ECONOMIC MIXING OF SILICA-RUBBER COMPOUNDS

Economic mixing of silica-rubber compounds

Interaction between the chemistry of the silica-silane reaction and the physics of mixing

By Wilma Dierkes

Cover design by Wilma Dierkes

Cover illustration:
  Front: Silica, a filler in rubber compounds, chemically resembles sand. When used as reinforcing filler, the silanol groups on the silica surface react with the silane coupling agent during mixing; this is the processing step in focus of this thesis. During vulcanization the silica-silane compound reacts with the polymer under formation of a filler-polymer network.
  Back: The 'hevea brasiliensis' tree is the source for natural rubber, one of the polymers used in tire compounding.
  Background: Giugiaro tread design from the 'Ultrac' tire, with permission from Vredestein Banden B.V., P.O. Box 27, 7500 AA Enschede, the Netherlands

ECONOMIC MIXING OF SILICA-RUBBER COMPOUNDS

INTERACTION BETWEEN
THE CHEMISTRY OF THE SILICA-SILANE REACTION
AND THE PHYSICS OF MIXING

PROEFSCHRIFT

ter verkrijging van

de graad van doctor aan de Universiteit Twente,

op gezag van de rector magnificus,

prof. dr. W.H.M. Zijm,

volgens besluit van het College van Promoties

in het openbaar te verdedigen

op vrijdag 22 April 2005 om 15.00 uur

door

Wilma Karola Dierkes

geboren op 24 December 1964

te Werlte (Duitsland)

Dit proefschrift is goedgekeurd door:

Promotor: Prof.dr.ir. J.W.M. Noordermeer

Das gute Wort

Sag' morgens mir ein gutes Wort
Bevor du gehst von Hause fort
Es kann soviel am Tag geschehn
Wer weiß, ob wir uns wiedersehn
Sag lieb ein Wort zur guten Nacht
Wer weiß, ob man noch früh erwacht
Das Leben ist so schnell vorbei
Und dann ist es nicht einerlei
Was du zuletzt zu mir gesagt
Was du zuletzt hast mich gefragt
Drum laß ein gutes Wort das letzte sein!
Bedenk – das letzte könnt's für immer sein!

Editha Theiler

PREFACE

'Objects in the rear view mirror are closer than they appear'

After three and a half years of doing experiments, evaluating and reporting I finally finished my Ph.D-thesis. When I started with this task, simultaneously with the begin of my employment as assistant professor at the Department of Rubber Technology, this moment seemed to be far away in the future. Now, looking back through these years, my perception is rather that time flew by and that the first day of my Ph.D-project is just a short time ago. But then, regarding all the events during these years, I must admit that it was the busiest period of my life, and that's why I enjoyed most of it so much after all. But it is not my merit alone; a lot of people contributed to the success of this period and I want to acknowledge their support.

I am especially thankful to Prof. Noordermeer for giving me the chance to write this thesis parallel to my work within his group at the University Twente. During the last few months, when I spent a lot of time to finish my thesis, he exempted me from a lot of other tasks, and I assume that he himself took over most of them. But he never mentioned it, so I am also grateful for giving me this freedom of mind to concentrate on the thesis without feeling guilty about other people doing the rest of my work. I also want to thank him for being the promoter of my thesis, for the discussions and the comments on my work.

I want to thank the members of the RBT group for their patience, understanding and cheering up during busy periods. During the last few months, when I was working at home a lot, they barely saw me. But they respected my absence and did not disturb me at my temporary home office. The work of Joost within my Ph.D-project merits special thanks, as he did most of the measurements in the laboratory; it was not the most exciting job to measure dozens and dozens of rubber samples. I want to thank Gerda for the administrative support during this period, and also for taking over some of my work during the busiest periods. At the same time I want to express my thanks to Karin, Genevieve and their colleges for their support in urgencies. I also want to honor the work of Marek as well as Geert as his predecessor in computer and software support. They kept my computer going, and I remember a lot comments of Marek concerning my computer I do not want to repeat. And thanks to Wilco for helping me with the layout of the cover.

I very much appreciated the fruitful discussions within the former 'silica group': Louis, Annemieke and Dries and Rabin.

Special thanks are dedicated to my paranimfen, Kannika and Louis, for their practical and mental support. It was a good decision to have one experienced paranimf to convincingly assure me that everything will turn out to be fine when nervousness took over and to have one inexperienced paranimf to join me in my ignorance about the whole procedure.

Adrie, Annemarie, Jan, Zlata and the SGA group supported me whenever necessary; they made my task a lot easier.

I am also grateful for the pleasant atmosphere and distraction created by all the colleges from PBM-, STEP- and MBT.

I am thankful for the support of all members of the Satpro project group, especially Kai-Udo for the administrative work he was doing besides the preparation of the experimental sessions and the meetings. Together with Niklas and Casper we were a good team and successfully produced a lot of rubber at the technical laboratory of ThyssenKrupp and at Vredestein Banden. Thanks for the good co-operation! I found a lot of benefit in the discussions with Dieter Berkemeier, Udo Görl, Peter Halaška, Kai-Udo Kelting, Harald Keuter, Andreas Limper, Urban Magnusson, Miroslav Maňas, Gerard Nijman, Casper van de Pol, Niklas Priebe and other guests during the project meetings. As Vredestein Banden put their production facility at our disposal, I want to acknowledge their contribution to this work as well. I want to express my regard for the employees of ThyssenKrupp Elastomertechnik for their support during the test sessions in the technical laboratory, especially Thomas, Mathilde, Matthias and Maik. GE Advanced Materials and Rheinchemie supported me with material and advise, therefore special thanks to Christine Lacroix and Thomas Früh.

Mein besonderer Dank gilt meiner Familie, insbesondere meinem Vater, die mir das Gefühl gab, jederzeit willkommen zu sein, die aber auch Verständnis dafür zeigte, dass die Doktorarbeit manchmal höhere Priorität hatte. Einen besonderen Beitrag hatte meine Mutter, die mich gut durch die schwierigsten Perioden der letzten dreieinhalb Jahre gebracht hat. Nicht zu vergessen meine Nichten, die einen besonderen Beitrag geleistet haben, indem Sie mich ab und zu an die wichtigen Dinge im Leben erinnert haben: Ablenkung und Spass.

And last but not least I want to thank my friends for not forgetting me even if they barely got any sign of life from me during busy periods.

Thanks to all the other people who crossed my way during this period and are not mentioned above.

Wilma

TABLE OF CONTENTS

INTRODUCTION

---

1. HISTORICAL OVERVIEW

The focus of this work is a material, which more than 5 centuries ago was discovered by the natives from Haiti to provide them with a material for one of their most popular leisure activity: They used the fluid tapped from one of their local trees to make a rebouncing ball for their favorite game. But they also used this material to facilitate the adversities of the daily life: They impregnated their clothing with this liquid to make it water-proof. The tree, from which they tapped the latex, was called 'caa-o-chu': weeping tree. The botanical name, which was given to this species later on, is Hevea Brasiliensis. The fluid they used for the various purposes, is nowadays known as latex. This material was brought to Europe, to the Academy of Science in Paris, in 1736. It did not take long for the scientists to discover an utterly important application of this material, for which it is still used and which gave the material its name: rubber. They used the dried latex to rub out the marks of black lead pencils. [1-4]

The next important step in rubber technology was made approximately a century later, when a skilled engineer discovered a way to overcome the stickiness and high degradability of raw rubber by mixing it with sulfur, white lead and oil of turpentine and drying it with heat. This process, which is still the heart of rubber technology, was named 'vulcanization' after the Roman God of Fire, Vulcan. The inventor of this process was Charles Goodyear. [3, 5]

When automobiles were invented, rubber became the material of choice to dampen the bumpiness of the roads. The first tires were solid; they consisted of a rubber sheet covered with fabric. By the end of the 19th century, a handy engineer developed air-filled tires, but it took one and a half decades and a lot of flat tires to get a breakthrough for this technology. The name of the inventor of the pneumatic tire is still well-known: André Michelin. [6]

And again a century later, in the late 20th century, another important progress in rubber technology was achieved: The replacement of carbon black by silica fillers, with the advantage of reduced rolling resistance of tires and, as a consequence, reduced fuel consumption of the vehicle. The importance of this

development is emphasized by the contemporary situation of limited reserves of non-regenerative energy and environmental problems. The fuel saving capacity of such a tire is 3% to 4% compared to a tire having treads made from compounds with carbon black, corresponding to a reduction of the rolling resistance of 20%. [7] This environmental and economical incentive of silica technology is important enough to overcome the higher production costs due to the difficult processing behavior and the higher material costs of these tires. This is the starting point of this thesis.

2. BACKGROUND OF THE INVESTIGATION

Silica compounds are difficult systems in terms of structure as well as processing behavior. This investigation focuses mainly on the processing behavior of this system, as influenced by the interaction of silica with the coupling agent as a first step in the formation of a network established by silica particles, coupling agent and polymer.

The structure of filled rubber compounds on a molecular scale, in particular when silica is used as filler, is not very well known. The main obstacle in investigating this system on nanoscale is the difficulty to find appropriate methods of sample preparation. A rubber compound consists of up to 15 components, which are vigorously mixed in an energy-intensive process. The viscoelastic compound is then brought into its final shape by vulcanization, resulting in a dense network comprising polymer chains and filler particles, with all the other ingredients embedded in the matrix. This makes a direct analysis of the material on microscopic scale difficult; the proper separation of parts of the system without changing its basic structure is problematic. An alternative is the investigation of this system as an entity, based on determining the mechanical and dynamical properties and developing models for the structure of the material. Numerous attempts to model the interaction between the filler and the polymer, which include phenomena such as molecular surface slippage and rearrangements of the polymer chains on the filler surface, particle displacements, molecular segment alignment, strong and weak binding forces and interparticle chain breakage, were developed. An overview of the most important models is given in chapter 2.

Mixing of silica with rubber is a challenge, as these materials are not very compatible in various aspects:

- o *Surface energy:* The surface free energy consists of a dispersive part and a specific part. The dispersive part of the surface energy of silica particles is low, resulting in a weak interaction between the polymer and the filler, thus a low reinforcing effect. The specific part of the surface energy is high with the consequence, that the interaction between the filler particles is very strong and that the viscosity of silica compounds is high. During mixing of

rubber with silica, the interparticle forces need to be overcome, and a link between the silica particles and the polymer has to be established. The use of a coupling agent, for example bis(triethoxysilyl- propyl)disulfane (TESPD), can serve both purposes: The viscosity of the compound during mixing is reduced and the reinforcing effect of the filler is increased. [8]

o *Solubility:* One condition of good mixing is an intensive contact between filler particles and polymer, as well as a homogenous distribution of the filler aggregates within the matrix. The first aspect, the intensive contact between the filler surface and the polymer matrix, depends on the surface area of the filler and on its wettability. The wettability is determined by the difference of the solubility parameters of the two components, which is quite significant in the case of silica and a non-polar polymer.

o *Structure of the filler:* Silica has a high structure; agglomerates and aggregates based on clusters of primary particles are characterized by a high surface area and a high percentage of void volume within the filler structure. As the direct interaction between the filler and the polymer is rather low, polymer chains can be connected to the filler only by physical processes: The polymer is entrapped in the voids of the filler structure resulting in occluded rubber. During mixing the structure of the filler has to be broken in order to increase the interaction between filler and polymer releasing a part of the occluded rubber. However, the final aggregate size distribution has an optimum: The filler should not be broken to the level of primary particles. [9]

o *Viscoelastic properties:* The polymer and the silica filler are materials with entirely different properties: The unfilled polymer is a viscoelastic material, and the filler consists of rigid particles. During mixing, the addition of silica primarily results in a steep increase of the viscosity of the compound due to the hydrodynamic effect, followed by a viscosity decrease due to breakdown of the filler structure and release of occluded rubber. During this phase, transition to non-linearity occurs, expressed by phenomena such as the Mullins effect (stress softening) and the Payne effect (modulus decrease with increasing strain amplitude due to breakdown of the filler-filler network).

These shortcomings in compatibility can be overcome by the application of coupling agents: They provide a bond between the filler and the polymer by forming a chemical link. The most commonly used coupling agents are silanes, and they react with the filler under formation of a silanol bond and with the polymer under formation of a sulfur bond. The application of a coupling agent greatly improves the processing behavior by reducing the specific surface energy and the solubility parameter of silica, and it enhances the properties of the final product by an increase of the dispersive component of the surface energy and the formation of a covalent filler-polymer network. [10] However, these improvements are accompanied by other problems:

- o *Ethanol formation*: During mixing the silane has to react with silanol groups on the surface of the filler under formation of ethanol. The ethanol in the compound competes with the silane for adsorption and reaction sites on the silica surface, resulting in a reduction of the silanization efficiency. Furthermore, ethanol condensation in the mixing chamber results in slipping of the compound along the mixing chamber walls with the consequence of a reduced mixing efficiency.

- o *Processing temperature*: The temperature window of the mixing process is limited at the lower end by the necessity to have a sufficient silanization rate and at the higher end by the risk of scorch caused by the sulfur moieties of the silane.

- o *Influence of other factors*: The kinetics of this process are complicated, as they depend on numerous factors such as structure, surface area and chemistry of the filler, characteristics of the coupling agent, composition of the compound as well as mixing protocol and equipment.

The application of coupling agents results in the formation of interpenetrating filler-polymer and polymer-polymer networks. This special network structure gives silica-filled rubber its special characteristics in terms of dynamic properties or, considering the most important final product: a tire, a lower rolling resistance and better wet grip.

3. AIM AND STRUCTURE OF THE INVESTIGATION

The aim of the thesis is twofold: to elucidate the different processes influencing mixing of a silica-rubber compound and to develop an improved mixing process. The mixing and silanization process will be analyzed from a theoretical point of view, but based on and verified by actual mixing experiments. After identification of the most important parameters influencing the mixing and silanization efficiency of silica compounds, these parameters will be further elaborated, theoretically and practically on laboratory scale, and verified on production scale.

The outcome the investigation will be a proposal of measures for improvement of mixing and silanization of silica compounds by adjustments of the mixing protocol and equipment. These measures shall enable the rubber processor to shorten the mixing cycle, thus to mix these compounds more economically. The quality of the material is required to be at least similar to the quality of the material produced in the conventional way.

The first part of the investigation is a screening of commonly used mixing technology in terms of their suitability for silica compounds. Investigated factors are the size of the mixing chamber and the rotor type, the time-temperature

profiles, the temperature control unit settings, the fill factor of the mixing chamber, an improved ventilation of the mixing chamber by working in an open mixer or by applying air injection in an open or a closed mixer, with or without providing a special outlet for the air stream.

The outcome of this part of the study is a ranking of the influencing parameters for the silanization efficiency. The most important parameters are further elaborated on laboratory scale. Once these measures are proven to enhance the silanization efficiency, they are scaled up to production scale. The compounds produced with the improved technology are compared to the compounds produced by the conventional process. Given that the material produced under improved conditions fulfills the specifications of the standard production control, tires are built using the compound for the tread. The tires undergo a complete test program to measure their performance and to compare them with tires having a standard tread.

This thesis reflects only a part of a project, with emphasis on the chemical background of silica mixing. A second thesis elaborated within this project will focus on the technical and economical aspects of mixing of a silica-silane-polymer system.

4. CONCEPT OF THE THESIS

After a brief introduction, the current state of the art concerning rubber reinforcement and rubber mixing with special attention to silica as a filler will be reviewed in *chapter 2*. One paragraph within this chapter is dedicated to the theoretical models to describe the interaction of carbon black or silica with the polymer and to explain the Payne effect. This chapter also includes an overview of the properties of silica with focus on their application as a filler.

In *chapter 3* the results of a phenomenological investigation of the mixing process are presented and discussed. Various parameters of the mixing and silanization process are investigated concerning their influence on the silanization efficiency.

The following *chapter 4* is a theoretical approach to the silica-silane-polymer system: The devolatilization of rubber compounds during mixing, including a chemical reaction, is modeled. The different processes and parameters influencing the devolatilization of the compound are discussed with respect to the silanization efficiency.

In *chapter 5* the kinetics of the silanization reaction with variation of different influencing factors are discussed. Reaction rates for different conditions are calculated and compared in order to get a better view on the dependence of the

time-temperature profile of the degree of silanization. Activation energies reflect the temperature sensitivity of the reaction.

Energy input is one of the most important parameters in rubber mixing, depending not only on the mixing equipment, but also on the compound properties. In *chapter 6,* the energy input during heating and silanization of the compounds is evaluated, again with variation of the most important influencing factors of the silanization.

Upscaling is one of the main problems in rubber processing, as a change of the dimensions of the mixer does not result in a proportional change of the mixing process parameters. The influence of an increase of mixer size in this special case, a mixing process combined with a chemical reaction, is investigated and discussed in *chapter 7*.

Chapter 8 is focused on coupling agents: Different types of coupling agents are investigated concerning their influence on the processing behavior of the compound and silanization efficiency.

5. REFERENCES

1. Brydson, J.A., in *Rubbery materials and their compounds*, 1988, Elsevier Science Publishers: Essex.
2. Natuurrubber, 2000, **20**(4).
3. Mark, H.F., Rubber Chem. Technol., 1988, **61**: p. G73.
4. Hofmann, W., in *Rubber Technology Handbook*, 1996, Hanser Publishers: Munich (Germany).
5. Blow, C.M., Hepburn, C., in *Rubber technology and manufacture*, 1982, Butterworths: London (Great Britain).
6. www.vintagecars.about.com/library/weekly/aa082298.htm.
7. Pauline, R., 12.02.1999, Compagnie Generale des Etablissements Michelin: EP 0 501227A1.
8. Wolff, S., Wang, M.J., Tan, E.H., in *Am. Chem. Soc. Rubber Div. conference*, 1993, Denver, Colorado (USA).
9. Reuvekamp, L.A.E.M., in *Thesis: Reactive mixing of silica and rubber for tyres and engine mounts*, 2003, Dept. Rubber Technol., Univ. Twente: Enschede (the Netherlands).
10. Wang, M.J., Wolff, S., Rubber Chem. Technol., 1992, **65**: p. 715.

FILLER REINFORCEMENT OF RUBBER

WITH SPECIAL ATTENTION TO SILICA FILLERS

Rubber is not simply an elastomer brought into a fixed shape by crosslinking, but contains a variety of different compounding ingredients like processing aids, protection and curing agents as well as a considerable amount of fillers. The fillers used in rubber compounding are characterized by their reinforcing effect, which ranges from inactive over semi-active to very active fillers. The designation 'active' or 'reinforcing' refers to the influence of the filler on compound viscosity and mechanical properties such as tensile strength, abrasion and tear resistance. Structure as well as surface properties of the filler are the main characteristics which determine the reinforcing effect. Active fillers are characterized by a large relative surface area and a high structure, both properties resulting in a strong physical and chemical interaction between the filler and the polymer. However, a highly active filler surface also results in strong interparticle forces, which negatively influence the processing behavior due to agglomeration of filler particles during mixing and storage of the compound.

Silica fillers are characterized by a high specific surface energy which results in a strong filler-filler interaction and a difficult processing behavior. The dispersive part of the surface energy is rather low, therefore the interaction between the filler and the polymer is not very strong and the reinforcing effect is weak. These shortcomings can be overcome by the use of a coupling agent, which chemically connects to the filler during mixing and to the polymer during vulcanization. Consequently, mixing of silica compounds is fundamentally different from mixing of carbon black compounds: In the case of silica, strong filler agglomerates have to be broken, the chemical reaction between filler and coupling agent has to take place, the reaction byproduct, ethanol, has to be removed and the filler-polymer network has to be established in the curing step. The structure of the final cured silica-containing rubber product is fundamentally different from the structure of carbon black reinforced rubber on molecular scale: The polymer is linked to the silica particles by covalent bonds, resulting in a strong filler-polymer network. Numerous models describe the correlation between the structure of the silica-polymer system and the special properties of this material making it especially suitable for tire tread application: a low hysteresis at high temperatures and low frequencies resulting in a low rolling resistance in combination with a good wet grip and abrasion resistance.

This chapter gives an overview over the fundamentals of rubber reinforcement and rubber mixing, both from a theoretical as well as a practical point of view.

1. RUBBER REINFORCEMENT

Elastomers in general are not used in their pure form, but are reinforced by fillers. The addition of fillers fundamentally changes the properties of rubber: Unfilled rubbers increase in modulus with increasing temperature, as predicted by the kinetic theory of rubber elasticity. The addition of fillers significantly changes the temperature coefficient of the modulus; it can even alter the sign of the coefficient resulting in a decrease of the modulus with increasing temperature. Another effect of blending fillers with rubber is the transition to non-linear behavior. The use of reinforcing fillers gives the material unique properties: a combination of high elasticity with high strength. Figure 1 illustrates the influence of the addition of increasing amounts of reinforcing fillers on various properties of an elastomer.
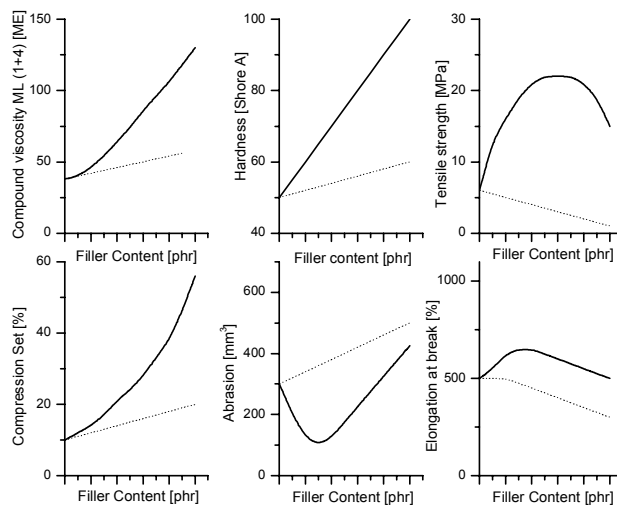
Figure 1: The influence of reinforcing fillers on the properties of an elastomer [2]
—— *active fillers* ---- *non-active fillers*

1.1. REINFORCING EFFECTS

A condition for filler reinforcement is the interaction between the filler particles and the polymer. These interactions can be strong, for example in the case of covalent bonds between functional groups on the filler surface and the polymer, or weak as in the case of physical attractive forces. When carbon black is blended with a polymer, the level of physical interaction is high. [3] In contrast to this, the interaction between silica particles and the polymer is very weak, and only by the use of a coupling agent a bond is formed between the filler and the polymer.

Besides the interaction between the polymer and the filler, an interaction between filler particles occurs, predominantly above a critical concentration threshold, the percolation threshold: The properties of the material change drastically, because a filler-filler network is established. This results for example in an overproportional increase of electrical conductivity of a carbon black filled compound. But even at

lower concentrations, the filler-filler interactions influence the material characteristics, as expressed by the Payne effect. Figure 2 illustrates the strain-dependence of the Payne effect and the strain-independent contributions to the shear modulus for carbon black filled compounds [4] and silica filled compounds.
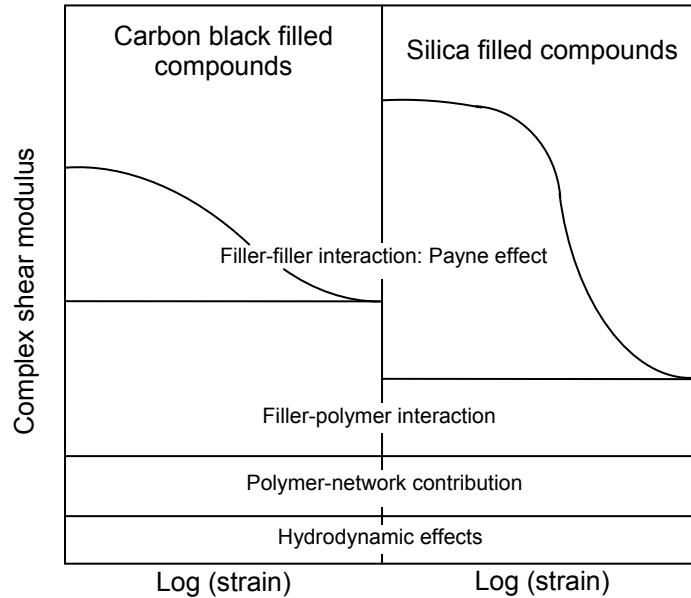

Figure 2: Effects contributing to the complex shear modulus

The main contributions to the complex shear modulus are the hydrodynamic effect, the polymer network, the filler-polymer and the filler-filler interaction.

1.1.1. Hydrodynamic effect

The addition of particles to a viscous fluid results in an increase of the viscosity of the fluid, commonly designated as the hydrodynamic effect. [5] In a polymeric matrix this effect is also measured as an increase of the modulus. The phenomenon was modeled by *Einstein* almost a century ago, and he described the viscosity increase by rigid spherical particles dispersed in a liquid by the following equation: [6, 7]

$$\eta_f = \eta_0(1 + 2.5\phi)$$ *Eq. 1*

In this equation, η_f is the viscosity of the fluid containing the particles, η_0 is the viscosity of the pure fluid and ϕ is the volume fraction of the particles. Einstein made the following assumptions for his model:

o Perfect wettability of the spheres
o Uniform spherical particles
o No interaction between the particles

Especially the last two requirements are rarely met in filler-polymer systems. This discrepancy between Einstein's theory and practical experience was taken into consideration by an additional term, introduced by *Guth and Gold*: [8]

$$\eta_f = \eta_0(1 + 2.5\phi + 14.1\phi^2)$$

Eq. 2

The term Guth and Gold added, is again a function of the filler volume fraction ϕ to the power of two, emphasizing the influence of the filler concentration.

In the case of an elastic matrix, the viscosities of the material can be replaced by the shear moduli, as shown by *Smallwood*: [9]

$$G_f = G_0(1 + 2.5\phi + 14.1\phi^2)$$

Eq. 3

The addition of the filler increases the shear modulus of the pure elastomer G_0 and results in a shear modulus G_f for the filled compound. The same correlation holds for the Young's modulus E. A correction for the non-spherical shape of the filler particles, a shape factor f_S, was added by *Guth*, resulting in the following equation: [10]

$$G_f = G_0(1 + 0.67f_S \cdot \phi + 1.62f_S^2 \cdot \phi^2)$$

Eq. 4

The shape factor f_s represents the ratio of the longest dimension to the shortest dimension of the particle. The modulus as calculated by Equations 3 and 4 is independent of the applied strain.

1.1.2. Filler-polymer interaction

The filler-polymer related effects are determined by the special structure of the filler in the rubber matrix and its interaction with the polymer. The occluded rubber contributes to this effect: Polymer chains are trapped in the voids of the filler agglomerates and aggregates; they are immobilized and shielded from deformation. They do not contribute to the elastic behavior of the matrix, as their properties resemble the properties of the rigid filler particles rather than the properties of the elastic and flexible free polymer chains. Occluded rubber increases the effective filler loading and thus the strain independent contribution to the modulus. The filler-polymer interaction can be attributed to physical interactions, for example van der Waals forces, or chemical reactions as in the case of a silica-coupling agent system. [11-14]

1.1.3. Polymer network contribution

The polymer network formed during vulcanization is the third strain-independent contribution to the modulus: The modulus is proportional to the concentration of elastically active network chains υ and the absolute temperature T, with the proportionality constant being the Boltzmann constant k_B:

$$G_0 = \upsilon \cdot k_B \cdot T \qquad\qquad \textit{Eq. 5}$$

1.1.4. Filler-filler interaction: Payne effect

The strain-dependent contribution to the modulus is caused by filler-filler interactions. This effect was first brought into focus by Payne, and he interpreted the sigmoidal decrease of the storage modulus versus the double strain amplitude in logarithmic scale from a limiting zero-amplitude value to a high amplitude plateau as the result of the breakage of physical bonds between filler particles, for example van der Waals or London forces. This effect is largely reversible once the strain is released and is independent of the type of polymer, but is dependent on the type of filler. Figure 2 shows the key difference between carbon black and silica: The Payne-effect is stronger for silica, as a consequence of the strong interparticle forces between the filler particles. [14-17]

1.2. DYNAMIC MECHANICAL PROPERTIES OF REINFORCED RUBBER

The tire performance is related to the dynamic mechanical properties of the material. Rolling resistance, for example, is related to the hysteresis. When energy is brought into the material, it is partly dissipated into the tire material as heat and partly stored elastically. The energy input into a viscoelastic material can be modeled at sinusoidal shear deformation $\gamma(t)$ of an angular frequency ω. The shear stress response $\sigma(t)$ is also sinusoidal, but out of phase with the strain:

$$\gamma(t) = \gamma_0 \sin(\omega t) \qquad\qquad \textit{Eq. 6}$$

$$\sigma(t) = \sigma_0 \sin(\omega t + \delta) = (\sigma_0 \cos\delta)\sin\omega t + (\sigma_0 \sin\delta)\cos\omega t \qquad\qquad \textit{Eq. 7}$$

γ_0 is the maximum strain amplitude, σ_0 is the shear response at maximum strain, t is the time and δ is the phase angle. The phase angle is graphically illustrated in Figure 3:
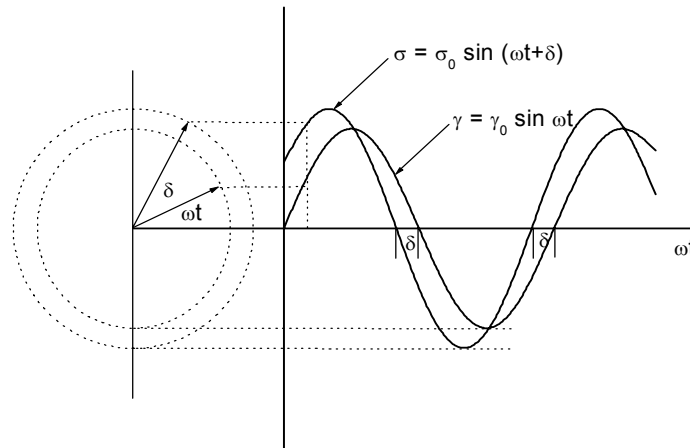

Figure 3: Illustration of the phase angle for the delay of the stress response on sinusoidal deformation

The shear stress signal can be separated into two contributions, one in phase with the strain and one 90° out of phase with the strain. The two components can be described by defining two moduli:

$$G' = \frac{\sigma_0}{\gamma_0} \cos \delta \qquad\qquad \textit{Eq. 8}$$

$$G'' = \frac{\sigma_0}{\gamma_0} \sin \delta \qquad\qquad \textit{Eq. 9}$$

G' is the component in phase and G" is the component out of phase with the oscillatory strain. The correlation between strain and stress is expressed by combining Equations 7 to 9:

$$\sigma(t) = \gamma_0 [G' \sin \omega t + G'' \cos \omega t] \qquad\qquad \textit{Eq. 10}$$

The two components are the real and the imaginary part of the shear modulus G*, when written in a complex form:

$$G^* = G' + iG'' \qquad\qquad \textit{Eq. 11}$$

or:

$$G^{*2} = G'^2 + G''^2 \qquad\qquad \textit{Eq. 12}$$

G' is the storage or elastic modulus and G" is the loss or viscous modulus. Using these two moduli, the phase angle is defined as follows:

$$G''/G' = \tan \delta \qquad\qquad \textit{Eq. 13}$$

Both moduli depend on frequency as well as on temperature. Figure 4 shows the frequency-dependence of the storage and loss modulus.
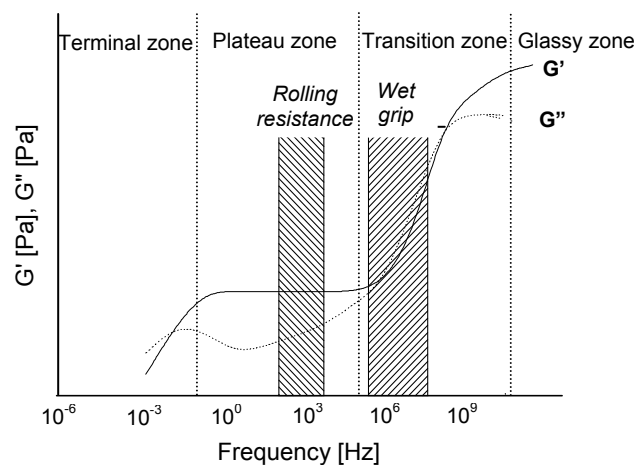

Figure 4: The frequency-dependence of the storage modulus G'
and the loss modulus G" [18]

The frequency-dependence of the modulus is a result of chain and segment mobility in the material. At low frequencies, in the terminal zone, the time scales of one cycle of stress application and the enforced chain movements are equal: The polymer chains can follow the applied strain without delay and without loss of energy. With increasing frequencies of the applied strain, entanglements are no longer able to follow the applied strain, they act as temporary crosslinks and the material shows elasticity. All other movements are still taking place within the time scale of the load cycle. This region of a constant storage modulus and a minimum in loss modulus is called the rubber plateau. With further increasing frequency the material comes into a transition zone between the rubbery state and the glassy state, which is characterized by a strongly decreasing mobility of the molecules relative to the frequency, with the consequence that both moduli strongly increase. Finally the material enters the glassy state: The material has a high modulus, the result of the rigidity of the polymer chains at these high frequencies. The molecules are not flexible enough to follow the applied strain, only small local chain movements occur. In the transition zones energy dissipation is high, with a maximum of the loss modulus. [18]

The frequency region of rolling resistance and wet skid are indicated in Figure 4: Rolling resistance is a characteristic of the rolling tire, and the angular frequency of a rolling tire is within the rubbery zone. Wet skid is a high frequency phenomenon, in the transition zone between the rubbery and the glassy state, typically in the megahertz region. The position of wet skid on the frequency scale shows, that the glass transition temperature has a strong influence on this property of a tire: Materials with a high glass transition temperature are preferred, as their wet skid resistance is high. [19, 20]

The above discussion of the frequency-dependence of the dynamic properties shows, that these properties are dependent on the mobility of the polymer chains, which is influenced by the temperature of the material. Figure 5 shows the temperature profile of the phase angle, the elastic and the viscous modulus and the correlation with the most important tire properties.
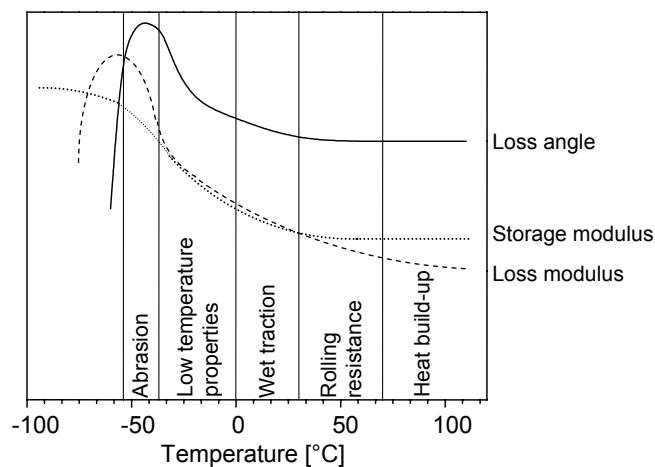

Figure 5: The temperature profile of the phase angle, the elastic and the viscous modulus and the correlation with tire properties [21, 22]

15

At low temperatures around the glass transition point, the polymer is in a glassy state with high moduli, and the phase angle is at a maximum. In the following rubbery region, the molecular mobility is high enough to follow the applied dynamic strain; energy dissipation decreases and finally reaches a plateau.

The glass transition temperature of the material gives an indication of the low temperature performance of the tire, as it indicates the limit of the elastic behavior. A correlation between the glass transition temperature and abrasion resistance is generally accepted. [21, 23, 24] The temperature range above 0°C up to ambient temperatures correlates to the prevailing road temperatures, and the phase angle in this temperature range gives an indication of the skid behavior or traction, particularly on wet roads. In this temperature range the phase angle should be as high as possible to ensure good traction. The next temperature zone is representative for the temperature of a running tire and the phase angle in this temperature range correlates with the rolling resistance: Damping should be low, resulting in a low rolling resistance. At further temperature increase, the material starts to degrade and driving safety is reduced. Therefore heat build-up should be low in order to restrain the temperature increase as far as possible. [23]

The dynamic properties are not only influenced by the type of polymer, but also by the filler used in the compound, or, more accurately, by the interaction of the filler with the polymer. The effect of carbon black on hysteresis depends primarily on the particle size of the filler and is related to breakdown and reformation of the agglomerations and the network, to slippage of polymer chains around the periphery of the filler clusters and the presence of occluded rubber. [25] Figure 6 shows the difference of the temperature profiles of carbon black and silica filled rubber compounds.
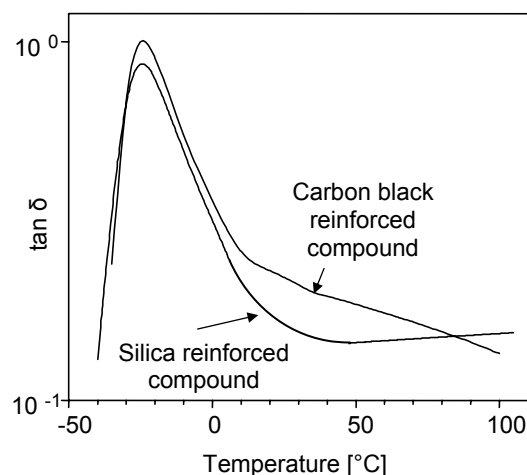

Figure 6: Temperature profiles of the phase angle
for a carbon black filled and a silica filled compound [26]

The most prominent difference between the two filler materials is the increase of the phase angle at higher temperatures for the silica filled compounds: With increasing temperature, the filler-filler interactions for silica are reduced, the filler-

filler bonds are easier broken and the rate of network breakdown and reformation is increasing, resulting in an increasing energy dissipation. A crossover point with the phase angle of the carbon black filled compound is found in the range of 80°C to 90°C. The benefit of replacing carbon black by silica lies in the reduced hysteresis in the temperature range around 60°C, the typical range for rolling resistance: The rolling resistance of silica filled compounds is lower compared to carbon black filled compounds. [26]

2. RUBBER MIXING

Mixing of rubber compounds is a rather complicated process as components differing in structure, viscosity and rheological behavior have to be homogenized. Physical processes, for example the adsorption of polymers or other additives onto filler surfaces and the incorporation of polymers into voids of the filler structure, need to occur. In the case of silica, a chemical reaction between the coupling agent and the silanol groups on the filler surface has to take place. Besides this, the mixing equipment, in general an internal mixer, is not very flexible and a short-term adjustment of the mixing conditions is difficult. Different mixing processes have to take place in order to guarantee a homogenous blend of all the compound ingredients on the required scale: laminar, distributive and dispersive mixing.

2.1. THEORETICAL BACKGROUND

2.1.1. Different mixing processes
The following types of mixing are the main processes necessary for a good particulation and homogenization of the compound ingredients: [1, 27, 28]

o *Extensive or laminar mixing*: The primary mechanism of this mixing process is convection associated with deformation of the matrix in an internal mixer. This process takes place in the channels between the rotor shaft and the mixer wall.

o *Distributive mixing*: The randomness of the spatial distribution of a minor constituent within a matrix is increased without change in the dimensions of this constituent. Examples are the distribution of a carbon black or accelerator masterbatch throughout a polymer matrix. This type of mixing takes place in the region between the rotor shaft and the mixing chamber wall as well as in the free volume above the rotors.

o *Intensive or dispersive mixing*: The size of the clusters of the minor constituent is reduced. Examples are the breakdown of carbon black or silica agglomerates into smaller aggregates and primary particles. Filler agglomerates are broken, when the stress level within the deforming matrix exceeds the cohesive forces or surface tension forces of the agglomerates.

The area in the mixing chamber with sufficiently high shear forces is the clearance between the rotor tip and the mixing chamber wall.

The most challenging part of rubber mixing is the dispersion of the filler: The filler agglomerates have to be broken into smaller particles, the aggregates, but not completely to the level of primary particles. An optimal particle size distribution has to be achieved in order get the best properties for the final rubber product. [29]

2.1.2. Mixing with fillers: dispersive mixing

Mixing of rubber is not just a process with the aim of a homogenous distribution of the compound additives in the polymer matrix, but includes processes such as plasticization, incorporation of solids and dispersion. During mixing all these processes take place, but depending on the mixing parameters and the degree of mixing the rate of the different processes changes.

On macroscopic scale the dispersion of a filler into a polymer matrix shows the following stages: [28]

o The filler smears into striations following the deformation pattern of the polymer
o Agglomerates up to 10 to 100 micrometer in size appear
o Agglomerates are continuously broken and aggregates with an average size of 100 nanometers till 0.5 micrometers appear
o Smaller aggregates and primary particles appear on the expense of larger aggregates and agglomerates

Figure 7 illustrates the transition from large agglomerates into smaller aggregates and primary particles, and gives an indication of their dimensions.

20 nm

Primary particles

100 nm

Aggregates

10 µm

Agglomerates
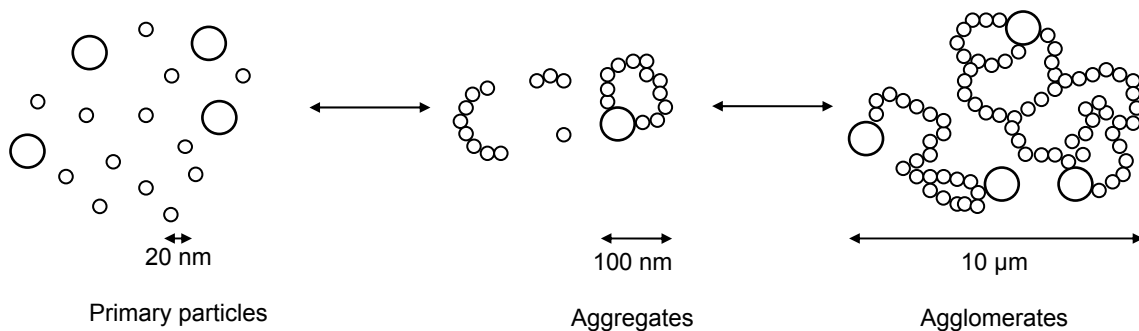
Figure 7: Filler aggregation and dispersion [30]

Based on these phenomena, *Yoshida* [31] described mixing as a three step process: transposition, insertion and breaking of the disperse system. During transposition the system is subjected to stretching deformation by shearing forces, which increases the interface between the disperse phase and the matrix, and results in a gradual insertion of the disperse phase into the matrix. The particles of the dispersed phase are disrupted by shearing forces, and the size of

agglomerates and aggregates is reduced. The degree to which the filler finally has to be dispersed depends on the quality requirements of the compound: the higher the degree of dispersion, the better the properties. But there is a lower limit to the aggregate size as the properties deteriorate with very small aggregate sizes and an increasing amount of primary particles. [29, 32] A more refined model of dispersive mixing separates the process into four different steps: [33-35]

o   Incorporation
o   Plasticization
o   Dispersion
o   Distribution

In the initial stages of mixing before incorporation starts, two processes take place: The first process involves large deformations and subsequent relaxation of rubber domains, during which filler aggregates are sandwiched between rubber layers. The second mechanism is based on the disintegration of the rubber into small particles, which are blended with the filler agglomerates and finally seal them inside. [33, 36, 37]

2.1.2.1.   Incorporation

The incorporation of the filler is subdivided into two phases: formation of a rubber shell around the filler particles followed by filling up the voids within the filler agglomerates, in other words between the filler aggregates. [31] It includes a subdivision step: breaking of large agglomerates into smaller entities. [33-35]

2.1.2.2.   Mastication and plasticization

Mastication and plasticization take place during the whole mixing process and result in a change of the rheological properties of the compound, especially a viscosity decrease of the polymer matrix by degradation of the elastomer chains. [33-36] Figure 8 gives a schematic view of the viscosity changes during mixing and the contributions of temperature increase and polymer breakdown to the viscosity decrease.
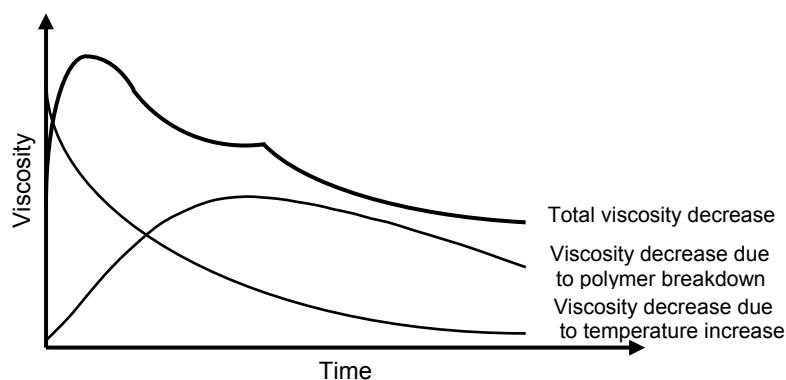

Figure 8: Contributions of polymer breakdown and
temperature increase to the viscosity decrease [38]

2.1.2.3. Dispersion

At the end of the incorporation stage the majority of the filler is present as agglomerates. They act as large, rigid particles, whose effective volume is higher than that of the filler alone due to rubber trapped inside the filler voids and the rubber immobilized on the surface. [27] The bound and occluded rubber increases the rate of dispersive mixing by increasing the effective radii of the filler particles: larger effective radii lead to higher stress during mixing.[39, 40] The filler agglomerates are successively broken to their ultimate size, mainly by shear stress. Parallel with the reduction of the agglomerate size the interface between the matrix and the filler is increased, and the filler particles are distributed homogenously throughout the rubber matrix. [41] When the filler agglomerates decrease in size, the occluded rubber concentration is reduced. The viscosity of the compound decreases [12] and finally reaches a plateau region. [42] In general, the average particle size reaches a minimum value and a further energy input does not result in a reduction of the size of the filler aggregates any more, as the mixing and dispersion efficiency is decreasing with reduced viscosity of the compound. [43]

2.1.2.4. Distribution

In the distributive mixing step particles are spread homogenously throughout the polymer matrix without changing their size and physical appearance. The thermodynamic driving force for this process is the entropy increase of the blend. [41]

Figure 9 illustrates the different mixing stages with respect to filler subdivision, incorporation, dispersion and distribution.
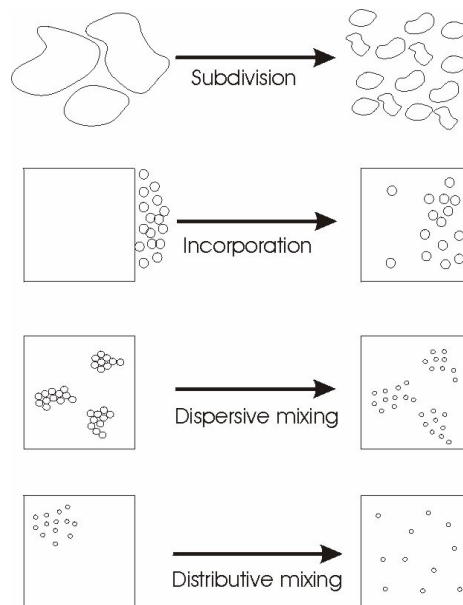

Figure 9: Illustration of the different mixing stages for filler-polymer systems [34]

2.1.3. Dispersion mechanisms

Two forces are involved in agglomerate breakup: cohesive forces within the agglomerates and hydrodynamic forces inducing the breakup of the clusters. [44] Numerous models for the dispersion process are published, but most of them take only one of these forces into consideration.

Models based on cohesive interparticle forces within the agglomerates are developed by *Rumpf* [45], *Cheng* [46, 47], *Hartley and Parvitt* [48], *Sonntag and Russell* [49, 50] and *Kendall* [73]. Another category of models is based on hydrodynamic forces and they differ in the definition of the agglomerates: Some models consider agglomerates as two touching rigid spheres of different radii with a total volume equal to that of the agglomerate (*Nir and Acrivos* [51]), other approaches describe agglomerates as homogenous spheres undergoing bulk motion as single entities, neglecting the fluid interstitial velocity through the clusters (*Bagster* [52, 53], *Adler* [53]).

For a complete description of filler dispersion both forces - cohesive and hydrodynamic – have to be taken into consideration. *Manas-Zloczower and Feke* [54] base their model on both forces. They describe the silica-rubber system as rigid spheres in a matrix undergoing simple shear. The fraction of agglomerates broken by the applied flow field Z can be calculated as follows:

$$Z = \frac{\chi \mu \dot{\gamma}}{TS} \qquad\qquad Eq. \ 14$$

$\dot{\gamma}$ is the shear rate, χ reflects the geometry of the breakup process, µ is the velocity of the suspending fluid and TS is the tensile strength of the agglomerate. Z scales the magnitude of the hydrodynamic forces acting to rupture the agglomerate relative to the cohesive forces of the agglomerate. [55, 56] An extension of this model takes various flow geometries into consideration, resulting in different values of Z for simple shear, pure elongation, uniaxial and biaxial extension. [54]

The reduction of the particle diameter is found to be a first-order process [57, 58] corresponding to an exponential mixing torque decay. [59]

Two basic mechanisms for filler dispersion are discussed in literature: the onion model and the fracture model. [60, 61] In the onion model, rubber flows around a filler agglomerate and scrapes small aggregates from its surface, which are distributed in the matrix. The size of the agglomerates gradually decreases. [62] This mechanism occurs preferably in the rolling pool of material in front of the rotor flights, as illustrated in Figure 10. [63]

A simulation of the onion model assumes that the radius of the aggregates peeled off the agglomerates is 0.1 µm. In this case the diameter of the particles after n steps d_n can be calculated from the diameter of the agglomerates d_0: [62]

$$d_n = d_0 - 0{,}2n \qquad\qquad \textit{Eq. 15}$$

The second mechanism is fracture of the agglomerates, reducing their size to about half of the original size with each fracture step. [44, 55, 64-67] This process mainly occurs in the clearance between the rotor flight and the mixing chamber wall. During each rotor revolution a small portion of the compound passes the clearance, where stresses are high enough to cause disagglomeration by fracture. [68] This well-dispersed part of the compound is then distributively mixed into the remaining material.

The simulation of the fraction model is based on the fracture of agglomerates into two equal parts, which are assumed to be spherical. The distribution of the agglomerate sizes after n fracture steps is described as follows: [62]

$$d_n = d_0 \big/ (2^n)^{1/3} \qquad\qquad \textit{Eq. 16}$$

This equation gives the correlation between the diameter of the initial agglomerate, d_0, and the diameter of the final aggregate after n steps of the simulation, d_n.

2.2. MIXING EQUIPMENT: INTERNAL MIXERS

2.2.1. *Flow and forces in an internal mixer*
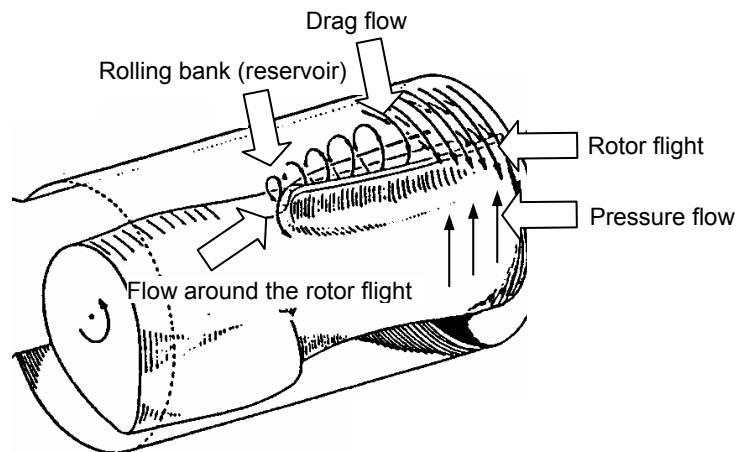
Figure 10: Flow paths within a hemisphere of an internal mixer [63]

Tracing the material in a mixing chamber of an internal mixer on a macroscopic scale shows, that a reservoir of material is situated in the space above the rotors. This region has two critical functions: Incorporation of the material fed into the mixer and exchange of material between the two hemispheres of the mixing chamber. A part of the material is collected by the rotor flight and swept into the area in front of the flight, in either hemisphere of the mixing chamber. [69] The amount of the collected material depends on the fill factor and the relative rotor

position in case that friction is applied. [69] During one rotor turn the material is distributed within the mixing chamber by a flow between rotor tip and chamber wall and between rotor shaft and chamber wall as well as by the flow around the end of the rotor flight, as illustrated in Figure 10. The remaining material returns to the reservoir. [63]

Using an appropriate fill factor, the region in front of the flight is permanently filled with rubber. The flow in this region is a summation of drag flow and pressure flow: The drag flow is caused by the motion of the rotor relative to the chamber wall, and the pressure flow is induced by the pressure difference behind the rotor and in front of the rotor. Behind the rotor tip, voids are present even at very high fill factors, resulting in a low pressure and providing the basis for disordering, necessary for intensive and extensive mixing.

The drag flow in the clearance between flight tip and chamber wall causes a layer of material to be sheeted out onto the wall of the mixing chamber (Figure 11). This layer finally separates again from the wall and undergoes elastic recovery. It is swept up and incorporated again by the flow front of the material being pumped around. [69]
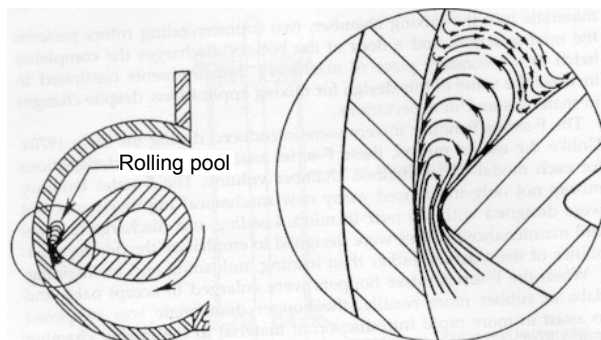
*Figure 11: The rolling pool of material in front of a rotor flight
and the formation of the wall layer*

The high-shear region between the rotor flight tip and the chamber wall is the only region within an internal mixer with unidirectional flow; in all other region random flow occurs. [63] This area is the most important one for a good mixing efficiency as shearing forces and elongation deformations are high. All other areas are less effective in mixing; only macroscopic transport of material resulting in homogenization on a larger scale occurs, and the material moves either in an axial direction or from one hemisphere to the other. [37, 43]

2.2.2. Dispersion in an internal mixer

Dispersion occurs mainly in the high-shear region of the mixer, the clearance between the rotor tip and the mixer wall. The width of the rotor tip is of great importance for the total shear as well as for the residence time of the material in the high shear zone. [34] The amount of material passing this zone can be

estimated by calculating its volume and comparing it to the total free volume of the mixing chamber. In the case of a laboratory Banbury mixer, the ratio of the volume of the high shear zone to the total free volume of the mixing chamber is approximately 15%. [43] The spiraling axial flow of the rolling bank in front of the rotor flight also contributes to dispersive mixing. [63] The volume of the rolling bank depends on the fill factor and the rotor speed: With increasing rotor speeds the volume of the rolling bank is reduced, and more and more material occupies the space behind the rotor tip. [70]

The shear stress in the clearance between flight tip and chamber wall has to surpass a critical value, the stress required for breaking the agglomerates, in order to be effective in dispersion. If the shear stress is only slightly higher than the critical stress, only those agglomerates that are favorably oriented to the unidirectional flow in the clearance – with their long axis perpendicular to the stream lines - will break. The remaining agglomerates will finally become aligned with the flow without any further dispersive or distributive effect. [71, 72] The stress in the clearance between the flight tip and the chamber wall depends on the depth and width of the channel: [73] The maximum shear stress varies inversely with the flight tip clearance, making the shear stress very sensitive to variations of the clearance and requiring very narrow clearances for high shear stresses. [72]

The shear not only depends on the geometry of the mixing chamber, but also on the viscosity of the compound: High shear stresses are especially effective in high-viscosity media. Therefore the mixing efficiency is improved by high filler loadings, low mixing temperatures and low oil concentrations. [33, 34, 74]

2.3. THE MIXING PROCESS

The mixing process can be controlled and analyzed by fingerprints: time profiles of temperature, torque, energy input, ram pressure or other parameters monitored during the mixing process. Especially the torque profile gives a good view of the different steps of the mixing process.

2.3.1. *Analysis of torque-time profiles of a mixing cycle*

Figure 12 shows a generalized torque-time profile of a mixing cycle for a carbon black compound, which is characterized by two torque maxima. The first torque maximum corresponds to the point when all ingredients so far added to the compound are forced into the mixing chamber and the ram reaches its final position. Time and height of the maximum depend on the composition of the compound, the fill factor of the mixing chamber, the activity and structure of the filler as well as the bound rubber fraction. [31, 75] The region between the start of the mixing cycle and the first minimum is the region, in which mainly mastication of the polymer takes place and dispersion starts. In the next zone dispersion and distribution of the additives including the filler occurs, and a second torque maximum is observed. This torque maximum corresponds to the incorporation of the filler: the agglomerates are wetted by the polymer, entrapped air is removed

and the compound reaches its final density. [31] Filler dispersion and polymer breakdown result in a fast torque decrease after the second peak down to a dispersion degree above 90%, and the kinetics can be described by a first order law: The rate of agglomerate breakdown is proportional to the concentration of the agglomerates. This period of steep torque reduction is followed by a period of a slower torque decrease, during which polymer breakdown and dispersion occur to a very limited degree, shearing is reduced and homogenization starts. [59, 76]
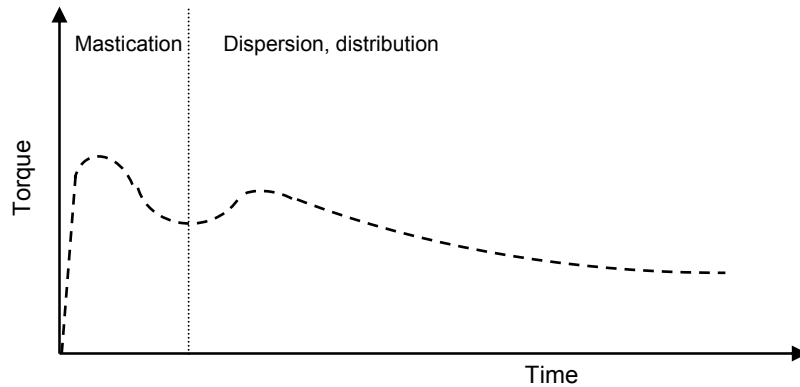
Figure 12: Generalized torque-time profile of a mixing cycle

2.3.2. Parameters influencing the mixing process

The following parameters are the most important ones to determine the mixing efficiency:

o Geometrical design of the mixing chamber and the rotor
o Fill factor
o Rotor speed
o Temperature control unit settings
o Ram pressure

2.3.2.1. Geometrical design of the mixing chamber and the rotor

The first internal mixers used in the rubber industry were equipped with tangential rotors, with the main characteristic that the circumferences of the two rotors do not interfere: the rotors can turn at uneven speed. Especially for silica compounds mixers with intermeshing rotors are becoming more and more common. These rotors are positioned close to each other and can therefore not run with friction. Figure 13 shows examples of tangential and intermeshing rotors.
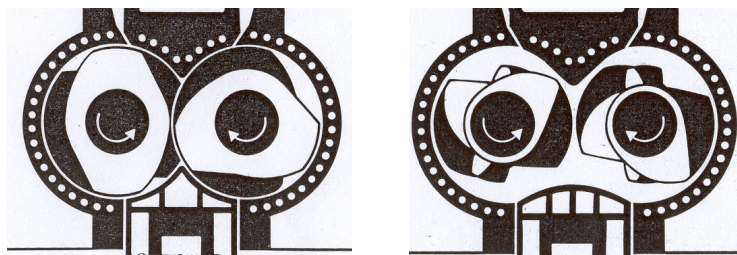
Figure 13: Intermeshing (left) and tangential (right) rotor geometry

Tangential rotors are characterized by a main material flow from the two sides to the center of the mixing chamber, and axial recesses result in an intensive flow near the side of the mixing chamber. The tangential rotor geometry is the preferred one for high machine efficiency, fast feeding and incorporation of the material into the mixing chamber as well as short mixing cycles.

Intermeshing rotors in general also have axial recesses in order to improve flow and to allow higher fill factors. The mixing efficiency of intermeshing rotors is higher compared to tangential rotors due to the enforced formation of thin layers between the rotors. For comparable mixing protocols the total power consumption per unit time is higher and the temperature of the batch is on a lower level thanks to a higher cooling efficiency. [77, 78]

Other important characteristics of rotors in general are the length of the flight and the helix angle, as these parameters influence internal flow and the extent of dispersive mixing. [79] The rotor geometry has a significant influence on the intake behavior: If the intake behavior is insufficient, the rubber compound is pulled into the area between the rotors with a delay. Tangential rotors show a better intake behavior compared to intermeshing rotors. [77] The clearance between the rotor tip and the chamber wall affects the dispersion of the filler: With increasing clearance the relative material flow through this region increases resulting in a faster dispersion and better homogeneity. However, a wider clearance results in a lower stress level at the tip and thus in a lower efficiency of dispersion. [72, 80] Effective mixing not only takes place in the area between the rotor tip and the chamber wall, but also in the rolling pool in front of the rotor flight. The mixing efficiency can be improved by an increase of the volume of material in the rolling pools, thus by introducing more flights. Changing from a two-flight rotor to a four-flight rotor has the additional advantage, that the force-balance on the rotor shaft is better. [36]

2.3.2.2. Fill factor

The capacity of a mixer can be increased by increasing the fill factor within a limited range. As long as the rotor speed is adjusted in order to keep the discharge temperature constant, the quality of the compound is only slightly influenced. At constant rotor speed with consequently increasing discharge temperature the quality improves to a maximum due to reduced stick slip and then deteriorates again: More material is caught in dead zones of the mixer and is entering the mixing process with a delay. The lower limit of the fill factor is determined by the necessity to have sufficient wall contact for cooling. [77, 81, 82] The optimal fill factor increases with increasing ram pressure and decreases with increasing rotor speed. [59]

Typical fill factor values are in the range of 60% to 70%, with extreme values up to 86% for carbon black incorporation into SBR and down to 40% for carbon black-filled NR. [77] Overloading the mixer with more than 10% of the optimal fill factor is counterproductive, as it increases power consumption and mixing time, but does not result in improvements of the batch quality. [82] The optimal fill factor changes

with the viscosity of the compound: Especially during silica mixing, the mixing chamber tends to be underfilled as the viscosity is strongly decreasing due to the silanization reaction. [83, 84]

2.3.2.3. Rotor speed

Increasing the rotor speed is another possibility to improve the compound quality, but with the disadvantage of a higher discharge temperature. A higher rotor speed increases the total shear applied to the compound resulting in a faster and more efficient mixing. [85] The fill factor can be reduced simultaneously in order to keep the discharge temperature constant, without negative influence on the dispersion of the filler. [83, 86] Rotors running at the same speed without friction have the advantage that the homogeneity in temperature and viscosity is better compared to rotors running with friction. [87]

2.3.2.4. Temperature control unit settings

The temperature of the cooling medium influences the temperature profile of the mixing cycle and the final temperature of the compound. However, the influence of the cooling temperature is limited: Change of the cooling temperature in a tangential laboratory mixer results in an under-proportional change in compound temperature. [77] Physical properties such as modulus, tensile strength and elongation at break are all deteriorating with increasing cooling temperature, with a final drastic decrease due to scorch reactions. [82]

2.3.2.5. Ram pressure

An increase in ram pressure results in a shorter mixing cycle, as the incorporation time of the additives, especially the fillers, is reduced. Dispersion and the final quality of the compound are not influenced by ram pressure, as it has no direct influence on the shear stress. However, a higher ram pressure indirectly increases shear stress by decreasing the voids in the material, increasing the contact area between the components and reducing slippage. [34] When the mixer is fully loaded, an increase of the ram pressure results in an increase of the power consumption: Within a limited range, the torque of the rotors is proportional to the ram pressure. Compared to the effect of the variation of the fill factor, rotor speed and mixing time, variation of the ram pressure has a minor influence. [83]

2.4. PROCESSING OF SILICA COMPOUNDS

As the addition of silica to the elastomer results in a strong increase of the viscosity, the filler in general is added in two portions, with the coupling agent added together with the first filler portion. Other additives which can interfere with the silanization reaction should be avoided in this early stage of mixing. Zinc oxide should therefore be added during the final mixing step together with the curing additives. [88]

The temperature window for mixing of silica compounds is rather narrow, limited by the decreasing silanization rate and increasing risk of scorch. High

temperatures improve the silanization rate due to the temperature dependence of the reaction and a reduced sterical hindrance of the silylpropyl group of the coupling agent by increased thermal mobility. [29, 89] The mixing temperature should be in the range of 145°C to 155°C to achieve a good silanization and to avoid pre-crosslinking. Experience shows, that at a discharge temperature of 155°C the primary reaction is completed after approximately 8 minutes, when mixing is done in two separate steps. 3 to 5 steps and a total mixing time of approximately 11 minutes are necessary to fully complete the silanization including the secondary reaction. The reaction rate is increased with increasing concentration of the silane, but finally reaches a plateau: The rate is limited by the reduced amount of accessible silanol groups on the silica surface. [90]

The silica surface is covered by silanol groups, responsible for the strong interparticle forces. Silica particles tend to agglomerate, they are difficult to disperse and re-agglomerate after mixing. [91] One of the effects of re-agglomeration is the reduction of processability during storage: The viscosity of a compound increases during storage, with an increasing rate at higher temperatures. The viscosity increase follows a second order kinetic law, suggesting that the process is based either on coalescence of filler-bound rubber entities or re-agglomeration of filler particles. The tendency of re-agglomeration is influenced by the water content of the silica: A higher water content results in a lower rate of viscosity increase during storage due to a shielding effect of the water molecules on the surface of the silica, which reduces the interparticle forces. [92]

3. SILICA AS A REINFORCING FILLER

3.1. SILICA VERSUS CARBON BLACK

Silica compared to carbon black is characterized by weaker filler-polymer interactions and stronger filler-filler interactions. This results in a higher compound viscosity, a higher modulus at low strain amplitudes, a lower modulus at high strain amplitudes and a lower bound rubber content. [93] However, the combination of silica with a coupling agent has a higher reinforcing effect and different dynamic mechanical properties compared to carbon black. [94] The main influence on the mechanical properties when replacing carbon black by silica combined with a coupling agent is found for:

- o Tear, abrasion and heat resistance
- o Flex stability
- o Hardness, stiffness and modulus
- o Tack
- o Heat build up
- o Resilience

The stronger reinforcing effect of silica compared to carbon black allows the reduction of the filler content without any negative influence on the property profile, but with an additional positive effect on elasticity due to the higher ratio of elastic component to damping filler. This results in an additional reduction of the rolling resistance.

The stability of the covalent silica-polymer network results in a lower rate of breaking and reformation of the silica-polymer bonds compared to the carbon black-polymer network during a deformation cycle, resulting in a decrease of the loss modulus. A low value of the loss modulus together with a high value of the storage modulus results in a low value of the phase angle. As both, loss modulus and storage modulus, depend on deformation, the phase angle is also influenced by the applied strain: It increases with increasing deformation. [91]

3.2. SILICA PROPERTIES AND SURFACE CHARACTERISTICS

The primary filler characteristics influencing elastomer reinforcement are:

o   Surface chemistry, structure and relative surface area
o   Particle size and particle size distribution
o   Structure of the filler aggregates, agglomerates and primary particles

The rubber-filler interface formed during mixing is primarily responsible for the level of properties such as abrasion resistance, tensile strength and tear propagation. The structure of the filler network influences the viscoelastic properties like elasticity, loss modulus and hysteresis.

3.2.1. Surface chemistry

The surface of silica is covered by a layer of acidic silanol groups and different siloxane groups: geminal, vicinal, clustered and isolated groups. [91, 95] The functional groups are randomly distributed over the whole surface, [96] in contrast to carbon black, where the functional groups are preferably located on the edges of the crystallites. The silanol groups on the surface of different silica particles interact with each other, resulting in strong agglomerates due to the hydrogen bonds between the silanol groups. [89, 97] The moieties on the silica surface also interact with basic accelerators, resulting in reduced curing rates and lower crosslink densities. [91, 98, 99] They can react with other chemical compounds such as stearic acid, polyalcohols and amines. These compounds compete with the coupling agent for adsorption sites on the filler surface, reduce the concentration of free surface silanol groups and thus the silanization efficiency. [90]

The silica surface has a tendency to adsorb moisture due to the hydrophilic character of the filler. This adversely influences the curing reaction and hence the properties of the final product. However, a certain moisture content is required for the silanization reaction, as hydrolysis of the ethoxy groups of the coupling agent is a precondition for the secondary reaction to take place. [91, 100-102]

The average size of silica aggregates in a rubber matrix depends on the surface concentration of the silanol groups: A higher number of silanol groups per unit surface area results in an increase of aggregate size, leading to a higher concentration of occluded rubber. [103] The relative surface area has an ambivalent influence on processing and properties of a rubber compound: On one hand it has a negative influence on the processing behavior, as a larger surface area results in a higher compound viscosity, and compound additives like accelerators are inactivated on the filler surface to a higher degree. On the other hand, a higher surface area has a positive influence on filler dispersion. [104]

3.2.2. Surface energy

The energy distribution of the silica surface is inhomogeneous due to the distribution of silanol and siloxane groups and impurities. [105] The surface energy γ_s of fillers is comprised of a dispersive and a specific component, γ_s^d and γ_s^{sp} respectively: [106, 107]

$$\gamma_s = \gamma_s^d + \gamma_s^{sp} \hspace{3cm} Eq. \ 17$$

The dispersive component, based for example on London forces, is responsible for the rubber-filler interaction. [91] This component is rather low in the case of silica, thus resulting in a low reinforcing effect, expressed by very low concentrations of bound rubber and a low modulus at medium and large strain amplitudes. [108] However, polymer chains are entrapped in voids of the silica agglomerates and aggregates: occluded rubber. [97] The dispersive component is influenced by the degree of hydration of the silica: Increasing water contents are reducing the dispersive component even further. [109] The specific component characterizes the interaction between the filler particles, and examples of these forces are dipole-dipole forces, induced dipole forces or hydrogen bonds. The contribution of the specific forces to the surface energy is higher for silica compared to carbon black. [105] The balance of the dispersive and specific surface forces results in the unfavorable situation, that the filler-filler interaction is high and the interaction with the polymer is low for silica, with the consequence, that viscosity as well as Payne effect are high. [108] These effects can be reduced by using coupling agents, silanes for example, together with the silica filler.

The reaction of silica with a silane results in a decrease of the specific component of the surface energy, leading to a decrease of the interaction between the silica particles. [110, 111] This facilitates filler incorporation and dispersion and reduces filler agglomeration. However, it also reduces the filler-polymer interaction, resulting in a reduction of the reinforcing effect. [112, 113] Therefore, the coupling agent contains a rubber-reactive group, which allows the formation of covalent bonds between the polymer and the coupling agent, thus providing a chemical link between silica particles and polymer during curing of the compound. [110, 111]

3.3. THE SILICA-POLYMER INTERACTION

One of the models for the adsorption of polymers on the surface of carbon black is based on the uncoiling of the polymeric chains and multiple adsorption of these chains onto the surface of the filler. The released adsorption enthalpy is partly changing the chain conformation entropy, enabling the chains to abandon their coiled conformation and to take the form of trains. With several contacts per polymer chain the bonding strength of a polymer molecule is in the range of a chemisorptive interaction.

The intensity of wetting of the filler by a polymer depends on the difference of the solubility parameters: [114, 115] The surface concentration of adsorbed trains is inversely proportional to the difference of the solubility-parameters between the polymer and the filler. [116] The solubility parameters for some polymers and fillers are given in Table I. For the silica-polymer system the difference of the solubility parameters is significant, with the effect that the two materials are difficult to blend. When a coupling agent is used, a hydrophobic shell is formed around the filler particle and the solubility parameter of the filler is reduced, the difference in the solubility parameters decreases and the compatibility of the two materials increases.

Table I: Solubility parameters of common compounding ingredients [114]

Material	Hildebrand solubility parameter
FKM, silicones	7-7,5
PE, EPM, EPDM	8
NR, BR,IIR	8-8,5
SBR, low molecular weight resins	8,5-9
CR, CSM, some NBR	9-9,5
Typical lubricants and process aids	8,5-9,5
PVC, ECO, ACM, some NBR	9,5-10
Carbon black	12-15
Clay, whiting, talk	13-14
Silica (untreated)	14-18

3.4. SILICA-SILANE REACTION

The formation of a hydrophobic shell around the silica particle by the silica-silane reaction prevents the formation of a filler-filler network due to the reduction of the specific surface energy. [22] Prior to the chemical reaction of the silane with the silanol groups on the silica surface, the silane molecule has to make contact with the silica surface by adsorption. [117, 118] Then the chemical reaction of silica with an alkoxysilyl moiety of the coupling agent takes place in a two-step, endothermic reaction. [119] The primary step is the reaction of alkoxy groups with silanol groups on the filler surface. [90] Two possible mechanisms are reported: Direct reaction of the silanol groups with the alkoxy groups of the coupling-agent, and hydrolysis of the alkoxy groups followed by a condensation reaction with the silanol groups. [120, 121] The fact, that the rate of silanization is influenced by the moisture content, is an indication that a hydrolysis step is involved. The reaction follows a pseudo-first order kinetic law. [90, 122] Figure 14 shows the mechanism of the primary reaction.
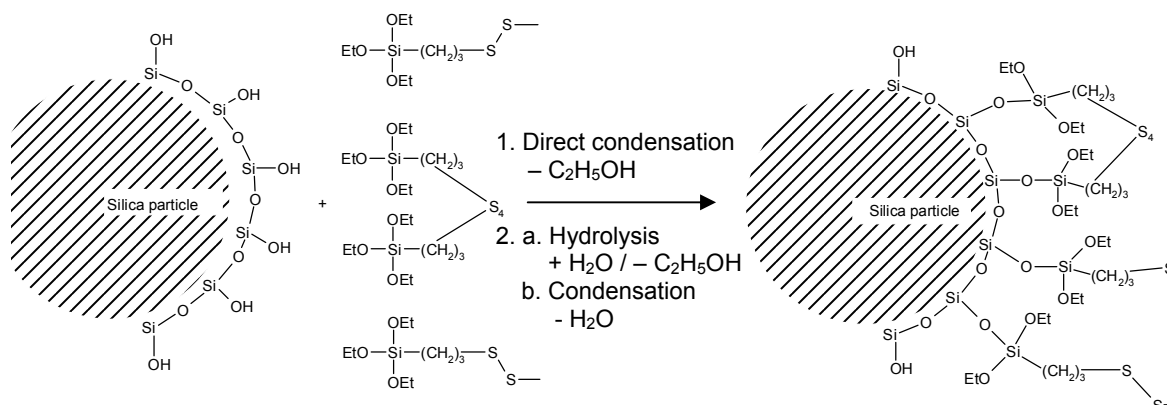
Figure 14: The primary reaction of silica with a silane [110]

The secondary reaction (Figure 15) is a condensation reaction between adjacent molecules of the coupling agent on the filler surface or between alkoxy groups of the coupling agent and silanol groups of the silica. It is generally accepted, that a hydrolysis step is involved in the reaction. In comparison to the primary reaction this step is slower with a factor of approximately 10. The energy of activation for both reactions, the primary and the secondary, is within the range of 30 to 50 kJ/mol. This value is rather low, indicating that the temperature dependence of the reaction rate is not very strong. The rates of both reactions are influenced by the acidity of the matrix, and the reaction is acid as well as alkaline catalyzed. The reaction rate is reduced by steric hindrance and an electron donating effect of the leaving group. [123] Not all ethoxy groups react during the silanization reaction: The reaction results in two silane-silica bonds per silyl group, with one hydrolyzed ethoxy group remaining. [124] But as the secondary reaction has only a slight influence on the properties of the compound, the incomplete reaction does not negatively influence the final quality of the material. [90]
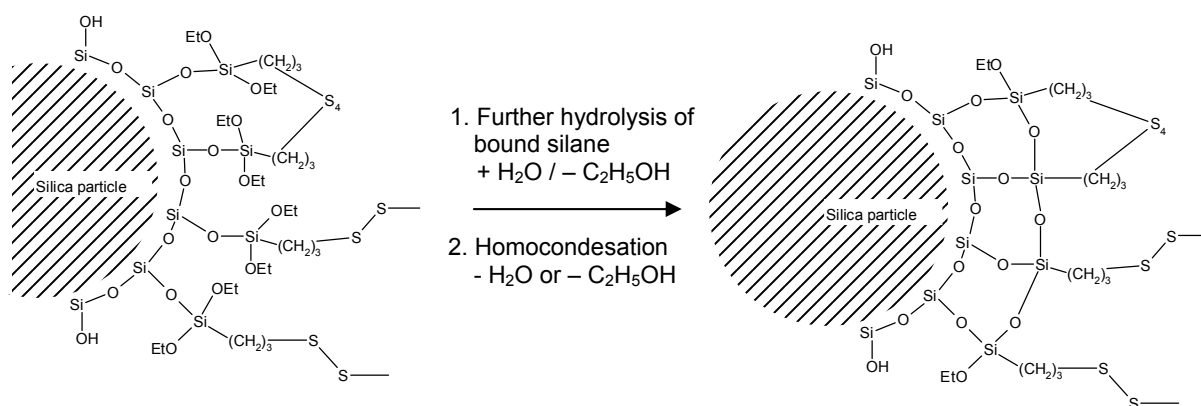
Figure 15: The secondary reaction of silica with a silane

The coupling agents need a moiety enabling them to react with the polymer during vulcanization in order to be reinforcing. This is shown in experiments with coupling agents, which can react with the filler but not with the polymer: The reinforcing effect is reduced, as the formation of bound rubber is impossible. [24, 125] In general, the moiety reacting with the polymer is a sulfur group, either a poly- or disulfidic group or a blocked sulfur group. Other functional groups used to link the coupling agents to the polymer are double bonds, which have to be activated by the addition of an active sulfur-compound or by the generation of a radical moiety in order to have a simultaneous crosslinking of the polymer and the coupling agent with comparable reaction rates during curing.

The polysulfidic moieties of the silanes are unstable, and the cleavage of the sulfur groups results in active sulfur moieties, very probably radicals, which react with the polymer under formation of a filler-silane-polymer bond. [3, 126-128] *Görl et al.* studied the reaction mechanism of the silane-polymer reaction with model compounds, and they propose a mechanism, in which an intermediate polysulfide is formed by the reaction of the silane, which is already bound to the silica, with an accelerator containing a disulfidic moiety. This polysulfide substitutes the allylic hydrogen atom on the polymer chain, and the accelerator part is released. Finally a chemical bond is formed between the polymer chains and the filler. [129-131] Figure 16 shows a general reaction scheme for the formation of the filler-polymer bond:

33
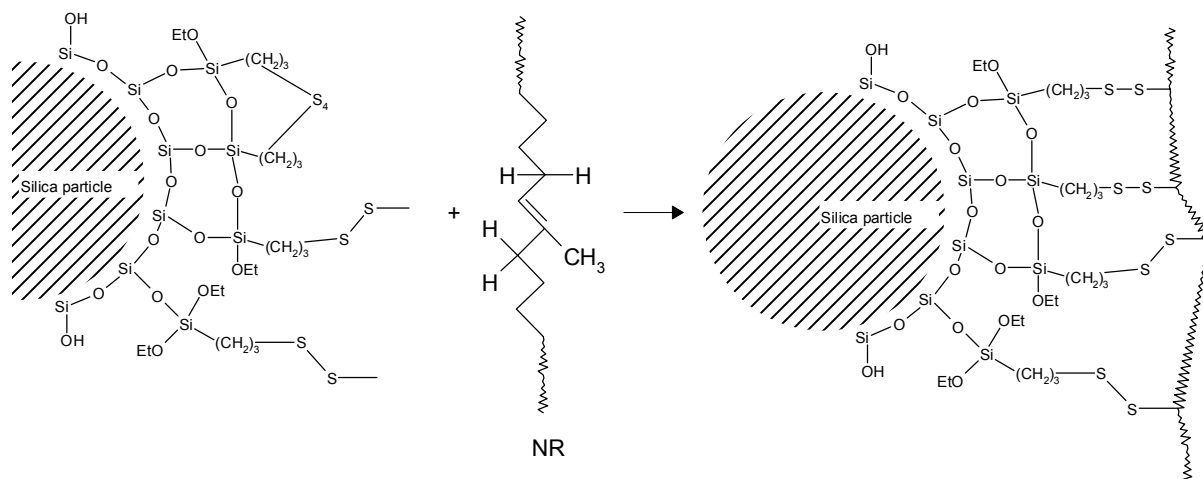
Figure 16: General reaction scheme of a polysulfidic silane with an unsaturated polymer

4. MODELS OF THE POLYMER-FILLER INTERACTIONS

4.1. THE PAYNE EFFECT

The introduction of filler particles such as carbon black or silica into a rubber matrix strongly influences the viscoelastic behavior of the material. One of the phenomena is the Payne effect: When a sinusoidal deformation is applied, the storage modulus decreases until it reaches a constant value, as illustrated in Figure 2. The Payne effect is temperature-dependent: With increasing temperature the difference between the storage modulus at low strains and the modulus at high strains decreases due to the strong reduction of the initial modulus. [132] In the temperature interval between 20°C and 90°C the reduction of the storage modulus at low strain amplitudes is approximately 50%, whereas the storage modulus at high amplitudes remains more or less unchanged with increasing temperature. [15] The difference between the maximum value measured at low strains and the minimum plateau value measured at high strains depends on type and concentration of the filler, elastomer matrix and compound ingredients, which influence the filler-elastomer interaction. [133]

Numerous models have been developed to describe the Payne effect based on hydrodynamic effects, filler-filler interactions, filler-polymer interactions or combinations thereof.

4.1.1. Hydrodynamic effect
The early model of *Guth and Gold* is based on the hydrodynamic interaction of carbon black particles: When a particle is suspended in a fluid in motion, the velocity profile near the particle is disturbed. A second particle, which is placed into the same area, is subjected to an altered flow field.

The modulus of a carbon black filled elastomer matrix can be predicted from the modulus of the unfilled material with due allowance for occluded rubber, as explained in paragraph 1.1.1. At filler loadings higher than 50 phr (parts per hundred rubber) the calculation becomes inaccurate, as the assumption of rigid particles without interaction is no longer valid. Equation 3 is in accordance with measurements on compounds with filler concentrations up to 20 phr and on compounds with higher filler concentrations up to 50 phr when measured at high strain amplitudes. The main shortcomings of this model are, that filler structure and strain dependence are not taken into consideration. [10, 25]

4.1.2. Filler-filler interaction

The model Payne proposed, is based on direct interparticle forces, for example London or van der Waals forces. [125] At very low strain amplitudes the filler-filler contacts are intact and contribute to the modulus of the material, whereas with increasing strain amplitudes the contacts start to break. This process is reversible: The filler tends to re-agglomerate once the strain is released, and this process results in a maximum of the loss modulus as a function of strain amplitude. [133, 134] A strong indication for the existence of such a filler network is the existence of the percolation threshold of carbon black filled rubber compounds. One shortcoming of this model is, that the interparticle forces are too weak to explain the high modulus at low strains. Another shortcoming is the high calculated value of the strain at which the abrupt change in modulus occurs. The strain value predicted from his model is approximately 5% to 8%, compared to values in the range of 0.01% as measured in carbon black-oil systems.

Wang et al. [93, 108, 135] propose different models depending on the affinity of the filler and the polymer. If filler and polymer are highly incompatible, as in the case of silica and a non-polar polymer, the filler particles are in direct contact with each other. In the case of carbon black blended with a non-polar polymer, the filler particles are covered by a polymer shell and the network is formed by a joint shell mechanism. The filler network formed by direct contact between the filler particles is more rigid than the joint-shell network and starts to break at lower strain amplitudes.

A filler-filler network based on attractive van der Waals forces and repulsive Lennard-Jones forces is proposed by *Kraus*. [136] The filler particles act as large multifunctional crosslink sites, which cause non-affine deformation leading to strain amplification. [125] Van der Waals interaction between particles provides a ready mechanism for energy storage; energy loss is the result of frictional forces between the filler particles and the polymer. In this model it is assumed that the filler-filler contacts are periodically broken and reformed under a periodic sinusoidal strain γ. As the strain amplitude is increased, an increasing number of contacts will be broken: The rate of breakage, R_b, is a function of the maximum amplitude of the strain γ_0 and is proportional to the number of contacts N_c:

$$R_b = k_b \gamma_0^m N_c \qquad\qquad Eq. \ 18$$

The constant k_b is the rate constant for the breakage process. The rate of agglomeration R_a is proportional to the number of broken contacts, which is expressed as the difference between the number of elastically active contacts at zero deformation N_0 and the remaining contacts N_c at a given strain γ, and is assumed to vary with γ_0^{-m}:

$$R_a = k_a \gamma_0^{-m} (N_0 - N_c) \qquad Eq.\ 19$$

The constant k_a is the rate constant of the agglomeration process. From these two basic equations, Kraus derived equations describing the storage modulus G' and loss modulus G" of the agglomerate network at any strain amplitude and in equilibrium:

$$\frac{G'-G'_\infty}{G'_0-G'_\infty} = \frac{1}{1+\left(\dfrac{\gamma_0}{\gamma_c}\right)^{2m}} \qquad Eq.\ 20$$

$$\frac{G''-G''_\infty}{G''_0-G''_\infty} = \frac{2\left(\dfrac{\gamma_0}{\gamma_c}\right)^{m}}{1+\left(\dfrac{\gamma_0}{\gamma_c}\right)^{2m}} \qquad Eq.\ 21$$

G'$_\infty$ and G"$_\infty$ are the moduli at high strain amplitudes, and G'$_0$ and G"$_0$ represent the moduli at zero strain. γ_c is the strain half-width amplitude, the strain at which the step of the storage modulus has decreased to half its value at zero strain, and is defined as:

$$\gamma_c = \left(\frac{k_a}{k_b}\right)^{1/2m} \qquad Eq.\ 22$$

γ_c depends on the filler type and concentration and on the type of polymer in the rubber matrix, and the factor m depends on the surface structure of the filler. [137] Combining Equations 20 and 21, an expression for the phase angle can be derived:

$$\tan\delta = \frac{G''_\infty\left[\left(\dfrac{\gamma_0}{\gamma_c}\right)^{m/2} - \left(\dfrac{\gamma_0}{\gamma_c}\right)^{-m/2}\right]^2 + 2G''_0}{G'_\infty\left(\dfrac{\gamma_0}{\gamma_c}\right)^{m} + G'_0\left(\dfrac{\gamma_0}{\gamma_c}\right)^{-m}} \qquad Eq.\ 23$$

These results are in good agreement with the experimental data published by Payne. However, this model is not able to predict the values of the very high and

very low strain moduli, neither the influence of frequency, temperature, filler concentration and dispersion.

Extensions of this model are published by *Klüppel et al.* [137] Their models are based either on the percolation or on the kinetic cluster-cluster aggregation theory. Both models take the fractal characteristics of the filler-filler network into consideration, and the elastic modulus of the material is a function of the dimensions of the fractal unit cells, the number of primary particles in the backbone of the unit cells and the elastic modulus of the filler particles.

Huber and Vilgis [133, 138] investigated the influence of the disordered filler structure on the reinforcement of elastomers. In their model the filler network has a fractal structure and is based on clusters of filler particles. The energy-elastic contribution of the rigid filler network prevails at small strains, whereas at large strain the hydrodynamic effect and the filler-polymer interaction prevail.

4.1.3.   Filler-filler and filler-polymer interaction
A combination of filler aggregates and occluded rubber is the basis of the model developed by *Medalia.* [25, 139] According to his model the dynamic properties of reinforced rubber are strongly influenced by the amount of immobilized polymer chains. A portion of the polymer is trapped within the voids of the filler agglomerates and aggregates and thereby shielded from deformation. Under increasing stress application, the filler aggregates break and entrapped rubber is successively released.

Drozdov and Dorfmann [140] developed a model of two interpenetrating networks: one comprises semiflexible polymer chains connected to temporary nodes, whereas the second network is formed by filler aggregates and agglomerates. The polymer chains connected to the network nodes are in equilibrium of breakage and reformation, and the kinetics of this process is comparable to the kinetic of ad- and desorption processes. The filler-filler network is not fully developed at low filler concentrations, changes in the viscoelastic response are associated with transformations occurring in the surface layers around the filler particles and aggregates. At higher filler concentrations a network is formed and interactions between the filler network and the matrix are dominant.

Gerspacher [141, 142] states that the filler-filler network is contributing to energy dissipation by de- and re-agglomeration. At low strains, below 10%, the carbon black network is destroyed, whereas the polymer network stores energy. When the strain is released, the filler-filler network is re-established with energetic input from the polymer network. At high strains two dissipative processes are assumed to take place: The above-described re-agglomeration of the filler particles under formation of a network, and a second process of successive formation of sub-networks, whose size is dependent on the applied strain and the filler morphology. The sub-networks are trapped within the polymer network, which is the deformation and energy carrier.

Freund and Niedermeier [143] did a comparative study of carbon black and silica in a polar as well as a non-polar elastomer matrix. They investigated the Payne effect of these materials in order to elucidate the prevailing mechanism: filler networking or polymer adsorption. Their conclusion is, that in carbon black filled compounds adsorption is prevailing and in silica filled compounds filler networking is dominant.

Wagner et al. [144] emphasize the contribution of entanglements between bound rubber and the polymer chains in the rubber matrix in the transition zone between the filler surface and the polymer matrix. *Funt* further refined this model by including filler-polymer interactions: The polymer chains are adsorbed onto the filler surface, resulting in a secondary network. This bound rubber has a reduced mobility and influences the dynamic properties of the material. Two mechanisms of reinforcement are proposed: Hydrodynamic interactions, which dominate at high strains, and chain entanglements in a transition zone between immobilized bound rubber on the filler surface and mobile rubber chains in the matrix. [125]

Maier and Göritz [145] assume an adsorption kinetic of the polymer chains onto the surface of carbon black according to the Langmuir model: They assume an energetic homogenous surface with a monomolecular coverage of polymer chain segments, which do not interact with each other. The network density increases in the proximity of the filler surface due to the adsorption-desorption equilibrium. They further assume a distribution of the bonding strength as a function of the number of adsorbed segments per polymer chain, and define stable and unstable bonds. The first polymer molecules to be adsorbed onto the filler surface during a mixing process are strongly bound: After the first contact with the filler surface, adjacent polymer chain segments attach to neighboring positions, resulting in a multiple bonding of the molecule to the filler surface. Polymer molecules, which are adsorbed on a later stage, will be adsorbed on single free adsorption sites, resulting in a weak bond. The adsorption rate is assumed to be constant, and the adsorption energy is in the range of adsorption energies of van der Waals forces. The desorption rate of unstable links depends on the strain amplitude γ. With increasing amplitude of deformation mainly rupture of unstable van der Waals bonds occurs, and the network density is reduced resulting in a decrease of the modulus. In equilibrium, adsorption and desorption rate are equal, and the density of unstable bonds $D_{N,U}(\gamma)$ at a given strain amplitude γ can be calculated from the density of unstable bonds at zero strain $D^0_{N,U}$:

$$D_{N,U}(\gamma) = \frac{D^0_{N,U}}{1+c\gamma} \qquad\qquad \textit{Eq. 24}$$

The constant c is a factor summarizing the kinetic constants of adsorption and desorption.

The quantitative description of the storage modulus G' is based on entropy elasticity and is a function of network density D_N and the absolute temperature T:

$$G' = D_N \cdot k_B \cdot T \qquad\qquad \textit{Eq. 25}$$

The factor k_B is the Boltzmann constant. Three network contributions are distinguished: a chemical network formed by stable bonds with the density $D_{N,C}$, a stable physical network formed by multiple adsorption with the density $D_{N,S}$ and an unstable physical network formed by single adsorption with the density $D_{N,U}$:

$$D_N = D_{N,C} + D_{N,S} + D_{N,U} \qquad\qquad \textit{Eq. 26}$$

$$G'(\gamma) = \left(D_{N,C} + D_{N,S} + D_{N,U}(\gamma)\right)k_B T \qquad\qquad \textit{Eq. 27}$$

The combination of Equation 24 and Equation 27 results in an expression for the storage modulus as a function of the strain amplitude:

$$G'(\gamma) = \left(D_{N,C} + D_{N,S} + \frac{D_{N,U}^0}{1+c\gamma} \right) k_B T \qquad\qquad \textit{Eq. 28}$$

This model correctly predicts the non-linear behavior of the storage and loss modulus, but it is not accurate enough to quantify the strain, temperature or frequency dependence of the modulus. [133]

Gauthier et al. [146] propose a model, in which filler particles are linked by an adsorbed layer of polymer. They distinguish two areas in a filled rubber matrix: areas of non-reinforced material and highly reinforced areas. In the reinforced areas the filler particles are linked by bound rubber. The morphology of this system is described by a three step repetition: Firstly, the effective modulus of the rubber matrix including bound rubber and occluded rubber is calculated. Secondly, the matrix is considered to be homogenous having a modulus as calculated in the first step, with highly reinforced zones embedded into this matrix containing filler, bound rubber and occluded rubber. Last, the effective modulus of the actual composite is calculated.

4.2. INTERACTION OF CARBON BLACK WITH A POLYMER

In well mixed compounds, the final structure of carbon black aggregates in rubber is a grapelike arrangement of spherical carbon black particles fused together. Three different regions around the aggregates are distinguished: [147]

o *Region 1*: A thin, tightly bound layer of polymer is connected to the filler surface. This surface layer is rigid and behaves like the filler particle itself.

o *Region 2*: A shell of loosely bound rubber, eventually forming connective filaments between filler aggregates. The material in this region is flexible and can undergo large deformations.

○ *Region 3*: The polymer does not interact with the filler and is mobile.

At higher filler concentrations, a three-dimensional network of bound rubber–filler particle units connected by soft polymer units is formed. [148] The aggregates have a diameter of approximately 50 to 100 nanometers, and the surrounding loosely bound rubber shell has a thickness of 3-6 nm. [148]

The shell of strongly bound polymer chains has a very high modulus, and the concentration of carbon black in this shell is estimated to be approximately 200 phr. Polymer chains are randomly attached to the filler particles, independent of their molecular weight. However, during storage longer polymer chains are favorably attached to the filler surface. [107] The connection between this bound rubber shell and the surrounding rubber matrix is established by entanglements. [149] Due to the immobilization, this shell does not incorporate curing agents during the productive mixing step: a composite of a polymer system and a carbon black system with different properties is formed. [24, 150-159]

The volume of the immobilized rubber directly influences the dynamic properties. The influence of carbon black particles covered by a shell of immobilized rubber on the Young's modulus E can be calculated using the Guth-Gold equation [8] with a correction for occluded rubber (see also Equation 3): [160]

$$E_f / E_0 = 1 + 2.5\phi' + 14.1(\phi')^2 \qquad\qquad \textit{Eq. 29}$$

ϕ' is the effective volume fraction of the filler including the immobilized fraction of the polymer. This correlation between the Young's modulus of the reinforced material, E_f, and the gum vulcanizate, E_0, holds for equilibrium conditions and conditions near equilibrium such as low strains and low rates of strains. [160] A forth factor taking the filler properties into consideration was proposed by *Tan et al*. [93]:

$$E_f = E_0(1 + 2.5\phi' + 14.1\phi'^2) + a_m(\phi - \phi_{crit})^{a_s} \qquad \textit{Eq. 30}$$

The constants a_m and a_s represent the filler morphology and the surface characteristics, respectively. ϕ_{crit} is the critical filler volume fraction, which is defined as the volume fraction limiting the validity of the Guth-Gold equation, and ϕ is the actual filler volume fraction in the compound. Rubber molecules bound to the surface of filler particles are not fully immobilized over the whole chain length, thus only a part of the occluded rubber is effective in contributing to the relative modulus described in Equations 29 and 30. This effect is taken into consideration by the occluded volume effectiveness factor F_o, which represents the ratio of the effective volume of the occluded rubber calculated from its contribution to the modulus and the actual volume of occluded rubber calculated from DBP absorption. The values for the effectiveness factor for temperatures above room temperature and equilibrium are close to 0.5, showing that approximately half of the occluded rubber is immobilized. This part forms a hard, undeformable shell

and is effective in increasing the modulus. Physically, the shell of occluded rubber presents a continuum: in poorly shielded regions the deformation is comparable to the deformation of the matrix, whereas in well-shielded regions close to the filler surface no deformation takes place. The modulus of the shell then varies continuously from the shell-matrix boundary to the shell-filler boundary. [160] A more simplified model of the shell is made under the assumption, that the shell is homogenous over its thickness and has an average modulus with a value between the modulus of the filler and the modulus of the matrix. [161, 162] At higher temperatures, the factor F_0 exponentially decreases. [160] This is explained with a molecular slippage mechanism: If the rubber molecules are not chemically or physically bound to the filler surface, they are able to slip over the surface of the filler particles releasing the applied stress. This effect will be more pronounced at higher temperatures. [163]

4.3. INTERACTION OF SILICA WITH A POLYMER

Strauß et al. [164] developed a model for the silica-polymer interaction based on adsorption. They derived the modulus G_f of a filled rubber matrix in quasi-permanent contact with the filler particles in a swollen vulcanizate from the Einstein-Smallwood equation:

$$G_f = G_0 \left(1 + C_{ES} \cdot \phi\right)$$

Eq. 31

G_o is the modulus of the matrix without filler particles and ϕ is the volume fraction of the filler. C_{ES} is the Einstein-Smallwood parameter, which depends only on the shape of the filler particles and for these systems generally is equal to 2.5 (see paragraph 1.1.1. and 4.2.). They differentiate three areas in the compound: the rubber matrix, the rigid filler particles and a shell of one monolayer of polymer around the particles, in which the polymer molecules make contact with the filler. This effectively increases the crosslink density of the system and reduces the effective length of the polymer chains according to:

$$y_{p,f} = \frac{y_p}{1 + C_{ES} \cdot \phi}$$

Eq. 32

y_p is the average number of strain-invariant units of the polymer between the crosslinks, and determines the mean size of the free polymer segments. $y_{p,f}$ is the reduced average size of polymer segments in a filled compound under consideration of the filler-polymer contacts. A comparable relationship is found for the maximum uniaxial strain that can be applied to a single chain, λ_m:

$$\lambda_{m,f}^2 = \frac{\lambda_m^2}{1 + C_{ES} \cdot \phi}$$

Eq. 33

$\lambda_{m,f}$ is the reduced strain in the polymer-filler system under consideration of polymer-polymer and filler-polymer bridges. This model is based on the following assumptions:

o   Energy-equivalence of the chains in the network
o   Quasi-permanent polymer-filler contacts
o   Slipping of the adhesional contacts on extension
o   Strain-independent contact density
o   Equilibrium of adsorption and desorption, constant density of contact elements

The validity of this model was verified by swelling experiments. The silica was fully silanized with a monofunctional saturated oligomeric silane, prohibiting direct filler-matrix interactions. The degree of swelling of this compound was found to be equal to the swelling of an unfilled compound. This phenomenon is explained with an equilibrium Langmuir-adsorption of the silane onto the filler surface. The adsorption isotherm of this system can be described by the following equation:

$$\Gamma = \Gamma_0 \frac{c_L}{c_L + (b_{ad/de}/RT)}$$

Eq. 34

The surface concentration of the adsorbent Γ is proportional to the concentration of a monolayer of the adsorbent Γ_0, with the proportionality factor depending on the concentration of the absorbed molecules in the matrix c_L, the ratio of adsorption to desorption $b_{ad/de}$ and the temperature T. For a partly covered surface the following assumptions are made:

o   Energetically equal adsorption sites on the silica surface
o   Adsorption of a monolayer
o   Equivalent filler particles
o   Average concentration of occupied sites equal for all particles
o   Silane molecules randomly anchored to the filler particles
o   No lateral interaction between the silane molecules
o   Polymer segments in contact with adsorption sites not occupied by silane molecules

An increase of the surface concentration of the silane results in a reduction of the filler-polymer contacts by a factor ξ, and the Einstein Smallwood relationship becomes:

$$G_f = G_o(1 + \xi \cdot C_{ES} \cdot \phi)$$

Eq. 35

The factor ξ is defined as follows:

$$\xi = 1 - \frac{\Gamma}{\Gamma_0} = \frac{b_{ad/de}}{c_L + b_{ad/de}}$$

Eq. 36

The adsorption kinetics of octyltrimethoxy-silane on glass fibers were investigated by *Eklund et al.* [165] For low surface concentrations of the silane they confirmed that the kinetics can be described according to a Langmuir law. However, the model failed for higher surface concentrations, as a plateau value corresponding to a monolayer was not reached. The adsorption was more accurately described by a Freundlich isotherm, in which the adsorption enthalpy depends exponentially on the degree of surface coverage and the adsorption is not limited to a monolayer.

5. STARTING POINT AND FOCUS OF THE PROJECT

The replacement of carbon black by silica in rubber compounds has its advantages in terms of material properties: Improved mechanical and dynamic properties due to a strong, covalent filler-polymer network formed during mixing and vulcanization. However, processing of these compounds is still a difficult challenge due to:

o Agglomeration of the filler by strong interparticle forces resulting in a poor dispersion of the aggregates

o Poor interaction between the filler and the polymer requiring a coupling agent, which connects the filler to the polymer

o High initial viscosity of the filler-polymer blend and strong decrease of viscosity during mixing

o Reaction of the filler with the coupling agent during the mixing cycle and in a mixer, which is not specially designed for a chemical reaction

o Compound devolatilization of the silanization by-product ethanol and removal of the alcohol out of the mixing chamber

o Reduction of the mixing efficiency by condensation of ethanol in the mixing chamber

o Increased scorch sensitivity due to the commonly used sulfur containing coupling agents

o Narrow operational temperature window limited by the decrease of the silanization rate at low temperatures and the scorch risk at higher temperatures

The commonly used mixing technology is optimized for blending of elastomers with carbon black as filler and can not easily be adjusted to the requirements of silica compounds, neither is the installation of new, specially designed mixers an

option due to the high investment costs. In actual practice, the mixing protocol in general is adjusted in order to guarantee a good dispersion and silanization of the filler, but at the expense of mixing capacity: The compounds are mixed in several steps in order to limit the temperature load. This procedure delivers compounds of a good quality, but reduces the capacity and increases the costs of the material.

This brief summary reflects the situation concerning silica mixing: The rubber processor faces a number of problems when processing silica compounds, but there is a lack of appropriate solutions. Research and development activities focused on processing improvements of silica compounds are few, leaving mainly empirical approaches to solve the problems.

The scope of this project is to provide solutions for the improvement of the mixing process of silica compounds based on existing technology: The commonly used mixing equipment shall be adjusted in order to increase the mixing capacity by a more efficient silanization. The first part of the study is dedicated to an evaluation of existing mixing technology in terms of suitability for the mixing process as well as for the chemical silanization reaction. The second part of the study is focused on the development and implementation of mixer adjustments, which increase the silanization rate by improving the devolatilization of the compound. In the third part, the most promising measures are scaled up and their efficiency is verified on production scale, including tire building using these materials and their testing.

6. REFERENCES

1. Leblanc, J.L., Prog. Trends Rheol., 1988. **II**: p. 32.
2. Mushack, R., Lüttich, R., Bachmann, W., Eur. Rubber J. **July/August 1996**: p. 24.
3. Dannenberg, E.M., Rubber Chem. Technol., 1975. **48**: p. 410.
4. Payne, A.R., Rubber Plast. Age. **August 1961**: p. 963.
5. Donnet, J.B., Rubber Chem. Technol., 1998. **71**: p. 323.
6. Einstein, A., Ann. der Physik, 1906. **19**: p. 289.
7. Einstein, A., Ann. der Physik, 1911. **34**: p. 591.
8. Guth, E., Gold, O., Phys. Rev., 1938. **53**: p. 322.
9. Smallwood, H.M., J. Appl. Phys., 1944. **15**: p. 758.
10. Guth, E., J. Appl. Mech., 1945. **16**: p. 20.
11. Brennan, J.J., Jermyn, T.E., J. Appl. Polym. Sci., 1965. **9**: p. 2749.
12. Boonstra, B.B., Medalia, A.I., Rubber Chem. Technol., 1963. **36**: p. 115.
13. Medalia, A.I., Rubber Chem. Technol., 1974. **47**: p. 411.
14. Medalia, A.I., Rubber Chem. Technol., 1978. **51**: p. 437.
15. Payne, A.R., Whittaker, R.E., Rubber Chem. Technol., 1971. **44**: p. 440.
16. Wolff, S., Goerl, U., Wang, M.-J., Wolff, W., Eur. Rubber J., January 1994: p. 16.
17. Payne, A.R., J. Appl. Polym. Sci., 1963. **7**: p. 873.
18. Hall, D.E., Moreland, J.C. in *Am. Chem. Soc. Rubber Div. conference*. April 4-6, 2000. Dallas, Texas.
19. Yanovsky, Y.G., Zaikov, G.E., in *Encyclopedia of fluid mechanics*. 1990, Gulf Publishing Company: Houston.
20. Ferry, J.D., in *Viscoelastic properties of polymers*. 1980, John Wiley & Sons: New York.
21. Nordsiek, K.H., Kautsch. Gummi Kunstst., 1985. **38**: p. 178.
22. Wang, M.-J., Rubber Chem. Technol., 1997. **71**: p. 520.
23. Heinrich, G., Kautsch. Gummi Kunstst., 1992. **45**: p. 173.
24. ten Brinke, J.W., in *Thesis: Silica reinforced tyre rubbers*. 2002, Dept. Rubber Technol., Univ. Twente: Enschede (the Netherlands).
25. Medalia, A.I., Rubber Chem. Technol., 1973. **46**: p. 877.
26. Wang, M.-J., Rubber Chem. Technol., 1998. **71**: p. 520.
27. Johnson, P.S., Elastomerics. **January 1983**: p. 9.
28. Chohan, R.K., David, B., Nir, A., Tadmor, Z., Int. Polym. Pro., 1987. **2**(1): p. 13.
29. Reuvekamp, L.A.E.M., *Reactive mixing of silica and rubber for tyres and engine mounts*, in *Thesis: Reactive mixing of silica and rubber for tyres and engine mounts*. 2003, Dept. Rubber Technol., Univ. Twente: Enschede (the Netherlands).
30. Li, Y., Wang, M.J., Zhang, T., Zhang, F., Fu, X., Rubber Chem. Technol., 1994. **67**: p. 693.
31. Yoshida, T., Int. Polym. Sci. Technol., 1993. **20**(6): p. 29.
32. Leblanc, J.L., Kautsch. Gummi Kunstst., 2001. **54**(6): p. 327.
33. Nakajima, N., Rubber Chem. Technol., 1980. **53**: p. 1088.
34. Palmgren, H., Rubber Chem. Technol., 1975. **48**: p. 462.
35. Tokita, N., Pliskin, T., Rubber Chem. Technol., 1973. **46**: p. 1166.
36. Nakajima, N. *Energy measures of efficient mixing*. in *Proceedings ACS Rubber Division Conf., October 8-11, 1981*. Detroit, Michigan.
37. Nakajima, N., Harrell, E.R., Seil, D.A. *Energy balance and heat transfer in mixing of elastomer compounds with the internal mixer*. in *Proceedings ACS Rubber Division Conf., October 8-11, 1981*. Detroit, Michigan.
38. Jentsch, J., Michael, H., Flohrer, J., Plaste Kautsch., 1983. **30**(4): p. 216.
39. Dizon, E.S., Micek, E.J., Scott, C.E., J. Elast. Plast., 1976. **8**: p. 414.
40. Dizon, E.S., Rubber Chem. Technol., 1976. **49**: p. 12.
41. Vostroknitov, E.G., Badenkov, P.F., Novikov, M. I., Prozorovskaya, N.V., Reztsova, E.V., Sov. Rubber Technol., 1971. **30**(3): p. 11.
42. Clarke, J., Freakley, P.K., Rubber Chem. Technol., 1994. **67**: p. 700.
43. Nakajima, N., Harrell, E.R., Rubber Chem. Technol., 1984. **57**: p. 153.
44. Manas-Zloczower, I., in *Mixing and compounding of polymers*, I. Manas-Zloczower, Tadmor, Z., Editor. 1994, Hanser: Cincinnati (USA). p. 55.
45. Rumpf, H., W.A. Knepper, Editor. 1962, Wiley-Interscience: New York.
46. Cheng, D.C.-H., Proc. Soc. Anal. Chem., 1973. **10**: p. 17.
47. Cheng, D.C.-H., Farley, R., Valentin, F.H.H., Inst. Chem. Eng. Symp. Ser., 1968. **29**: p. 14.
48. Hartley, P.A., Parfitt, G.D., Langmuir, 1985. **1**: p. 651.

49.   Sonntag, R.C., Russel, W.B., Coll. Interf. Sci., 1987. **115**: p. 378.
50.   Kendall, K., Powder Metall., 1988. **31**: p. 28.
51.   Nir, A., Acrivos, A., J. Fluid Mech., 1973. **59**: p. 209.
52.   Bagster, D.F., Tomi, D., Chem. Eng. Sci., 1974. **29**: p. 1773.
53.   Adler, P.M., Mills, P.M., J. Rheol., 1979. **23**(1): p. 519.
54.   Manas-Zloczower, I., Feke, D.L., Int. Polym. Process. J., 1989. **IV**(1): p. 3.
55.   Manas-Zloczower, I., Nir, A., Tadmor, Z., Rubber Chem. Technol., 1982. **55**: p. 1250.
56.   Manas-Zloczower, I., Nir, A., Tadmor, Z., Polym. Compos., 1985. **6**(4): p. 222.
57.   Rwei, S.P., Manas-Zloczower, I., Polym. Eng. Sci., 1990. **30**(11): p. 701.
58.   Rwei, S.P., Manas-Zloczower, I., Polym. Eng. Sci., 1991. **31**(8): p. 558.
59.   Cotton, G.R., Rubber Chem. Technol., 1984. **57**: p. 118.
60.   Shiga, S., Furuta, M., Rubber Chem. Technol., 1985. **58**: p. 1.
61.   Shiga, S., Furuta, M., Nippon Gomu Kyokaishi, 1982. **55**: p. 491.
62.   Clarke, H.J., Freakley, P.K., Plast. Rubber Compos. Proc., 1995. **24**(5): p. 261.
63.   Leblanc, J.L., Prog. Trends Rheol., 1988. **II**: p. 32-43.
64.   Manas-Zloczower, I., Cheng, H., Macromol. Symp., 1996. **112**: p. 77.
65.   Manas-Zloczower, I., Tadmor, Z., Rubber Chem. Technol., 1984. **57**: p. 48.
66.   Manas-Zloczower, I., Rubber Chem. Technol., 1994. **67**: p. 504.
67.   Manas-Zloczower, I., Tadmor, Z. *Dynamics of agglomerate size distribution in linear shear flow fields*. in *Polym. Pro. Soc., 3d meeting*. 1987. Stuttgart (Germany).
68.   Scurati, A., Manas-Zloczower, I., Feke, D.L., Rubber Chem. Technol., 2002. **75**: p. 726.
69.   Freakley, P.K., Wan Idris, W.Y., Rubber Chem. Technol., 1979. **52**: p. 134.
70.   Freakley, P.K., Patel, S.R., Rubber Chem. Technol., 1985. **58**: p. 751.
71.   McKelvey, J.M., in *Polymer processing*. 1962, Textile Book: New York, ch. 12.
72.   Funt, J.M., *Mixing of rubbers*. 1977, Rubber and Plastics Research Association of Great Britain: Shawbury (Great Britain).
73.   Tadmor, Z., Gogos, C.G., *Principles of polymer processing*. 1979, Wiley Interscience: New York.
74.   Tokita, N., Pliskin, T., Rubber Chem. Technol., 173. **46**: p. 1166.
75.   Cotton, G.R., Kautsch. Gummi Kunstst., 1985. **38**(8): p. 705.
76.   Turetzky, S.B., van Buskirk, P.R., Gunberg, P.F., Rubber Chem. Technol., 1976. **49**: p. 1.
77.   Wiedmann, W.M., Schmid, H.M., Rubber Chem. Technol., 1982. **55**: p. 363.
78.   Noordermeer, J.W.M., Wilms, M.M., in *Handbook of applied polymer processing technology*, N.P. Cheremisinoff, Cheremisinoff, P.N., Editor. 1996, Marcel Dekker: New York. p. 549.
79.   Melotto, M.A., in *The mixing of rubber*, R.F. Grossman, Editor. 1997, Chapman & Hall: London. p. 1.
80.   Inoue, K., Hashizume, S., Fukui, T., Asai, T., Kobe Steel Eng. Rep., 1982. **32**: p. 77.
81.   Wiedmann, W.M., Schmid, H.M., Koch, H. *Rheologisch-thermisches Verhalten von Gummiknetern*. in *Int. Kautschuk-Tagung*. 1980. Berlin, Germany.
82.   Dolezal, P.T., Johnson, P.S., Rubber Chem. Technol., 1980. **53**: p. 251.
83.   Schmid, H.-M., Kautsch. Gummi Kunstst., 1982. **35**(8): p. 674.
84.   Berkemeier, D., Haeder, W., Rinker, M., Rubber World. **July 2001**: p. 34.
85.   Johnson, P.S., Elastomerics, 1983(January): p. 9-16.
86.   O'Connor, G.E., Putman, J.B., Rubber Chem. Technol., 1978. **51**: p. 799.
87.   Inoue, K., in *Mixing and compounding of polymers*, I. Manas-Zloczower, Tadmor, Z., Editor. 1994, Hanser: Cincinnati (USA). p. 619.
88.   Reuvekamp, L.A.E.M., ten Brinke, J.W., van Swaaij, P.J., Noordermeer, J.W.M., Rubber Chem. Technol., 2004. **77**(1): p. 34.
89.   Patkar, S.D., Evans, L.R., Waddel, W.H., Rubber Plast. News. **September 1997**: p. 237.
90.   Luginsland, H.-D. *Processing of the organo silane Si 69*. in *11. SRC conference*. 1999. Puchov, Poland.
91.   Wolff, S., Goerl, U., Wang,M.-J., Wolff, S., Eur. Rubber J., 1994. **16**(January 1994): p. 16-19.
92.   Schaal, S., Coran, A.Y., Mowdood, S.K., Rubber Chem. Technol., 2001. **73**: p. 240.
93.   Wolff, S., Wang, M.-J., Tan, E.-H., Kautsch. Gummi Kunstst., 1994. **47**(2): p. 102.
94.   Okel, T.A., Patkar, S.D., Bice, J.-A.E., Prog. Rubber Plast. Technol., 1999. **15**(1): p. 1.
95.   Hair, M.L., Hertl, W., J. Phys. Chem., 1970. **74**(1): p. 91.
96.   Wang, M.-J., Wolff, S., Kautsch. Gummi Kunstst., 1992. **45**(1): p. 11.
97.   Yatsuyanagi, F., Suzuki, N., Ito, M., Kaidou, H., Polym. J., 2002. **34**(5): p. 332.

98.   Wolff, S., Rubber Chem. Technol., 1996. **69**: p. 325.
99.   Kataoka, T., Zetterlund, B., Yamada, B., Plast. Rubber Comp., 2003. **32**(7): p. 291.
100.   Hockley, J.A., Pethica, B.A., Trans. Faraday Soc., 1961. **57**: p. 2247.
101.   Bassett, D.R.E., Boucher, A., Zettlemoyer, A.C., J. Coll. Interf. Sci., 1968. **27**: p. 649.
102.   Ansarifar, A., Azhar, A., Song, M., J. Rubber Res., 2003. **6**(3): p. 129.
103.   Sawanobori, J., Ono, S., Ito, M., Kobunshi Ronbunshu, 2000. **57**: p. 356.
104.   Blume, A. *Analytical properties of silica - a key for understanding silica reinforcement*. in *Am. Chem. Soc. Rubber Div. conference*. 1999. Chicago, Illinois.
105.   Wang, M.J., Wolff, S., Rubber Chem. Technol., 1992. **65**: p. 715.
106.   Vidal, A., Haidar, B., Die Angewandte Makromolekulare Chemie, 1992. **202/203**: p. 133.
107.   Leblanc, J.L., Prog. Polym Sci., 2002. **2**: p. 627.
108.   Wolff, S., Wang, M.-J., Rubber Chem. Technol., 1992. **65**(2): p. 329.
109.   Wolff, S., Wang, M.-J., Rubber Chem. Technol., 1991. **64**(4): p. 559.
110.   Hunsche, A., Görl, U., Mueller, A., Knaack, M., Goebel, Th., Kautsch. Gummi Kunstst., 1997. **50**(12): p. 881.
111.   Görl, U., Hunsche, A., Mueller, A., Koban, H.G., Rubber Chem. Technol., 1997. **70**: p. 608.
112.   Parent, J.S., Mrkoci, M.I., Hennigar, S.L., Plast. Rubber Comp., 2003. **32**(3): p. 114.
113.   Ray, S., Bhowmick, A.K., Bandyopadhyay, S., Rubber Chem. Technol., 2003. **76**: p. 1092.
114.   Grossman, R.F., in *The mixing of rubber*, R.F. Grossman, Editor. 1997, Chapman & Hall: London. p. 25.
115.   Schuster, R.H. *Selective interactions in elastomers, a base for compatibility and polymer-filler interaction*. in *Am. Chem. Soc. Rubber Div. conference*. October 1995. Cleveland, Ohio.
116.   Schuster, R.H., Int. Polym. Sci. Technol., 1996. **23**(11): p. 9.
117.   Matisons, J.G., Jokinen, A.E., Rosenholm, J.B., J. Coll. Interf. Sci., 1997. **194**: p. 263.
118.   Burneau, A., Gallas, J.-P., in *The surface properties of silicas*, A.P. Legrand, Editor. 1988, John Wiley & Sons: Chicester (Great Britain).
119.   Nakajima, N., Shieh, W.J., Wang, Z.G., Int. Polym. Pro., 1991. **VI**: p. 4.
120.   Sindorf, D.W., Marciel, G.E., J. Phys. Chem., 1982. **86**: p. 5208.
121.   Sindorf, D.W., Marciel, G.E., J. Am. Chem. Soc., 1983. **86**(105): p. 3736.
122.   Hunsche, A., Görl, U., Koban, H.G., Lehmann, Th., Kautsch. Gummi Kunstst., 1998. **51**(7-8): p. 525.
123.   Pohl, E.R., Chaves, A., Danehey, C.T., Sussman, A., Benett, V., in *Silanes and other coupling agents*, K.L. Mittal, Editor. 2000, VSP: Utrecht (the Netherlands).
124.   Marrone, M., Montanari, T., Busca, G., Conzatti, I., Costa, G., Castellano, M., Turturro, A., J. Phys. Chem. B, 2004. **108**: p. 3563.
125.   Funt, J.M., Rubber Chem. Technol., 1987. **61**: p. 842.
126.   Cruse, R.W., Hofstetter, M.H., Panzer, L.M., Pickwell, R.J., Rubber Plast. News, 1997: p. 14.
127.   Datta, R.N., Das, P.K., Mandal, S.K., Basu, D.K., Kautsch. Gummi Kunstst., 1988. **41**: p. 157.
128.   Debnath, S.C., Datta, R.N.; Noordermeer, J.W.M., Rubber Chem. Technol., 2003. **76**(5): p. 1311.
129.   Görl, U., Parkhouse, A., Kautsch. Gummi Kunstst., 1999. **52**: p. 493.
130.   Hasse, A., Klockmann, O., Wehmeier, A., Luginsland, H.D. in *Am. Chem. Soc. Rubber Div. conference*. October 16-19, 2001. Cleveland, Ohio.
131.   Luginsland, H.D., Fröhlich, J., Wehmeier, A. in *Seminar of the 'Deutsche Kautschuk Gesellschaft' on soft matter nano structuring and reinforcement*. May 22, 2001. Hannover (Germany).
132.   Payne, A.R., *Reinforcement of elastomers*. 1965, Interscience: New York.
133.   Chazeau, L., Brown, J.D., Yanyo, L.C., Sternstein, S.S., Polym. Comp., 2000. **21**(2): p. 202.
134.   Payne, A.R., J. Appl. Sci., 1962. **6**(19): p. 57.
135.   Ouyang, G.B., Tokita, N., Wang, M.-J. in *Am. Chem. Soc. Rubber Div. conference*. October 17-20, 1995. Cleveland, Ohio.
136.   Krauss, G., J. Appl. Polym. Sci., 1984. **39**: p. 75.
137.   Klüppel, M., Kautsch. Gummi Kunstst., 1997. **50**(4): p. 282.
138.   Huber, G., Vilgis, T.A., Kautsch. Gummi Kunstst., 1999. **52**: p. 102.
139.   Medalia, A.I., J. Coll. Interf. Sci., 1970. **32**: p. 115.
140.   Drozdov, A.D., Dorfmann, A., Polym. Eng. Sci., 2002. **42**: p. 591.

141. Gerspacher, M., O'Farrel, C.P., Yang, H.H., Wampler, W.A. *A proposed mechanism for the reinforcement of elastomers by carbon black*. in *Am. Chem. Soc. Rubber Div. conference*. May 1996. Montreal, Canada.
142. Gerspacher, M., O'Farrel, C.P., Yang, H.H., Tricot, C., Rubber World, 1996. **214**: p. 27.
143. Freund, B., Niedermeier, W., Kautsch. Gummi Kunstst., 1998. **51**: p. 444.
144. Wagner, M.P., Rbber Chem. Technol., 1976. **49**: p. 703-774.
145. Maier, P.G., Göritz, D., Kautsch. Gummi Kunstst., 1996. **49**: p. 18.
146. Gauthier, C., Reynaud, E., Vassoile, R., Ladouce-Stelandre, L., Polymer, 2004. **45**: p. 2761.
147. Kaufman, S., J. Polym. Sci., 1979. **9**: p. 829.
148. Leblanc, J.L., Progr. Rubber Plast. Technol., 1994. **10**(2): p. 112.
149. Banet, L.L., Rubber Chem.Technol., 1974. **47**: p. 858.
150. Ahagon, A., J. Appl. Polym. Sci., 1989. **44**: p. 217.
151. Kaufmann, S., Slichter, W.P., Davies, D.D., J. Polym. Sci., 1971. **A-2**(9): p. 829.
152. O'Brien, J., Cashell, E., Wardell, G.E., McBrierty, V.J., Macromol., 1976. **9**: p. 653.
153. Kenny, J.C., McBrierty, V.J., Rigbi, Z., Douglass, D.C., Macromol., 1991. **24**: p. 436.
154. Serizawa, H., Ito, M., Kanamoto, T., Tanaka, K., Nomura, A., Polym. J., 1982. **14**: p. 149.
155. Litvinov, V.M., in *Organosilicon chemistry: From molecules to materials II*. 1996, VCH: Weinheim.
156. Litvinov, V.M., Steeman, P.A.M., Macromolecules, 1999. **32**: p. 8476.
157. McBrierty, V.J., Kenny, J.C., Kautsch. Gummi Kunstst., 1994. **47**: p. 342.
158. Legrand, A.P., Lecomte, N., Vidal, A., Haider, B., Papirer, E., J. Appl. Polym. Sci., 1992. **46**(2223).
159. Ono, S., Ito, M., Tokumitsu, H., Seki, K., J. Appl. Polym. Sci., 1999. **74**: p. 2529.
160. Medalia, A.I., Rubber Chem. Technol., 1972. **45**: p. 1171.
161. Kerner, E.H., Proc. Phys. Soc., 1956. **69B**: p. 808.
162. Nielsen, N.E., Appl. Polym. Symp., 1969. **12**: p. 249.
163. Dannenberg, E.M., Trans. Inst. Rubber Ind., 1966. **42**: p. 943.
164. Strauß, M., Kilian, H.G., Freund, B., Wolff, S., Coll. Polym. Sci., 1994. **272**: p. 1208.
165. Eklund, T., Bäckmann, J., Idmann, P., Norström, A.A.E., Rosenholm, J.B., in *Silanes and other coupling agents*, K.L. Mittal, Editor. 2000, VSP: Utrecht. p. 55.

PHENOMENOLOGICAL APPROACH

OF THE DISPERSION AND SILANIZATION PROCESS

IN AN INTERNAL MIXER

In this investigation, different adjustments of the mixing equipment and process parameters of the silanization step are analyzed in terms of their potential to improve the efficiency of the silanization reaction. Parameters investigated are working in an open mixer, application of air injection, variation of the rotor type as well as temperature control settings of the mixer and the rotor.

All measures, which increase the ethanol transfer out of the compound, improve the silanization efficiency. Parameters influencing the mass transfer across the compound/vapor interphase are: rotor speed, fill factor, compound temperature and removal of ethanol out of the vapor phase in the mixing chamber by working in an open mixer or using air injection. The same factors influence the cooling efficiency of the mixer, together with a direct influence thereon of the temperature of the mixing chamber and the rotors. Other factors which increase the silanization efficiency are a higher efficiency of the energy input, a reduced ethanol condensation in the mixer, a lower ethanol concentration in the compound, a better wall contact between the compound and the mixer wall as well as a good intake behavior.

The most preferred measure to improve the silanization efficiency, which can easily be implemented, is air injection: During the silanization step, existing valves in the mixer can be used to inject a strong current of air. This measure can be enhanced by providing an outlet for the air stream, for example by working in an open mixer. During the silanization step the mixer is used as an open reactor with the basic functions of keeping the temperature level constant, creating fresh surfaces and homogenizing the compound. Thus, the most appropriate mixer design is a tandem system with a traditional internal mixer for the mixing and dispersion step and a separate open reactor for the silanization step.

1. INTRODUCTION

It is common practice to mix silica compounds in traditional 'black' mixing equipment. The internal mixers for rubber are designed for dispersion and mixing, but not for a chemical reaction as required in the case of silica compounds. Therefore, these compounds require additional steps to complete the reaction between the silanol groups of the silica and the ethoxy groups of the coupling agent (see chapter 2). During the silanization reaction the hydrophilic character of the silica filler surface is changed to a more hydrophobic one, increasing the compatibility of the filler with the polymer. The coupling agent reacts with the polar silanol groups on the silica surface forming a shell around the filler particle with carbon and sulfur atoms on the outside. This primary reaction takes place at room temperature, although to a very limited extent. Only at temperatures above 130ºC, the reaction rate is high enough to achieve a sufficient degree of silanization during the mixing cycle. In the second step of the silanization reaction the remaining ethoxy groups of the coupling agent react with adjacent ethoxy groups or silanol groups. This step is slower compared to the primary reaction and therefore requires a higher temperature level for completion within a mixing cycle. [1] The sulfur contained in the commonly used coupling agents is necessary to build the filler-polymer network during vulcanization, giving the silica compound its special property profile. At the same time it is the limiting factor for the rate of the silanization reaction: The upper limit of the temperature window during processing is given by the risk of scorch. Therefore, the temperature range for the silanization reaction is limited, from approximately 130ºC to 150ºC, depending on the type of coupling agent and silica, the mixing process and the type of mixing equipment. [2] In order to stay in this relatively narrow temperature window and close to 150ºC, silica compounds require several mixing stages.

Ethanol formation during the coupling reaction between silica and silane is another problem. Each gram of silane used in the compound forms approximately 0.5 grams of ethanol when all ethoxy groups react. In a production plant, where large batch sizes are processed, this accounts for a considerable amount of alcohol, which partly devolatilizes out of the compound, then recondenses or is removed from the mixing chamber. When ethanol recondenses in the mixing chamber, it causes slippage of the compound and results in less effective mixing and cooling. Additionally, high ethanol concentrations in the compound result in a decrease of the silanization rate.

These shortcomings of silica compound processing have mainly been approached from the raw materials side: Highly dispersible silica types were introduced, and new silanes were developed with the aim to reduce the scorch risk during mixing and silanization and allow working at high temperatures. [3-7]

Some work was done to improve processing of silica compounds, for example by adjustments of the compounding protocol or by choosing a more appropriate mixer. [8] The scorch risk can be reduced by the addition of zinc oxide in the final mixing step instead of the first mixing step, and this widens the temperature window to higher silanization temperatures. [9] In terms of mixing equipment, an intermeshing mixer is preferred because this one is characterized by a tight temperature control allowing working closer to the scorch temperature compared to tangential mixers. [10]

In this chapter different processing parameters of the silanization step are analyzed concerning their potential to improve the silanization efficiency.

2.   INVESTIGATED PROCESSING PARAMETERS

The following factors, which are expected to have an influence on the silanization efficiency, are investigated:

- *Pressure-less mixing:* The silanization step was done pressure-less in an open mixer. The fill factors used in these experiments were optimized in terms of intake behavior, silanization efficiency and mixer capacity.

- *Air injection:* A very strong current of air was blown through the mixing chamber in order to drag out ethanol.

- *Mixer temperation:* The TCU settings (cooling water temperature of the mixing chamber, the rotors and the ram) were varied in order to improve the cooling efficiency or to reduce condensation of ethanol.

- *Mixer opening:* When silanization was carried out with the ram up, the mixer opening was adjusted in order to improve the intake behavior.

- *Different rotor types:* Mixers with different rotor designs and capacities were compared.

3. EXPERIMENTAL

To study the relationship between mixer variables and silanization efficiency, one large masterbatch was prepared, which was further mixed and silanized in different laboratory and production mixers under various conditions.

All investigations are done using a passenger car tire tread masterbatch based on a blend of S-SBR and BR with 83.5 phr silica and a coupling agent, either TESPT or TESPD. (The complete recipe can not be revealed due to

confidentiality reasons.) The compound was mixed and predispersed in a 320 l intermeshing mixer. A typical fingerprint of the mixing step is shown in Figure 1.

3.1. Preparation of the Masterbatch
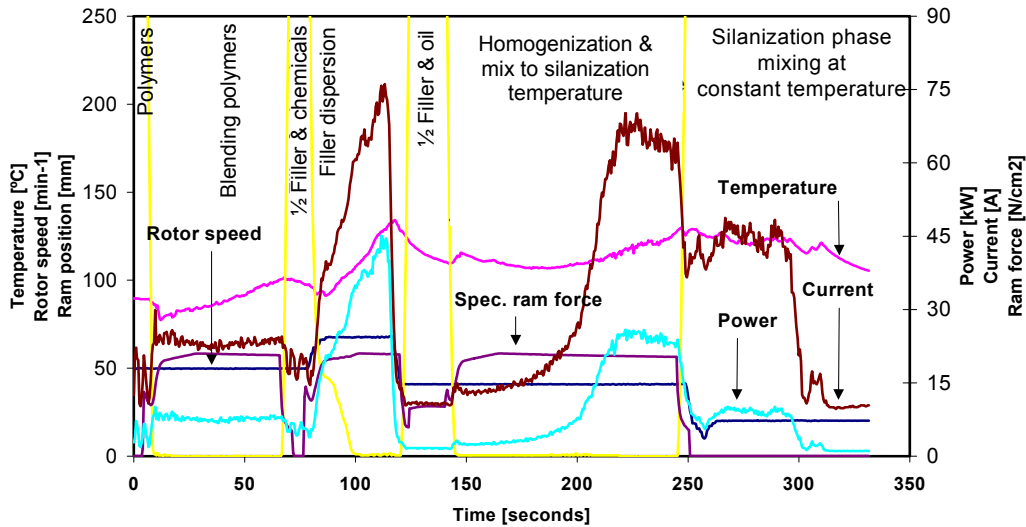
Figure 1: Fingerprint of masterbatch mixing

The masterbatch reached the starting temperature for the silanization, 130ºC, approximately 60 seconds before the material was discharged: The silanization reaction took place to a very limited extent during this period. Such a predispersed, but not silanized compound was also used in all investigations discussed in chapters 5-8.

3.2. The Mixing Equipment

Five different mixers are used for the investigations of this chapter: three intermeshing mixers, I5, I45 and I320, and two tangential mixers, T4 and T7. Within this project, in the experiments described in chapters 5 through 8, different rotor types are used, and a complete overview is given in Table I. The notation for the mixer/rotor combinations consists of a letter indicating the rotor type ('I' for intermeshing, 'T' for tangential), followed by a number signifying the size of the mixing chamber.

The intermeshing rotor with PES5 geometry and the tangential rotor with ZZ2 geometry are standard rotors used in rubber mixing. The ZZ2 rotor has two opposing central wings and two short wings to drag the material from the chamber ends. The tangential rotor with the F4W-geometry (full four wing) has a larger wing in a smaller angle compared to the ZZ2 rotor, resulting in a higher efficiency in terms of laminar mixing and dispersion. The SI rotor has two long wings in opposite positions, forcing the material to a stronger axial deflection.

52

Table I: Mixers and rotors used in the investigation and their notations

	Net mixer volume [liter]	Rotor type	Number of long/(short) flights	Rotor tip clearance [mm]	Net mixer volume [liter]	Rotor type	Number of long/short flights	Rotor tip clearance [mm]
I5	5.5	PES5	3	3.3	6.4	I5-SI	3	*unknown*
I45	49.0	PES5	3	3.4				
I320	320	PES3	3	*unknown*				
T4	3.6	ZZ2	2/2	1.5				
T7	7.6	F4W	2/2	1.8	8.4	T7-SI	2/2	1.4

3.3. SETUP OF THE EXPERIMENTS ON SILANIZATION EFFICIENCY

For all experiments, predispersed masterbatches as described in 3.1. are used. This masterbatch was fed into the mixer and brought to silanization temperature as fast as possible, with the mixing chamber closed. Once the silanization temperature was reached, the temperature was kept constant by adjustment of the rotor speed during the silanization step. In the open mixer mode, the ram was lifted after the silanization temperature was reached and was held in this position during silanization. After the silanization step the compound was discharged and the compound temperature was controlled using a pyrometer.

3.4. SAMPLE PREPARATION AND ANALYSIS

During the experiments, the Mooney viscosity of the compounds was measured directly after discharge of the compound, giving a first indication of the dispersion of the filler and the degree of silanization. More accurate results on the degree of silanization are gained by measuring the Payne effect (see chapter 2). The samples used for further evaluation were quenched in liquid nitrogen immediately after discharge in order to avoid ongoing silanization. They are cooled during storage to prevent further silanization and reagglomeration of the filler. [11]

The following equipment and procedures are used for the preparation and analysis of the compounds discussed below, but also in the investigations described in chapter 5 through 8:

o *Compound temperature*: The compound temperature was monitored during mixing, heating and silanization by thermocouples installed in the mixing chamber, in general in the bottom part of the mixing chamber and in the side plates. Prior to the experiments, the correlation of the automatically monitored temperature inside the mixer and the actual compound temperature was determined. The actual compound temperature was measured outside the mixer using a pyrometer (Almemo 2290-4, Therm

2288-2) immediately after discharge of the batch. The highest temperature value had to be in accordance with the chosen silanization temperature within a limit of ± 2ºC.

o *Viscosity ML(1+4), 100ºC*: The viscosity of the compounds was measured immediately after discharge of the batch using a shearing disk viscometer. The measurements were done on two similar machines from Frank (1987, 1988). In general, three separate samples per experiment were measured, and if the variation between the three values exceeded ± 1.5 MU, additional measurements were done. The average value of the measured viscosities was taken as the final viscosity of the compound.

o *Payne effect (difference in storage modulus G' at small strains and at high strains):* Measurements were done using a Rubber Process Analyzer RPA 2000 from Alpha Technologies. Storage modulus, loss modulus, complex modulus and loss angle were measured as a function of strain in the range between 0.56% and 100% at a temperature of 100ºC and a frequency of 0.5 Hz. This measurement is widely accepted as a measurement of the Payne effect, in spite of the fact that these measurements are normally limited to the linear region. The variation of the measurements within one batch was determined to be ± 5%.

o *Evaporated ethanol*: The relative amount of ethanol in the vapor phase just above the mixer opening was measured by adsorption on active coal, followed by thermal desorption and quantitative determination by gas chromatography. Adsorption of ethanol was done by guiding a calibrated vapor stream (in the range of 500 ml per minute) from the lower hopper region just above the mixing chamber opening through the test tubes filled with active coal. Desorption was carried out in a Programmed Thermal Desorber PTO-132 (Meyvis & Co.) with nitrogen as the purging gas at 350ºC. The desorbed ethanol was collected in a heated chamber with a temperature of 300ºC and a volume of 300 ml. The amount of ethanol was determined with a Varian 3700 gas chromatograph equipped with a 2.5 meter Carbopack C column coated with 5% Carbolax 20M at 235ºC. A flame ionization detector was used at a temperature of 270ºC. The accuracy of these measurements was ± 2%. This measurement was possible only in the open mixer mode.

o *Water content*: The water content was measured by a Karl-Fischer titration using a Karl Fischer Coulometer 652 (Metrohm). The water was evaporated out of a rubber sample with a thickness of approximately 0.5 mm during 30 minutes in a Büchi T050 oven, which was purged with nitrogen. The measurement was done with a delay of 10 seconds. The accuracy of these measurements was approximately ± 3% within one sample and ± 5% within a complete batch.

4. RESULTS

4.1. PRESSURE-LESS MIXING

One of the key parameters for an efficient silanization was assumed to be the ethanol concentration in the compound and in the vapor phase in the mixer. A measure to reduce the concentration is working pressure-less in an open mixer during the silanization step. Figure 2 shows the increase in silanization efficiency by using the mixer as an open reactor, as quantified with the Payne effect. Results are given for different mixers and different fill factors, with silanization carried out in a closed mixer compared to the open mixer mode using the same conditions. Table II shows the experimental setup of this series of experiments. The fill factor used in the first part of this investigation, 60%, is in the lower range of fill factors used in actual practice for rubber mixing under standard conditions in a closed mixer. The lower fill factors were chosen on the basis of a fill factor study for silanization in an open mixer: Figure 3. This study showed that a fill factor of 40% for intermeshing mixers and a fill factor of 45% for tangential mixers is the best compromise between good intake behaviour on one hand and reduction of the mixer capacity on the other hand.

A significant improvement of the silanization efficiency was achieved when silanization was done in an open mixer in both cases, with a high fill factor as well as with a reduced, optimized fill factor. The effect was more pronounced in intermeshing mixers compared to tangential mixers. The results found on small scale were verified on larger scale in the intermeshing I45 mixer: The absolute level of silanization was independent of mixer size, but did depend on the fill factor, as illustrated in Figures 2 and 3: A higher fill factor generally resulted in a higher Payne effect, indicating a lower silanization efficiency.
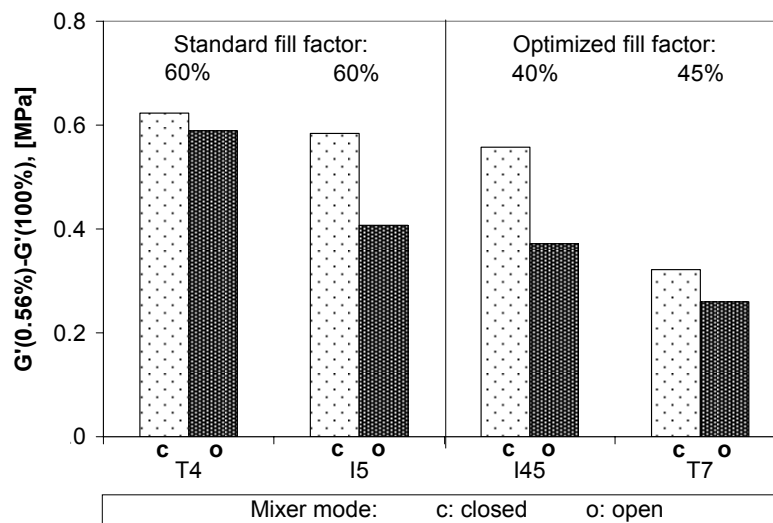
Figure 2: Effect of silanization in an open mixer

Table II: Parameters for the experiments shown in Figure 2

Mixer	-	T4	I5	I45	T7
Rotor type	-	ZZ2	PES5	PES5	F4W
Fill factor	[%]	60	60	40	45
TCU settings	[ºC]	90	90	40	60
Silanization temperature	[ºC]	145	145	145	145
Silanization time	[minutes]	150	150	150	150
Air injection	[on/off]	off	off	off	off
Mixer mode	[open/closed]	variable	variable	variable	variable
Coupling agent		TESPT	TESPT	TESPT	TESPD
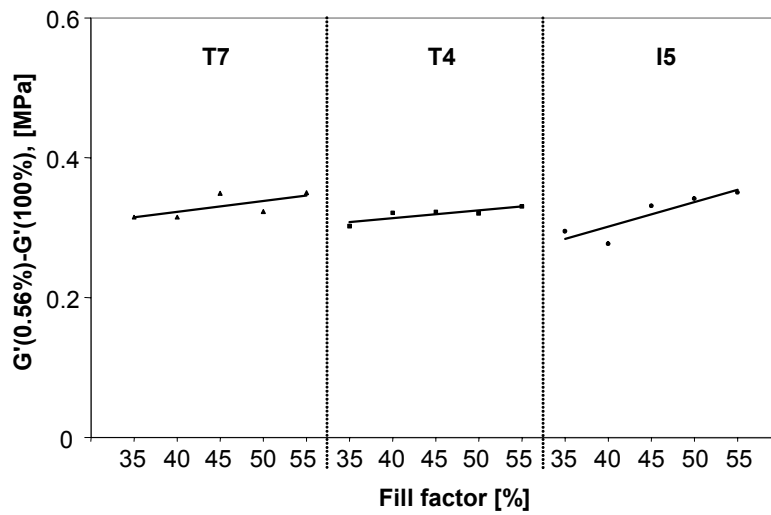
Figure 3: Fill factor studies for working in an open mixer

Table III: Parameters for the experiments shown in Figure 3

Mixer	-	T7	T4	I5
Rotor type	-	F4W	ZZ2	PES5
Fill factor	[%]	variable	variable	variable
TCU settings	[ºC]	60	60	60
Silanization temperature	[ºC]	145	145	145
Silanization time	[minutes]	60	60	60
Air injection	[on/off]	off	off	off
Mixer mode	[open/closed]	open	open	open
Coupling agent		TESPD	TESPD	TESPD

4.2. AIR INJECTION

Ventilation of the mixing chamber is significantly improved by air injection: A strong current of air is blown through the mixing chamber. This air stream drags ethanol out of the mixing chamber and cools the material. For these experiments the compound was warmed up to the silanization temperature in a closed mixer using a high rotor speed. When the compound reached the final temperature, air injection was switched on and the rotor speed was adjusted in order to keep the temperature at a constant level.

Figure 4 shows the effect of air injection on the silanization efficiency in the closed I45 mixer at different degrees of filling. A significant improvement can be achieved by this measure: The Payne effect of the compound silanized with air injection is significantly lower than the Payne effect of the compound silanized under the same conditions, but without air injection. The effect is less pronounced for high fill factors.
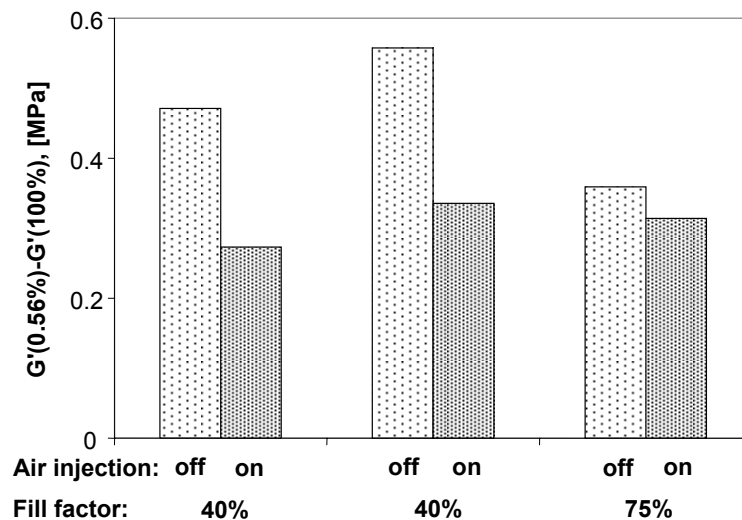
Figure 4: Effect of air injection in a closed mixer (I45)

Table IV: Parameters for the experiments shown in Figure 4

Mixer	-	I45	I45	I45
Rotor type	-	PES5	PES5	PES5
Fill factor	[%]	40	40	75
TCU settings	[°C]	40	40	40
Silanization temperature	[°C]	145	145	145
Silanization time	[minutes]	150	150	60
Air injection	[on/off]	variable	variable	variable
Mixer mode	[open/closed]	closed	closed	closed
Coupling agent		TESPT	TESPT	TESPT

Studies on the influence of the moisture content on the silanization efficiency have shown, that the reaction rate increased with increasing water concentrations, as the ethoxy groups are hydrolyzed during the secondary reaction prior to silanization. [1, 12] Therefore the effect of air injection on the water content of the compound was measured: Figure 5 shows that the moisture content of the compound is reduced by approximately 15 % after silanization for 150 seconds at 145ºC by applying air injection. The same figure also shows the total amount of evaporated ethanol during the silanization reaction, which is correlated to the Payne effect: The lower the Payne effect, thus the higher the silanization efficiency, the higher the amount of evaporated ethanol during the silanization step.
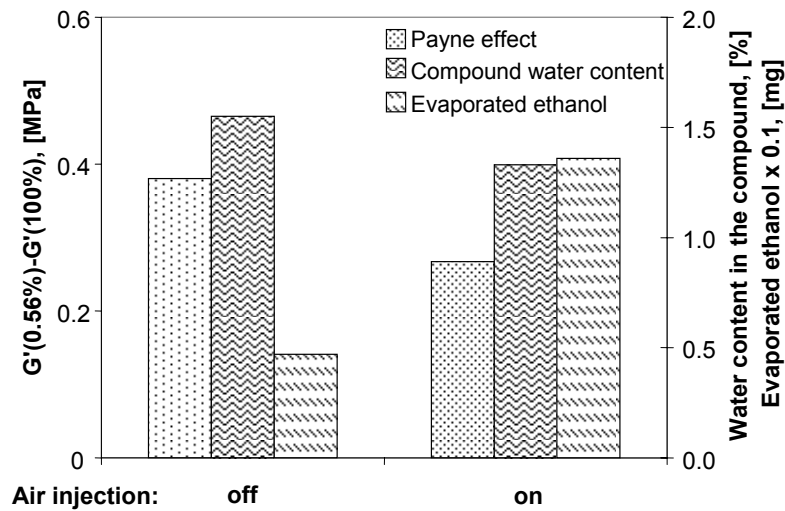
Figure 5: Influence of air injection on the water concentration in the compound and the amount of evaporated ethanol

Table V: Parameters for the experiments shown in Figure 5

Mixer	-	I45
Rotor type	-	PES5
Fill factor	[%]	40
TCU settings	[ºC]	40
Silanization temperature	[ºC]	145
Silanization time	[minutes]	150
Air injection	[on/off]	variable
Mixer mode	[open/closed]	closed
Coupling agent		TESPT

As air injection had a significant positive influence of the silanization efficiency, trials on production scale in the I320 mixer were carried out: Figure 6. Two series of 10 batches each were produced according to the standard mixing protocol and with air injection into the closed mixer respectively. The

compounds silanized with air injection passed the standard quality control tests and were used for passenger car tire building as tread material. These tires were tested in an indoor and outdoor test program and were found to show similar performance compared to the tires having treads made from standard compounds. In terms of driving safety on natural ice and snow, the tires with treads based on compounds produced with air injection even showed some improved performance. A summary of the results of these tire tests is given in annex 1.
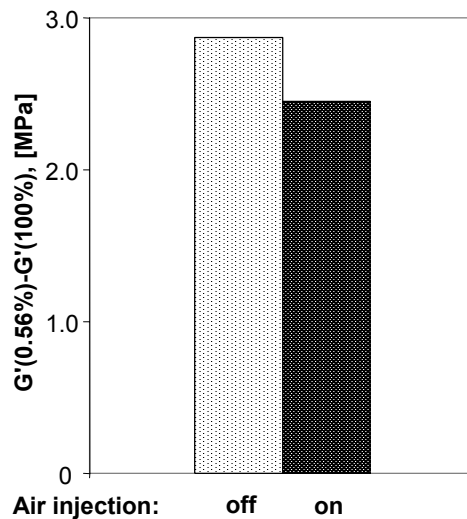
Figure 6: Influence of air injection on the silanization

in a closed mixer on production scale (I320)

Table VI: Parameters for the experiments shown in Figure 6

Mixer	-	I320
Rotor type	-	PES3
Fill factor	[%]	59
TCU settings (rotor/mixer wall)	[ºC]	35/45
Final silanization temperature	[ºC]	155
Silanization time	[minutes]	3
Air injection	[on/off]	variable
Mixer mode	[open/closed]	closed
Coupling agent		TESPD

4.3. COMBINATION OF WORKING IN AN OPEN MIXER AND AIR INJECTION

Several series of experiments were carried out in order to investigate the superimposed effects of both measures. Figure 7 shows, that an additional reduction of the Payne effect can be achieved by combining both measures: The lowest Payne effect, thus the highest degree of silanization, is found for silanization in an open mixer together with air injection. Looking at the single

measures, a stronger reduction of the Payne effect is found for air injection compared to the effect of the open mixer mode alone.
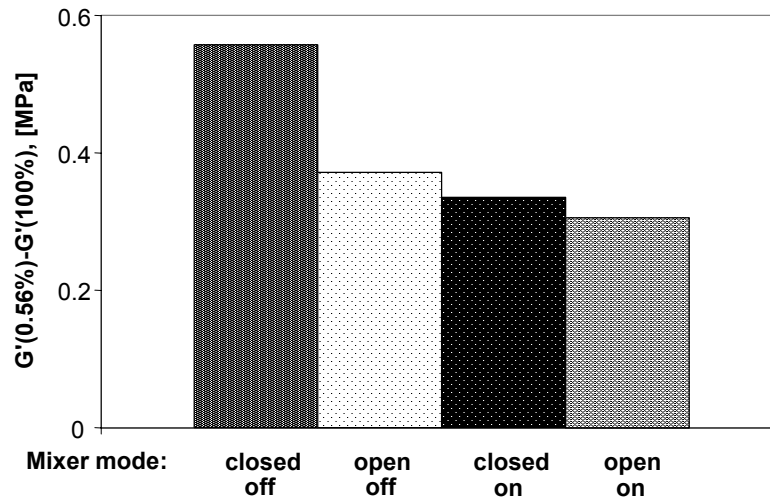
Figure 7: Effect of mixing in an open mixer and
in a closed mixer combined with air injection

Table VII: Parameters for the experiments shown in Figure 7

Mixer		I45
Rotor type		PES5
Fill factor	[%]	40
TCU settings	[°C]	40
Silanization temperature	[°C]	145
Silanization time	[minutes]	150
Air injection	[on/off]	Variable
Mixer mode	[open/closed]	Variable
Coupling agent		TESPT

Figure 8 shows other examples for the combination of air injection with working in an open mixer. In this case, the silanization was done in the open mixer mode, and the figure shows the results of the comparison between working with air injection and without air injection. The two series only differ in the type of coupling agent used (see Table VIII). In both cases an additional reduction of the Payne effect can be achieved by using air injection.
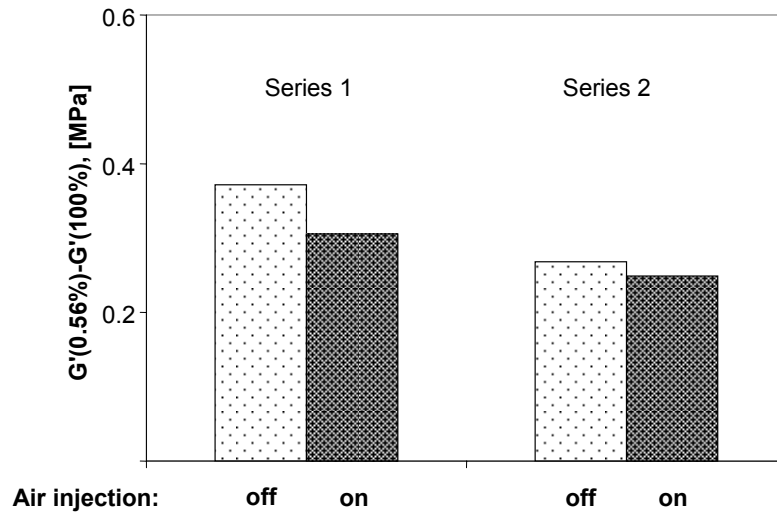
Figure 8: Effect of air injection in an open mixer (I45)

Table VIII: Parameters for the experiments shown in Figure 8

		Series 1	Series 2
Mixer	-	I45	I45
Rotor type	-	PES5	PES5
Fill factor	[%]	40	40
TCU settings	[ºC]	40	40
Silanization temperature	[ºC]	145	145
Silanization time	[minutes]	150	150
Air injection	[on/off]	variable	variable
Mixer mode	[open/closed]	open	open
Coupling agent		TESPT	TESPD

4.4.   MIXER TEMPERATURE

Figure 9 illustrates the influence of the temperature control unit (TCU) settings on the silanization efficiency: A lower temperature of the cooling media results in a lower Payne effect, thus in a higher silanization rate in the cooling temperature range between 60º and 90ºC. No difference is found any more at cooling temperatures above 90ºC.
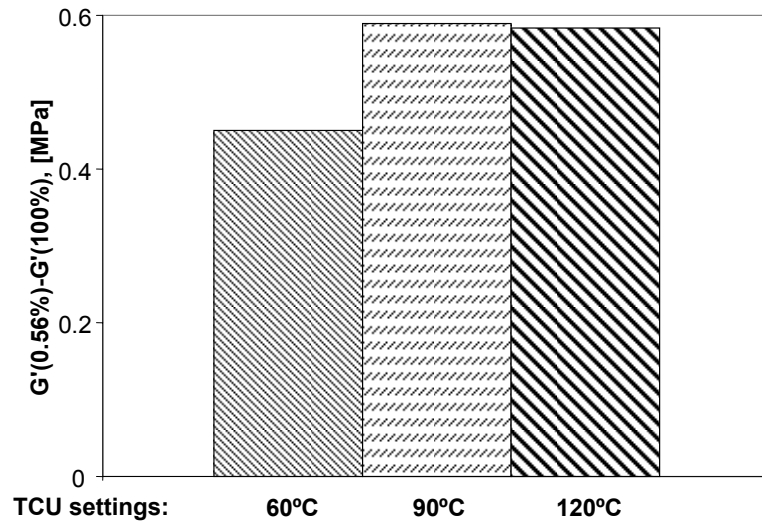
Figure 9: Effect of the cooling water temperature

Table IX: Parameters for the experiments shown in Figure 9

Mixer	-	T4
Rotor type	-	ZZ2
Fill factor	[%]	60
TCU settings	[ºC]	variable
Silanization temperature	[ºC]	145
Silanization time	[minutes]	150
Air injection	[on/off]	off
Mixer mode	[open/closed]	open
Coupling agent		TESPT

Figure 10 shows the situation, when different zones within the mixer are set at different temperature levels. Again, the lowest temperature settings result in the highest degree of silanization. The absolute values of the Payne effect with decreasing cooling temperature are significantly lower compared to the situation shown in Figure 9.

For silanization in a closed mixer, the upper part of the mixing chamber, particularly the ram, is the area where condensation of ethanol is most pronounced. The liquid ethanol covering the mixer walls influences the material flow in the mixer as well as the heat transfer from the compound through the mixer walls to the cooling media. Reducing the alcohol condensation, for example by heating the ram, is therefore expected to positively influence the silanization efficiency. Figure 11 shows the influence of this measure in combination with air injection. In both cases, with and without air injection, heating of the ram works counterproductive: It results in a higher Payne effect, thus lower silanization efficiency. Silanization in a mixer with a heated ram and without air injection results in the highest Payne effect and the lowest specific

energy input; whereas the highest energy input is required for silanization with ram heating on and air injection on.
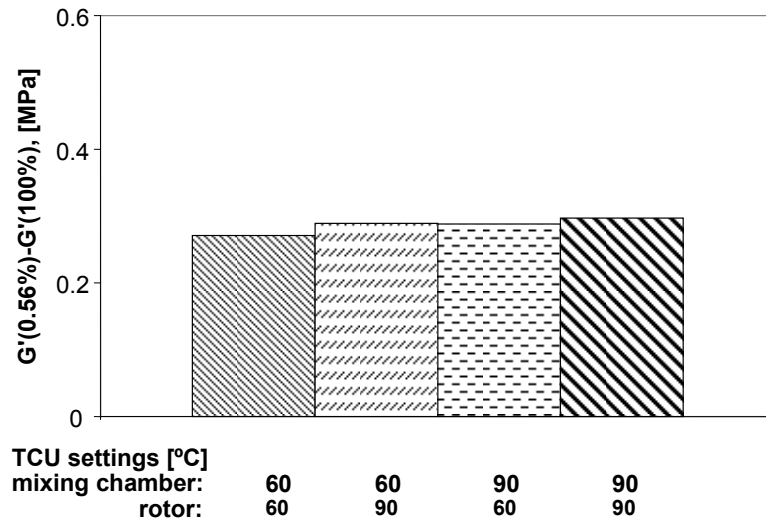
Figure 10: Effect of different cooling temperatures of the rotor and the mixing chamber

Table X: Parameters for the experiments shown in Figure 10

Mixer	-	T7
Rotor type	-	F4W
Fill factor	[%]	45
TCU settings	[ºC]	variable
Silanization temperature	[ºC]	145
Silanization time	[minutes]	150
Air injection	[on/off]	off
Mixer mode	[open/closed]	open
Coupling agent		TESPD
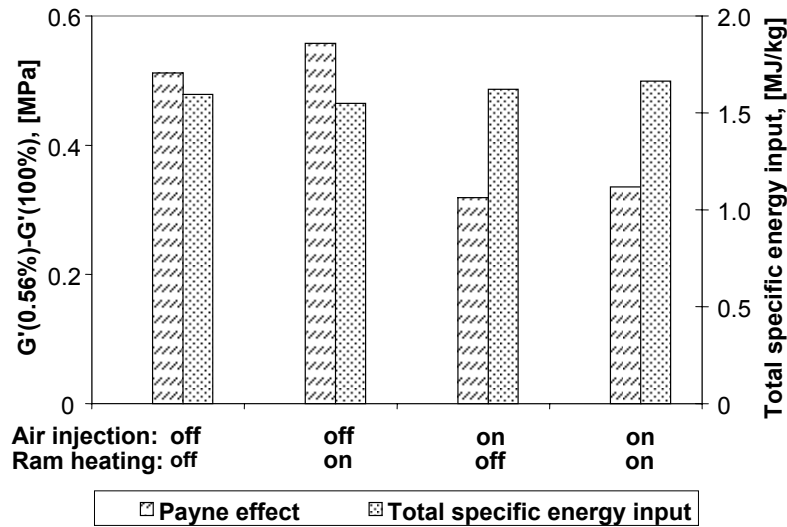
Figure 11: Effect of ram heating combined with air injection

Table XI: Parameters for the experiments shown in Figure 11

Mixer	-	I45
Rotor type	-	PES5
Fill factor	[%]	40
TCU settings	[ºC]	40
Silanization temperature	[ºC]	145
Silanization time	[minutes]	150
Air injection	[on, off]	variable
Mixer mode	[open, closed]	closed
Ram heating	[on, off]	var.
Coupling agent		TESPT

4.5.   ALTERNATIVE HOPPER CONSTRUCTIONS

The shortcomings of working in an open mixer are the irregular intake behavior and a missing pressure during mixing. Both effects reduce the mixing effect, energy input into the compound and the surface renewal rate, finally resulting in a lower silanization efficiency. In order to avoid this negative effect, the hopper opening was redesigned. In one set of experiments, the mixing chamber was closed by a perforated plate instead of the ram: During mixing, pressure was applied and the compound could not be pushed up into the hopper. At the same time ethanol could evaporate out of the mixing chamber. The second design was a reduced hopper opening area by using a frame with a smaller opening, again preventing that the compound was pushed up into the hopper and at the same time allowing ethanol to escape out of the mixing chamber. Figure 12 shows the effect of these alternative hopper designs in combination

with air injection. All measures result in a reduction of the Payne effect, with only slight differences between the alternative designs and production parameters.
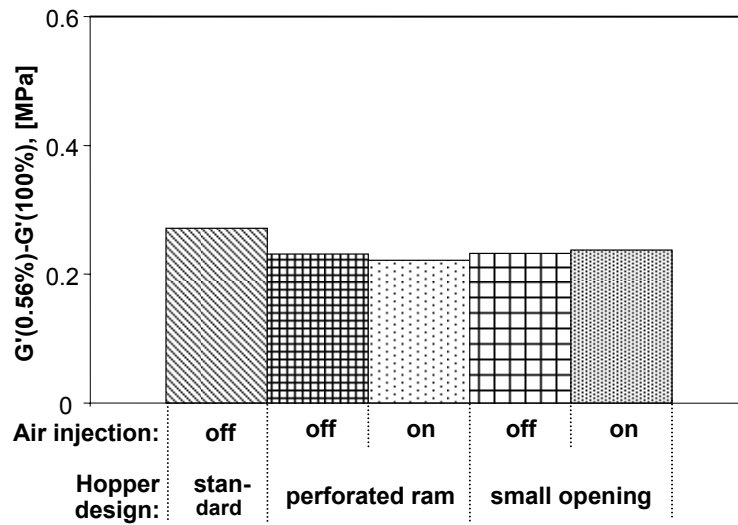
Figure 12: Effect of different hopper constructions in combination with air injection

Table XII: Parameters for the experiments shown in Figure 12

Mixer	-	I5
Rotor type	-	PES5
Fill factor	[%]	40
TCU settings	[°C]	60
Silanization temperature	[°C]	145
Silanization time	[minutes]	150
Air injection	[on, off]	variable
Standard mixer mode	[open/closed]	open
Coupling agent		TESPT

4.6. ROTOR TYPE

Different rotor designs were tested on laboratory scale: The F4W, the PES5 and the ZZ2 rotors are standard rotor geometries used in the rubber industry, and the two SI rotors are new prototypes. In these series of experiments, the first heating of the compound was done in the closed mixer, and silanization was done in the open mixer mode. A reduced, optimized fill factor was used (Table XIII). The degree of silanization was measured as a function of the silanization temperature and time. Figure 13 shows the silanization efficiency of the different rotors, and Figures 14 and 15 show the specific energy input and the total number of revolutions during the silanization phase. This last parameter was defined as the number of revolutions in the specified time period needed to keep the temperature constant.
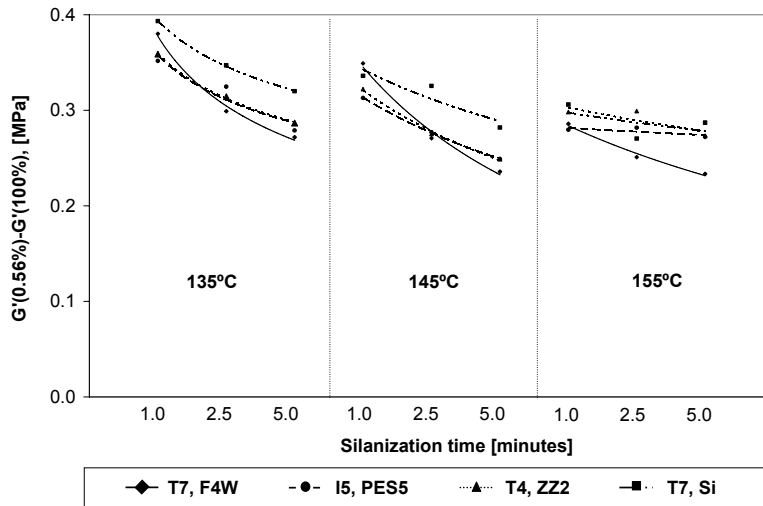
*Figure 13: Silanization efficiency of different rotor types
at different silanization temperatures*
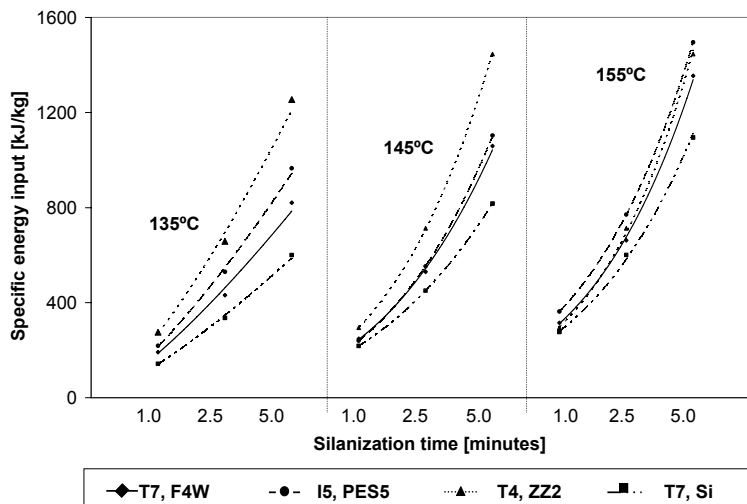
*Figure 14: Specific energy input during silanization depending
on the rotor type at different silanization temperatures*
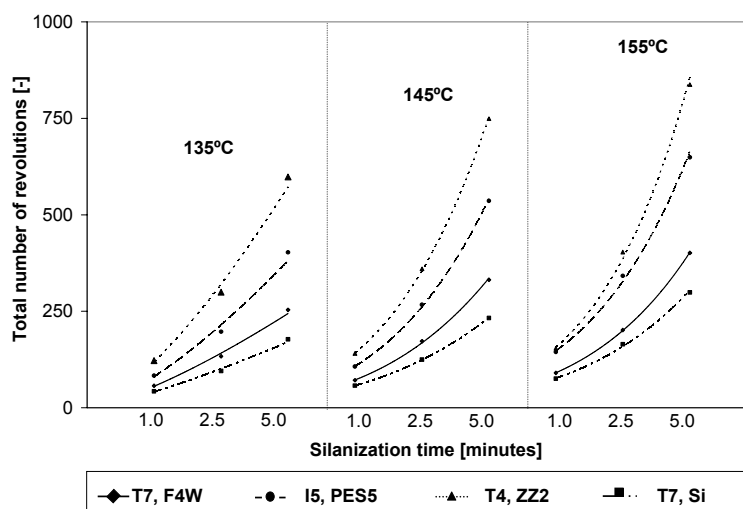
*Figure 15: Total number of revolutions during silanization depending
on the rotor type at different silanization temperatures*

Table XIII: Parameters for the experiments shown in Figures 13 to 15

Mixer	-	T7	I5	T4	T7
Rotor type	-	F4W	PES5	ZZ2	T7-SI
Fill factor	[%]	40	45	45	45
TCU settings	[ºC]	60	60	60	60
Silanization temperature	[ºC]	variable	variable	variable	variable
Silanization time	[minutes]	variable	variable	variable	variable
Air injection	[on/off]	off	off	off	off
Mixer mode	[open/closed]	open	open	open	open
Coupling agent		TESPD	TESPD	TESPD	TESPD

The different rotor types show only slight differences in terms of silanization efficiency with the exception of the T7-SI rotor, which shows a significantly lower efficiency during the whole period of silanization at all temperatures. The compound silanized in the mixer equipped with the F4W rotor shows a higher Payne effect at short silanization times and at lower temperatures, compared to the compound silanized in the mixers with the PES5 and the ZZ2 rotor, respectively. After 2.5 minutes of silanization the degree of silanization is similar in the three cases; only at the highest temperature and at longer silanization periods the compound silanized with the F4W mixer shows a lower Payne effect. The specific energy input for the different mixers differs significantly: The T4 mixer with the ZZ2 rotor has the highest energy input, while the T7 mixer with the T7-SI rotor has the lowest energy input. The mixers equipped with the PES5 rotor and the F4W rotor take an intermediate position, and only at a low temperature, 135ºC, the mixer with the PES5 rotor has a significantly higher specific energy input compared to the mixer with the F4W rotor. At higher silanization temperatures, the difference between the mixers with the different rotor types diminishes, and at 155ºC only slight differences are left. The number of revolutions during silanization shows a clear trend within the whole temperature window: The compound silanized in the mixer with the ZZ2 rotor undergoes the highest number of revolutions, followed by the compound silanized in the mixer with the PES5 rotor. The difference in the total number of revolutions is less pronounced between the mixer with the F4W rotor and the T7-SI rotor; the mixer equipped with the T7-SI rotor shows the lowest values. The difference between the total number of revolutions is higher the longer the silanization period.

5. DISCUSSION

The concentrations of ethanol in the compound as well as in the vapor phase of the mixing chamber are the main influencing factors for the rate of silanization, as ethanol is competing with the silane molecules for adsorption sites on the

silica surface (see chapter 2): The faster the devolatilization of the compound, the lower the degree of adsorption of ethanol on the silica surface. Furthermore, ethanol condensation in the mixing chamber is negatively affecting the efficiency of energy transfer into the compound as well as the cooling efficiency. One possibility to achieve an efficient devolatilization of the compound and to reduce ethanol condensation is a decrease of the ethanol concentration in the vapor phase of the mixing chamber. This can be achieved by working in an open mixer, thus using the mixer as an open reactor during the silanization phase. This is only possible when dispersion of the filler is no longer necessary during the silanization phase: This is the case in the experimental setup used in this investigation, as the degree of filler dispersion of the masterbatch was already on a high level of about 91% to 93%, and the dispersion is further improved during the heating period prior to silanization. The compound is heated up from room temperature to the final silanization temperature in a closed mixer at a high rotor speed, applying high shear, resulting in good distributive and dispersive mixing. The results of the comparative investigation of pressure-less silanization in an open mixer and silanization in a closed mixer, both carried out under the same conditions, prove this point: Silanization in an open mixer, where ethanol can escape out of the mixing chamber, results in a lower Payne effect (Figure 2).

A shortcoming of working in an open mixer with a standard fill factor is the irregular intake behaviour: The compound is pushed up into the hopper opening where it remains for a certain period of time before it is pulled into the mixing chamber again, resulting in overall poor mixing and devolatilization. The intake behaviour can be improved by a reduction of the fill factor. A combination of both measures, pressure-less silanization and reduced fill factor, leads to a superimposed positive effect on the silanization efficiency.

The fill factor influences the silanization efficiency (Figure 3): The lower the fill factor, the lower the total amount of ethanol generated in the mixing chamber. Additionally, the frequency, with which a certain portion of the compound is passing the gap between the rotors as well as between the rotor and the mixer wall, is higher with a lower fill factor. The material is sheeted out to a higher extent and evaporation of ethanol out of the compound is enhanced. The influence of the fill factor on the Payne effect is more pronounced in the intermeshing mixer due to the more irregular intake behavior compared to the tangential mixer; therefore the benefit that can be gained by adjustment of the fill factor and improvement of the intake behavior is bigger for the intermeshing mixer.

A very efficient way to improve the silanization efficiency is a strong current of air passing through the mixing chamber (Figure 4). The injected air drags ethanol out of the vapor phase of the mixing chamber, thus increasing the driving force for ethanol transfer across the compound/vapor interphase and reducing condensation of alcohol in the mixing chamber. The reduction of the

ethanol concentration in the compound shifts the balance of adsorption of ethanol and the silane onto the filler surface to the silane side, resulting in a higher degree of silanization. Another factor is the cooling effect of the air current, requiring a higher rotor speed to keep the temperature at a given level. This results in a more effective mixing and a higher surface renewal rate of the compound, additionally enhancing devolatilization.

The higher silanization efficiency is not only expressed in the lower Payne effect values, but also in the higher total amount of evaporated ethanol as shown in Figure 5. The higher the degree of silanization, the higher the number of ethoxy groups which did react under formation of ethanol, thus the higher the concentration of ethanol in the compound. As the concentration difference between the compound and the vapor phase is the driving force for devolatilization, this will result in a higher devolatilization rate and thus in higher ethanol concentrations in the vapor phase of the mixing chamber.

Evaporation of ethanol will be accompanied by evaporation of water. The water content of the batch has an influence on the silanization: The reaction rate increases with increasing moisture content of the silica up to a level of approximately 7%, measured in model compound systems. [1, 12] This value corresponds to an average moisture content in the compound of 2.0 to 2.5%, the evaporation of water during mixing not taken into consideration. Measurements of the water concentration in the compound silanized with and without air injection respectively show, that the moisture content is only slightly influenced by air injection: It is not seen that the silanization rate is significantly influenced by a reduction of the moisture content when air injection is applied.

As air injection turned out to be a very effective measure, production tests were carried out to confirm the observations in small scale mixing. These tests reproduced the trend found on smaller scale: Air injection reduces the Payne effect, thus increases the silanization efficiency (Figure 6). This measure is relatively easy to implement in a production mixer: existing valves, for example the valves used for oil injection, can be used during the silanization step to inject the air. The production results, as well as the tire tests, did not show any negative influence of air injection compared to the material produced according to the standard process, but tire tests did show positive effects on the tire performance (see annex 1). Therefore, the production process can be changed to implement air injection without any further adjustments of the compound and the processing parameters with the exception of rotor speed, which might have to be adjusted to compensate for the cooling effect of air injection.

The combination of both measures, working in an open mixer with air injection, results in an addition of both effects, as illustrated in Figures 7 and 8. Ethanol concentration, which is already lowered by working in an open mixer, can be further reduced by air injection. As the air current used for these experiments is very strong, it can be assumed, that the ethanol concentration in the vapor

phase is very low. Air injection alone results in a slightly lower silanization efficiency compared to the combination of working in an open mixer together with air injection: When air injection is used in a closed mixer, the air can not escape fast enough, representing a bottleneck for the air stream. A further improvement of the silanization efficiency when air injection is used can be achieved by implementing outlets for the air.

The temperature control unit settings influence the heat transfer from the compound to the cooling water. A higher cooling efficiency results in a higher energy input necessary to keep the temperature at a constant level. This requires a higher rotor speed, resulting in an increased renewal rate of the surface of the compound. As the rate of devolatilization of the rubber compound is mainly determined by the surface renewal rate, this measure will enhance devolatilization and thus improve the silanization efficiency. The decrease of the Payne effect with decreasing cooling water temperature, as illustrated in Figures 9 and 10, gives evidence of this effect. The effect is more pronounced for the experiments carried out in the T4 mixer with the ZZ2 rotors (Figure 9): In this case, the Payne effect is on a higher level compared to the situation in the T7 mixer with the F4W rotor (Figure 10), so the benefit that can be gained by decreasing the cooling temperature of the T4 mixer is higher than the benefit that can be gained in the T7 mixer. After silanization in the T7 mixer, the Payne effect values are very low, close to minimum achievable values; therefore the effect of a reduction of the cooling temperature is less pronounced compared to the situation in the T4 mixer.

The area in the mixing chamber underneath the ram is critical for the mixing efficiency. Practical experience shows, that an excessive condensation of ethanol is found in this area, resulting in stick slip behavior. The material is not regularly pulled into the area between the rotors and is therefore passing the high shear zones less frequently. Condensation of ethanol might be reduced by heating the ram, and this should result in an improvement of the mixing behavior and an increase of the silanization efficiency. However, ram heating turned out to have a negative effect on the silanization efficiency. In this case two contradictory effects are superimposed: Firstly, a reduced condensation on the ram due to the higher ram temperature improves the mixing behavior: If wetting of the compound surface by condensed ethanol is reduced, the compound is less slip-sensitive and the material is pulled into the rotor-rotor gap more regularly. This results in a more effective mixing and a more effective silanization, because the devolatilization rate is increased due to the higher surface renewal rates. The second aspect is the thermal balance of the compound, which is also affected by the ram heating: A higher temperature level of the ram increases the material temperature, thus decreases the energy input required to keep the temperature level required for silanization. A lower energy input results in a lower surface renewal rate and a lower silanization efficiency, as explained above. If the cooling effect of air injection is also taken into consideration, the compound silanized in a mixer with the ram heating off

and the air injection on should show the lowest Payne effect values, combined with a high specific energy input. This conclusion can indeed be drawn from Figure 11.

The balance of these two effects, less condensation versus heating of the compound, determines the final effect of ram heating on the silanization efficiency: In this case, the negative effect of the reduction of the surface renewal rate is more pronounced than the positive effect of reduced slip, resulting in a negative influence of ram heating. Another effect that has to be taken into consideration, is scorch: If the material remains in the area underneath the heated ram for a longer period, it might heat up too far and scorch reactions may occur.

The experiments with different hopper constructions shown in Figure 12 underline once again, that ethanol removal is a crucial point for the improvement of the silanization efficiency. It also shows that silanization with air injection and exertion of pressure, the case of the mixer closed with a perforated ram, results in the highest silanization efficiency. Improving the intake behavior of the compound during silanization in an open mixer by reducing the hopper opening area also has a positive effect, but the effect is less pronounced compared to the other alternative: The shearing forces, which are applied in the mixer with the perforated ram, further improve the dispersion and silanization of the filler. The standard mixer mode in this case was silanization in an open mixer, which already resulted in a higher silanization efficiency compared to silanization in a closed mixer. The additional effect achieved by adjusting the hopper design is not very large compared to the effects of the open mixer mode.

The influence of rotor design on silanization behavior is comparatively limited. The most prominent difference between the four rotor types compared in this series of experiments is the low silanization efficiency of the T7-SI rotor (Figure 13). This rotor was originally designed for a good intake behavior, important as silanization was done in an open mixer, and for a good temperature control. However, the low silanization efficiency is an indication that these improvements are not effective for the present case. One explanation for the insufficient performance of the T7-SI rotor is the total number of revolutions, as shown in Figure 15: The number is significantly lower compared to all other cases, resulting in a low surface renewal rate and a low devolatilization rate. The silanization rate of the mixer with the ZZ2 rotor is comparable to the rate measured for the other two rotors, the PES5 rotor and the F4W, but with the disadvantage of a high energy input for the mixer equipped with the ZZ2 rotor. The performances of the mixer with the PES5 rotor and the mixer with the F4W are comparable up to 145ºC; only at higher temperatures the mixer with the F4W rotor shows lower Payne effect values. However, at these high temperatures the risk of scorch is higher using the F4W rotor, as the temperature control is less effective.

6. CONCLUSIONS

In this investigation different mixers, rotors and mixing process variations were tested concerning their influence on the efficiency of the silanization process on laboratory scale as well as in a production plant. The following factors were found to increase the silanization efficiency:

○ *Mixing pressure-less in an open mixer:* After mixing and dispersion, the following silanization step can be done in a pressure-less mode in an open mixer. This enhances ethanol evaporation and thus increases the silanization efficiency. The best way to achieve this is working with two mixers: one standard mixer (preferably with intermeshing rotor geometry) for mixing and dispersion, followed by the silanization step done in a specially designed reactor. The role of the silanization reactor is to keep the temperature on the desired level, to create a high level of fresh surface for devolatilization of the compound and to allow the ethanol to escape out of the reactor.

○ *Air injection:* This measure has a positive effect on the silanization efficiency without negatively influencing the properties of the material. If air injection is applied during silanization in a closed mixer, the air outlet is the bottleneck. The combination of air injection with working in an open mixer adds the positive effects of the two measures.

○ *Temperature control settings:* Intensive cooling of the mixing chamber and the rotors increases the silanization efficiency due to a better devolatilization of the compound.

○ *Rotor design:* The differences in silanization efficiency observed between the rotors tested in this study are rather small. All commonly used rotor types (ZZ2, PES5, F4W) perform similarly. The intermeshing PES5 rotor gives the best overall performance, as it combines good silanization efficiency with low energy requirements.

Table XIV shows the different processing parameters, which are identified in this investigation to have an influence on the silanization efficiency. The cooling efficiency is the most important factor, as it is influenced by all processing parameters except for the type of coupling agent used in the compound. Another important factor is the ethanol transfer across the compound/vapor interphase that is influenced by rotor speed, fill factor, compound temperature, mixer mode and the application of air injection. Factors like ethanol condensation, energy input, ethanol concentration in the vapor phase, contact between the mixer wall and the compound and intake behavior are other factors influencing the silanization efficiency. For an optimization of the equipment and the process for silanization the first two factors, cooling efficiency and ethanol transport out of the compound, must be optimized.

*Table XIV: The influence of different processing parameters
on the factors influencing the silanization efficiency*

Factors improving the silanization efficiency / Operational processing parameters	Reduction of ethanol condensation	Increase of cooling efficiency	Increase of mass transfer (devolatilization)	Increase of energy input	Decrease of energy input efficiency	Reduction of ethanol concentration in vapor	Improving wall contact	Improving intake behavior
Rotor speed		↑	↑					x
Fill factor	x	↑	↓		↓	↓	↑	x
TCU settings	↑	↓		↓		↓	↑	
Compound temperature		↑	↑	↑	↑	↓		x
Open/closed mixer	o	c	o		x	o	c	c
Air injection	↑	↑	↑	↑		↑		
Coupling agent [1]	x				x	x		

[1] *Coupling agent not influencing the rheology of the compound*

↑ Increase, ↓ decrease of the processing parameter for improvement

x No clear influence

7. REFERENCES

1. Luginsland, H.-D., in *11. SRC conference*, 1999, Puchov, Poland.
2. Reuvekamp, L.A.E.M., ten Brinke, J.W., van Swaaij, P.J., Noordermeer, J.W.M., in *Kautschuk Herbst Kolloquium*, 2000, Hannover, Germany.
3. Reuvekamp, L.A.E.M., in *Thesis: Reactive mixing of silica and rubber for tyres and engine mounts*, 2003, Dept. Rubber Technol., Univ. Twente: Enschede (the Netherlands).
4. Joshi, P.G., Cruse, R.W., Pickwell, R.J., Weller, K.J., Hofstetter, M.H., Pohl, E.R., Stout, M.F., Osterholtz, M.F., 2002, http://www.cromptoncorp.com/ck_prd/tpr_us_en_x_nxtsilane.pdf.
5. Früh, T., Steger, L., Heiliger, L., in *Kautschuk Herbst Kolloquium*, 2002, Hannover, Germany.
6. ten Brinke, J.W., van Swaaij, P.J., Reuvekamp, L.A.E.M., Noordermeer, J.W.M., in *Am. Chem. Soc. Rubber Div. conf.*, October 17-21, 2001, Cleveland, Ohio.
7. Joshi, P.G., Cruse, R.W., Pickwell, R.J., Weller, K.J., Sloan, W.E., Hofstetter, M., Pohl, E.R., Stout, M.F., Tire Technol. Int., **2004**: p. 166.
8. Peter, J., Sandau, H., 23.3.1999, Continental AG: DE 199 13 047 A 1.
9. Reuvekamp, L.A.E.M., Debnath, S.C., ten Brinke, J.W., van Swaaij, P.J., Noordermeer, J.W.M., in *Am. Chem. Soc. Rubber Div. conf.*, October 8-11, 2002, Pittsburgh, Pennsylvania.
10. Berkemeier, D., Haeder, W., Rinker, M., Rubber World, **July 2001**: p. 34.
11. Lin, C., in *Am. Chem. Soc. Rubber Div. conf.*, October 17-19, 2001, Cleveland, Ohio.
12. Hunsche, A., Görl, U., Koban, H.G., Lehmann, Th., Kautsch. Gummi Kunstst., 1998, **51**(7-8): p. 525.

CHEMICAL ENGINEERING MODEL

OF

DEVOLATILIZATION IN AN INTERNAL MIXER

During mixing of a rubber compound containing silica and silane, the mixer is not only used for the dispersion of the filler and other ingredients, but also for a chemical reaction. These two functionalities of the mixer result in opposite processing requirements: A good dispersion is reached by high shearing forces, increasing the compound temperature. The silanization is not depending on high shearing forces; it is positively influenced by high temperatures, but with an increasing risk of pre-scorch. Another drawback is the fact, that the equilibrium between the ethanol concentration and the vapor phase in the void space of the mixing chamber and in the rubber phase is limiting the reaction rate of the silanization. Devolatilization of the compound is a crucial factor for the efficiency of the silanization reaction.

In this chapter a model for devolatilization of a rubber compound in an internal mixer is developed, including a chemical reaction replenishing the volatile component during the devolatilization process. The model is based on the penetration theory, with the main contribution to the devolatilization being the mass transfer. It is compared with experimental data, resulting in the conclusion that the situation in the internal mixer can best be described by mass transport between the surface layer of the rubber phase and the vapor phase.

1. INTRODUCTION

Devolatilization during mixing in an internal mixer is based on a flux of the volatile component across the interphase between the rubber compound and the free space in the mixing chamber, the vapor phase. The rubber phase has a characteristic distribution and flow pattern in the mixing chamber, that can basically be described by rolling pools of material in front of the rotor flights and a periodically refreshed layer of material covering the walls of the mixing chamber. Figure 1 shows these areas and the material flows as modeled for an extruder process. This flow pattern can be transferred to the situation in an internal mixer: a pool of material is rotating in front of each rotor flight, and a part of the material is wiped onto the mixer chamber wall. [1]
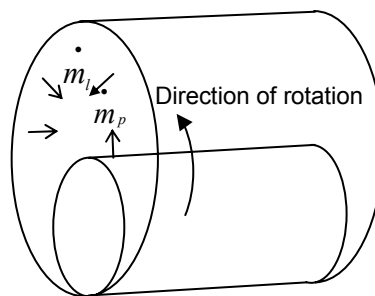
Figure 1: Devolatilization from the wall layer and rotating pool in an internal mixer

The model consists of two cylindrical pools of material, one of them solid and representing the material pool in front of the screw flight, the other one hollow and representing the layer on the barrel wall. Both pools rotate with the same circumferential speed and they touch in the tip clearance. The flows of the volatile components are both directed into the void space, with the flow out of the wall layer indicated by subscript l, and the flow out of the pool in front of the flights indicated by subscript p.

All the models for the devolatilization of highly viscous materials described in literature are based on extrusion processes, in general using vacuum technology. The model developed by *Latinen* [2] is focused on extrusion processes with the attempt to include the effect of axial dispersion. It is based on two separate processes: devolatilization from the layer wiped on the barrel wall and devolatilization from the surface of the material pool. Depletion of the volatile component takes place by molecular diffusion through the outer layer of the film on the wall and of the rotating pool material, and by evaporation from the interphases with the vapor phase. In this model the wall layer is assumed to be continually refreshed by the wiping action of the screw, the characteristic feature of the penetration model. Shortcomings of this model are a difference between the predicted and actual surface areas for diffusion, and the neglected viscoelastic properties of the material.

A different approach was used by *Coughlin* and *Canevari*. [3] They modeled devolatilization in a single-screw extruder as unsteady state mass transfer from a stagnant film. Estimations for the diffusion coefficients and the mass transfer coefficients for a drying process show, that this process is more accurately described by a mass transfer coefficient model than by an effective diffusion coefficient model.

Roberts [4] estimated the ratio of the devolatilization rate from the wall layer and the pool material surface in an extruder. He identified the wiped wall layer as a major contributor to devolatilization due to its large surface area.

Biesenberger [1] looked at devolatilization in a single-screw extruder by using the separation of the material into the wall layer and the rotating pool. Geometrical and processing parameters as well as the efficiency are summarized in dimensionless numbers. Special attention was paid to the residence time as a consequence of changes of the screw speed and the wall layer thickness. The estimated values of the diffusivity ID from different research groups were compared with calculated data with the result, that the calculated values were in general higher than the measured values. This lead to the conclusion that a mechanism far more rapid than diffusion is rate-determining in devolatilization.

The first approach to model devolatilization of a polymeric solution in a co-rotating intermeshing twin-screw extruder was done by *Collins, Denson* and *Astarita*. [5, 6] They defined the devolatilization process as evaporation from the semi-infinite layer on the mixing chamber wall and the pool of material. The mass transfer rate during devolatilization was described in terms of a liquid phase mass transfer coefficient, a driving force and the surface area effective in devolatilization. The mass transfer coefficient depends on material properties, process variables and equipment variables. The basic model used was the penetration model, and it predicts the influence of the rotor speed correctly. However, in fitting their model to actual measurements, they had to conclude that the model overestimates the surface area for mass transfer of the wall layer and the pool.

Valsamis [7, 8] based his work on the models developed by Biesenberger and Denson. He determined the influence of geometric parameters, operational conditions and physical properties on the efficiency of devolatilization in a non-intermeshing, counter-rotating twin-screw mixing extruder. Temperature, rotor speed, fill factor and flow rate were identified as main operational and independent variables of the process.

Foster and *Lindt* [9, 10] used a penetration diffusion approach to model the mass transfer for devolatilization in the same type of extruder as used by Valsamis. As a condition to the application of the penetration theory they define unsteady-state diffusion in every fluid element at the liquid-vapor interphase. The surface

replacement rate must be high enough to result in an exposure time of the interphase significantly shorter than the characteristic time for diffusion, resulting in only a limited contribution of diffusion to the devolatilization.

Keum and *White* [11] analyzed the devolatilization in intermeshing co-rotating twin-screw extruders. They stated, that bubble-free devolatilization can be described by the penetration theory. The efficiency of the devolatilization is increasing with screw speed and initial feed rate of the volatile component. The interfacial area was found to be independent of barrel temperature. However, the mass transfer coefficient was found to increase with barrel temperature as well as with increasing screw speed. They correlated the efficiency of removal of the volatile component with the Hildebrand solubility parameters.

The model of extruder-devolatilization developed by *Wang* [12-14] was also based on the penetration theory, but with the assumption that the exposure time of the surface of the material is not constant, but has a certain distribution. This corresponds to the surface replacement theory described in paragraph 3.3. They related the efficiency of devolatilization to a dimensionless number representing the geometry of the local interphase between the devolatilized material and the vapor, as well as the exposure time.

2. MASS BALANCE

The microscopic mass balance for the volatile component of a volume element consists of a diffusion term, a flow term and a term for a chemical reaction:

$$\frac{\partial c}{\partial t} = \underbrace{\text{ID}\ \frac{\partial^2 c}{\partial x^2} + \text{ID}\ \frac{\partial^2 c}{\partial y^2} + \text{ID}\ \frac{\partial^2 c}{\partial z^2}}_{\text{Diffusion}} \underbrace{- v_x \frac{\partial c}{\partial x} - v_y \frac{\partial c}{\partial y} - v_z \frac{\partial c}{\partial z}}_{\text{Flow}} + \underbrace{CR}_{\text{Reaction}} \qquad \textit{Eq. 1}$$

In this equation, c is the concentration, ID is the diffusion coefficient, v is the velocity of the volume elements and CR is a term representing the contribution of the chemical reaction. The flow term describes the exchange of the position of volume elements due to flow of the material. It is dependent on the velocity of the volume elements and the concentration gradient. The exchange rate is low for laminar flow and high for turbulent flow. Only viscous flow is taken into consideration, because elastic flow, the reversible exchange of volume elements, does not result in a net flow and is therefore not changing the local concentration within the material.

2.1. DIFFUSION

Diffusion is described by *Fick*'s law. The driving force for diffusion is a concentration gradient within the material, resulting in a flow of a component

from areas of high concentration to areas of low concentration. As the concentration is represented as a second derivative, this term is stronger influenced by the concentration gradient than the flow term. It is proportional to the diffusion coefficient ID. This coefficient represents the mass transfer through a surface and is expressed in the rate per area and per unit time. It is based on the Brownian motion law.

The diffusion of a volatile component in a rubber compound in an internal mixer can be described as the diffusion in thin, periodically renewed layers, either on the chamber wall or on the surface of the rolling pool in front of the rotor flight. These layers can be modeled as semi-infinite slabs in which diffusion is uni-directional:

$$\frac{\partial c}{\partial t} = -ID \ \frac{\partial^2 c}{\partial x^2}$$

Eq. 2

The initial concentration of the volatile component at time t = 0 at any x-value is c_i. At infinite time t = ∞ the concentration of the component at the interphase reaches equilibrium with the vapor phase, c_{eq}. The solution to Equation 2 using these boundary conditions is an error-function: [9]

$$\frac{c - c_{eq}}{c_i - c_{eq}} = -erf \ \frac{x}{\sqrt{4 \cdot ID \cdot t}}$$

Eq. 3

The following assumptions are made:

o   The diffusion coefficient is independent of the concentration of the volatile component and the temperature
o   The penetration depth for diffusion is small compared to the layer thickness
o   The initial concentration of the volatile component is uniform within the layer and equal to the concentration in the pool of material

Diffusion coefficients for volatile components in polymeric materials given in literature are in the range of 10^{-9} m^2 sec^{-1} [1, 7], whereas exposure times of the layer on the chamber wall are less than 1 second. Assuming diffusion in a semi-infinite slab, the calculation of the concentration gradient of the volatile material is confined to a very thin layer of the order of 0.05 mm. [4] The thickness of the layer on the chamber wall may be assumed to be equal to the clearance between the flight tip and the chamber wall. In standard mixing equipment this clearance is a few millimeters up to one centimeter, depending on the size of the mixer. Thus, the thickness of the layer is much larger than the thickness over which the concentration gradient is established during one period of exposure. The semi-infinite slab has an initial uniform concentration c_i, and diffusion occurs from the surface into a reservoir with a lower concentration of the volatile material.

The extent, to which diffusion occurs, depends on the diffusion coefficient ID, the concentration gradient within the rubber material and the temperature. The diffusion coefficient is a measure of the mobility of the volatile component in the matrix. The driving force for a molecule to diffuse through the matrix is the affinity between the molecule and the matrix material. This affinity is related to chemical compatibility, dipole-dipole interactions and van der Waals forces. A way to quantify the affinity is to compare the solubility parameters of the volatile component and the matrix: the closer the solubility parameters, the higher the affinity. Another influencing factor for diffusion is the friction force generated when molecules are migrating through the matrix. Systems with a low affinity between the matrix material and the diffusing components, with dense matrix materials and bulky diffusing components have low diffusivity.

2.2. Material Flow Across the Interphase With a Vapor Phase

In the absence of a chemical reaction, mass transfer of the volatile component by flow is characterized by the velocity of the volume elements moving to the interphase due to external forces. This movement can follow the typical flow patterns like laminar flow, turbulent flow or any stages in between, but it can also be a special flow pattern caused by the particular processing device. In an internal mixer, the flow induced mass transfer is caused by periodically wiping a thin layer of material onto the chamber wall and refreshing the surface of the rolling pool of material in front of the rotor flights.

If diffusion is slow, mass transfer is dominated by the flow of material in the mixing equipment. Material having a concentration of the volatile component c_i is transported from the pool to the surface. At the interphase with the vapor phase, mass transfer occurs and the concentration of the volatile component in the surface layer changes into the equilibrium concentration c_{eq}. The mass flux is then proportional to the difference between the actual concentration of the volatile component in the pool material c_i and the equilibrium concentration in the surface layer c_{eq}, and to the mass transfer coefficient k_{MT}:

$$\dot{m} = k_{MT}(c_i - c_{eq}) \qquad \qquad Eq.\ 4$$

The volatile component in the surface layer is in equilibrium with the adjacent phase, in this case a vapor phase containing the volatile component with a partial pressure p. This equilibrium is determined by Henry's law, with k_H being Henry's constant:

$$c_{eq} = p / k_H \qquad \qquad Eq.\ 5$$

Figure 2 illustrates the concentration profile within the pool material changing in time.
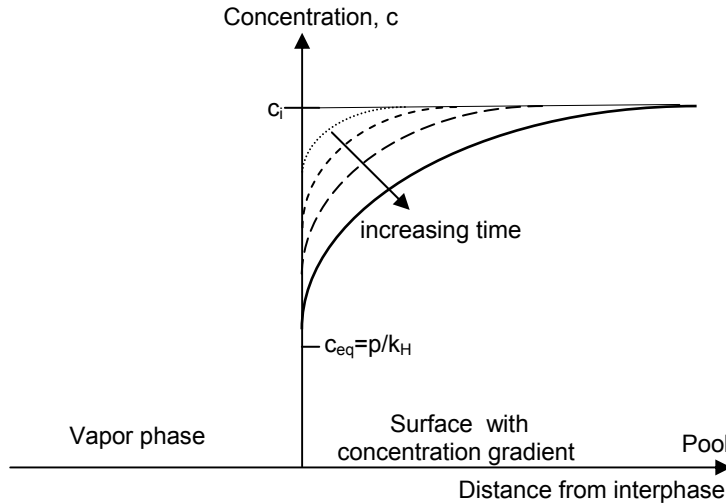
Figure 2: Concentration profile in the surface layer
as a function of the distance from the interphase

2.3. MATERIAL FLOW ACROSS THE INTERPHASE IN COMBINATION WITH A CHEMICAL REACTION

The rate of change of the concentration of the volatile component due to a chemical reaction depends on the order of the reaction. For a first order reaction, the reaction rate R is proportional to one of the concentrations of the starting component, for example the concentration of the silane coupling agent c, with k_I being the proportionality factor or reaction rate constant of a first order reaction:

$$R = k_I \cdot c \qquad\qquad \textit{Eq. 6}$$

The primary reaction, the reaction of the first ethoxy-moiety of a silyl group, is much faster than the secondary reaction, the reaction of the remaining ethoxy groups. [15-19] The kinetics of the reaction are determined by the former reaction, the reaction of one ethoxy group per silyl group with a silanol-moiety resulting in one molecule of ethanol. The secondary reaction is not necessary for the attachment of the coupling agent to the silica.

In this case the concentration in a closed system changes in time according to the following expression:

$$\frac{dc}{dt} = -k_I \cdot c \qquad\qquad \textit{Eq. 7}$$

The starting concentration at time t = 0 is c_0. Integration of Equation 7 results in:

$$\ln \frac{c}{c_0} = k_I \cdot t \qquad\qquad Eq.\ 8$$

The concentration of the coupling agent, which is related to the concentration of the volatile component ethanol in the reactor, is changing exponentially with reaction time t, if no concentration changes due to mass flux through the interphase occur.

In a combination of chemical reaction and mass flux through the interphase, equilibrium between the vapor phase and the surface layer of the bulk material is finally reached, and the concentration of the volatile component in the surface layer of the bulk of material reaches the equilibrium value according to Henry's law, c_{eq}. The concentration of the volatile component in the bulk of material reaches a steady state, c_{ss}: Concentration changes due to mass transfer and to the chemical reaction balance each other. The mass transfer reduces the concentration of the volatile component at the interphase, but at the same time it is replenished by the chemical reaction and the flow of material. The material balance is given by Equation 9:

$$A \cdot k_{MT} \cdot (c_{eq} - c_{ss}) = k_I \cdot V \cdot c_{ss} \qquad\qquad Eq.\ 9$$

The mass flux between the bulk and the vapor phase is determined by the surface area across which the mass transfer occurs, A, and the difference of the concentration of the volatile component in the bulk of material c_{ss}, and the equilibrium concentration in the surface layer c_{eq}. The change in the amount of the volatile component by the chemical reaction is proportional to the volume of the reacting media V and the concentration of the volatile component c_{ss}, with a proportionality factor k_I. Elimination of the steady state concentration c_{ss} shows, that the mass flux per unit length and time depends on geometrical factors such as volume and surface area of the bulk material, kinetic factors such as mass transfer coefficient and reaction rate constant as well as the concentration of the volatile component in equilibrium with the vapor phase:

$$\dot{m}_{l,t} = \frac{V}{A} k_I \cdot c_{eq} \left(\frac{A \cdot k_{MT}}{A \cdot k_{MT} + V \cdot k_I} \right) \qquad\qquad Eq.\ 10$$

3. MATERIAL TRANSFER BY FLOW AND DIFFUSION: FILM, PENETRATION AND SURFACE REPLACEMENT THEORIES

The exchange of material between the vapor phase and the bulk rubber phase in a mixing device consists of a diffusion and a material flow part. For the further specification of the mass transfer coefficient k_{MT}, three theories for the

material transfer between these phases are known: film theory, penetration theory and surface replacement theory.

3.1. FILM THEORY [20-22]

This theory, developed by *Hatta*, assumes a linear concentration gradient within a thin surface layer: the film. Mass transfer occurs only by diffusion, with the concentration gradient Δc over the thickness of the film being the driving force. The mass flux m, in mol per square meter per second, is then calculated as follows:

$$\dot{m} = k_{MT} \cdot \Delta c = \frac{\text{ID}}{\delta} \Delta c \qquad \text{Eq. 11}$$

The mass transfer coefficient k_{MT} is determined by the diffusion coefficient ID and the film thickness δ:

$$k_{MT} = \text{ID}/\delta \qquad \text{Eq. 12}$$

This theory is based on a static film with a constant thickness δ. The time-dependence of the mass flux is given by the changes in time of the concentration gradient within the film. The diffusion coefficient ID for liquid systems is of the order of 10^{-9} $m^2 sec^{-1}$, resulting in mass transfer coefficients in the range of 10^{-5} to 10^{-6} $m\ sec^{-1}$ for films with a thickness between 1 and 0.1 mm.

3.2. PENETRATION THEORY [21]

In this theory introduced by *Higbie*, small flow elements are transported to the interphase, for example in turbulent flow, where they stay for a characteristic time of exposure t_e. After the exposure, these elements return into the bulk of the material to be mixed again with the pool material. In this case, the mass flux additionally depends on the exposure time t_e:

$$\dot{m} = k_{MT} \cdot \Delta c = 2 \cdot \Delta c \sqrt{\text{ID}/\pi \cdot t_e} \qquad \text{Eq. 13}$$

The exposure time t_e is equal for all flow elements and determined by the flow pattern of the material. The mass transfer coefficient depends on the exposure time as well as on the diffusion coefficient:

$$k_{MT} = 2\sqrt{\text{ID}/\pi \cdot t_e} \qquad \text{Eq. 14}$$

The mass transfer coefficient for liquid systems is of the order of 10^{-6} $m\ sec^{-1}$.

3.3. SURFACE REPLACEMENT THEORY [21]

This theory, developed by *Danckwaerts*, is an extension of the penetration theory. It assumes the exposure time to be variable, and its distribution is given by the following equation:

$$f(t_e) = RR \cdot e^{-RR \cdot t}$$

Eq. 15

This distribution depends on the fractional replacement rate of the area exposed to penetration, RR. According to this theory the mass transfer coefficient is proportional to the square root of RR and ID:

$$k_{MT} = \sqrt{RR \cdot \mathrm{ID}}$$

Eq. 16

Equations 12, 14 and 16 are valid for systems with purely physical changes of concentrations. However, these theories can also be applied to systems wherein a chemical reaction takes place, since a reaction in general only marginally influences the flow pattern of the material. In the case of a combination of mass transfer and chemical reaction two time scales have to be taken into consideration. The first one is the time scale of diffusion, exposure time and surface replacement rate, and the second one is the time scale of the chemical reaction. [21]

Diffusion becomes the dominating process when the mass transfer due to flow is very small: this is the case when the exposure time of the surface layer in the penetration theory or the average lifetime of the volume element in the surface replacement theory is long compared to the time necessary for diffusion through the layer. Very thin films also result in an increase of the contribution of diffusion to mass transfer.

3.4. SUITABILITY OF THE THEORIES FOR RUBBER MIXING

The main difference between the three model theories is the balance between diffusion and material flow: the film theory describes the mass flux as the resultant of diffusion only, whereas the penetration and the surface replacement theories contain both processes: mass flux by diffusion and by material flow.

If a chemical reaction has to be taken into account, the ratio of the concentration change due to mass transfer versus the change due to the chemical reaction determines the difference between the models. If the chemical reaction is very fast (high value of the reaction constant k_l), the starting components are present in very low concentrations and the products of the chemical reaction are present in high concentrations. The concentrations are not significantly changed by mass transfer, thus no differences will be seen

between the different models. A similar reasoning is valid for a very slow reaction: the concentration of the starting components is very high and the product concentration is low, again resulting in almost constant concentrations. Only in a case, when the concentration changes due to mass transfer and chemical reaction are of the same order of magnitude, both processes mutually influence each other and differences will be found, depending on the model that is used. Figure 3 shows the reaction factor, the ratio of the mass transfer coefficients with and without chemical reaction, depending on the reaction constant for a first order reaction k_l.

The penetration model and the surface replacement model differ slightly in the case that the rate of the chemical reaction and mass transfer are of the same order. For large values of these characteristic times, the system reaches a steady state diffusion-reaction pattern, and in this case the two models do coincide.
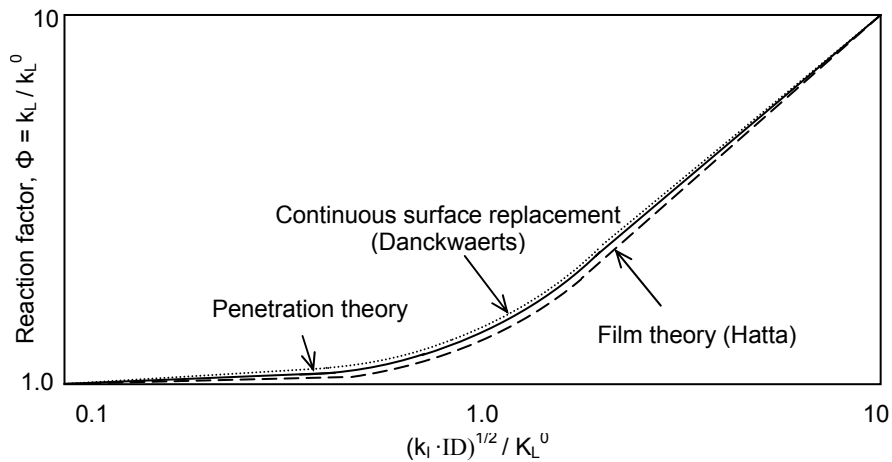
Figure 3: Comparison of the three model theories of mass transfer, combined with a first order chemical reaction [20]

For the silanization step of silica compound mixing, the major part of the devolatilization takes place in a layer on the mixing chamber wall, while this layer is constantly renewed by the rotor movement. The film theory does not hold as it is based on a static film with a time-dependent decreasing concentration gradient over the film thickness. In an internal mixer the wall layer is periodically refreshed by the rotor movement, resulting in a constant exposure time of the surface of the film at constant rotor speed, the characteristic parameter of the penetration model. Therefore, the penetration theory is the most appropriate for this case.

4. THE PENETRATION THEORY APPLIED TO A RUBBER MIXER USED FOR DEVOLATILIZATION WITHOUT CHEMICAL REACTION

Devolatilization, for example the removal of residual solvent or monomer from a polymer solution, is an important unit operation in polymer processing. In practice, it is mainly done in extruders equipped with vacuum units. Therefore, most theories to describe this process are based on extruder devolatilization. [12] In the following paragraph, the penetration theory will be applied to devolatilization in an internal mixer.

Looking at the flow pattern in an internal mixer, the predominant characteristic is surface replacement of the layer on the chamber wall as observed in a tangential mixer, and of the surface of the pool material in front of the rotor flight. The constant exposure time t_e of the wall layer and the pool surface is the determining factor for the mass flow of the volatile component. In the following the penetration theory will be further detailed for this case.

The following assumptions are made:

o The flows are fully developed
o The pool material is homogeneous
o The concentration of the volatile component in the layer on the mixing chamber wall is renewed with every pass of the rotor flight
o The extraction is isothermal
o The diffusion coefficient is independent of the concentration of the volatile component in the rubber compound
o The concentration of the volatile component in the vapor phase is uniform
o No bubble formation or foaming of the rubber compound
o The longest relaxation time of the compound material is shorter than the exposure time of the wall layer
o The resistance to mass transfer across the interphase is negligible

The rubber compound in the mixing chamber is divided into two areas with different mass flow characteristics: the layer on the mixing chamber wall and the rolling pool of material in front of the rotor flight. This situation is illustrated in Figure 4, where the cylindrical geometry of the mixer walls is represented in a planar manner.
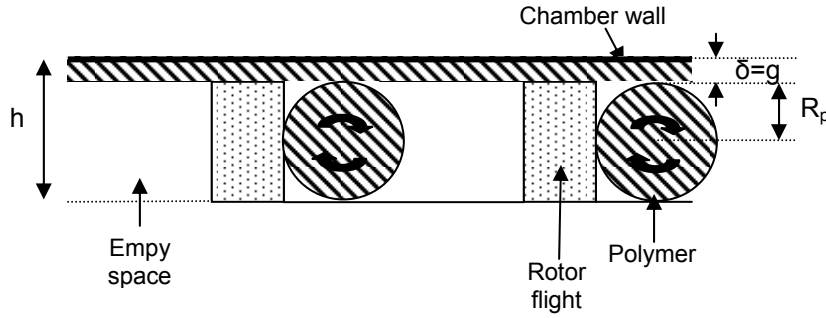
Figure 4: Cross section of a partially filled mixing chamber

During the revolution of the rotor, material from the pool is wiped onto the mixing chamber wall, and this layer is periodically renewed. The lifetime of the layer, the exposure time $t_{e,l}$, is the time between two adjacent flights passing a certain position, and is determined by the rotor speed N and the number of flights n_f:

$$t_{e,l} = \frac{1}{N \cdot n_f}$$

Eq. 17

The shape of the pool material in front of the flight will be approximated to be cylindrical. The surface replacement rate of this area can now be calculated from the rotor speed N, multiplied by a factor representing the ratio of the wall circumference of one mixer hemisphere and the pool circumference. The exposure time of the pool surface $t_{e,p}$ is:

$$t_{e,p} = \frac{1}{N_p} = \frac{1}{N \cdot R_M} \sqrt{\frac{V_M \cdot FF}{4\pi \cdot L_M} - g \cdot R_M}$$

Eq. 18

N_p is the surface renewal rate of the pool, V_M is the net volume of the mixing chamber, FF is the fill factor, L_M is the length of the mixing chamber, g is the clearance between the rotor tip and the mixing chamber wall and R_M is the radius of the mixing chamber. The expression under the square root is the radius of the pools, expressed in dimensions of the mixing chamber and the fill factor. An estimation of the exposure time for a 50 liter mixer with a fill factor of 70%, running with a rotor speed of 60 rpm and having a rotor with two flights, results in a wall layer exposure time of 0.5 seconds and a pool surface exposure time of approximately 0.3 seconds.

The surface of the wall layer A_l can be simulated by two flat slabs with a length equal to the free part of the inner circumference of the mixing chamber and the second dimension taken as the length of the rotor, L_M:

$$A_l = 4\pi \cdot R_M \cdot L_M$$

Eq. 19

87

It is assumed that the mixing chamber consists of two identical parts with each half of the full inner surface. The wall layer is released from the wall immediately due to the relaxation of the material resulting in contraction. Therefore the wall layer has two interphases with the vapor phase in the mixing chamber, one towards the wall and one towards the middle of the mixing chamber. The actual situation in a mixer varies between this situation of a complete wall layer and a situation, in which the wall layer contracts that far, that the layer breaks and separate volume elements are formed. [23, 24]

The volume of the pools depend on the fill factor, therefore their surface area is also dependent on the fill factor. The volume of the wall layer is constant, determined by the geometrical dimensions of the mixer, given that sufficient material is present. All additional material goes into the pools in front of each rotor. Their surface area can be calculated from the total volume of the compound by subtracting the volume of the wall layer and dividing by 4, corresponding to one pool in front of each rotor flight.

$$A_p = 8\pi \cdot L_M \sqrt{\frac{V_M \cdot FF}{4\pi \cdot L_M} - g \cdot R_M} \qquad \qquad \textit{Eq. 20}$$

In this calculation the individual geometrical factors such as the helix angle of the flights, the ratio of tip clearance to wall layer thickness, the land width of the flights as well as surface roughness of the compound surface are not taken into consideration. The calculation of the surface area of the wall layer and the pool using the above mentioned data results in areas of 1.5 m^2 and 0.9 m^2, respectively, for the 50 liter mixer.

This model is valid for the situation in a tangential mixer with a complete wall layer and 4 pools, one in front of each rotor flight. The following assumptions are made for this model:

- Each rotor has two long flights
- All material is distributed between the 4 pools and the surface layer
- The pools rotate, and their complete surface area is in contact with the vapor phase

With respect to the wall layer the following situation is assumed:

- It exists in half of the circumference of each mixing chamber hemisphere
- It exists during the period between the passes of two rotor flights
- It releases from the wall immediately after passage of the rotor flight without change of surface area

The situation in a mixer with intermeshing rotors is different: The wall layer does not exist, and all the material is distributed in cylindrical pools. Additionally to the pools in front of each rotor flight, another pool exists above the clearance between the two rotors where the material is brought into the mixer, and is assumed to exist over the whole length of the mixing chamber. This pool is larger than the pools in front of the rotor flights and serves as a reservoir of material, with which the rotor flights exchange material when they are passing. For this mixer type it is assumed that the volume of the large reservoir pool is double compared to the volume of one small pool in front of a rotor wing. The reservoir turns with the same circumferential speed as the rotor tip, and the surfaces of the reservoir pool as well as the flight pools are continuously renewed. In this case, the surface areas and the exposure times are calculated as follows:

$$A_p = 8\pi \cdot L_M \sqrt{\frac{V_M \cdot FF}{6\pi \cdot L_M}} \qquad\qquad Eq.\ 21$$

$$A_{res} = 2\sqrt{2}\pi \cdot L_M \sqrt{\frac{V_M \cdot FF}{6\pi \cdot L_M}} \qquad\qquad Eq.\ 22$$

$$t_{e,p} = \frac{\sqrt{V_M \cdot FF / 6\pi \cdot L_M}}{N \cdot R_M} \qquad\qquad Eq.\ 23$$

$$t_{e,res} = \frac{\sqrt{V_M \cdot FF / 3\pi \cdot L_M}}{N \cdot R_M} \qquad\qquad Eq.\ 24$$

For a 50 liter intermeshing mixer with a fill factor of 70% and a rotor speed of 60 rpm, the exposure time of the surface of the pools in front of the rotor flights is 0.23 seconds, and the exposure time of the surface of the reservoir pool is 0.33 seconds. The surface areas are 0.8 m^2 and 0.28 m^2, respectively.

As explained earlier, the most appropriate model for a mixer is the penetration model. In this case the amount of the volatile component removed per unit time from a unit area of the surface, q, is proportional to the mass transfer coefficient and to the concentration difference between the actual concentration c in the rubber compound and the equilibrium concentration of the volatile component at the interphase c_{eq}: [7]

$$q = k_{MT}(c - c_{eq}) = 2\sqrt{\frac{ID}{\pi t_e}}(c - c_{eq}) \qquad\qquad Eq.\ 25$$

The total rate of devolatilization Q is the product of q and the area A across which devolatilization occurs:

$$Q = q \cdot A = 2\sqrt{\frac{\text{ID}}{\pi \cdot t_e}}(c - c_{eq})A \qquad \textit{Eq. 26}$$

The partial rates of devolatilization for the layer on the mixing chamber wall Q_l and the pool surface Q_p are:

$$Q_l = 2\sqrt{\frac{\text{ID}}{\pi \cdot t_{e,l}}}(c - c_{eq})A_l \qquad \textit{Eq. 27}$$

$$Q_p = 2\sqrt{\frac{\text{ID}}{\pi \cdot t_{e,p}}}(c - c_{eq})A_p \qquad \textit{Eq. 28}$$

5. EFFICIENCY OF MASS TRANSFER IN AN INTERNAL MIXER [1]

The efficiency of mass transfer by evaporation for one step can be defined as follows:

$$E_j \equiv \frac{c_{j-1} - c_j}{c_{j-1} - c_{eq}} \qquad \textit{Eq. 29}$$

For the wall layer, one step is defined as the period between two passes of adjacent flights. For step j, the situation just before the layer is refreshed is compared with the situation before the layer is deposited or, in other words, at the end of the prior step with the subscript j-1. The efficiency of such an evaporation step E_j is given by the ratio of the actual reduction of the concentration of the volatile component in the matrix, c_{j-1}-c_j, and the theoretically maximum achievable reduction of the concentration, c_{j-1}-c_{eq}. The concentration c_j is the concentration at the end of the evaporation step, c_{j-1} is the starting concentration being similar to the end concentration of the prior step, and c_{eq} is the equilibrium concentration of the volatile component in the rubber matrix at the interphase with the vapor phase. This equation is valid under the assumption that density and volume of the system are not changing due to the devolatilization.

The concentration change within one step then depends on the time of exposure of the surface t_e, which is the time period until the layer is completely renewed by the rotor movement:

$$c_{j-1} - c_j = f(t_e) = \int_0^{t_e} r(t)dt \qquad \textit{Eq. 30}$$

The rate function r(t) is an expression for the evaporation per unit volume and time. It is proportional to the ratio S_V of the total evaporation area to the volume of the batch, to the concentration difference as the driving force of the evaporation and to the mass transfer coefficient k_{MT}:

$$r(t) = S_V[c(t) - c_{eq}]k_{MT} \qquad \textit{Eq. 31}$$

The rate function r(t) in Equation 31 can be averaged over time, and this equation can then be expressed in the following way:

$$k_{MT} \cdot S_V = \frac{r(t)}{[c_{j-1} - c_{eq}]} = \frac{\frac{1}{t_e}f(t_e)}{[c_{j-1} - c_{eq}]} = \frac{c_{j-1} - c_j}{t_e[c_{j-1} - c_{eq}]} = \frac{E_j}{t_e} \qquad \textit{Eq. 32}$$

The efficiency of one evaporation step E_j can be calculated from the mass transfer coefficient k_{MT}, the ratio of the area of evaporation to the batch volume S_v and the exposure time t_e:

$$E_j = \frac{c_{j-1} - c_j}{c_{j-1} - c_{eq}} = S_v \cdot k_{MT} \cdot t_e = \frac{A}{V} \cdot \frac{2}{\sqrt{\pi}} \sqrt{\frac{ID}{N \cdot n_f}} \qquad \textit{Eq. 33}$$

Equation 33 shows, that the efficiency of one single step depends on the following factors:

o *Diffusion coefficient ID*: The higher the diffusion coefficient, the higher the efficiency. The effect is limited due to the proportionality to the square root of *ID*. As a consequence, the efficiency can slightly be increased by raising the diffusion coefficient, for example by a higher temperature.

o *Rotor speed N*: A lower rotor speed increases the exposure time, whereby the efficiency of the devolatilization between two rotor flight passes increases.

o *Number of rotor flights*: A higher number of flights decreases the exposure time and thus decreases the efficiency of the devolatilization within one step. If the efficiency for a given period of devolatilization is calculated, a higher number of flights results in an increased total efficiency.

- ○ *Surface area A*: A larger surface area through which mass transport occurs increases the efficiency.

- ○ *Volume V*: The larger the volume of the material, the lower the devolatilization efficiency caused by the decreasing surface to volume ratio.

For a multiple step devolatilization process, it is assumed that the degree of devolatilization relative to the concentration difference with the equilibrium concentration is equal for each step, resulting in a steady-state component balance for the whole process:

$$E_j = \frac{c_{j-1} - c_j}{c_{j-1} - c_{eq}} = const \qquad\qquad Eq.\ 34$$

The whole devolatilization process in the mixer can then be regarded as a series of n_R reactors, with E_j being equal for all steps of the cascade of reactors. The overall efficiency E is then determined by the concentration after n_R steps, c_{n_R}, the concentration at the beginning, c_0, and the equilibrium concentration, c_{eq}:

$$E = \frac{c_0 - c_{n_R}}{c_0 - c_{eq}} \qquad\qquad Eq.\ 35$$

This equation can be transformed into a function of the number of steps:

$$1 - E = \frac{c_0 - c_{eq}}{c_0 - c_{eq}} - \frac{c_0 - c_{n_R}}{c_0 - c_{eq}} = \frac{c_{n_R} - c_{eq}}{c_0 - c_{eq}} = (1 + \Psi)^{-n_R} \qquad\qquad Eq.\ 36$$

with

$$\Psi \equiv \frac{E_j}{1 - E_j} \qquad\qquad Eq.\ 37$$

Transformation of the very left and very right part of Equation 36 into an expression for the overall efficiency E results in:

$$E = 1 - e^{-n_R \Psi} \qquad\qquad Eq.\ 38$$

The efficiency of one single step, E_j, is rather low; therefore the value of Ψ is very small:

$$\Psi = \frac{E_j}{1 - E_j} \ll 1 \qquad\qquad Eq.\ 39$$

As E_j is close to zero, $(1-E_j)$ is close to 1, and Ψ can be taken equal to E_j. By replacing Ψ in Equation 38 by the efficiency for one step, E_j, we get the following expression:

$$E = 1 - e^{-n_R \cdot E_j} \qquad \textit{Eq. 40}$$

As shown in Figure 4 for a mixer with tangential rotor geometry, the total evaporation is divided into evaporation from the wall layer and evaporation from the pool material. The wall layer with a surface area A_l exists for a period $t_{e,l}$, and the pool with a surface area A_p exists for a period $t_{e,p}$. The efficiency of one step is the sum of the partial efficiencies multiplied by the respective volume ratios. If the partial rates of devolatilization are calculated according to Equations 27 and 28, the efficiency for a single step E_j is given by:

$$E_j = 2\sqrt{\frac{\text{ID}}{\pi t_{e,p}}} t_{e,p} \cdot S_{V,p} \frac{V_p}{V} + \sqrt{\frac{\text{ID}}{\pi t_{e,l}}} t_{e,l} \cdot S_{V,l} \frac{V_l}{V} = 2\frac{\sqrt{\frac{\text{ID}}{\pi}}}{V} \left(A_p \sqrt{t_{e,p}} + A_l \sqrt{t_{e,l}} \right) \qquad \textit{Eq. 41}$$

By replacing the efficiency E_j in Equation 41 by Equation 40, the following expression for the overall efficiency of a process of n_R stages results:

$$E = 1 - \exp\left[-\frac{2 \cdot n_R \sqrt{\frac{\text{ID}}{\pi}}}{V} (A_p \sqrt{t_{e,p}} + A_l \sqrt{t_{e,l}}) \right] \qquad \textit{Eq. 42}$$

In a mixer with intermeshing rotor geometry the same equation is valid, when the wall layer exposure time and surface area is replaced by the respective time and area of the reservoir pool.

This equation shows that the overall efficiency of the devolatilization process in the internal mixer depends on the following factors:

○ Number of steps n_R, being equal to the number of passes of the flights of one rotor over each position
○ Total volume of the compound in the mixer V
○ Surface area of the wall layer and the pool, A_l and A_p
○ Exposure time of the surface of the wall layer and the pool, $t_{e,l}$ and $t_{e,p}$

The processing parameters such as temperature, rotor speed, fill factor and ram pressure are influencing the above mentioned parameters. The machine parameters such as gap clearance, channel clearance, dimensions of the mixing chamber and the rotor as well as net volume are influencing the volume, the surface area of the pool and the exposure time of the pool.

6. MODELING THE INFLUENCE OF DIFFERENT PARAMETERS ON THE DEVOLATILIZATION EFFICIENCY

In order to visualize the influence of number of passes, rotor speed, fill factor and mixer size on the devolatilization efficiency, Equation 42 is detailed for a hypothetical internal mixer using the parameters as given in Table I.

6.1. INFLUENCE OF THE ROTOR SPEED

Table I shows the standard parameters used in the calculations below. If different parameters are used, they are explicitly indicated for the respective figures.

Table I: Parameters used for the modeling of the devolatilization efficiency

		Tangential	Intermeshing
Volume of the mixing chamber, V_M	$[m^3]$	0.05	0.05
Standard fill factor, FF	[%]	0.7	0.7
Standard rotor speed, N	[rpm]	60	60
Diameter mixing chamber, D_M	[m]	0.43	0.62
Length mixing chamber, L_M	[m]	0.55	0.55
Rotor tip clearance, g	[m]	0.004	---
Exposure time of the pool surface, $t_{e,p}$	[seconds]	0.30	0.16
Exposure time of the wall layer, $t_{e,l}$	[seconds]	0.50	---
Exposure time of the reservoir pool, $t_{e,res}$	[seconds]	---	0.23
Surface area of the pool, A_p	$[m^2]$	0.90	0.80
Surface area of the wall layer, A_l	$[m^2]$	1.49	---
Surface area of the reservoir pool, A_{res}	$[m^2]$	---	0.28
Diffusion coefficient, ID	$[m^2\ sec^{-1}]$	10^{-9}	10^{-9}

The diffusion coefficient used in the modeling is an average value for diffusion in a liquid matrix at ambient temperature. Diffusion coefficients in polymeric materials are difficult to calculate as they strongly depend on concentration of the volatile component and temperature. Temperature dependence is not taken into consideration for the calculation. [7]

Figure 5 shows the influence of rotor speed on the efficiency of the devolatilization in a tangential and an intermeshing mixer, calculated according to Equation 42. The efficiency is calculated as a function of the number of passes of the flights over a certain position along the chamber wall.
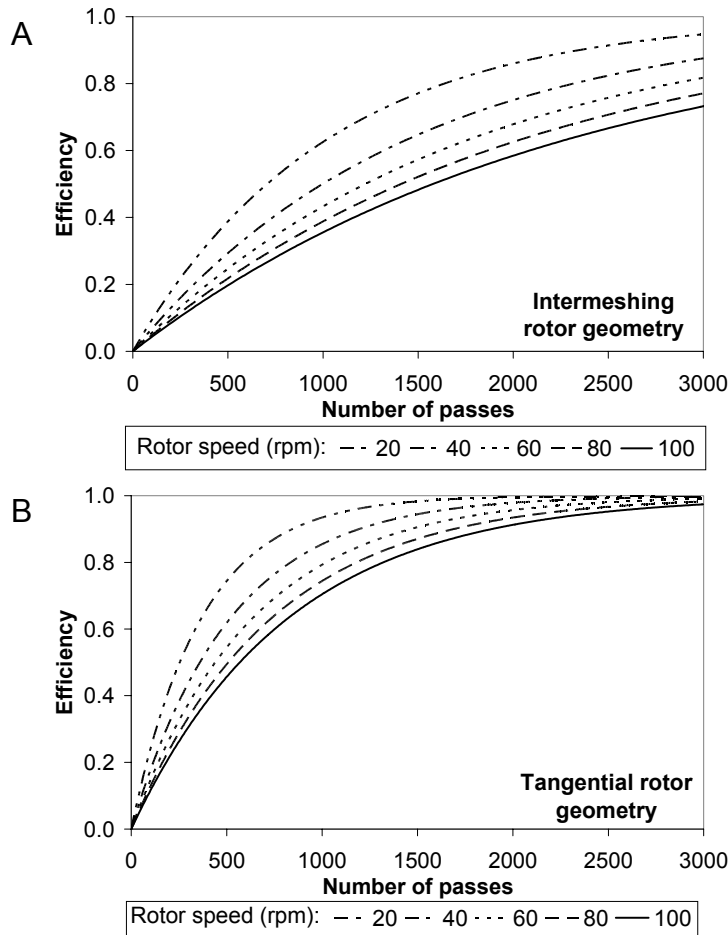
*Figure 5A and B: The influence of the rotor speed
on the efficiency versus number of passes*

A lower rotor speed results in a higher efficiency for the same number of passes. This is a consequence of the longer total exposure time, which is the product of the exposure time per pass and the number of passes. In Figure 6 the efficiency as a function of the total exposure time is shown. For a given total exposure time, which is equal to the process time, a higher rotor speed results in higher efficiency: The frequency of surface replacement is higher. Therefore, devolatilization is more efficient, as the driving force, the difference between the actual concentration in the bulk and the equilibrium concentration of the volatile component in the surface layer of the pool or wall layer and the concentration in the vapor phase, is maximized in each pass.
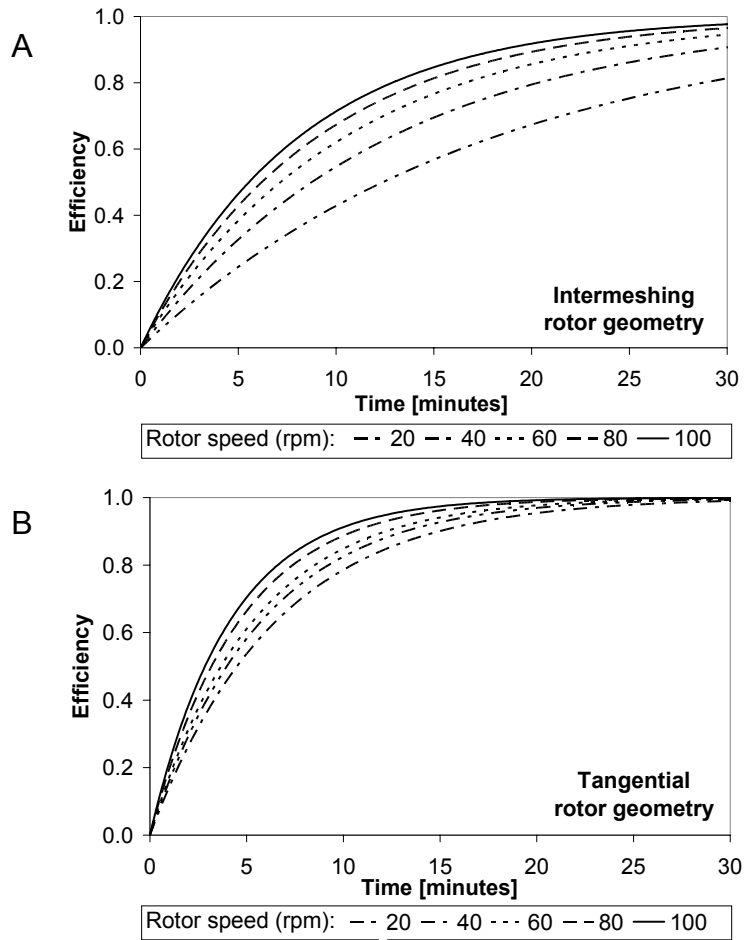
*Figure 6A and B: The influence of the rotor speed
on the efficiency versus time*

In this simulation, the mixer with tangential rotor geometry is more efficient than the mixer with intermeshing rotors. This due to the higher total free surface area of the compound in the tangential mixer compared to the compound in the intermeshing mixer: For the standard mixer and parameters given in Table I, the total free surface area of the compound in the tangential mixer is 2.4 m^2, and the free surface area in the intermeshing mixer is 1.1 m^2. As the efficiency of the silanization is strongly affected by ethanol transport across the interphase between the rubber phase and the vapor phase in the mixer, a larger free surface area will positively influence evaporation and silanization.

6.2. INFLUENCE OF FILL FACTOR

The influence of the fill factor on the efficiency of the devolatilization process is illustrated in Figure 7.
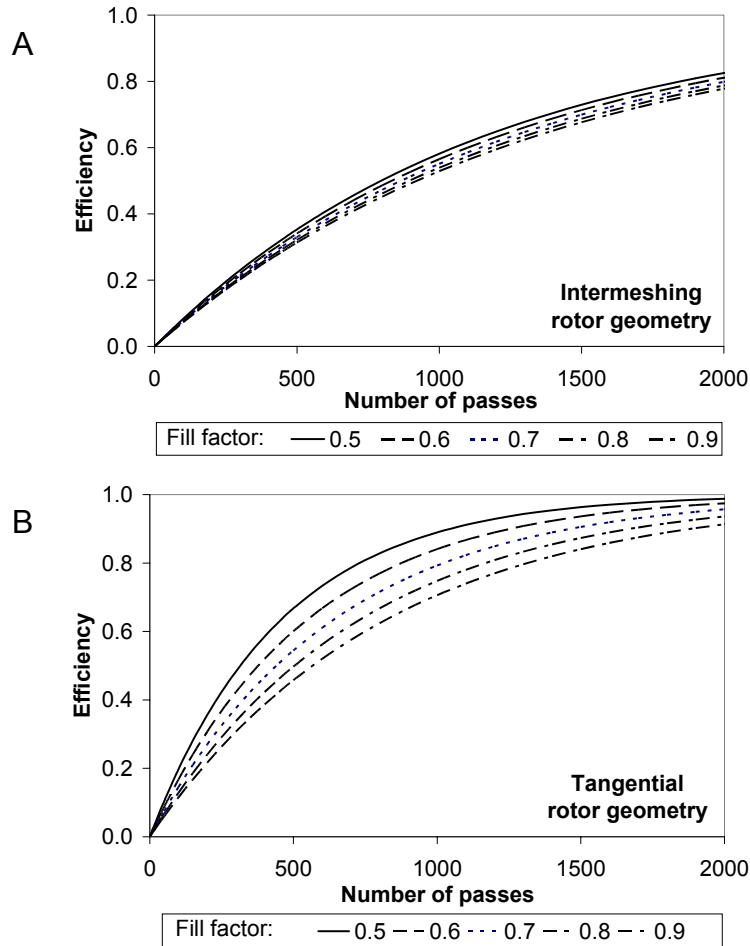
*Figure 7A and B: The influence of the fill factor
on the efficiency versus number of passes*

A lower fill factor, with all other parameters kept constant, results in a higher efficiency. This is a consequence of three factors: an increasing void volume in the mixer, an increasing ratio of surface area to volume of the compound and an increasing surface renewal rate with decreasing fill factors. Devolatilization in a mixer with intermeshing rotors is less sensitive to fill factor variations.

The decreasing dispersion efficiency of the mixing process, once a threshold value of the fill factor is surpassed, is not taken into consideration. In this case the devolatilization efficiency will decrease, because the coupling agent and the filler are not homogenously distributed, resulting in concentration mismatches of the two components.

6.3. UPSCALING

Figure 8 shows the influence of the scale up of the mixing chamber on the devolatilization efficiency.
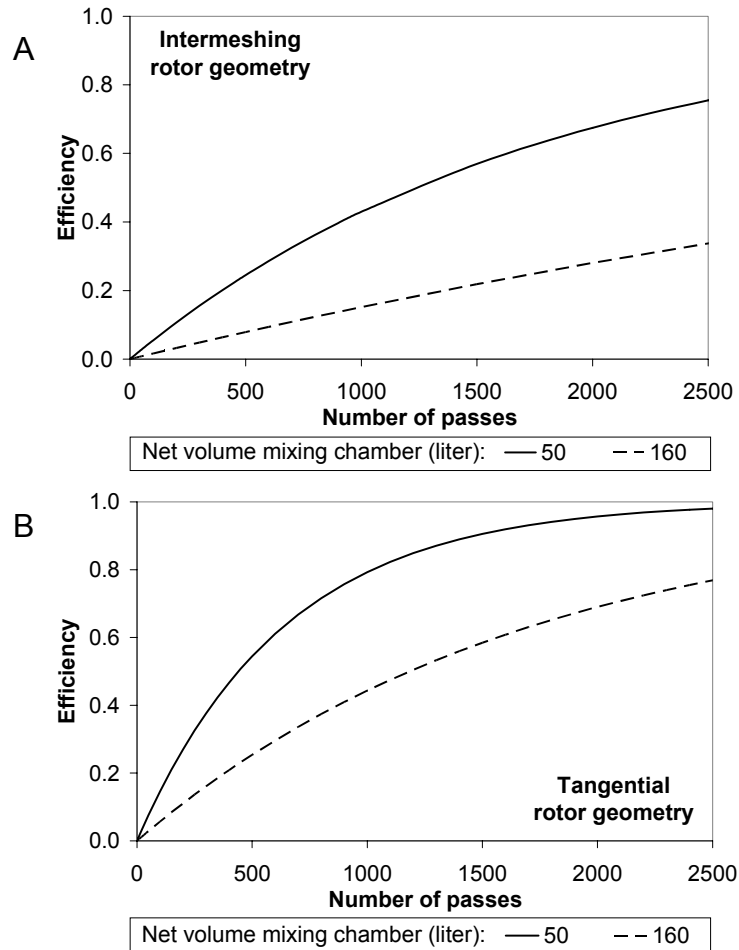
*Figure 8A and B: The influence of the mixing chamber volume
on the efficiency versus number of passes*

As usual, upscaling is done in a geometrical, proportional manner with the diameter and the length of the mixing chamber increased. [25] The surface areas of the pool, A_p, and of the wall layer, A_l, are increased accordingly. The volume of the pool and the layer on the mixer wall are also recalculated. All other factors are as given in Table I. A variation of the rotor clearance, the gap between the rotor flight and the mixing chamber wall, other than proportionality is not taken into consideration. A variation of these geometrical parameters would influence the wall layer thickness and the shearing forces applied to the rubber material, but both factors are not directly influencing the devolatilization efficiency, as defined by the penetration theory.

Upscaling has a drastic effect on the devolatilization efficiency: the number of passes to reach 90% efficiency is three times higher for a 160 liter tangential mixer compared to a 50 liter tangential mixer. The reason for the loss of

efficiency in upscaling is the decrease of the ratio of surface area to compound volume: this ratio is approximately 40 for the 50 liter mixer and 25 for the 160 liter mixer. The smaller mixer has a relatively larger surface area per unit volume, resulting in a faster devolatilization.

7. THE PENETRATION THEORY APPLIED TO A RUBBER MIXER USED FOR DEVOLATILIZATION WITH CHEMICAL REACTION BETWEEN SILICA AND SILANE

7.1 EXTENSION OF THE MODEL TO INCLUDE A CHEMICAL REACTION

The model can be extended to include a chemical reaction: Equations 27 and 28 allow the calculation of the mass transfer of the volatile component, as it depends on the concentration difference between the actual concentration c and the equilibrium concentration c_{eq} at the interphase. When a chemical reaction is involved, the actual concentration in the rubber material not only depends on the mass transfer due to flow and diffusion, but also depends on the reaction rate.

In paragraph 2.3., Equation 7, the reaction rate of a first order equation is defined as follows:

$$\frac{dc}{dt} = -k_I \cdot c \qquad\qquad Eq.\ 43$$

The concentration c is referring to either one of the starting components. Integration of this equation results in the following expression:

$$\ln\frac{c}{c_0} = k_I \cdot t \qquad\qquad Eq.\ 44$$

The concentration c_0 is the initial concentration of the rate-determining starting component, and c is the actual concentration of this component at time t. The molar concentration of the reaction product c_{rp} is correlated to the concentration of the starting component by the stochiometric equation for the reaction.

In the present case it is assumed that one molecule of the starting product reacts to give one molecule of the final product. In the case of the triethoxysilane as starting material this implies that only one ethoxy group per silane molecule is reacting, resulting in one ethanol molecule. This assumption is justified as the reaction rate of the primary reaction, the reaction with the first ethoxy group of a silane molecule, is significantly faster than the reaction of the second and third ethoxy group. [15, 16, 19] Equation 44 can be transformed into an exponential expression:

$$c = c_0 \cdot e^{-k_I \cdot t} \qquad\qquad \textit{Eq. 45}$$

Replacing the concentration of one of the starting materials, c, by the concentration of a reaction product, c_{rp}, results in:

$$c_{rp} = c_0 - c = c_0 - c_0 \cdot e^{-k_I \cdot t} = c_0 (1 - e^{-k_I \cdot t}) \qquad\qquad \textit{Eq. 46}$$

For the system silica-coupling agent in a rubber compound, two periods can be distinguished: the initial period of the reaction between the silica and the ethoxy groups of the coupling agent, during which the concentration of the coupling agent decreases and the ethanol-concentration in the rubber matrix increases according to the first order kinetic law. After this period, equilibrium is reached and the concentration of ethanol does not change any more: the rate of ethanol generation is equal to the rate of devolatilization by mass transfer.

During the first period, the mass transfer rate for a volatile reaction product is expressed by Equation 26, however now with c being the concentration of the reaction product, the volatile component ethanol. This concentration of the reaction product c corresponds to the expression for c_{rp} in Equation 46. The equilibrium concentration of the volatile component c_{eq} is given by Henry's law: Equation 5. The expression for the flow rate then results in:

$$Q = 2 \sqrt{\frac{\mathrm{ID}}{\pi \cdot t_e}} [c_0 (1 - e^{-k \cdot t}) - \frac{p}{k_H}] A \qquad\qquad \textit{Eq. 47}$$

The flow rate of the volatile reaction product can be increased by an increase of the diffusion coefficient ID of the volatile component in the rubber matrix, by decrease of the exposure time t_e, by an increase of the concentration of the volatile component in the surface layer and by an increase of the surface area. The factor representing Henry's law has to decrease for an increase of the flow rate: Reducing the partial pressure of the volatile component in the empty space in the mixer as much as possible also has a positive effect.

After a certain time the second period begins: The generation of ethanol by the chemical reaction and the depletion of the rubber matrix due to mass transfer reach equilibrium with a constant concentration of ethanol in the rubber matrix. At this stage the mass transfer per unit time to the empty space is equal to the amount of volatile product generated by the chemical reaction. The chemical reaction as such is also in an equilibrium state, expressed by a constant ratio K_{CR} of the concentration of the reaction product c_{rp} to the actual concentration of the starting material c_{sm} (silane):

$$\frac{c_{rp}}{c_{sm}} = K_{CR}$$

Eq. 48

In this practical case, c_{sm} represents the silane concentration and c_{rp} the ethanol concentration. This equation is valid under the earlier mentioned assumption that only the first ethoxy group of the silane reacts to account for the first order reaction.

The expression for the flow rate, Equation 47, again has to be applied to the devolatilization from the wall layer and from the pool of rubber, subscript l and p respectively, similar to Equations 27 and 28. The concentration $c_{rp,eq}$ represents the concentration of the reaction product in the chemical equilibrium as defined by Equation 48. The concentration c_{eq} refers to the equilibrium between the surface of the rubber material and the vapor phase at the interphase.

$$Q = 2\sqrt{\frac{\mathrm{ID}}{\pi \cdot t_{e,l}}}(c_{rp,eq} - c_{eq})A_l + 2\sqrt{\frac{\mathrm{ID}}{\pi \cdot t_{e,p}}}(c_{rp,eq} - c_{eq})A_p$$

Eq. 49

The equilibrium of the chemical reaction is shifted by mass transfer: Without the contribution of the chemical reaction, the equilibrium concentration of the volatile product in the rubber compound would slowly be reduced by mass transfer. The chemical reaction results in an immediate replenishing of the concentration according to the above mentioned first order kinetics. When mass transfer and chemical reaction remain in balance, the concentration changes due to both processes are similar and the material balance can be calculated by combining Equation 43 with Equation 49:

$$Q\frac{t}{V} = [2\sqrt{\frac{\mathrm{ID}}{\pi \cdot t_{e,l}}}(c - c_{eq})A_l + 2\sqrt{\frac{\mathrm{ID}}{\pi t_{e,p}}}(c - c_{eq})A_p]\frac{t}{V} = k_I \cdot c \cdot t \quad (t > t_{eq})$$

Eq. 50

7.2 COMPARISON OF THE CALCULATED MASS FLUX WITH AND WITHOUT CHEMICAL REACTION, WITH ACTUAL MEASUREMENTS

Figure 9 shows the devolatilization of a compound in an internal mixer during a continuous mixing cycle, with and without chemical reaction. The amount of volatile component removed from the rubber compound without chemical reaction as a function of time is calculated by Equation 51. This equation is the combination of Equations 27 and 28, giving the partial rates of devolatilization for the pool material and the wall layer, multiplied by time.

$$Q \cdot t = [2\sqrt{\frac{\text{ID}}{\pi \cdot t_{e,l}}}(c - c_{eq})A_l + 2\sqrt{\frac{\text{ID}}{\pi \cdot t_{e,p}}}(c - c_{eq})A_p] \cdot t \qquad \textit{Eq. 51}$$

The parameters given in Table I are used for the modeling. The ethanol concentration c_{eq} in the rubber material in equilibrium with the vapor phase is assumed to have a constant value of 0.01 kg m^{-3}. The assumption is justified by the observation that the concentration of ethanol in the void space of the mixing chamber, the partial pressure, reaches saturation. Ethanol is either transported out of the mixing chamber by ventilation or condensation on cooler parts of the mixing chamber. The initial value of the actual concentration c is chosen to be equal to the measured steady state concentration of ethanol in the rubber material, 0.21 kg m^3. This value was measured after 20 minutes of silanization at 135ºC in a 7 liter tangential mixer with a good reproducibility.
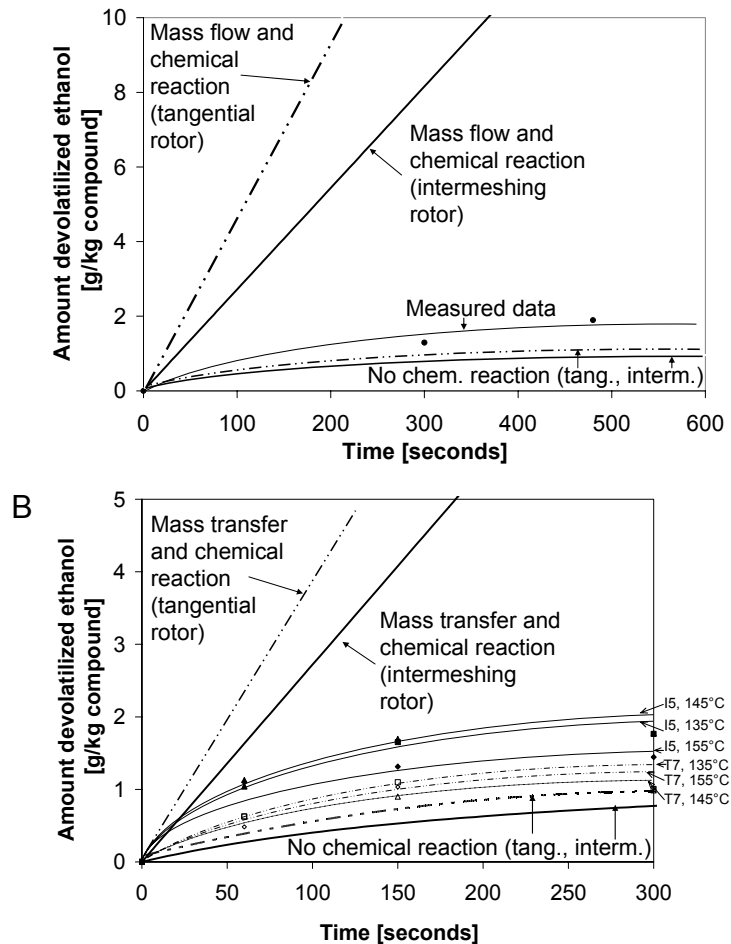

Figure 9A and B: Devolatilization model and actual measurements
(A: literature data [26, 27], B: project measurements)

The case, that mass flux is combined with a chemical reaction, is also shown in Figure 9. In this case, equilibrium between mass flux and chemical reaction is assumed, resulting in steady state conditions characterized by a constant

concentration of ethanol in the compound. The calculation of the mass flux is made according to Equation 50, which describes the steady state situation in which all removed ethanol is immediately replenished by ethanol generated in the chemical reaction. Again the data in Table I are used for the calculation, c_{eq} is 0.01 kg m^{-3} and c_{ss} is 0.21 kg m^{-3}.

The lines illustrating the actual measurements are positioned in between the theoretical lines representing the two different cases. It indicates that steady state equilibrium between the chemical reaction and the mass flux is not reached. The amount of ethanol transported out of the rubber compound is higher than the amount of ethanol generated by the silanization reaction, resulting in a decreasing concentration of ethanol in the rubber compound.

The experimental lines correspond better to the simulated case without chemical reaction. The generation of ethanol by the chemical reaction is significantly slower than the ethanol transport out of the compound. The efficiency of the silanization is then predominantly influenced by the physical process of ethanol transport across the interphase with the vapor phase in the mixing chamber. The simulation of the mass transfer with and without chemical reaction again results in a higher devolatilization rate for the mixer with tangential rotors, as seen earlier.

The measurements shown Figure 9B show a different trend: They result in a higher devolatilization rate for the intermeshing mixer. One of the reasons for the contradictory results is the choice of the model. In the model for the tangential mixer, it is assumed that a stable wall layer exists during the total exposure time, and that this layer is released from the mixer wall resulting in two interphases. This assumption leads to a maximum surface area, which in a mixer actually may not exist. The wall layer will partly retract from the wall, but the distance to the wall will be small, and the vapor phase between the wall and the compound will be saturated with ethanol very rapidly. A part of the wall layer may contract that far, that the layer breaks, resulting in a reduced surface area. Another assumption is the availability of the complete surface of the pool material, but in actual practice the pool will touch the mixer wall and the rotors, and the effective surface area will be smaller. The model for the situation in the intermeshing mixer is also different from the actual situation: The material will be sheeted out in the narrow gap between the rotors, and possibly some material will be sheeted out or particulated in the gap between the rotor tip and the mixing chamber wall, both effects resulting in an increase of the surface area in the intermeshing mixer.

Another critical point of this comparison is the experimental setup of the investigations shown in Figure 9B, which are not exactly the same. In this particular case, the main difference between the two series of experiments is the number of flights on the rotor: The intermeshing rotor has three flights, while the tangential rotor has only two large flights. This will again improve the

efficiency of the silanization in the mixer with the intermeshing rotor, as the surface area is increased.

All these differences between the actual situation and the idealized situation as assumed in the model will result in a smaller surface area for the compound in the mixer with the tangential rotor geometry and a larger surface area for the compound in the mixer with the intermeshing rotor geometry, which can result in an inversion of the trend.

8.   CONCLUSIONS

The devolatilization of a component in an internal mixer can be described by a model based on the penetration theory. The main characteristic of this model is the separation of the bulk of material into two parts: a layer periodically wiped onto the wall of the mixing chamber, and a pool of material rotating in front of the rotor flights. This flow pattern results in a constant exposure time of the interphase between the material and the vapor phase in the void space of the internal mixer.

Devolatilization occurs according to two different mechanisms: molecular diffusion between the fluid elements in the surface layer of the wall film and the pool, and mass transport between the rubber phase and the vapor phase due to evaporation of the volatile component. As the diffusion rate of a liquid or a gas in a polymeric matrix is rather low, the main contribution to devolatilization is based on the mass transport between the surface layer of the polymeric material and the vapor phase.

The model for silanization in an internal mixer, as developed here, demonstrates the following positive factors to enhance the silanization:

- o   High operation temperature (limited by scorch phenomena) in order to raise the speed of the silane reaction with silica and the diffusion coefficient of the ethanol formed
- o   Small mixer volume, rather than large
- o   Low fill factor of the mixer
- o   High rotor speed
- o   Long reaction/mixing time
- o   Low partial pressure of ethanol in the void space of the mixer

Verification of the experimental model with experimental data shows, that under conditions depicted above the silanization reaction proceeds fast in the early mixing stages of the mixing procedure. The reaction can be considered as far progressed by the time devolatilization starts. The main driving force for the silanization is then the removal of ethanol from the compound. The extra ethanol still produced in second instance during the devolatilization operation – as a result of the chemical equilibrium reaction or of the reaction of the second and third ethoxy groups of the silane – plays a minor role.

The efficiency of the devolatilization process depends on processing conditions, for example rotor speed and fill factor. It depends on the mixer design, for example number of rotor flights and the size of the mixer, and the material characteristics. The diffusion coefficient of the volatile component in the polymeric matrix is of minor influence.

The silanization process has to be described by a model consisting of mass transfer combined with a chemical reaction. Two limiting cases have been theoretically modeled: mass transfer alone and the combination of mass transfer with a chemical reaction replenishing the evaporated component. Comparison of the experimental data of the silanization in an internal mixer shows that this process does not reach the steady state, indicating that the devolatilization of the rubber compound by mass transfer is much faster than replenishment by the chemical reaction.

The two models chosen for the flow in a mixer with tangential and intermeshing rotor geometry, respectively, illustrate the two extreme cases for each mixer, with the result that the tangential mixer performs better due to a larger surface area of the compound. The real situation in an internal mixer will differ from these cases, and the difference of the free surface area of the compound between a tangential mixer and an intermeshing mixer will be less pronounced.

9. REFERENCES

1. Biesenberger, J.A., Sebastian, D. H., *Principles of polymerization engineering*, 1983, Wiley-Interscience: New York.
2. Latinen, G.A., Am. Chem. Soc. Adv. Chem. Ser., 1961, **34**: p. 235.
3. Coughlin, R.W., Canevari, G.P., AIChE J., 1969, **15**(4): p. 560.
4. Roberts, G.W., AIChe J., 1970, **16**(5): p. 878.
5. Denson, C.D., in *Advances in chemical engineering*, J. Wei, Editor, 1983, Harcourt Brace Jovanovich: New York, p. 61.
6. Collins, G.P., Denson, C.D., Astarita, G., AIChE J., 1985, **31**(8): p. 1288.
7. Valsamis, L.N., Canedo, E.L., in *ANTEC*, 1989, New York, USA.
8. Valsamis, L.N., Canedo, E.L., Int. Polym. Proc., 1989, **IV**(4): p. 247.
9. Foster, R.W., Lindt, J.T., Polym. Eng. Sci., 1990, **30**(11): p. 621.
10. Foster, R.W., Lindt, J.T., Polym. Eng. Sci., 1990, **30**(7): p. 424.
11. Keum, J., White, J.L., Int. Polym. Pro., 2004, **XIX**(2): p. 101.
12. Wang, N.H., Sakai, T., Hashimoto, N., Int. Polym. Pro., 1995, **X**(4): p. 296.
13. Wang, N.H., Polym. Eng. Sci., 2000, **40**(8): p. 1833.
14. Wang, N.H., Chem. Eng. Technol., 2001, **24**(9): p. 957.
15. Luginsland, H.-D., in *11. SRC conference*, 1999, Puchov, Poland.
16. Luginsland, D., Hasse, A., in *Am. Chem. Soc. Rubber Div. conference*, April 4-6, 2000, Dallas,Texas.
17. Hunsche, A., Görl, U., Koban, H.G., Lehmann, Th., Kautsch. Gummi Kunstst., 1998, **51**(7-8): p. 525.
18. Hunsche, A., Görl, U., Mueller, A., Knaack, M., Goebel, Th., Kautsch. Gummi Kunstst., 1997, **50**(12): p. 881.
19. Görl, U., Hunsche, A., Mueller, A., Koban, H.G., Rubber Chem. Technol., 1997, **70**: p. 608.
20. Hatta, S., Tohoku Imperial U. Techn. Rep., 1928, **10**: p. 119.
21. Sherwood, K.S., Pigford, R.L., Wilke, C.R., in *Engineering series*, J.J. Carbery, Peters, M.S., Schowalter, W.R., Wei, J., Editor, 1975, McGraw-Hill: New York.
22. Hatta, S., Tohoku Imperial U. Techn. Rep., 1932, **8**: p. 1.
23. Nijman, G., 2004, personal communication.
24. Limper, A., 2004, personal communication.
25. Funt, J.M., *Mixing of rubbers*, 1977, Rubber and Plastics Research Association of Great Britain: Shawbury (Great Britain).
26. Görl, U., Parkhouse, A., Kautsch. Gummi Kunstst., 1999, **52**: p. 493.
27. Görl, U., Munzenberg, J., Luginsland, H.D., Müller, A., Kautsch. Gummi Kunstst., 1999, **52**: p. 588.

CHAPTER 5

INFLUENCE OF THE MIXING PROCESS

ON THE SILANIZATION KINETICS

This chapter gives an overview of the kinetics of the silanization reaction. Literature data from investigations on model compounds as well as rubber compounds are compared with the results from an analysis of the mixing parameters in an internal mixer on laboratory scale.

The mixing and silanization processes are analyzed in terms of mixer design and process variables. Different rotor geometries and rotor/mixer combinations are tested concerning their performance during the chemical reaction of silanization. Process variables such as fill factor, temperature control settings, air injection and ram position are investigated in order to elucidate their influence on the rate of silanization at different temperatures.

The most effective way to increase the silanization rate is removal of ethanol. This can be accomplished by working in an open mixer with an adjusted fill factor or by applying air injection in order to drag out the ethanol. Air injection allows for an increase of the apparent reaction rate at 145ºC by more than a factor of 2.

Efficient cooling by choosing a low temperature for the cooling fluid and a reduction of the fill factor increase the silanization rate at higher temperatures. Comparison of the different combinations of rotor geometry and mixing chamber does not result in a clear picture: The silanization rate depends on several factors related to the mixing equipment, and all combinations can be optimized by choosing the appropriate processing conditions.

1. INTRODUCTION

The silanization reaction is not a simple single-step reaction, but consists of several steps:

- ○ Diffusion of the silane coupling agent molecules to the active sites on the filler surface
- ○ Adsorption of the silane molecules onto the filler surface
- ○ Hydrolysis of ethoxy groups of the coupling agent
- ○ Reaction of the ethoxy groups with the silanol groups of the filler (primary reaction)
- ○ Reaction of the hydrolyzed ethoxy groups with silanol groups of the silica or adjacent silane molecules (secondary reaction)

In a rubber compound these reactions are preceded by dispersion and distribution of the filler and blending with the coupling agent. Further side-reactions may occur such as homocondensation of the silane without being bound to the filler surface and adsorption of ethanol onto the filler surface.

If all these reactions are taken into consideration, the kinetic of the silanization reaction depends on numerous factors. The diffusion of the silane depends on the temperature of the matrix and the type of silane, the compatibility of the silane with the polymer matrix and steric properties of the silane. The adsorption of the coupling agent is influenced by the surface concentration and accessibility of the silanol groups on the silica surface. The equilibrium concentration of the silane-molecules adsorbed on the silica surface is also depending on the temperature and the presence of other polar molecules that can be adsorbed. The ethoxy groups of the silane molecules react with water in a stepwise process of hydrolysis, but at the same time condensation of the reactive silanol groups occurs, resulting in an equilibrium concentration of more than 10 different reaction products. [1] The kinetics of these reactions are rather complicated, but under certain conditions they can be summarized in a pseudo first order reaction. [2] The primary reaction, the reaction of one ethoxy group per silane molecule with a siloxane group of the filler is a single-step reaction, whose reaction rate depends on the concentration of the reactants and the pH value of the reaction media. The secondary reaction again is a stepwise reaction comprising the hydrolysis and condensation steps, resulting in a variety of factors determining the kinetics of this reaction.

However, the kinetic law can be simplified by identifying the rate-determining step, and by assuring that concentrations of some of the starting components are constant or in excess. It is generally accepted that the overall reaction can be described by a first order reaction law:

$$\frac{d[ethanol]}{dt} = -\frac{d[silane]}{dt} = k_I \cdot [silane] \qquad \qquad \textit{Eq. 1}$$

The term k_l is a pseudo first order constant, as it summarizes the actual reaction rate constant and all other constant factors of the above-mentioned reactions.

Other factors influencing the kinetics are the type of coupling agent, filler characteristics and reaction conditions.

1.1.   THE SILANE

Polarity, geometry and type of functional groups determine the reaction kinetics of a silane. The silanes used for the present application differ in general in terms of the functional group bound to the propyl group. A comparison between the commonly used bis(triethoxysilylpropyl)tetrasulfane and a thiocyanato-propyl-triethoxysilane showed, that the efficiency of the silanization reaction was not influenced by the functional group. However, the reaction rate was different: the thiocyanato-silane reacted faster than the tetrasulfane-silane, probably due to the higher polarity of the former, resulting in a higher affinity to the polar silica surface. [3]

The steric properties of the silane molecule affect the mobility of the silane in the matrix and limit the availability of silanol groups on the filler surface, once the silane is bond to the filler surface. The compatibility of the silane with the filler and the matrix is determined by the differences in polarity and solubility factors. A low compatibility results in a difficult homogenous distribution of the coupling agent in the matrix.

Increasing concentrations of the coupling agent result in an increase of the rate of hydrophobation and shielding of the silica surface during mixing. However, higher concentrations of the coupling agent result in a lower efficiency of the silanization reaction relative to the amount of silane. [3, 4]

1.2.   THE FILLER

Structure of the filler, acidity, moisture content as well as concentration and availability of the silanol groups on the surface are major influencing factors for the kinetic of the reaction with the silane. The structure of the filler influences the silanization kinetic as it is an important characteristic for the filler dispersibility and availability of the silanol groups. The concentration of silanol groups as one component in the silanization reaction is directly determining the rate of silanization. Commonly used silica types have approximately 4 to 5 silanol groups per nm^2 surface. [2, 5-9]

Acidity of the filler has an influence on the reaction rate of the silanization, besides its influence on the curing characteristics. The silanization reaction is catalyzed by bases and by acids. Both, high pH values as well as low pH values are increasing the reaction rate, mainly by increasing the rate of

hydrolysis of the ethoxy groups of the silane. Bases have a stronger effect compared to acids. The primary reaction is more sensitive to the acidity of the reaction media than the secondary reaction. [3, 10, 11]

Both reaction rates, the rate of the primary reaction as well as the rate of the secondary reaction, are influenced by moisture content. The primary reaction is accelerated by increasing concentrations of water in the filler, but it is less sensitive to moisture than the secondary reaction. The rate of the primary step is increasing with increasing moisture content of the filler up to approximately 6%, while the rate of the secondary reaction increases at even higher moisture contents. [4, 11, 12]

1.3. REACTION CONDITIONS

The reaction conditions, such as the presence of other compounding ingredients, reaction temperature, energy input and ethanol removal, influence the silanization reaction. The competing reaction of other additives such as zinc oxide, stearic acid, alcohols and amines influence the kinetics of the silanization reaction as they block active sites on the filler surface. Amines, either as a part of the silane molecule or added separately, have a high affinity to the silica surface and are easily adsorbed, but at the same time they have a catalytic effect on the hydrolysis reaction. [2, 13, 14]

The rates of the primary and the secondary reaction are depending on the temperature. The primary reaction, the reaction of one ethoxy group per silyl group of the coupling agent, starts at lower temperatures than the secondary reaction, during which siloxane bonds are formed between the remaining hydrolyzed ethoxy-moieties or with the silanol groups on the silica surface. It is assumed that at reaction temperatures below approximately 50ºC mainly the primary reaction takes place. This assumption is based on the fact that at this temperature the maximum amount of ethanol generated during the silanization reaction is not exceeding 2 mol of ethanol per mol silane. Homocondensation between silane molecules can also take place, with the ratio between coupling to the filler surface and homocondensation depending on the surface concentration of the silanol groups and their accessibility, as well as the reaction temperature: With increasing temperatures the reaction rate of homocondensation increases. [11, 12, 15, 16] The ratio of the homocondensation of the silane to the reaction of the coupling agent with silanol groups on the silica surface is low under the commonly used processing conditions. The degree of homocondensation is reduced with decreasing moisture contents [10] and by the pH approaching a value of 4.5. [17]

The silanization reaction proceeds even at ambient temperature, a phenomenon well known from storage of this type of compounds. Treated silica samples stored for several months at room temperature showed a decrease in the number of ethoxy groups. Ethanol was generated as a product of either

hydrolysis or silanization. This effect was more pronounced when the storage container was not sealed, an indication that absorption of moisture [3] or the presence of oxygen influenced the kinetics of the silanization reaction.

The secondary reaction, the reaction of the remaining ethoxy groups with either silanol groups or other adjacent ethoxy groups, requires higher temperatures. At silica mixing temperatures, in the temperature interval between 140ºC and 160ºC, this reaction takes place to a significant extent. However, for a given temperature the rate of the secondary reaction is lower compared to the rate of the primary reaction by approximately one order of magnitude. As hydrolysis of the ethoxy groups is necessary, this reaction is catalyzed by moisture as well as by the acidity of the matrix. Kinetic investigations of model systems containing only filler and coupling agent have shown that for the major part of the silicon atoms of the coupling agent only two out of three ethoxy groups react. Taking into consideration the geometrical structure of the silanol groups of the silica and the hydrolyzed silane, it becomes clear that bonding of one silyl group to the filler surface by three siloxane bonds is possible only by strong distortion of the bonding angles, resulting in a low stability. It is commonly assumed that only one ethoxy group is chemically bound to the silica surface and that the remaining ethoxy groups undergo a condensation reaction with adjacent silane molecules. This is in accordance with the fact, that a monoethoxy-silane has the same performance as the triethoxy-silane in terms of silanization and properties of the final material. [18] Looking at the silicon atoms on the filler surface, indications are found that geminal groups are more reactive than isolated silanol groups. [3]

2. KINETICS INVESTIGATED BY MODEL COMPOUND INVESTIGATIONS

For model compound investigations of the silanization kinetics, squalene, a hexamer of isoprene, has widely been used as polymer. Decane, methanol or acetone were used as inert solvents. The preferred analytical method for the quantitative determination of the starting material, the silane, as well as the reaction product, ethanol, is High Pressure Liquid Chromatography (HPLC). Both components allow monitoring the reaction rate, but the analysis of ethanol gives less accurate results as side reactions change the ethanol concentration: The silane splits off ethanol even without coupling to the filler surface due to homocondensation. Furthermore, ethanol is physically adsorbed and chemically bound to the filler surface. The adsorbed ethanol can be removed by treatment with diethyleneglycol monobutylether, but the chemically bound ethanol can not be removed and can therefore not be detected. [11, 12, 15]

3. KINETICS INVESTIGATED IN RUBBER COMPOUNDS

The progress of the silanization reaction in real rubber compounds can be monitored by several methods:

3.1. VISCOSITY MEASUREMENTS

The further the silanization reaction proceeds, the better the dispersion of the filler particles in the compound, resulting in a reduction of the viscosity. Shortcomings of this measurement are the sensitivity to other reactions influencing the viscosity: scorch reactions resulting in a viscosity increase, and polymer breakdown as well as ethanol dissolved in the rubber compound leading to a reduction of the viscosity.

3.2. PAYNE EFFECT MEASUREMENTS

The Payne effect allows for a direct measurement of the dispersion and hydrophobation of the filler, as it measures the interparticle forces between the filler aggregates (see chapter 2), making it independent of most other influencing factors mentioned in paragraph 3.1. The Payne effect not only gives an indication of the silanization reaction, it also measures the hydrophobation effect of the silane used. Only adsorption of ethanol will influence the results as it also hydrophobizes the surface of the filler. Most investigations on the dispersion of silica and the silanization reaction make use of the Payne-effect.

3.3. ETHANOL MEASUREMENTS

Ethanol generated during the hydrolysis and silanization reaction can be measured online by encapsulating the mixer and analyzing ethanol quantitatively with a flame ionization detector (FID). The accuracy of this method is reported to be approximately ± 20%. [19] These measurements can also be done off-line by adsorbing ethanol on, for example, active coal and measuring the amount of ethanol after desorption by gas chromatography (GC). The critical point of the former method is the difficulty to completely encapsulate a rubber mixer to ensure that all ethanol is actually collected and analyzed. Common for both methods is the fact that ethanol condensed in the mixer and dissolved in the rubber is not detected. The concentration of ethanol in the compound during the different test series varied between 0.2 to 0.5 gram ethanol per kilogram compound. The average percentage of the total amount of ethanol, which is dissolved in rubber, amounts to approximately 10 %, under the assumption that 0.35 gram ethanol per kilogram compound is dissolved and 5 ethoxy groups from each silane molecule react.

3.4. MEASUREMENT OF THE COUPLING AGENT

The non-reacted coupling agent can also be measured by HPLC after extraction from the silanized compound. This method suffers from a low accuracy, as it is difficult to separate the silane from other compounding ingredients also soluble in the extraction fluid.

4. DETAILED DESCRIPTION OF THE KINETICS OF THE SILANIZATION REACTION

4.1. TEMPERATURE-DEPENDENCE

Hunsche et al. investigated the silanization reaction between silane coupling agents and silica in dispersion, avoiding the influence of other rubber compounding additives on the kinetics of the reaction. [3, 12] Tests were done in two temperature intervals: between 30°C and 60°C with the aim to measure the primary reaction, and between 120°C and 160°C in order to measure the combined primary and secondary reactions. Conclusions concerning the secondary reaction were drawn by comparing the results of the combined primary and secondary reaction with the temperature-extrapolated effects of the primary reaction. Extrapolation of the kinetics of the primary reaction to higher temperatures was done using the Arrhenius-equation:

$$\ln k_R = \ln A - \frac{E_A}{RT} \qquad\qquad Eq.\ 2$$

This equation allows for calculation of the rate constant k_r for different temperatures T, once the constant A and the activation energy E_A for a given temperature interval are known. [3, 11, 12, 15] A comparison of the rate of ethanol generation at 50°C and 120°C showed that the kinetics of the reaction differ, depending on the temperature (Figures 1 and 2). At 50°C the silanization reaction showed an exponential increase of ethanol generation in time, characteristic for a first order reaction. A series with increasing silane concentrations resulted in a decrease of the reaction rate relative to the initial concentration of the silane. This implies that other factors like a blockage of the silanol sites on the silica surface by the silane as well as by the ethanol formed is influencing the reaction rate. The distance between silane molecules bound to the silica surface is influencing the reaction rate: If the silane concentration is low, the distance between the silane molecules is large and homocondensation is inhibited. [11, 12, 15]

At 120° the initial reaction rate is very high due to the fact that the fast primary reaction and the slower secondary reaction take place simultaneously. A sharp and almost linear increase of the amount of generated ethanol was found for

the first period of silanization. In the second period, the reaction rate slowed down considerably (Figure 2). [11, 12, 15]
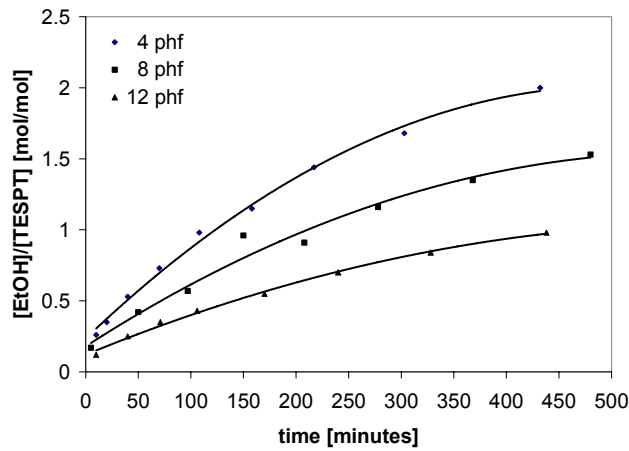
Figure 1: Ethanol generation in a dispersion of silica and silane in n-decane at 50°C (primary reaction; phf = parts per hundred filler) [12]
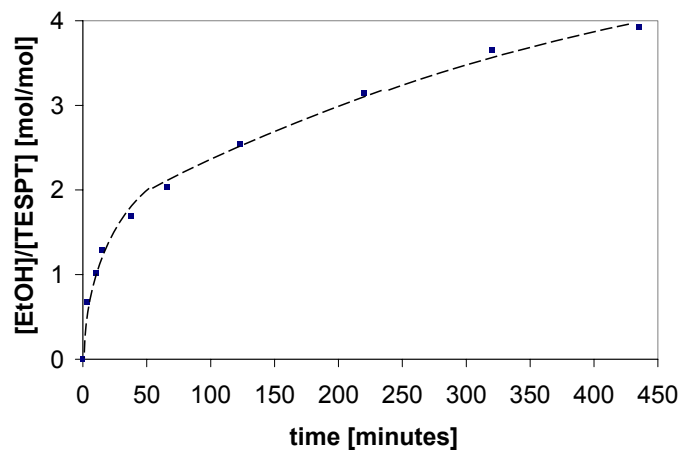
Figure 2: Ethanol generation in a dispersion of silica and silane in n-decane at 120°C (primary and secondary reaction) [12]

4.2. INFLUENCE OF OTHER COMPOUNDING ADDITIVES

Reuvekamp [13, 18] investigated the influence of other compounding additives such as zinc oxide and stearic acid on the kinetics of the silanization reaction. Both additives were slightly reducing the reaction rate of the silanization at temperatures around 140°C. The silanization rate increased by 30% to 50% depending on the reaction media for compounds without zinc oxide addition during the silanization step. The effect found for stearic acid was less pronounced. These results are in agreement with the work done by *Kim and van der Kooi.* [20]

114

4.3. Influence of the Type of Silane

Numerous publications and patents propose different silanes for the hydrophobation of silica in rubber compounds, mainly differing in the functional groups connected to the triethoxysilylpropyl group, but most of these molecules are not thoroughly investigated concerning their influence on the kinetics and efficiency of the silanization reaction. [21-34] For MPS (3-methacryloxypropyl trimethoxysilane), a monofunctional silane with only one silyl group, the adsorption process and the kinetics of the silanization reaction were studied by *Posthumus et al.* [10] Model studies in methanol at 70ºC were used to elucidate the reaction mechanism. The hydrolysis step was identified as the rate-determining step of this reaction. This step can be described by a pseudo first order kinetic law and is acid and base-catalyzed. [35] The amount of coupling agent chemically bound to the silica surface was limited to a monolayer, with the silane molecules oriented parallel to the silica surface. The measured total amount of MPS that could be chemisorbed onto the silica surface was 3.8 µmol/m^2 [36], being slightly higher than the theoretically calculated value of 3.0 µmol/m^2 for a parallel orientation of the molecules in a monolayer on a silica with a BET surface of 191 m^2/g. The parallel orientated monolayer was assumed to be stabilized by hydrogen bonds between the silanol groups of the silica particles and the carbonyl-moieties of the coupling agent. [10]

Bifunctional silanes such as TESPT and TESPD will behave differently: Initially the molecules are attached with one siloxane bond only, and their orientation will be perpendicular to the surface as they have a low affinity with the polar silica surface. Molecules bound to the silica surface by both silyl groups are bended over the surface of the silica particle, resulting in a parallel orientation. This structure is more stable compared to the structure of MPS on silica, because the bifunctional molecule is bound chemically on both ends. Only after breaking of the sulfur-bridge in the middle part of the bifunctional silane, the molecule will no longer be fixed to the silica surface on both ends and the orientation will change to a perpendicular one. Finally, the orientation of the bis(triethoxysilylpropyl) sulfane molecules will be a mixture of perpendicular and parallel orientations. The silica surface will partly be covered by more than one layer, due to homocondensation between the silanol groups of the second silyl group of the silane molecules already bound to the silica surface and free silane molecules, resulting in the attachment of a higher layer.

4.4. Adsorption of the Coupling Agents

Basically three models for the adsorption of a silane onto silica are discussed in the literature. The first one is a vertical model, in which silane molecules are attached to the silica surface in a perpendicular orientation. Higher layers of silane are chemisorbed onto the first layer. The second model postulates the reaction of all ethoxy groups of one silyl group with silanol groups on the silica surface. The third model describes the reaction of one ethoxy moiety per silyl

group bound to the silica surface, and the second and third hydrolyzed ethoxy group undergoing a homocondensation reaction with adjacent silane molecules. This model is the most probable one, as it is geometrically sound and in accordance with the two-step reaction mechanism. Figure 3 shows the configuration of the silane molecules on the silica surface according to this model. [11, 37]

$$
\begin{array}{ccc}
& R & \\
& | & \\
EtO-Si-OEt & \\
& | & \\
& O & \\
& | & \\
\hline
& \text{Silica surface} &
\end{array}
\qquad
\begin{array}{ccc}
R & & R \\
| & & | \\
-O-Si-O-Si-O- \\
| & & | \\
O & & O \\
| & & | \\
\hline
& \text{Silica surface} &
\end{array}
$$
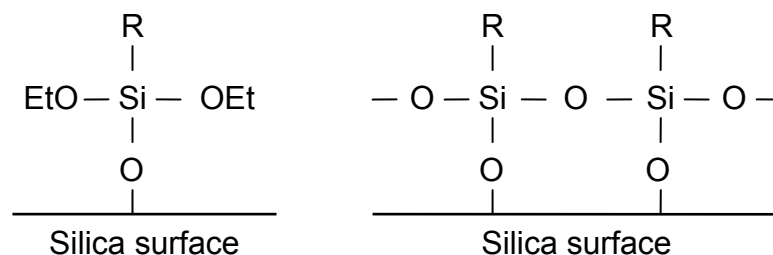
Figure 3: Silane molecules attached to the silica surface according to model 3 [11]

Blum et al. investigated the hydrolysis and adsorption on silica surfaces of mono-functional silane coupling agents in acetone-water mixtures. [2] Adsorption of the hydrolyzed silanes onto the surface of the silica was analyzed by Langmuir-plots: The amount of adsorbed coupling agent reached a maximum, interpreted as the completion of a monolayer. The amount of an aminopropylsilane adsorbed in a monolayer corresponded to approximately 1 silane molecule per surface hydroxyl group of the silica, which for this type of silica sums up to 6.6 $\mu mol/m^2$. This degree of coverage is only possible when the silane molecules are packed perpendicular to the filler surface. [2]

5. KINETICS OF THE SILANIZATION REACTION IN A RUBBER MATRIX AS INFLUENCED BY THE PROCESSING CONDITIONS

Table I gives an overview of the reaction constants of the silanization reaction measured in model compounds, published by different authors. The reaction rate for the primary reaction at low temperatures (30°C to 60°C) is low: The silanization reaction in this temperature range is very slow. The activation energy for this step is not very high, showing that the reaction rate does not strongly depend on temperature. The rates of the complete reaction in the temperature range around 140°C are higher by at least a factor of 10, with the absolute value depending on the silanization parameters. The secondary reaction alone is rather slow in the temperature range between 120°C and 140°C. At 160°C the rate of the secondary reaction is significantly increased. The activation energy given for this step only is low: This is surprising as the temperature dependence is very strong, especially in the temperature range between 140°C and 160°C.

Table I: Reaction constants for the model compound silanization in different media

Tempe-rature	Reaction rate	Activation energy	Reaction media	Reaction step	Ref.
[ºC]	[1/minute]	[kJ/mol]			
30	0.00080				
40	0.0015	47	n-Decane	Primary reaction	[12]
50	0.0027				
60	0.0043				
70		37.8	Methanol	Primary reaction	[10]
120	0.0055				
140	0.0080	28	n-Decane	Secondary reaction	[12]
160	0.12				

5.1. EXPERIMENTAL

For the present study, one large masterbatch was prepared as starting material. This predispersed compound contained all ingredients except the curing additives. They were mixed separately in different laboratory and production mixers under various conditions.

5.1.1. Preparation of the masterbatch

All investigations were done using a passenger car tire tread masterbatch based on a blend of S-SBR and BR with 83.5 phr silica and a silane as coupling agent (TESPT or TESPD). This compound was mixed and pre-dispersed in a 320 liter intermeshing mixer, with a dump temperature of approximately 130ºC. The primary silanization reaction was assumed to have taken place to a very limited extent only during this first mixing step.

5.1.2. The silanization experiments

For all experiments the pre-dispersed masterbatch was used. This masterbatch was brought to the final silanization temperature under consideration as fast as possible in the internal mixer, with the ram closed. After reaching the silanization temperature, this temperature level was kept constant during the whole period of silanization by adjustment of the rotor speed.

5.1.3. Analysis of the samples

As a first indication of the dispersion of the filler and the degree of silanization, the Mooney viscosity of the material (ML(1+4), 100ºC) was measured immediately after the silanization step. The measurements were done with a Mooney Viscometer 2000 E (Alpha Technologies).

The Payne effect was measured with the aid of a Rubber Process Analyzer RPA 2000 (Alpha Technologies) in a strain sweep (strain: 0.56%-100%,

temperature: 100ºC, frequency: 0.5 Hz). As the samples were not measured immediately after the test, they were stored at low temperatures in order to avoid further silanization and re-agglomeration of the filler. The reaction rates and activation energies for the silanization reaction were calculated using the Payne effect data according to ISO 53529: The Payne effect PE was measured as a function of the silanization time at different temperatures, in general 135ºC, 145ºC and 155ºC. The reaction constant for a first order reaction was then calculated according to Equations 3 and 4:

$$k_r = \frac{\ln(1 - x_1) - \ln(1 - x_2)}{t_2 - t_1} \qquad\qquad Eq.\ 3$$

$$x = \frac{PE(t) - PE_0}{PE_\infty - PE_0} \qquad\qquad Eq.\ 4$$

The reaction variable x was calculated from the Payne effect at time t PE(t), the Payne effect of the starting material PE_0 and the Payne effect for a fully silanized compound PE_∞. The reaction constant k_r is given by the slope of the line of the logarithm of (1-x) as a function of time, see Figure 4. The activation energy was calculated from the reaction constants k_r at different temperatures:

$$k_r = k_0 \exp\frac{-E_a}{R \cdot T} \qquad\qquad Eq.\ 5$$

In the graph showing the logarithm of k_r as a function of the reciprocal temperature, the slope of the line gives the value of the activation energy, as illustrated in Figure 5.
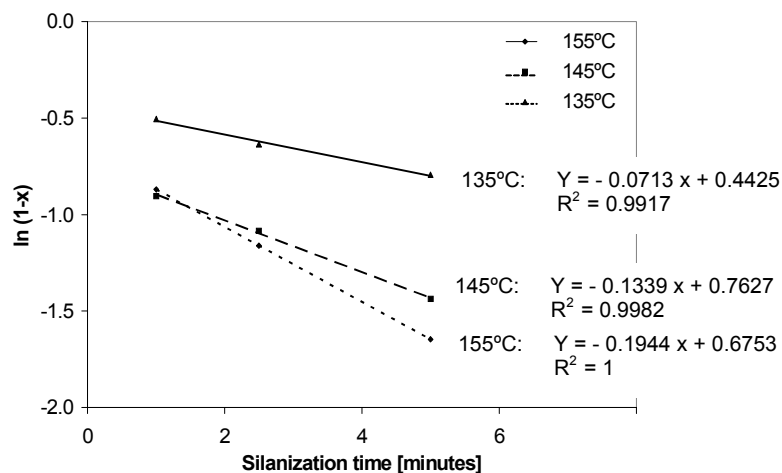
Figure 4: Determination of the reaction constant at different temperatures
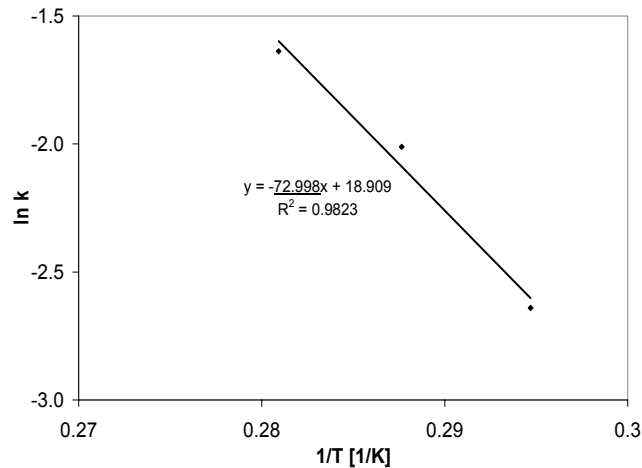
Figure 5: Determination of the activation energy

5.1.4. Mixing equipment for the silanization tests

Four different mixing chambers were used for this investigation: three laboratory mixers with an effective volume of approximately 3.6 liter, 5.5 liter and 7.6 liter. Different rotors were used in the experiments, determining the precise effective volume of the mixing chamber/rotor combinations. One production scale mixer with an intermeshing pair of rotors was used, having an effective volume of 49 liter. In the following paragraphs the mixers are described by indicating the type of rotors ('I' for intermeshing, 'T' for tangential) followed by the mixer size. The compound temperature was monitored during the reaction by a thermocouple installed in the mixing chamber. After discharge the temperature of the compound was verified with a pyrometer. A detailed description of the experimental setup is given in chapter 3.

5.1.5. Factors investigated

The following factors, which are expected to have an influence on the silanization kinetics, were evaluated: size of the mixing chamber, rotor type, fill factor, temperature control unit settings, air injection into the mixing chamber with pressurized air and ram position.

5.2. RESULTS

Tables II through VII show the results of different series of silanization experiments carried out under different processing conditions. The temperature interval for the experiments was in general 135ºC to 155ºC, and the reaction times were 1, 2.5 and 5 minutes. The lowest achievable value of the Payne effect, necessary for the calculation of the reaction rate constants, was measured at a compound after silanization at 135ºC during 20 minutes. Starting value was the Payne effect of the masterbatch.

5.2.1. Variation of the rotor geometry

Two series of experiments (Table II and III) were carried out with different rotors in the same mixing chamber. These experiments allow the direct

119

comparison of the influence of the rotor geometry and exclude the influence of the design of the mixing chamber.

Table II: Kinetic data for the silanization with different rotors in the same mixing chamber

Variable processing conditions		
Rotor type	PES5	I5-SI
Rate of silanization		
Temperature [ºC]	k_r [minute^{-1}]	k_r [minute^{-1}]
135	0.085	0.086
145	0.117	0.148
155	(0.016)	-
Activation energy		
	[kJ/mol]	[kJ/mol]
	45	77

Mixer: I5
TCU settings: 60ºC
Ram position: up
Ventilation: on
Air injection: off
Coupling agent: TESPD
Fill factor: 40%

The same reaction rate at 135ºC was found for both rotor types, but at 145ºC the two rotors behaved differently: the silanization rate was significantly higher for the I5-SI rotor compared to the PES5 rotor. When the temperature was further increased, the Payne effect of the materials mixed with the I5-SI rotor showed only slight differences depending on silanization time, making it impossible to calculate the reaction rate. The silanization rate in the mixer with the PES5 rotor at 155ºC showed the same trend: only small changes of the Payne effect were measured between 1 minute and 5 minutes of silanization time, resulting in very low reaction rates for this period.

Table III: Kinetic data for the silanization with different rotors in the same mixing chamber

Variable processing conditions		
Rotor type	F4W	T7-SI
Rate of silanization		
Temperature [ºC]	k_r [minute^{-1}]	k_r [minute^{-1}]
135	(0.143)	0.067
145	0.051	0.089
155	0.086	0.211
Activation energy		
	[kJ/mol]	[kJ/mol]
	33	56

Mixer: T7
TCU settings: 60ºC
Ram position: up
Ventilation: on
Air injection: off
Coupling agent: TESPD
Fill factor: 45%

Table III shows the results of a comparative investigation of the T7-SI rotor and the tangential F4W rotor in the 7.5 liter mixing chamber. The F4W rotor results in a high silanization rate at the lowest temperature, 135°C. In the temperature range between 145°C and 155°C, the rate is on a significantly lower level, with a slight increase when the temperature is raised from 145°C to 155°C. In this temperature range, the average silanization rate is lower for the mixer equipped with the F4W rotors compared to the T7-SI rotor. The compound silanized with the T7-SI rotor shows the expected increase of silanization rate with increasing temperature. The activation energy, calculated for the temperature interval between 145°C and 155°C, is lower for the silanization with the F4W rotor compared to the T7-SI rotor.

5.2.2. Variation of the mixing chamber and the rotor geometry

In this series of experiments the influence of the rotor geometry in different mixing chambers was investigated. The rotors were mounted in mixers differing in size with a factor of about 2. The fill factors were adjusted to the rotor geometry; they were optimized in a fill factor study done prior to these experiments.

Table IV: Kinetic data for the silanization with different rotors and mixing chambers at low fill factors

Variable processing conditions			
Mixer type	I5	T4	T7
Rotor type	PES5	ZZ2	T7-SI
Fill factor	40%	45%	45%
Rate of silanization			
Temperature	k_r	k_r	k_r
[°C]	[minute^{-1}]	[minute^{-1}]	[minute^{-1}]
135	0.085	0.085	0.067
145	0.117	0.108	0.089
155	(0.016)	(0.060)	0.211
Activation energy			
	[kJ/mol]	[kJ/mol]	[kJ/mol]
	45	33	42

TCU settings: 60°C
Ram position: up
Ventilation: on
Air injection: off
Coupling agent: TESPD

Only slight differences concerning the silanization rate were found at low temperatures. The reaction rates at 135ºC were similar for the silanization in the I5 and T4 mixer, only the T7 mixer showed a slightly lower rate at this temperature. At 145ºC the differences became more pronounced: The silanization rate was highest in the I5 mixer, followed by the T4 mixer. At this temperature, the T7 mixer showed the slowest reaction rate. At the highest temperature, 155ºC, only the silanization in the tangential mixer (T7) was still

measurable. The reaction rate at this temperature more than doubled compared to the silanization rate at 145ºC. The activation energies of the I5 and T7 mixer were in the same range and comparable to the activation energies measured in the model reactions as given in Table I. The activation energy of the tangential T4 mixer was lower.

The same type of investigation was done at higher fill factors (see Table V). In this case, mainly the differences in intake behavior are expected to become visible.

Table V: Kinetic data for the silanization with different rotors and mixing chambers at a high fill factor

Variable processing conditions		
Mixer type	I5	T4
Rotor type	PES5	ZZ2
Rate of silanization		
Temperature	k_r	k_r
[ºC]	[minute^{-1}]	[minute^{-1}]
135	0.071	0.089
145	0.134	0.112
155	0.194	(0.008)
Activation energy		
	[kJ/mol]	[kJ/mol]
	56	33

TCU settings:	60ºC
Ram position:	up
Ventilation:	on
Air injection:	off
Coupling agent:	TESPT
Fill factor:	60%

At low temperatures around 135ºC, the reaction rate in the tangential T4 mixer was slightly higher compared to the intermeshing I5 mixer. The intermeshing mixer with the PES5 rotor showed higher silanization rates compared to the tangential mixer for temperatures in the range of 145ºC. The reaction rate was increasing significantly between 145ºC and 155ºC in the intermeshing mixer, but in the tangential mixer the reaction rate at 155ºC was very low, in accordance with the results of Table IV. The activation energy of the silanization in the tangential mixer was low compared to the activation energy in the intermeshing mixer.

5.2.3. Variation of the fill factor and TCU settings

The fill factor is an important influencing factor for the rate and efficiency of the silanization reaction, especially when working in an open mixer. The cooling efficiency, determined by the temperature control unit (TCU) settings, as well as the contact between the compound and the mixing chamber wall, are other influencing factors. In this series the best case scenario, low fill factor and low

cooling temperature, was compared to the other extreme, high fill factor and high cooling temperature.

Table VI: Variation of the fill factor together with the temperature control unit settings

Variable processing conditions		
Fill factor	60%	40%
TCU settings	90	60
Rate of silanization		
Temperature [ºC]	k_r [minute^{-1}]	k_r [minute^{-1}]
145	0.134	0.099

Mixer: I5
Rotor: PES5
Ram position: down
Ventilation: on
Air injection: off
Coupling agent: TESPT

At 145ºC, the reaction rate of the combination of a high fill factor with a high cooling temperature resulted in a higher reaction rate.

5.2.4. Influence of air injection

In these experiments the silanization was carried out in a production scale mixer of 49 liters, with the mixer being closed during the silanization reaction.

Table VII: Kinetic data of the effect of air injection

Variable processing conditions		
Air injection	on	off
Rate of silanization		
Temperature [ºC]	k_r [minute^{-1}]	k_r [minute^{-1}]
145	0.870	0.339

Mixer: I45
Rotor: PES5
TCU settings 40ºC
Ram position: up
Ventilation: on
Coupling agent: TESPD
Fill factor: 55%

These results show clearly, that air injection improves the rate and degree of silanization considerably, the k_r value is up to tenfold the values measured with the various other mixer and rotor settings.

6. DISCUSSION

A general problem with respect to the evaluation of the results from Tables II to VII is the silanization rate as measured at 155ºC. In some cases, the Payne effect did not change significantly any more during the time interval used in this investigation, resulting in low values for the reaction rate at this temperature. In these cases, the silanization reaction proceeded to a high extent already before the measurement started, in the period necessary for warming up the

compound to 155ºC and the first minute of the reaction. The increase of the reaction rate at high temperatures is in accordance with the values in Table I. The measured values of the Payne effect at the different time intervals were already low, close to the minimum value for full silanization. The change in the degree of silanization between 1 minute and 5 minutes was rather small, resulting in low values of the calculated reaction rate. These results are indicated with brackets in Tables II to VII, and they are not further used for the evaluation of the kinetics of the silanization. The absolute values of the Payne effect, that is the final degree of silanization, are not taken into consideration, as they are discussed in chapter 3.

Tables II and III show the influence of rotor geometry without alteration of any other processing parameters. Comparing the intermeshing PES5 rotor with the I5-SI rotor, both rotors perform more or less equal at low temperatures, but at 145ºC the silanization rate in the mixer with the I5-SI rotor is significantly higher. At 155ºC both rotors show very low rates of silanization, indicating that the reaction at this temperature is very fast and almost already complete within the warming up period and the first minute of silanization, as explained above. The rate of silanization in the mixer with the I5-SI rotor is higher in the commonly used temperature range for silanization. However, the absolute level of the measured Payne effect after silanization is higher for the compounds silanized in the mixer with the I5-SI rotor within the temperature-time window of these experiments, as shown in chapter 3. This indicates, that silanization during the heating period occurs to a minor extent, resulting in a higher value of the Payne effect at the beginning of the silanization step. This results in a lower final degree of silanization, even though the reaction rate is higher compared to the compound silanized in the mixer with the PES5 rotor.

The activation energy for the silanization using the I5-SI rotor is higher compared to the PES5 rotor, reflecting the stronger temperature dependence of the silanization in this mixer. The activation energy for the reaction done in the mixer with the PES5 rotor is in the same range as the activation energies published by other authors (Table I), showing that the temperature dependence of the silanization in this case is independent of the reaction medium. Even though the silanization in a rubber compound consists of more steps compared to the model reaction, the rate determining steps show the same temperature dependence. Diffusion of the silane to the filler particles does apparently not influence the temperature-dependence, nor does the availability and reactivity of the water molecules, which is different when the silanization is taking place at temperatures above the boiling point of water. The situation is different for the I5-SI rotor: The activation energy is significantly higher, caused by the strong temperature influence on the reaction rate in the temperature interval between 135ºC and 145ºC. As the warming up periods for both systems are equal, a possible explanation is a better temperature-homogeneity of the batch, resulting in a higher average reaction rate during the silanization step.

At 135ºC, the silanization rate for the reaction in the T7 mixer with the F4W rotor is very high compared to the higher temperature range. This is caused by the high starting value of the Payne effect at 135ºC: In this case, the silanization takes place only to a very limited extent during the heating period: When the compound reaches the silanization temperature, 135ºC, the Payne effect is still high, reaches after 5 minutes of silanization the lowest value for the highest possible degree of silanization. For higher temperatures, the starting value of the Payne effect is lower, only slightly higher than the minimum value for full silanization. Therefore, the possible decrease during the silanization step is limited, resulting in low reaction rates at 145ºC and 155ºC. This also influences the activation energy for this temperature range, resulting in a low value.

The rates for the silanization with the T7-SI rotor are higher compared to the rates for silanization with the F4W rotor at 145ºC and 155ºC. Particularly at 155ºC, the compound silanized in the 7 liter mixer equipped with the T7-SI rotor shows a high reaction rate, indicating that for this mixer/rotor combination and high temperatures the main part of the silanization takes place during the period of investigation between 1 minute to 5 minutes. In this case the silanization reaction does not significantly occur during the heating period within the experimental temperature range. The comparison of the activation energies as shown in Table III gives a wrong impression, as in the case of the F4W rotor the silanization during the heating period is not taken into consideration.

The silanization rates for different mixer/rotor combinations are shown in Tables IV and V. Table IV shows the results of a series of experiments with low fill factors: As the silanization is done in an open mixer, the fill factor had to be reduced in order to improve the intake behavior of the compound. The intake behavior of a tangential mixer is in general better than the intake behavior of an intermeshing mixer; therefore the optimal fill factor is higher. Mixer size is not expected to have an influence on the reaction rate in this case, as the difference in the volume of the mixing chamber is rather small.

The intermeshing mixer shows a higher silanization rate compared to both tangential mixers as long as the silanization temperature is on a moderate level, around 145ºC. An explanation for this effect is found in the flow pattern of this mixer type: In intermeshing mixers the distance between the tips of the rotor flights and the rotor shaft is small in the space between the two rotors, the rubber compound is thinly sheeted out in this region and the ethanol generated during the silanization reaction can be removed efficiently out of the compound. Another reason for the good performance of this mixer type is the fact, that intermeshing mixers are more effective in dispersive mixing. This results in a better dispersion of the filler, thus improving the availability of the surface silanol groups.

For the I5 mixer with intermeshing rotor geometry as well as the T4 mixer with tangential rotor geometry the reaction rate is low at 155ºC, showing that the silanization is almost complete after a short reaction time at his temperature. The silanization rate measured in the mixer with the tangential T7-SI rotor at this temperature is higher, as the major part of the silanization actually happens during the silanization period and not during the warming up period. The activation energies measured for the silanization in the mixer using the PES5 and T7-SI rotor are comparable with the energies measured in model compounds as given in Table I, implying that the influence of the temperature is equal. Only for the tangential mixer with the ZZ2 rotor a lower value is measured. The activation energies given in Table IV are calculated for the temperature interval between 135ºC and 145ºC. If the activation energy for the T7 mixer is calculated for the interval from 135ºC to 155ºC, the resulting activation energy will be higher (83 kJ/mol), again reflecting the higher temperature sensitivity of the compound in the range between 145ºC and 155ºC.

Table V shows the difference between tangential and intermeshing rotors in terms of the silanization kinetics, but at higher fill factors. Working in an open mixer with higher fill factors results in a more irregular intake behavior: The compound is pushed up into the hopper region where it remains for a certain number of rotor revolutions before taken in again. The consequences are a lower mixing efficiency and a less efficient temperature control of the compound. At 135ºC, the silanization rate is higher in the tangential mixer. This may be due to temperature inhomogeneity, being higher in a tangential mixer. In some areas the compound may reach the silanization temperature very early, and the degree of silanization in these areas is higher compared to other areas. At higher temperatures, the mixer with the intermeshing rotor geometry performs better, as seen before: The intermeshing rotor is more effective in cooling and mixing, and both factors are positively influencing the silanization efficiency.

The intermeshing mixer performs better at moderate temperatures: at 145ºC the reaction is faster. At 155ºC the reaction rate of the intermeshing mixer is very high, again showing that the silanization is taking place during the period monitored for the silanization. This temperature dependence is also expressed in the value of the activation energy: The activation energy for the reaction in the intermeshing mixer is significantly higher than the energy calculated for the tangential mixer.

Variation of the fill factor together with the TCU settings affects the silanization rates as shown in Table VI. The reaction rate is higher for the mixer with a higher fill factor and a higher cooling temperature. This is a temperature effect: The compound heats up faster, as cooling is less intensive due to the higher temperature of the cooling liquid. The silanization temperature is reached very fast, and silanization is almost completely taking place during the silanization

period. When cooling is more efficient due to a lower cooling temperature, heating up is slower and silanization already proceeds to a significant extent during the heating phase in the temperature interval between 135ºC and 145ºC, when the heating rate is low. This results in a lower starting value of the Payne effect and a lower decrease during the silanization step.

Table VII clearly demonstrates the influence of air injection on the reaction rate: The rate of silanization more than doubles when air injection is applied. The air drags ethanol out of the compound and out of the mixing chamber, thus shifting the balance of the hydrolysis reaction of the ethoxy groups towards the silanol groups. It reduces the adsorption of ethanol onto the silica surface, resulting in a higher surface concentration of available adsorption sites on the filler surface, and shifting the balance between ad- and desorption of silane and ethanol to the silica-silane adsorbate site.

7. SUMMARY

Mixer design and processing parameters were systematically investigated concerning their influence on the silanization rate, in order to identify the most important factors for increasing the silanization rate in an internal mixer. The emphasis of this investigation was on the description of the kinetics of the silanization reaction, depending on the mixer and process parameters. The absolute level of silanization was not discussed in this chapter, as it was in the focus of chapter 3.

The silanization was carried out at 135ºC, 145ºC and 155ºC. The silanization rate for the highest temperature was in some cases very low due to the fact that the silanization was already almost complete after a short silanization period. Furthermore, the properties of the material after silanization at 155°C might be influenced by a scorch reaction. The kinetic evaluation of the data is therefore in general limited to the temperature range between 135ºC and 145ºC.

Different combinations of rotor geometry/mixing chamber for the silanization in an open mixer were compared in terms of reaction rate, and the direct comparison of the silanization with the PES5, ZZ2 and T7-SI rotor resulted in a decreasing silanization rate from the PES5 over the ZZ2 to the T7-SI at 145ºC. The temperature control unit settings influenced the silanization rate: The combination of a high fill factor and a high cooling temperature performed better than the combination of a low fill factor and a low cooling temperature. An investigation on the influence of air injection leads to the conclusion, that the reaction rate was more than doubled by this measure. This demonstrates that removal of ethanol is a crucial factor for increasing the silanization rate, as it reduces the adsorption of ethanol on the silica and shifts the balance of the silanization reaction towards the reaction products.

8. REFERENCES

1. Arkles, B., Steinmetz, J.R., Zazyczny, J., Metha, P., in *Silanes and other coupling agents*, K.L. Mittal, Editor. 1992, VSP BV: Utrecht. p. 91.
2. Blum, F.D., Meesiri, W., Kang, H.-J., Gambogi, J.E., in *Silanes and other coupling agents*, K.L. Mittal, Editor. 1992, VSP: Utrecht. p. 181.
3. Hunsche, A., Görl, U., Mueller, A., Knaack, M., Goebel, Th., Kautsch. Gummi Kunstst., 1997. **50**(12): p. 881.
4. Luginsland, H.-D. *Processing of the organo silane Si 69*. in *11. SRC conference*. 1999. Puchov, Poland.
5. Zaborski, M., Vidal, A., Ligner, G., Balard, H., Papirer, E., Burneau, A., Langmuir, 1989. **5**: p. 447.
6. Zhuravlev, L.T., Langmuir, 1987. **3**: p. 316.
7. Jesionowski, T., Zurawska, J., Krysztafkiewicz, A., J. Mat. Sci., 2002. **37**: p. 1621.
8. Iler, R.K., *The chemistry of silica*. 1979, John Wiley & Sons: New York.
9. Burneau, A., Gallas, J.-P., in *The surface properties of silicas*, A.P. Legrand, Editor. 1988, John Wiley & Sons: Chicester (Great Britain).
10. Posthumus, W., Magusin, P.C.M.M., Brokken-Zijp, J.C.M., Tinnemanns, A.H.A., van der Linde, R., J. Coll. Interface Sci., 2004. **269**: p. 109.
11. Görl, U., Hunsche, A., Mueller, A., Koban, H.G., Rubber Chem. Technol., 1997. **70**: p. 608.
12. Hunsche, A., Görl, U., Koban, H.G., Lehmann, Th., Kautsch. Gummi Kunstst., 1998. **51**(7-8): p. 525.
13. Reuvekamp, L.A.E.M., ten Brinke, J.W., van Swaaij, P.J., Noordermeer, J.W.M., Rubber Chem. Technol., 2004. **77**(1): p. 34.
14. Reuvekamp, L.A.E.M., ten Brinke, J.W., van Swaaij, P.J., Noordermeer, J.W.M., Rubber Chem. Technol., 2002. **75**(2): p. 187.
15. Goerl, U., Hunsche, A. *Advanced investigations into the silica/silane reaction system*. in *Am. Chem. Soc. Rubber Div. conference*. 1996. Louisville, Kentucky.
16. Luginsland, D., Hasse, A. *Processing of silica/silane filled tread compounds*. in *Am. Chem. Soc. Rubber Div. conference*. April 4-6, 2000. Dallas,Texas.
17. Miller, J.D., Ishida, H., Surf. Sci., 1984. **148**: p. 601.
18. Reuvekamp, L.A.E.M., in *Thesis: Reactive mixing of silica and rubber for tyres and engine mounts*. 2003, Dept. Rubber Technol., Univ. Twente: Enschede (the Netherlands).
19. Luginsland, D., Hasse, A. *Processing of silica/silane filled tread compounds*. in *Am. Chem. Soc. Rubber Div. conference*. 2000. Dallas,Texas.
20. Kim, K.-J., van der Kooi, J., Rubber World, 2002. **August 2002**.
21. Agostini, G., *Rubber composition and tire having tread thereof*. 17.02.1999, The Goodyear Tire & Rubber Company: EP 0 896 978 A2.
22. Kayser, F., Lauer, W., Materne, T.F.E., *Nitrogen containing siloxy compounds*. 14.02.2001, The Goodyear Tire & Rubber Company: EP 1 076 059 A1.
23. Kayser, F., Lauer, W., Materne, T.F.E., *Ether containing siloxy compounds*. 14.02.2001, The Goodyear Tire & Rubber Company: EP 1 076 061 A1.
24. Kayser, F., Lauer, W., Materne, T.F.E., *Unsaturated siloxy compounds*. 14.02.2001, The Goodyear Tire & Rubber Company: EP 1 076 060 A1.
25. Materne, T.F.E., Agostini, G., Visel, F., Cohen, M.P., *Unsymmetrical siloxy compounds*. 01.09.1999, The Goodyear Tire & Rubber Company: EP 0 939 081 A1.
26. Materne, T.F.E., *Siloxy compounds*. 01.09.1999, The Goodyear Tire & Rubber Company: EP 0 939 080 A1.
27. Materne, T.F.E., Agostini, G., Junio. M., *Rubber composition containing silanol modified carbon black*. 12.04.2000, The Goodyear Tire & Rubber Company: EP 0 992 535 A1.
28. Sandstrom, P.H., Smith, R.R., Pyle, K.J., *Tire with silica reinforced tread and/or sidewall components*. 29.03.2000, The Goodyear Tire & Rubber Company: EP 0 989 161 A1.
29. Wideman, L.G., Sandstrom, P.H., *Rubber composition containing a pyrazine compound*. 21.11.2001, Goodyear Technical Center Luxembourg: EP 0 860 469 B1.
30. Zimmer, R.J., Visel, F., Frank, U.E., Agostini, G., *Asymmetrical siloxy compounds*. 29.09.1999, The Goodyear Tire & Rubber Company: EP 0 945 456 A2.

31.   Barruel, P., Guennouni, N., *Polysilphide organosiloxanes which can be used as coupling agents, elastomer compositions containing same and elastomer articles from said compositions*. 08.04.2002, Rhodia Chemie: WO 02/083719 A1.

32.   Vidal, P.-L., *Rubber composition and tire having tread thereof*. 17.02.1999, Michelin Rech. Tech., Michelin Soc. Tech.: WO2004033548.

33.   ten Brinke, J.W., in *Thesis: Silica reinforced tyre rubbers*. 2002, Dept. Rubber Technol., Univ. Twente: Enschede (the Netherlands).

34.   Materne, T.F.E., Kayser, F., *Silica reinforced rubber composition used in tires*. 20.12.2000, The Goodyear Tire & Rubber Company: EP 1 061 097 A1.

35.   Pohl, E.R., Osterholtz, F.D., in *Molecular characterization of composite interfaces*, H. Ishida, Kumar, G., Editor. 1985, Plenum Press: New York.

36.   Nishiyama, N., Shick, R., Isida., H., J. Colloid Interface Sci., 1991. **143**: p. 146.

37.   Sindorf, D.W., Maciel, G.E., J. Am. Chem. Soc., 1983. **105**: p. 3767.

THERMAL BALANCE OF A MIXING PROCESS

INCLUDING

A CHEMICAL REACTION

The fingerprints of the mixing and silanization process allow an estimation of the different energy streams in an internal mixer. In this chapter, the heating and silanization step of the mixing process of silica-silane compounds are analyzed concerning the interaction of the energy balance and the silanization reaction.

The energetic effects involved in the chemical reaction and physical adsorption processes, taking place during mixing and silanization of silica-silane compounds, contribute only marginally to the energy balance of the whole process. They can in general be neglected in the overall energy balance.

However, the silanization reaction does influence the energy transfer to the cooling media: The ethanol formed during this reaction partially condenses on the mixing chamber walls, thus limiting the contact between the compound and the mixer walls. This reduces the cooling efficiency, resulting in a deviation from a linear correlation between the cooling efficiency and the temperature difference between the compound and the cooling media.

Other parameters influencing the cooling efficiency are fill factor, rotor speed, rotor design, processing mode (open mixer: ram up/closed mixer: ram down) and air injection.

1. INTRODUCTION

The energetic balance of a mixing process depends on various factors, mixer-, material- and process-related, that makes it difficult to derive processing parameters. In this chapter the special processing conditions of silica compounds are analyzed concerning their influence on the energy transfer to the cooling media. Factors discussed in this chapter are working in an open mixer, variation of the fill factor, temperature of the cooling media and of the compound, rotor speed, air injection, viscosity of the compound and the influence of the silanization reaction.

2. ENERGY BALANCES IN AN INTERNAL MIXER

2.1. ENERGY FLOWS IN AN INTERNAL MIXER, WITHOUT CHEMICAL REACTION

During the mixing process in an internal mixer, only a small percentage of the total energy Q_T is absorbed by the rubber compound, Q_C. The main part of the energy is distributed between electrical and mechanical energy losses Q_{EML} in the equipment itself, absorption by the mixing equipment Q_M and the cooling media Q_W, and energy losses to the environment Q_E, as shown in Figure 1. [1, 2]
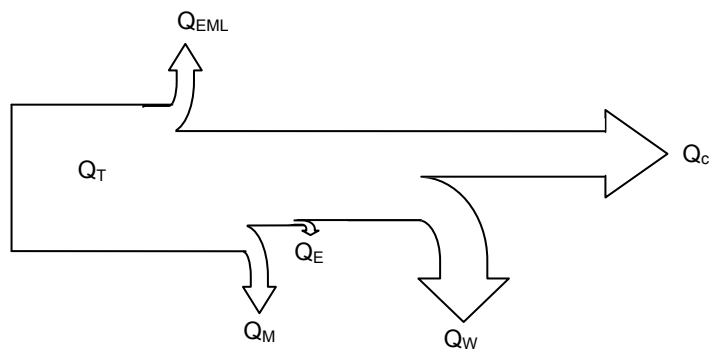

Figure 1: Energy flows during mixing in an internal mixer

The fingerprint of a mixing process allows an estimation of the ratios of the different energy flows into the rubber material, as explained in Figure 2.
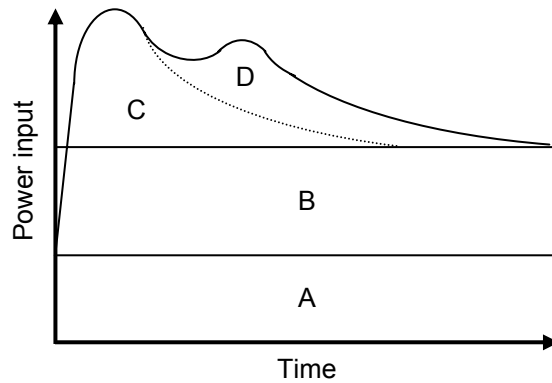
Figure 2: Generalized fingerprint of a mixing process [2]

For a powdered rubber compound with carbon black as filler, the energy consumed for mastication and comminution of the polymer, area A in Figure 2, is about one third of the total energy input. Area B represents the energy used for simple mixing in order to achieve a macroscopic homogenization by kneading and longitudinal cutback in the mixer. The energy consumed for incorporation of the filler is given by the area C, and area D is the energy necessary for the dispersion of the filler. [2] Various compound properties such as for example viscosity and complex modulus are changing as a consequence of the energy input. [3]

The energy balance during mixing in an internal mixer, without inclusion of a chemical reaction, can be expressed as follows: [1, 2]

$$Q_N = Q_T - Q_{EML} \qquad \text{Eq. 1}$$

The net energy input Q_N is equal to the total energy input Q_T reduced by the loss of energy due to the operation of the motor and other machinery Q_{EML}. The sum of the energy absorbed by the compound Q_c, the energy dissipated into the mixing equipment Q_M, the energy loss to the environment Q_E and the energy transfer by the cooling media, in general water, Q_w, is equally defined as the net energy input into the system Q_N:

$$Q_N = Q_C + Q_M + Q_E + Q_W \qquad \text{Eq. 2}$$

An estimation of the electrical and mechanical energy losses to the machinery, the ratio of Q_{EML}/Q_T, was experimentally done in a laboratory Banbury mixer for a compound containing powdered rubber and carbon black. This ratio was determined to be approximately 0.80, indicating that 20% of the total energy input was lost to the machinery. The relative energy absorption of the material, Q_c/Q_N, was measured to be 0.43. [4] Other sources calculated this ratio to be 0.36, based on an estimation of the energy required for rupture of the rubber. [2] The ratio of the energy dissipated into the mixer to the net energy input, Q_M/Q_N,

was approximately 0.13. The relative energy loss to the environment, Q_E/Q_N, was rather low and had an approximate value of 0.03. The relative energy transfer to the cooling media, Q_W/Q_N, was calculated to be 0.42. This ratio was decreasing with increasing mixer size, and reached values of 0.10 for large production-scale mixers. Generally not taken into account was the energy stored in the rubber due to elastic deformation, as this contribution was expected to be small compared to the net energy input Q_N. [4]

Table I gives average percentages of the energy streams as published in literature for a small scale laboratory mixer. [1, 2]

Table I: Energy flow in an internal mixer

Energy flow		Percentage of total energy [%]
Q_T	Total energy input	100
Q_{EML}	Electrical and mechanical losses	20
Q_N	Net energy input	80
Q_M	Heating of the mixer	10
Q_E	Environmental losses	3
Q_W	Energy to cooling water	34
Q_C	Enthalpy change of the compound	33

The discrepancy between the energy loss to the environment Q_E and the energy dissipation into the mixing machinery Q_M indicates, that the mixer temperature will rise slowly but steadily and that thermal equilibrium between heat accumulation and dissipation will only be achieved during long runs of similar compounds. This leads to the general problem of batch-to-batch variation, especially for the first few batches of a run.

The cooling efficiency is expressed by the ratio of Q_W/Q_N, the heat dissipated into the cooling water compared to the net energy input. Cooling is a result of heat conduction in three different areas: from the batch to the mixer wall, through the mixer wall and from the mixer wall into the cooling media. Especially during the initial phase of mixing, the thermal conductivity between the rubber compound and the mixer wall varies in time due to changes in wall adhesion: In the beginning of the mixing cycle the filler tends to adhere to the mixer wall making contact between rubber and steel, thus significantly increasing heat conduction across this barrier, especially in the case of carbon black. Once the filler is well dispersed, the compound is in permanent contact with the mixing chamber wall and the energy flux is more constant. [1, 2]

Figures 3 to 5 show the fingerprints of temperature and different energy streams during mixing and silanization, as measured during one representative silica mixing experiment.
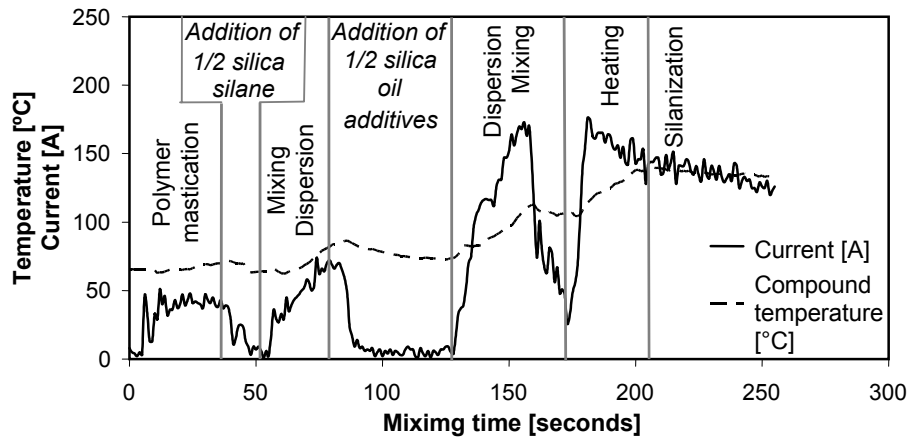
Figure 3: Fingerprint of temperature and current during mixing and silanization of silica compounds
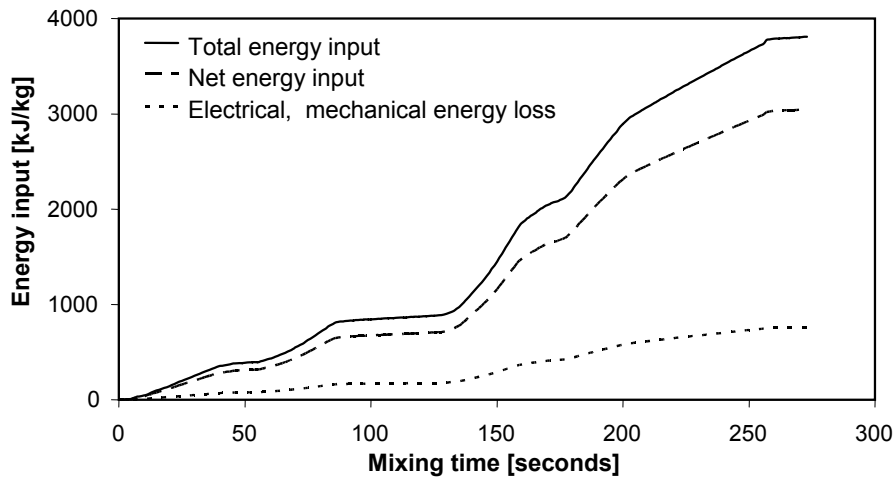

Figure 4: Energy streams during mixing and silanization of silica compounds
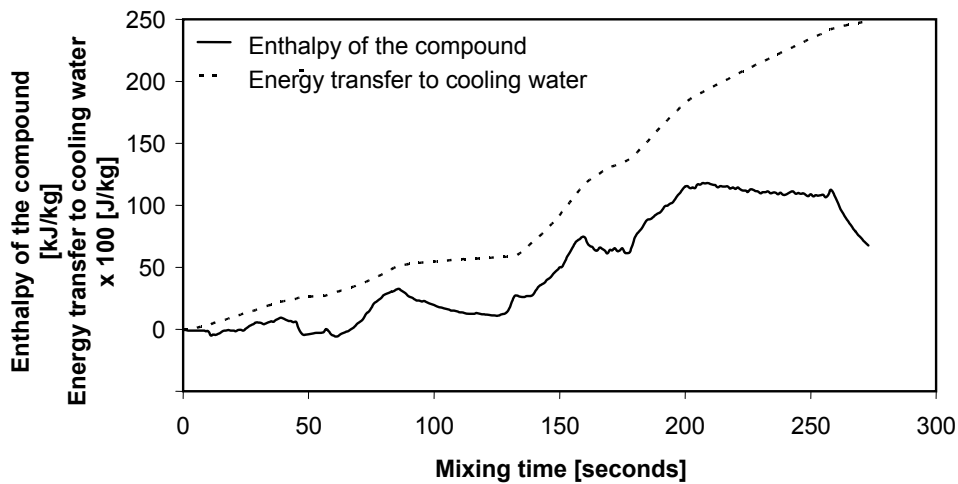

Figure 5: Energy balance of the compound and the cooling media during mixing and silanization of silica compounds

In Figure 3, a temperature and a current profile are shown, the latter being proportional to the torque. Figure 4 shows the total energy input as measured during the mixing cycle, and the calculated energy loss as well as the net energy input into the mixing equipment and compound. The enthalpy of the compound shown in Figure 5 is calculated from the temperature change during the process; energy changes due to a chemical reaction and adsorption of compound ingredients onto the filler surface are not taken into account. Making up the balance between the total energy input and the contributions as shown in Table I results in the energy transfer to the cooling water.

2.2. Heat Transfer from the Compound to the Cooling Media

Equation 3 correlates the energy transferred to the cooling water Q_W with the heat transfer coefficient κ, the heat transfer area A_{HT}, the time t and the temperature difference between the compound temperature and the temperature of the cooling media ΔT in the system: [4]

$$Q_W = \kappa \cdot A_{HT} \cdot t \cdot \Delta T \qquad \qquad Eq.\ 3$$

The heat transfer coefficient κ represents the overall heat transfer from the rubber compound to the cooling water. The heat transfer coefficients of rubber and steel are quite different: Steel is a very good heat conductor and has a very high κ-value, whereas rubber has a very low value. One problem arising from the low heat conductivity of rubber is the poor temperature-uniformity of a batch. The degree of non-uniformity depends on the viscoelasticity of the material as well as on the rotor geometry. The temperature is increased mainly by energy dissipated during the viscoelastic deformation and relaxation processes. As the shear forces show a wide variation within the mixing chamber, the energy input is strongly depending on the movement of a certain compound volume in the mixer. The heat flow between adjacent batch volume units is very limited due to the poor heat conductivity of the rubber. [1]

In most calculations, a temperature gradient within the rubber is not taken into consideration, in spite of the fact that practical experience shows that temperature differences within a batch are in the range of 10 to 20°C. The heat coefficient for the whole system then reduces to a function of the heat transfer coefficient between rubber and steel, α_{RS}, and the coefficient between steel and water, α_{SW}. Additionally, the heat conductivity of steel λ_H and the thickness of the mixer wall d_{wall} contribute to the heat transfer coefficient. The overall heat transfer coefficient κ is then calculated as follows: [4, 5]

$$\frac{1}{\kappa} = \frac{1}{\alpha_{RS}} + \frac{d_{wall}}{\lambda_H} + \frac{1}{\alpha_{SW}} \qquad \qquad Eq.\ 4$$

The heat transfer coefficient between rubber and steel, α_{RS}, depends on the elasticity of the material [6, 7] and the degree of mixing. The coefficient between steel and water α_{SW} depends on the circulation speed of the water and the existence of deposits on the inner surfaces of the cooling canals. The estimation of the heat transfer coefficient α_{SW} for a mixer with a volume of 110 liters results in a value of 750 W/m^2·K, calculated for a water flow rate of 70 liters/minute. The coefficient for a small mixer of 1.5 liter and a water flow rate of 15 liters/minute is roughly 550 W/m^2·K. [8] Other sources report values of α_{RS} in the range of 1100 to 6000 W/m^2·K, and values for α_{SW} between 2000 and 15.000 W/m^2·K in the case of water as a cooling media. [5] The thickness of the mixer walls d_{wall} varies between 10 and 100 mm, and the heat conductivity of steel λ is 45 to 60 W/m·K. [4, 5] The calculation of the overall heat transfer coefficient κ between rubber and cooling water results in values of 100 W/m^2·K to 250 W/m^2·K. [5, 8]

The main influencing factors for the cooling efficiency are the heat transfer area and the temperature difference between cooling media and rubber, as given in Equation 3. Rotor speed is also an influencing factor, as it determines the frequency of the renewal of the wall layer, thus the average temperature difference. The fill factor does not influence the cooling efficiency as long as the degree of filling is high enough to accomplish a complete coverage of the mixer walls (see chapter 4). The ratio of heat transfer area to mixing chamber volume increases with decreasing size of the mixer, resulting in higher cooling capacities for smaller size mixers. The ratio of surface area effective in cooling and mixing chamber volume is also higher for intermeshing mixers compared to tangential mixers. [9, 10] The cooling capacity increases proportionally with the temperature difference between rubber and cooling water: In the beginning of the mixing cycle, when the temperature gradient is small, only a small part of the energy input is dissipated into the water, resulting in a fast temperature increase. [5]

2.3. ENERGY BALANCE OF THE RUBBER COMPOUND IN THE MIXER, WITH CHEMICAL REACTION

The energy input into the compound is based on shear forces: During mixing the material is periodically passing zones of high shear forces, and a part of the mechanical energy is dissipating into the material as heat. The efficiency of the energy input by shearing is strongly depending on the viscosity of the material. The viscosity decreases with increasing degree of filler dispersion and silanization as well as with increasing temperature. The influence of temperature on viscosity η can be calculated by an Arrhenius-type of equation (Equation 5). It is a function of the absolute temperature T and activation energy E_A, with a proportionality factor F. R is the gas constant. [4, 11]

$$\eta = F \exp(E_A / RT) \qquad\qquad Eq.\ 5$$

The shear stress τ applied to a non-Newtonian material is proportional to the viscosity η and depends on the shear rate $\dot{\gamma}$: [12]

$$\tau = \eta \cdot \dot{\gamma}^{\,n} \qquad\qquad Eq.\ 6$$

The power law index n is in the range of 0.2 to 0.3 for most rubbers. [12]

The energy input into the compound is partly consumed for mixing, partly transferred to the cooling media and partly dissipated as heat, resulting in a temperature increase. For a compound without a chemical reaction the energy balance is limited to these three contributions. However, if a chemical reaction or a physical process is taking place, the energetic contributions of these processes have to be included into the energy balance as well. The total balance is then given in Equation 7:

$$Q_N = Q_C + Q_M + Q_E + Q_W + Q_{CR} + Q_{PP} \qquad\qquad Eq.\ 7$$

Q_{CR} and Q_{PP} are the energetic contributions of the chemical reaction and the physical processes, respectively. The contribution of the chemical reaction in the case of a silica-silane compound is the reaction of the silane with the filler surface, the hydrolysis of ethoxy groups and the homocondensation of silane molecules. If the reaction is fully completed, the reaction enthalpy is 91 kJ per kilogram of the TESPD-compound used in the present investigation. This value is calculated for the reaction of one ethoxy group per silyl group reacting directly with a silanol group of the silica surface and the remaining two ethoxy groups being hydrolyzed and undergoing homocondensation, and is based on the energies of the functional units of the molecules. [13]

The physical processes taking place during the silanization reaction are ad- and desorption processes. The physical adsorption of the silane as well as ethanol is contributing to the energy balance of the system. Adsorption enthalpies are in the range of 20 to 50 kJ/mol. Assuming that all ethoxy groups of the silane are adsorbed prior to the chemical reaction, either as such or as ethanol molecules, the total adsorption energy is about 6 to 16 kJ/kg compound. In comparison to the total energy input into the compound this quantity can be neglected.

In the experiments described in paragraph 3 and 4, the temperature during the silanization period was kept constant. In this case, the energy input into the compound, Q_C, is equal to the sum of the energy transferred to the cooling water Q_W and the energy contributions of the chemical reactions, Q_{CR}:

$$Q_C = Q_W + Q_{CR} \qquad\qquad Eq.\ 8$$

The energy input into the material Q_c mainly depends on mixer characteristics, process parameters and material properties. The energy transferred to the cooling media is correlated to the temperature difference between the cooling water and the compound. It also depends on rotor speed, as this determines the rate of renewal of the wall layer. The rate of the chemical reaction is influenced by the silanization temperature and the availability of free sites on the silica particles. The latter depends on the dispersion of the filler and the adsorption of ethanol and other compound ingredients.

3. EXPERIMENTAL SETUP

The experiments are carried out according to the experimental setup as described in detail in Chapter 3. Briefly summarized, the procedure was as follows:

- Preparation of a large masterbatch, in which the filler dispersion was almost complete, but silanization occurred only to a very limited extent
- Warming up of a portion of the masterbatch to the silanization temperature in a closed mixer without air injection
- Silanization at a constant temperature and adjustment of the rotor speed
- After silanization, the compound was discharged and the temperature was controlled

The temperature profile of the compound and the energy consumption of the mixer were automatically monitored during mixing, heating and silanization. The compound temperature was measured by thermocouples installed in the mixing chamber, in general in the bottom part of the mixing chamber and in the side plates. The energy flows were calculated from the total energy consumption according to Equation 7, with the energy flows Q_{EML}, Q_M and Q_E as given in Table I. For the experiments carried out in the open mixer mode, the ram was lifted after the silanization temperature was reached and was held in this position during silanization. All investigations were done using a passenger car tire tread masterbatch based on a blend of S-SBR and BR with 83.5 phr silica and a coupling agent, either TESPT or TESPD. The mixers used in this investigation are given in Table II. The notification 'I' stands for intermeshing, 'T' for tangential rotor geometry, and the number signifies the size of the mixing chamber.

Table II: Mixers used in the investigations

	Net mixer volume [liter]	Rotor type [-]
I5	5.5	PES5
I45	49.0	PES5
T4	3.6	ZZ2
T7	7.6	F4W

Table III gives an overview of the conditions for the experiments discussed in paragraph 4.

Table III: Overview of the experimental parameters

Figure	Mixing step	Mixer	Rotor type	Fill factor	TCU settings	Silanization temperature	Silanization time	Air injection	Mixer mode	Coupling agent
	[1]	-	-	%	[°C]	[°C]	[minutes]	[on/off]	[open/closed]	[2]
6	W	I5	PES5	var.	60	145	-	-	closed	MS, OS
7	W	I45	PES5	var.	40	145	-	-	closed	TESPT
8	S	I5	PES5	var.	60	145	1	off	open	TESPT
9	S	T4	ZZ2	var.	60	145	2.5	off	open	TESPT
10	S	I5	PES5	var.	60	145	2.5	off	closed	MS,OS
11	S	I5	PES5	67	60	var.	1.0 - 5.0	off	closed	MS, OS, TESPT
12	S	I5 T4 T7	PES5 ZZ2 F4W	40 45 45	60	var.	1.0 -5.0	off	open	TESPD
13	S	I5	PES5	40	60	var.	2.5	off	open	TESPT
14	W	T4 I5	ZZ2 PES5	60	var.	145	-	off	closed	TESPT
15	S	I45	PES5	40	40	145	var.	var.	var.	TESPD

[1] W: Warming up to silanization temperature

S: Silanization

[2] MS: Monomeric blocked silane (S-[3-(triethoxysilyl)propyl]ester of octanethionic acid)

OS: Oligomeric silane (bis(triethoxysilyl)polybutadiene)

TESPD: bis(triethoxysilylpropyl)disulfane

TESPT: bis(triethoxysilylpropyl)tetrasulfane

4. EXPERIMENTAL RESULTS

4.1. ENERGY FLOWS AS A FUNCTION OF THE FILL FACTOR

4.1.1. Energy flow during heating (no silanization)

Fill factor studies were carried out for different mixer/rotor combinations in the pressure-less mode, open mixer, as well as in a closed mixer. Figure 6 shows a series of experiments carried out in a 5.5 liter intermeshing mixer with the temperature control unit set at 60ºC. Two different compounds containing silanes differing in structure and molecular weight were used in this investigation: an oligomeric silane and a monomeric silane with a blocked thiol group. Details on these silanes are given in chapter 8. The heating period and the silanization period were analyzed in terms of energy flows. For the evaluation the energy contribution from silanization during this period was neglected, as the degree of silanization was assumed to be very low. Figure 6 shows the energy flows as well as the total number of revolutions for the two compounds at different fill factors.
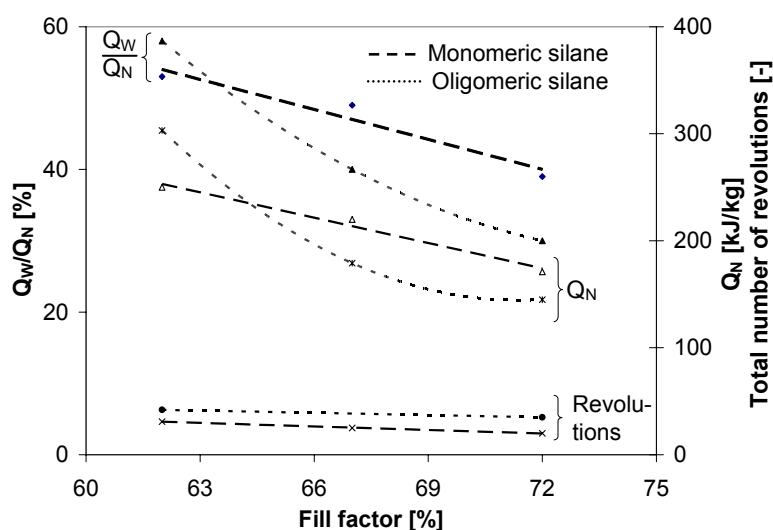
Figure 6: Net energy input Q_N, cooling efficiency Q_W/Q_N and total number of revolutions during warming as a function of the fill factor for compounds containing different silanes

The net energy input Q_N necessary for heating the material is reduced with increase of fill factor, and this effect is strongest for the compound with the oligomeric silane. The energy dissipated into the cooling water Q_W/Q_N also decreases with increasing fill factors. The compound with the oligomeric silane is more sensitive to a variation of the fill factor than the compound containing the monomeric silane. The total number of revolutions during the heating period is reduced with increasing fill factor, and the absolute values are slightly lower for the compound with the monomeric silane.

Figure 7 shows the influence of the fill factor on the cooling efficiency of the 49 liter intermeshing mixer. The energy dissipation into the cooling water is linearly

decreasing with increasing fill factor. However, compared to the measurements shown in Figure 6, the influence of the fill factor is less pronounced: The slope of the fitting line in Figure 7 is 0.6, compared to a slope of 1.4 for the fitting line for the compound with a comparable silane: the monomeric silane, as shown in Figure 6.
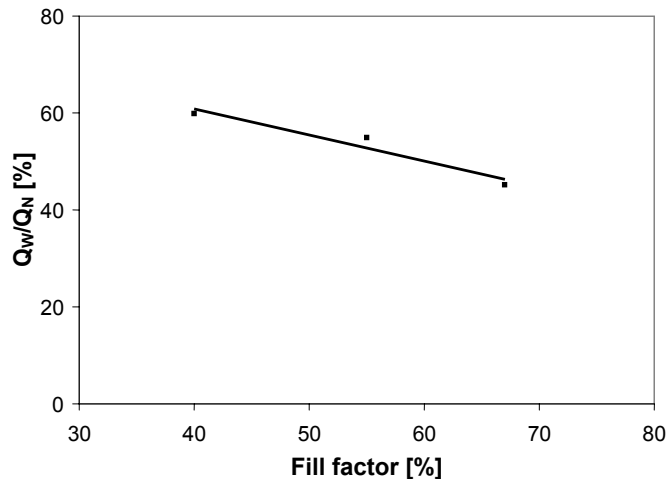
Figure 7: Energy transfer to the cooling water as a function of the fill factor during warming up in a closed mixer

4.1.2. *Energy flow during silanization at a constant temperature*
The energy dissipation into the cooling water during the silanization period was calculated from the total energy input by combining Equations 1, 2 and 8. The energy streams Q_{EML}, Q_N, Q_M and Q_E were quantified according to Table I. The energy contribution of the silanization reaction was calculated from the decrease in the Payne effect values with the assumption, that for a maximum degree of silanization 4 ethoxy groups per silane molecule, bis(triethoxysilyl-propyl)disulfane or –tetrasulfane, are reacting.

The values of the reaction energy were calculated to be less than 2 % of the energy input into the compound. The energy released during adsorption of silane and ethanol onto the filler was neglected.
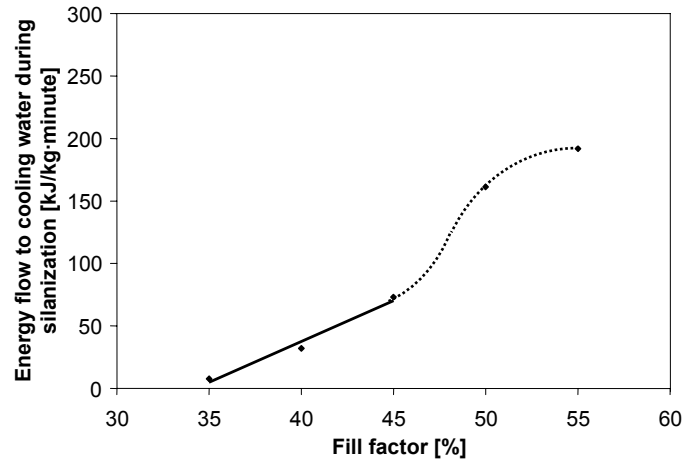
*Figure 8: Energy transfer to cooling water as a function
of the fill factor for silanization in an open mixer (I5)*
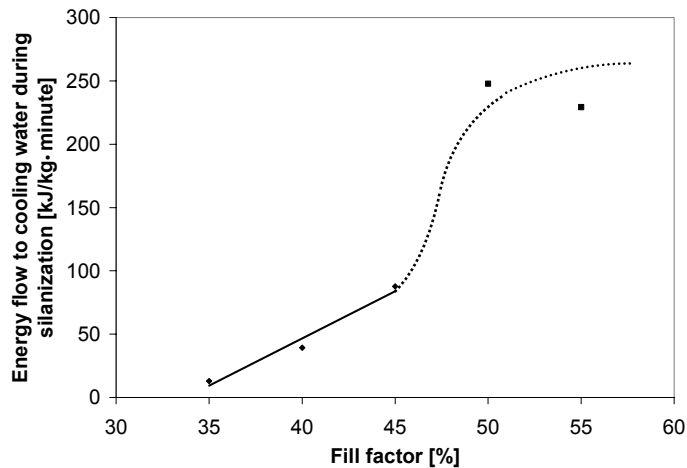
*Figure 9: Energy transfer to cooling water as a function
of the fill factor for silanization in an open mixer (T4)*

Figures 8 and 9 illustrate the energy flow to the cooling media as a function of the fill factor for silanization at a constant temperature in an open mixer. For low fill factors the energy flow increases proportionally with increasing fill factor. Between fill factors of 45% and 50% a discontinuity is observed: The energy dissipation increases significantly, and at the highest fill factors no univocal trend is found for the two mixers, possibly because the flow pattern is not properly developed at such high fill factors in open mixers.

143
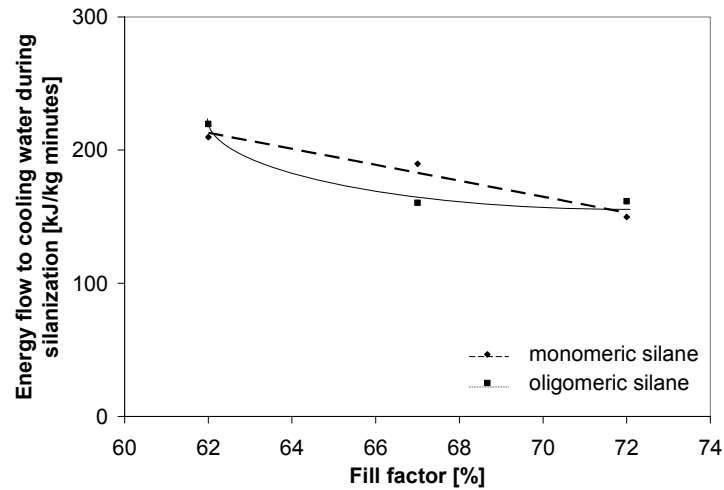
Figure 10: Energy transfer to cooling water
for silanization in a closed intermeshing mixer

The influence of the fill factor on the energy dissipation in a closed mixer for the silanization at a constant temperature is illustrated in Figure 10: With increasing fill factors a decrease in energy transfer to the cooling media is found. However, the influence of the fill factor on the cooling efficiency is not very strong. The energy flow for the compound containing the monomeric silane can be approximated by a linear correlation with the fill factor, whereas the compound with the oligomeric silane shows a polynomial correlation.

4.2. ENERGY FLOWS AS A FUNCTION OF THE DEGREE OF SILANIZATION
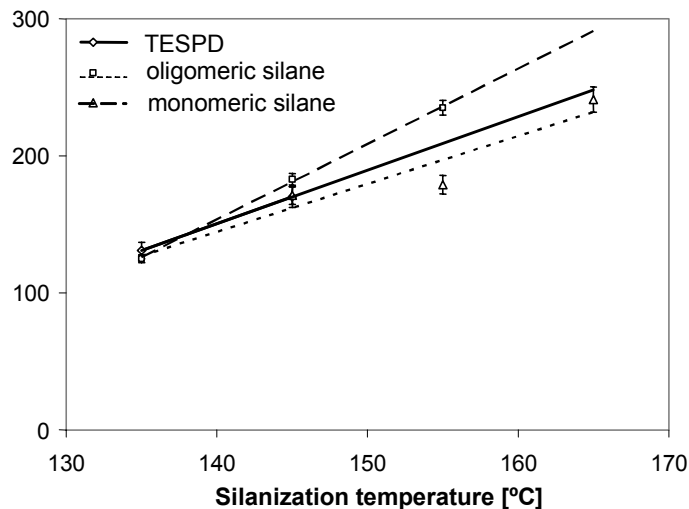
Figure 11: Energy transfer to the cooling water during silanization
at a constant temperature for compounds containing different silanes

In this series of experiments, compounds with three different silanes were compared. Two of the silanes are described in chapter 8, the polar monomeric silane and the oligomeric silane; the third silane is the non-polar monomeric

TESPD. In this series of experiments the rotor speed was varied within narrow limits in order to keep the temperature constant during the silanization period.

At a given temperature, the energy transfer into the cooling water is independent of the degree of silanization of the compound: The values of the energy transfer per unit time and mass are equal for different silanization periods. The values given in Figure 11 are average values for different silanization periods, and the variation of the individual values is represented by error bars. The energy transfer to the cooling media is quite similar for the compounds with TESPD and the oligomeric silane. Only the compound with the monomeric silane shows increased energy dissipation into the cooling water. The silanization temperature is influencing the energy flows: A higher compound temperature results in a higher amount of energy transferred to the cooling water, and a linear correlation is found.
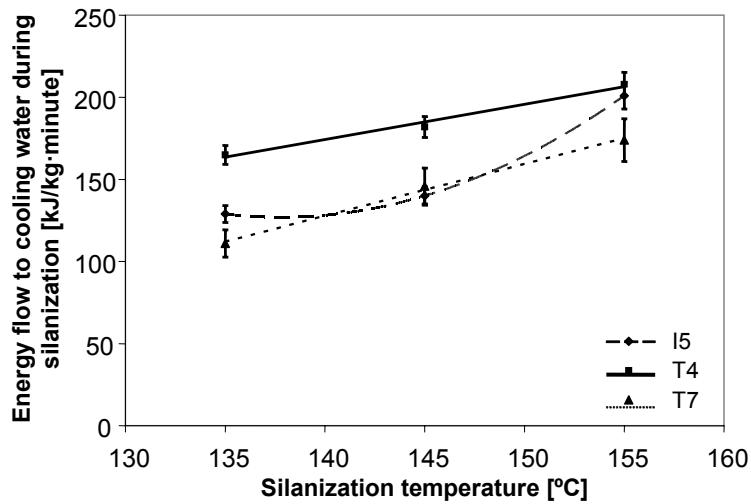
Figure 12: Energy transfer to the cooling water during silanization in an open mixer with variation of the rotor type

Figure 12 shows the energy flow to the cooling water for 3 different mixer types: the I5 mixer has a volume of 5.6 liter and intermeshing PES5 rotors, the T4 mixer has a volume of 3.6 liter and tangential ZZ2 rotors, and the T7 mixer has a volume of 7.6 liter and tangential F4W rotors. For these 3 types of mixers the energy transfer to the cooling media increases with increasing silanization temperature. The T4 mixer has the highest energy flow into the cooling water. The difference between the mixer with the full four wing rotors (T7) and the PES5 rotors (I5) is rather small. For lower temperatures their cooling efficiency is comparable; only at 155ºC the T7 mixer shows a slightly lower cooling efficiency.
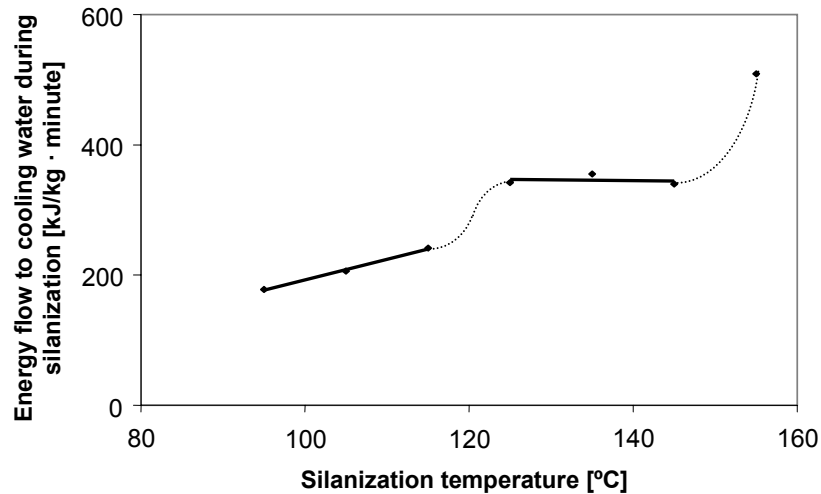
*Figure 13: Energy transfer to the cooling water as a function
of the silanization temperature in the intermeshing laboratory mixer*

Figure 13 shows the energy dissipation for the intermeshing mixer within a wider temperature interval. As expected, an increase of energy dissipation into the cooling water is found with increasing compound temperature. For low temperatures, the increase is strongest and a linear correlation with temperature is found. At temperatures between 120°C and 150°C, the increase of the energy dissipation into the water with increasing temperature is smaller and the absolute value is on a significantly higher level compared to the situation at lower temperatures. Between 145°C and 155°C, again a steep increase is measured.

4.3. ENERGY FLOW AS A FUNCTION OF THE TEMPERATURE CONTROL UNIT SETTINGS

The cooling efficiency, expressed by the percentage of the net energy input transferred into the cooling water, Q_W/Q_N, is reduced with increasing temperature of the cooling media, the temperature control unit settings (Figure 14). This trend is found for two different rotor types, a tangential as well as an intermeshing rotor, but the correlation with the cooling temperature is different: In the case of the intermeshing mixer (I5), a linear correlation is found, whereas in the case of the tangential mixer (T4), the cooling efficiency is decreasing rather exponentially. The net energy input decreases exponentially in both cases with increasing temperature settings, but the decrease is stronger in the case of the intermeshing mixer.

146
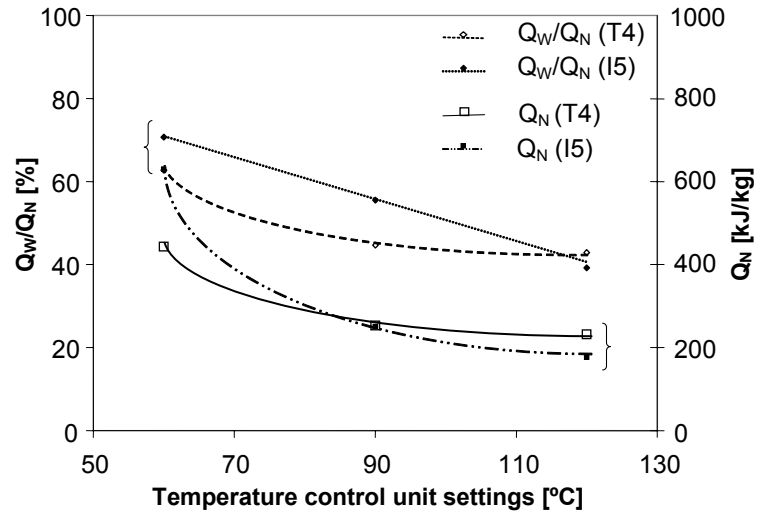
*Figure 14: Cooling efficiency Q_W/Q_N and net energy input Q_N
during warming up as a function of the temperature control unit settings*

4.4. INFLUENCE OF AIR INJECTION ON THE ENERGY BALANCE

In a different series of experiments the influence of air injection on the silanization process was investigated. Figure 15 shows the influence of air injection on the energy input during silanization at 145°C in the 45 liter intermeshing mixer, in an open as well as in a closed mixer. The two series differ in the duration of the silanization period (1.0 and 2.5 minutes, respectively), and in the coupling agent used (TESPD, TESPT). As the coupling agents are quite similar in structure and reactivity towards the filler, their effect on the energy balance is assumed to be similar. When air injection is used in order to remove ethanol out of the compound, the energy input required to keep the temperature level is higher. The maximum increase measured in these experiments is 25%. This effect is most pronounced for the silanization in the pressure-less mode (open mixer).
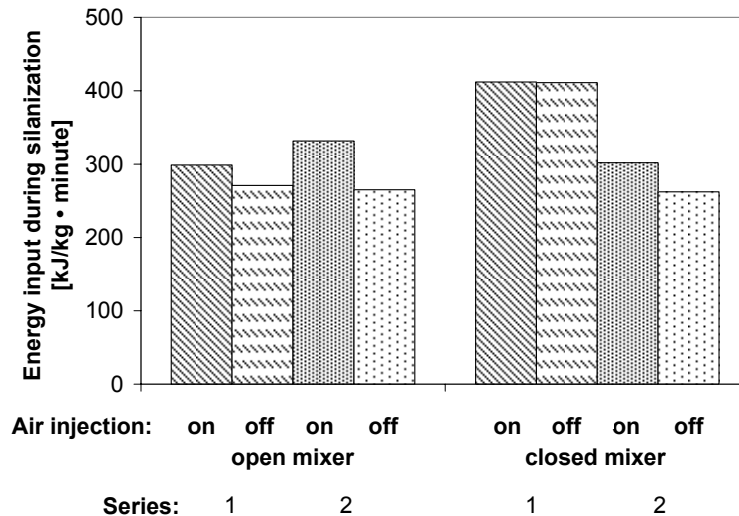
*Figure 15: The influence of air injection
on the energy input during the silanization period*

5. DISCUSSION

5.1. ENERGY FLOW AS A FUNCTION OF THE FILL FACTOR

Looking at the influence of the fill factor on the net energy input Q_N for heating up in a closed mixer, different correlations are found depending on the silane used in the compounds, as illustrated in Figure 6: For the compound containing the monomeric silane a linear correlation is found. The compound containing the oligomeric silane shows a reduced influence of the fill factor for higher degrees of filling, resulting in an exponential decrease of the energy input into the cooling media for increasing degrees of filling. The lower net energy input is also expressed in a lower total number of revolutions necessary during the heating up period. This result is in accordance with the general experience, that a higher fill factor results in a more efficient energy input.

Equation 3 shows, that the energy transfer to the cooling water is a function of the contact area and the temperature gradient across the mixing chamber wall. The influence of the temperature gradient is expressed by the temperature of the compound, but also by the total number of revolutions during the warming up period, a measure of the frequency of the renewal of the wall layer. This is a determining factor for the heat exchange between the compound and the cooling media: The higher the renewal rate, the higher the average temperature difference between the compound and the cooling water. The contact area between the compound and the mixer walls does not depend significantly on the fill factor, as described in the model in chapter 4, once a complete covering of the mixer wall is achieved. However, a higher fill factor does result in a smaller ratio of contact area to compound volume, thus negatively influencing the cooling efficiency.

The difference in the sensitivity to a variation of the fill factor, which depends on the silane, is somewhat unexpected, as during the studied period silanization is still of minor importance for the energy balance of the compound, and therefore both compounds should behave similarly. A possible explanation for this difference is based on a physical effect: The oligomeric silane reacts more like a polymer and is therefore more sensitive to shearing forces. Like the rubber polymer chains, the long silane molecules will be broken by shear forces, resulting in a stronger influence on the viscosity of the compound and an additional consumption of energy.

Figure 7 shows the influence of the fill factor on the cooling efficiency in the 45 liter intermeshing mixer. Compared to the experimental series of Figure 6, the size of the mixer is larger by a factor of approximately 10, the temperature control unit settings are lower (40ºC instead of 60ºC), and different silanes were used. Looking at the silanes used, the compound with TESPT (Figure 7) and the compound with the monomeric silane (Figure 6) are assumed to behave similarly within this evaluation: As the energy balance is established for the

heating period prior to silanization, the silane should not influence the energy flow. In this series of experiments the linear correlation between cooling efficiency and fill factor was reproduced: This correlation is independent of mixer size. However, the influence of the fill factor is less pronounced in the 45 liter mixer, and the absolute levels of dissipated energy are higher. The latter observation is somewhat unexpected, as an increasing mixer size generally results in a reduced cooling efficiency. In the 45 liter mixer this effect is counterbalanced by a lower temperature of the cooling media.

During the silanization period the temperature was kept constant, and for the process in an open mixer the cooling efficiency was seen to linearly increase with increasing fill factors for low degrees of filling, as illustrated in Figures 8 and 9. This is due to the increasing contact area between the rubber compound and the mixer wall. Once a certain threshold is reached, the cooling efficiency steps up significantly: Above these fill factors the mixer wall is completely covered and a further increase of the fill factor is not resulting in an improvement of the cooling efficiency. The threshold value for both mixer lies between 45% and 50% of filling. The energy dissipation into the cooling water will be influenced by the intake behavior as well, but this influence will be contrary to the influence shown in Figure 8 and 9: A higher fill factor results in a more irregular intake behavior with the consequence, that the cooling efficiency is reduced. Apparently the effect of wall coverage is more than counterbalancing the effect of intake behavior.

The situation during silanization in a closed mixer is different, as seen in Figure 10: In this case the energy dissipation decreases with increasing fill factor. For the fill factors used in the investigations, the degree of filling was high enough to accomplish a complete coverage of the mixer wall, and any additional compound in the mixer will lead to an increase of the volume of the rolling pool of material in front of the rotor flight. The ratio of the contact area with the mixer wall and the volume of the compound are reduced, and, as a consequence, the cooling efficiency becomes less.

5.2. ENERGY FLOW AS A FUNCTION OF THE DEGREE OF SILANIZATION

The energy dissipation into the cooling water is independent of the degree of silanization at a given temperature, but depends on the silanization temperature (Figure 11). The latter result was to be expected, as the cooling efficiency depends on the temperature difference between the compound and the cooling media. As stipulated by Equation 3, the correlation is linear. Therefore the driving force for the energy transfer between the rubber material and cooling water rises with increasing compound temperature. The constant values found for the energy dissipation to the cooling water at different degrees of silanization implies that the heat transfer is independent of the viscosity of the compound. The viscosity influences the flow behavior of the rubber

compound in the mixer, but apparently not to such an extent that the renewal of the rubber layer on the mixer wall by the rotor movement is influenced.

The comparison of the different rotor geometries in laboratory mixers of comparable sizes shows an unexpected result (Figure 12): The energy dissipation into the cooling water is highest for the T4 mixer with the tangential ZZ2 rotors. Generally, tangential mixers are known to have a lower cooling efficiency compared to mixers with intermeshing rotors. However, in the present case the series of experiments was done in an open mixer with the ram up, and in this mode the known better intake behavior of the tangential rotors plays a dominant role. The tangential rotor pulls the compound into the mixing chamber more frequently and regularly, thus increasing the contact time and renewal rate of the compound with the mixer wall, resulting in an improved cooling efficiency. Additionally, the volume of this mixer is only 2/3 of the volume of the intermeshing mixer, again resulting in a slight increase of the cooling efficiency.

Figure 13 provides a view on the cooling efficiency for a wider temperature window. It shows the energy transfer to the cooling water at a given constant temperature during the first 2.5 minutes of silanization after heating of the compound. Three different temperature regimes can be distinguished. At low temperatures, 95ºC to 115ºC, the energy transfer is proportional to the compound temperature, as stipulated by Equation 3 for a constant heat transfer area and heat transfer coefficient. Between 115ºC and 125ºC the heat transfer increases significantly with temperature. At temperatures between 125ºC and 145ºC, the energy flow is nearly independent of the temperature level. In this temperature window the increasing cooling efficiency due to the increasing temperature difference between the compound and the cooling media must be counterbalanced by another effect. As the silanization starts at the lower limit of this temperature range, a relation between the energy transfer and the chemical reaction must be assumed. Once the silanization starts, ethanol is formed as one of the reaction products. The ethanol evaporates under the given conditions, but re-condenses to a significant extent in the mixer on the cooled mixer walls, as their temperature is below the boiling point of ethanol. This results in stick-slip behavior of the compound, reducing the cooling efficiency. At even higher compound temperatures, again an increase in the energy dissipation is found: The temperature level of the whole system is now high enough to prevent the condensation of ethanol, thus to reduce slip effects.

5.3.   ENERGY FLOW AS A FUNCTION OF TEMPERATURE CONTROL SETTINGS

Equation 3 stipulates a linear correlation between the energy dissipation into the cooling water and the temperature difference between the compound and the cooling media. Figure 14 shows this correlation: The cooling efficiency is reduced with increasing temperature of the cooling water, but only in the case of the intermeshing mixer a linear correlation is found. In the tangential mixer,

the cooling efficiency is decreasing exponentially with increasing temperature of the cooling water. For a large temperature difference the cooling efficiency is high: approximately 2/3 of the net energy input is transferred to the cooling media. By increasing the cooling water temperature from 60ºC to 90ºC, the cooling efficiency is reduced to 45 %. For a further increase of the cooling temperature to 120ºC the cooling efficiency is only slightly further reduced: The energy flow to the cooling water mainly changes in the range between 60ºC and 90ºC. The boiling point of ethanol is within this temperature window: At temperatures above the boiling point of ethanol the condensation of the alcohol is reduced, resulting in less slip and a more efficient cooling. This increases the cooling efficiency at higher cooling temperatures compared to the influence of the temperature difference alone, resulting in the exponential decrease of the cooling efficiency instead of a linear correlation. In an intermeshing mixer the cooling efficiency is generally higher, with the result that the effect of ethanol condensation is less conspicuous.

5.4.   INFLUENCE OF AIR INJECTION ON THE ENERGY BALANCE

Comparative experiments with and without air injection were carried out in order to investigate the influence on the silanization efficiency. Besides the influence on the silanization reaction, air injection is expected to have an influence on the energy balance of the silanization process and on ethanol condensation. Figure 15 shows representative results of this comparative investigation: When air injection is used, a higher energy input is required to keep the temperature of the compound on a constant level. The stream of air is extracting ethanol together with energy from the compound, resulting in a cooling effect. This effect is more pronounced for mixing in an open mixer with the ram up, where the air can escape freely and therefore the throughput of air is higher compared to the situation in a closed mixer. Additionally, the evaporation of ethanol is consuming energy. Air injection also reduces the condensation of ethanol in the mixing chamber. This improves the wall contact of the compound, again an effect which results in a higher cooling efficiency.

The reduction of the ethanol concentration in the compound by dragging the alcohol out of material reduces the surface coverage of silica with ethanol and increases the concentration of free adsorption sites for the silane. This results in a direct increase of the silanization efficiency.

5.5.   GLOBAL VIEW ON THE INFLUENCING FACTORS
        FOR THE COOLING EFFICIENCY

In paragraph 5.1 through 5.4., correlations between the cooling efficiency and different mixing and silanization parameters were discussed. The correlation given by Equation 3, a linear correlation between the cooling efficiency calculated as Q_W/Q_N, and the difference between the compound temperature and the cooling water temperature ΔT, is observed for most of the operating

conditions. As an exception, the cooling efficiency of the tangential mixer operated in the pressure-less mode was found to be a function of the temperature difference ΔT to the power of 2, probably caused by stick-slip behavior due to ethanol condensation in the mixer. The fill factor influences the cooling efficiency, and depending on other processing conditions such as the operating mode (open, closed mixer) and type of silane used, either a linear or polynomial correlation is found. When a monomeric silane is used, the cooling efficiency depends linearly on the fill factor, independent of mixer size. Using an oligomeric silane, which has a stronger influence on the processing behavior of the compound, the cooling efficiency is found to be proportional to the fill factor to the second power. The energy flow to the cooling media is found to be independent of the viscosity of the compound. Rotor speed influences the cooling efficiency, as this is the determining factor for the frequency of the surface renewal, thus for the average temperature of the compound in contact with the mixer wall. A linear correlation is found between the cooling efficiency and the number of revolutions. The number of revolutions during the silanization period is of outstanding importance for the devolatilization of the compound and, as a consequence, for the silanization efficiency, as elaborated in chapter 4. If air injection is used to remove ethanol out of the system, the energy loss of the compound is increased due to the additional cooling of the material by the air stream. Other factors influencing the energy balance are related to the rotor type, such as the intake behavior in the pressure-less mode and the flow of the compound in the mixing chamber with special focus on the contact with cooled surfaces.

The correlation between the cooling efficiency and the different parameters P discussed above can be approximated according to the following engineering equation:

$$Q_W / Q_N = A \cdot P^n + B \qquad\qquad Eq.\ 9$$

A and B are arbitrary constants. In Table IV the coefficients for the correlation between the cooling efficiency and the different processing parameters are given.

*Table IV: Coefficients to describe the correlation between
the cooling efficiency and various processing parameters*

Parameter	n	Remarks
ΔT	1	In most cases a linear correlation
	2	Reduced cooling efficiency, e.g. due to stick slip from ethanol condensation
Fill factor	1	Monomeric silanes, small and medium size mixers, low fill factors in an open mixer
	2	Oligomeric silanes, high fill factors in an open mixer
Viscosity	0	
Number of revolutions	1	

6. CONCLUSIONS

For silica compounds, chemical and physical processes contribute to the energy balance of the silanization process. The enthalpies of the silanization reaction and the physisorption of silane and ethanol are low compared to the energy input into the rubber compound during mixing and silanization, and influence the energy balance only marginally.

The correlation between the heat transfer to cooling water and the temperature difference between compound temperature and cooling water temperature is found to be linear, as long as ethanol condensation in the mixing chamber is not affecting the cooling efficiency. The condensation of ethanol reduces the contact between mixer wall and the compound, resulting in a reduced cooling efficiency by slip effects.

The correlation between the fill factor and the cooling efficiency is found to be linear for different mixer sizes and for mixing and silanization in a closed as well as in an open mixer. Compounds containing a silane, which is strongly influencing the rheological behavior like an oligomeric silane, behave differently: In this case the correlation changes to a polynomial one. The viscosity of the compound does not influence the cooling efficiency.

Rotor speed influences the energy balance, as it determines the frequency of the wall layer renewal and, as a consequence, the average temperature of the rubber material in contact with the mixer wall. A linear correlation is observed between the number of revolutions and the energy dissipated into the cooling water.

7. REFERENCES

1. Nakajima, N., Harrell, E.R., Seil, D.A. *Energy balance and heat transfer in mixing of elastomer compounds with the internal mixer*. in *Proceedings ACS Rubber Division Conf., October 8-11, 1981*. Detroit, Michigan.
2. Nakajima, N., Harrell, E.R., Rubber Chem. Technol., 1984. **57**: p. 153.
3. Leblanc, J.L., Rubber World. **March 2001**: p. 28.
4. Palmgren, H., Rubber Chem. Technol., 1975. **48**: p. 462.
5. Kapitonov, E.M., Sov. Rubber Technol., 1968. **27**(4): p. 21.
6. Wiedmann, W.M., Schmid, H.M., Rubber Chem. Technol., 1982. **55**: p. 363.
7. Wiedmann, W.M., Schmid, H.M., Koch, H. *Rheologisch-thermisches Verhalten von Gummiknetern*. in *Int. Kautschuk-Tagung*. 1980. Berlin, Germany.
8. Menges, G., Grajewski, F., Sunder, J., Gummi Fasern Kunstst., 1988. **41**(2): p. 55.
9. Yoshida, T., Int. Polym. Sci. Technol., 1993. **20**(6): p. 29.
10. White, L., Europ. Rubber J. **March 1996**: p. 35.
11. Jentsch, J., Michael, H., Flohrer, J., Plaste Kautsch., 1983. **30**(4): p. 216.
12. Ghafouri, S.N., Rubber World. **March 2004**: p. 46.
13. Luo, Y.-R., in *Handbook of bond dissociation energies in organic compounds*. 2003, CRC Press: Boca Raton.

UPSCALING
OF THE MIXING PROCESS
IN AN INTERNAL MIXER
INCLUDING A CHEMICAL REACTION

In this chapter, the most important variables for upscaling of the mixing process of a rubber compound containing silica and a coupling agent will be investigated. The influence of the mixer and process parameters is different compared to the mixing process of carbon black compounds, as this process is not only based on physical mixing and dispersion, but also on a chemical reaction, for which mass transfer is crucial. The influencing factors for energy and mass transfer are basically the same, and as both, the efficiency of the physical mixing process and the chemical reaction, depend on these factors, they are more important in silica mixing compared to carbon black mixing.

In silica mixing, ethanol is formed during the silanization reaction and has to be removed from the rubber compound and out of the mixer: A low ethanol concentration in the vapor phase of the mixing chamber results in reduced concentrations of ethanol in the compound, thus in a higher rate of the silanization reaction. Mass transfer across the rubber/vapor interphase in the mixing chamber is determining these concentrations, therefore the ratio of surface area to volume of the compound should be maintained in upscaling. The exposure time of the compound surface and the renewal rate of the vapor phase in the mixer are important, as both influence ethanol transfer from the compound to the vapor phase. The fill factor influences the efficiency of energy input and ethanol formation per unit volume of the mixer. The dispersion efficiency is represented by the gap size, as the gap between rotor tip and mixer wall is the area in the mixing chamber with the highest shearing forces.

1.   INTRODUCTION

Various models for scaling up of the mixing process for rubber were developed, but none of these models is generally applicable without any shortcomings. The models in general are focused on one process parameter such as total shear or energy input; a model combining simple mixing, dispersion, mass transfer and a chemical reaction has not yet been published. The main problem of upscaling is the change of a variety of process parameters with the change in scale, mainly related to wall effects, dynamics and stability. Wall effects influence heat and mass transfer as well as the flow stability. In terms of dynamics the flow pattern in the mixer will be influenced by the geometrical dimensions, resulting in differences in shear stress applied to the compound. Stagnation zones change, as well as the residence time distributions for different zones in the mixer. Temperature and concentration gradients are influenced by the change in the surface-to-volume ratio. Consequently, the stability of the process becomes more sensitive to changes with increasing mixer size. If the rubber mixer is regarded as a chemical reactor, not only momentum and heat balance have to be taken into consideration, but also concentration changes due to the chemical reaction and mass transport need to be included.

After an overview of the various scaling principles of rubber mixing, designed primarily for dispersive and distributive mixing of reinforcing fillers, a series of experiments will be described to evaluate the consequences of the chemical silanization reaction on these scaling principles, as involved in silica mixing.

2.   SCALING LAWS FOR INTERNAL MIXERS

A number of alternative scaling principles for mixing of carbon black into a rubber matrix in an internal mixer have been described in literature [1,2], but none of the principles takes a chemical reaction into consideration, as this is not supposed to happen in this case. The following principles will be discussed:

1.   Simple geometric similarity
2.   Maximum shear stress
3.   Total shear
4.   Power input
5.   Mixing time
6.   Temperature profile
7.   Processing behavior (Weissenberg and Deborah numbers)
8.   Heat flow (Graetz and Griffiths numbers)
9.   Degree of filling
10. Energy balance (Brinkmann and Hersey numbers)

The geometrical dimensions of the mixing chamber used in the scaling principles described below are illustrated in Figure 1.
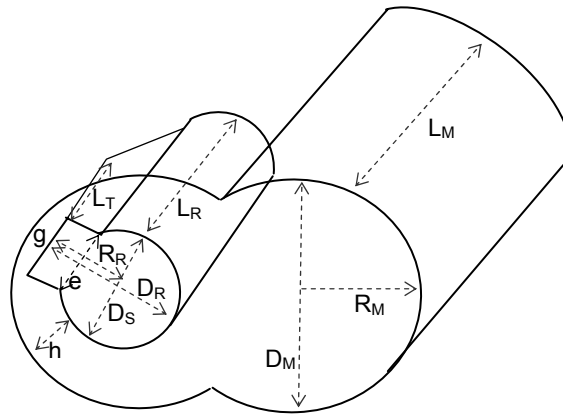
Figure 1: Notations of the geometrical dimensions of a mixing chamber

2.1. GEOMETRIC SIMILARITY

Early approaches to scale-up mixing processes in internal mixers are concentrated on geometrical parameters. Two fundamental aspects are: [3]

- The clearance between the rotor tip and the chamber wall must be equal at different scales

- The product of the number of revolutions and the diameter at the rotor tip must be constant

More elaborate geometrical models state, that the ratio of rotor length to diameter must be constant on the different scales, together with the ratio of the clearance between rotor tip and mixer wall, the rotor diameter and the cubic root of the volume of the mixers. [1] This approach is based on the assumption that the mechanical and heat transfer properties of the material all scale linearly with length. But as heat transfer is proportional to the contact area and heat generation is proportional to the volume of the mixer, the heat transfer characteristics of the mixer will change depending on the scale of the mixer.

2.2. MAXIMUM SHEAR STRESS

Another approach is upscaling with equal shear stress. The shear stress τ in a mixer depends on the viscosity of the compound η, the peripheral velocity v_p and the clearance between the rotor tip and the mixer wall g: [1]

$$\tau = \frac{\eta \cdot v_p}{g} \qquad\qquad Eq.\ 1$$

Scaling with constant shear stress results in the following ratios to be equal at both scales, represented by the prime and double prime:

$$\frac{N''}{N'} = \frac{g''}{g'} \cdot \frac{D'_R}{D''_R}$$

Eq. 2

The peripheral velocity v_p from Equation 1 is replaced by the rotor speed N and the diameter of the rotor D_R.

If dispersion of a filler is required, the maximum shear stress must be identical. The maximum shear stress τ_{max} is given by the power law of the material: [1]

$$\tau_{max} = k \cdot \dot{\gamma}_{max}^{n}$$

Eq .3

$\dot{\gamma}_{max}$ is the maximum shear rate. For rubber compounds k-values are in the range of 10^5 MPa, and a typical value for n is 0.3. The maximum shear rate can be separated into a term for pressure flow and a term for drag flow. Drag flow is determined by the rotor diameter D_R, the rotor speed N and the tip clearance g. Pressure flow is additionally depending on the channel clearance h, the tip width e and the diameter of the rotor shaft D_s: [1]

$$\dot{\gamma}_{max} = \frac{\pi \cdot D_R \cdot N}{g} \left[1 + \frac{3\left(\frac{D_S}{D_R} \cdot \frac{h}{g} - 1 \right)}{\frac{e}{\pi \cdot D_S}\left(\frac{h}{g}\right)^3 + 1} \right]$$

Eq. 4

Drag flow   Pressure flow

The contribution of the pressure flow term to the maximum shear rate is lower by approximately a factor of 2 compared to the drag flow term. The ratios between the geometrical parameters influencing the pressure flow are in general comparable for different brands and sizes of mixers, thus this term is nearly independent of mixer size. Therefore, upscaling will mainly influence the drag flow term, and the maximum shear stress is kept constant when the following ratio is constant: [1]

$$\left(\frac{D'_R \cdot N'}{g'} \right)^n = \left(\frac{D''_R \cdot N''}{g''} \right)^n$$

Eq. 5

This equation implies, that for geometrical similar machines the rotor speed at different scales should be similar as well.

To fulfill the criterion of constant maximum shear stress, a smaller mixer has to be run at a higher speed compared to a large scale production mixer, with the

result that relatively more energy is dissipated and that the temperature history will be different. [2]

In the context of the subject of this thesis, mass transfer of ethanol from the chemical reaction by surface refreshment, there is only one model known in literature, which takes the formation of fresh surface into account. The total shear criteria is expressed in terms of the number of rotors n_r, the radius of the mixing chamber R_M, the peripheral velocity of the rotor v_p, the length of the mixing chamber L_M, the mixing time t and the volume of the mixing chamber V_M. The coefficients C_1, C_2 and C_3 take into account the effective contact surface between the compound and the chamber wall, the ratio between the time of an effective volume to pass along the wall of a hemisphere and the duration of one revolution of the rotor, and the degree of filling respectively. No further evaluation of the coefficients C_1, C_2 and C_3 is done. [4]

$$\frac{2 \cdot \pi \cdot n_r \cdot R'_M \cdot v'_p \cdot L'_M \cdot t' \cdot C'_1 \cdot C'_2 \cdot C'_3}{V'_M} = \frac{2 \cdot \pi \cdot n_r \cdot R''_M \cdot v''_p \cdot L''_M \cdot t'' \cdot C''_1 \cdot C''_2 \cdot C''_3}{V''_M} \qquad Eq.\ 6$$

2.3. TOTAL SHEAR [1, 5]

Another method for upscaling of the mixing process of a rubber-filler compound is the total shear applied to the compound. A condition for the applicability of this method is, that the maximum stress attainable is higher than the critical stress value for particle dispersion. The total shear is the product of shear rate and mixing time t and is assumed to be proportional to the shear rate at the rotor tip, with a proportionality factor b summarizing the geometrical factors.

$$\overline{\gamma} = \dot{\gamma} \cdot t = b \cdot \dot{\gamma}_R \cdot t \qquad Eq.\ 7$$

$\overline{\gamma}$ is the total shear, $\dot{\gamma}$ is the shear rate and $\dot{\gamma}_R$ is the shear rate at the rotor tip. For geometrically similar mixers the ratio of the total shear to shear generated at the tip will be proportional.

The shear rate can be divided into a term of the shear rate in the channel between rotor shaft and mixer wall and the shear rate in the tip clearance area. The ratio of the shear rates is given by the ratio of the diameter at the rotor shaft D_S and the channel clearance h, as well as the ratio of the rotor diameter D_R and the tip clearance g:

$$\frac{\overline{\dot{\gamma}_h}}{\dot{\gamma}_g} = \frac{D_S/h}{D_R/g} \qquad Eq.\ 8$$

$\overline{\dot{\gamma}_h}$ is the shear rate in the channel, and $\overline{\dot{\gamma}_g}$ is the shear rate in the tip clearance. Another approach of upscaling with equal total shear is the use of a dimensionless number Γ calculated from the rotor diameter D_R over the clearance of the tip g, the calculated volume which is sheared by each revolution of the rotor V_s over the total batch volume V_b, the length of the tip clearance L_T over D_R, the rotor speed N and the mixing time t: [6]

$$\Gamma = \frac{\pi \cdot D_R}{g} \cdot \frac{V_s}{V_b} \cdot \frac{L_T}{\pi \cdot D_R} \cdot N \cdot t = K \cdot N \cdot t \qquad Eq.\ 9$$

The proportionality coefficient K is calculated from the geometrical factors and is called the dispersibility index.

2.4. POWER INPUT

For upscaling with equal power input the following assumptions are made: [4]

o   The total work input needed for mixing is mainly used for shearing the material

o   The total shear is directly proportional to the power consumption of the mixer

Equation 10 allows to calculate the work input based on the electrical power consumption profile P(t), the batch volume V_b and the geometrical factors summarized in the proportionality factor K_P: [6]

$$W = \frac{K_P}{V_b} \int_0^t P(t)dt \qquad Eq.\ 10$$

An alternative way to calculate the work input is using the torque profile T(t): [1]

$$W = \int_0^t \frac{2 \cdot \pi \cdot N(9,8 \cdot 10^{-6})}{V_b} T(t)dt \qquad Eq.\ 11$$

V_b is the volume of the batch and N is the rotor speed. Torque T is a function of shear stress in the tip clearance τ_g and in the channel between rotor shaft and chamber wall τ_h, as well as the geometrical parameters of the mixer: L_R is the length of the rotor, e is the tip width, D_R is the diameter of the rotor at the tip and D_S is the diameter of the rotor at the shaft:

$$T = L_R \left[\tau_g \frac{e \cdot D_R}{2} + \tau_h (\pi \cdot D_S - e) \frac{D_S}{2} \right]$$

Eq. 12

The shear stress can be replaced by a function of shear rate $\dot{\gamma}$ to the nth power for a power law fluid, see Equation 3. Equation 11 then becomes:

$$W = \frac{\overline{\dot{\gamma}}}{t} \int_0^t k \cdot \dot{\gamma}_R^{\,n} \left[1 + \left(\frac{\dot{\gamma}_S}{\dot{\gamma}_R} \right)^n \cdot \left(\frac{\pi \cdot D_S}{e} - 1 \right) \frac{D_S}{D_R} \right] dt$$

Eq. 13

The parameter k is the proportionality factor of the power law. This equation implies that the work input depends on the geometrical dimensions of the mixer and the shear rates. Scaling with similar work input calculated from the torque measurements gives good results in practice.

The power consumption P can also be calculated from the current using the line voltage LV, the area under the current-time curve A_{ct} and an empirical power factor: [1]

$$P = LV \cdot A_{CT} \cdot 0.9$$

Eq. 14

The assumptions made for this model are a complete filling of the high shear zone by the highly viscous fluid, a thermal history independent of the scale and a constant ram pressure. This way of scaling works well for mixers with similar design and for mixing under high shear conditions. [1]

Another approach is to calculate the power input from the peripheral velocity of the rotors v_p, the shear stress in the gap τ_g and the contact surface between the compound and the mixer wall A_l. In upscaling, the ratio of these parameters has to be kept constant: [4]

$$\frac{P'}{P''} = \frac{v'_p \cdot A'_l \cdot \tau'_g}{v''_p \cdot A''_l \cdot \tau''_g}$$

Eq. 15

Another upscaling model taking the fill factor into consideration, is given by Equation 16. The mixer is scaled up linearly, and the power requirement P on different scales varies with the product of fill factor FF and rotor speed N: [7]

$$\frac{P''}{P'} = \left(\frac{N''}{N'}\right)^{m+1} \left(\frac{FF''}{FF'}\right) \cdot c^3 \qquad\qquad \textit{Eq. 16}$$

The factor c is a dimensionless experimental constant. A shortcoming of this approach is the fact, that the scaling factor as such is not included. A more refined model includes this scaling factor u, as well as a function taking the geometrical factors into consideration: [1,7]

$$P = k \cdot u^3 \cdot f(geometry) \cdot N^{m+1} \cdot FF \qquad\qquad \textit{Eq. 17}$$

For two geometrically similar mixers filled to the same degree, the scaling law becomes: [1,7]

$$\frac{P'}{P''} = \frac{k'}{k''} u^3 \left(\frac{N'}{N''}\right)^{m+1} FF \qquad\qquad \textit{Eq. 18}$$

2.5. Constant Mixing Time

Constant mixing time as a criterion for upscaling may only be used in cases when the mixers are geometrically similar and running at the same speed. [1] The mathematical description of this scale-up criterion results in the following expression for mixers with similar geometrical shape: [8]

$$\frac{t''}{t'} = \frac{\overline{\dot{\gamma}}'_{max}}{\dot{\gamma}''_{max}} = \frac{N'}{N''} \qquad\qquad \textit{Eq. 19}$$

The ratios of the mixing times t, the maximum shear rates $\overline{\dot{\gamma}}_{max}$ and the rotor speed values N at the different scales have to be constant. Equation 19 is based on the assumption that the total number of revolutions, the product of mixing time t and the rotor speed N, is a determining factor for the mixing process. This approach is difficult to implement, as the effective mixing time very often is not equal to the total mixing time due to differences in intake behavior and stick-slip phenomena. Furthermore, the thermal history of the compound is not taken into consideration.

2.6. Constant Temperature Profile

If upscaling is done by keeping the temperature profile, the upscaled mixer has to run at lower rotor speeds with increasing mixer volume due to the lower

cooling efficiency. This results in lower shear rates, causing less energy dissipation into the material and less efficient filler dispersion, as well as longer mixing times. [1]

2.7. SIMILAR PROCESSING BEHAVIOR (WEISSENBERG AND DEBORAH NUMBERS) [1]

The dimensionless Weissenberg number (We) is the ratio of the relaxation time of the material λ and the time scale of the process t. For the mixing process of a rubber compound the latter is determined by the maximum strain rate. The Weissenberg number is then defined as follows:

$$We = \lambda/t \approx \lambda \cdot \dot{\gamma}_{max} = \lambda \cdot a \cdot N \qquad \text{Eq. 20}$$

$\dot{\gamma}_{max}$ is the maximum strain rate. The coefficient a summarizes geometrical factors including the rotor radius and the tip clearance. Weissenberg numbers smaller than unity characterize viscous material, and materials with values larger than unity show an increasing elasticity: The Weissenberg-number gives an indication of the viscoelasticity of the material and allows predicting the processing performance of the material on a mill or in a mixer.

The Deborah number De is independent of any geometrical dimensions and is defined as the ratio of the relaxation time λ and a residence time t, which in this case is the time of one period of revolution:

$$De = \lambda/t = \lambda \cdot 2 \cdot \pi \cdot N \qquad \text{Eq. 21}$$

A long relaxation time will result in a high value of the Deborah number, accentuating viscoelastic response and Newtonian behavior. [9] If the relaxation time of the material is longer than the time for one rotation of the rotor, the material can not relax completely and undergoes the following pass through the nip in a pre-stressed state. These effects are superimposed, the stress will increase subsequently until it finally exceeds the critical stress for wall slip: The material will no longer pass the gap between rotor tip and chamber wall. This flow instability is controlled by a critical Deborah number. Both, Deborah and Weissenberg numbers are influenced by the temperature, as the relaxation time is decreasing with increasing temperature.

Scaling with constant Weissenberg number and constant Deborah number is difficult, as these numbers are calculated from the relaxation time and rotor speed for a maximum strain rate. In upscaling, rotor speed often is reduced in

order to keep the temperature profile constant, resulting in a decrease of both numbers.

2.8. Similar Heat Flow (Graetz and Griffiths Numbers)

The Graetz number Gz is the ratio of heat conductivity to convective heat transfer in laminar flow: [10]

$$Gz = \frac{v_p \cdot g^2 \cdot \rho \cdot c_p}{\pi \cdot \alpha \cdot D_R}$$

Eq. 22

The heat conductivity of the rubber compound is given by α, v_p is the peripheral rotor speed, g is the tip clearance, ρ is the density, c_p is the heat capacity of the compound and D_R is the diameter at the rotor tip.

The Griffiths number Gr is defined as the ratio of viscous dissipation to convective heat transfer: [1]

$$Gr = \frac{\eta_o v^2}{\alpha \cdot b}$$

Eq. 23

Contrary to the Graetz number, the Griffiths number is temperature-dependent, taken into account by the factor b. This factor is defined by the temperature dependence of the viscosity:

$$\eta = \eta_0 \cdot \exp(-b \cdot [T - T_0])$$

Eq. 24

Upscaling with constant Graetz and Griffiths numbers means a similar temperature history on different scales. A constant Graetz number requires the product of the rotor speed N and the tip clearance g to the second power to be constant. A constant Griffiths number is expressed in constant values of the product of rotor speed N and the diameter of the rotor at the tip D_R, both to the second power. If the geometry of the mixer is scaled up according to the following expression,

$$\frac{D''_R}{D'_R} = \frac{(g'')^2}{(g')^2}$$

Eq. 25

both numbers will be constant. This implies that the diameter of the rotor at the tip D_R should scale linearly and the tip clearance g should scale to the second power.

2.9. DEGREE OF FILLING [1]

The degree of filling is a major factor in power calculation, since shearing takes place and energy is dissipated only in sections with complete filling over the whole channel height. There is an optimum degree of filling for a specific compound and rotor system, independent of mixer size. Nonetheless it might be required to decrease the fill factor slightly in order to avoid an unwanted temperature increase when scaling up. As a rule of thumb, a reduction of the fill factor with 10% results in an average temperature decrease of 20°C.

2.10. ENERGY BALANCE (BRINKMANN AND HERSEY NUMBERS)

The energy balance is expressed by the Brinkmann number Br and the Hersey number Hs. The former is the ratio of viscous heat generation to heat conduction, and the latter is the ratio of viscous heat generation to the change in energy content. The Brinkmann number can be calculated as follows:

$$Br = \left(\frac{\eta}{\alpha \cdot \Delta T}\right) \cdot \frac{1}{v} \cdot \frac{R_R^2 \cdot v_p^2}{g} \qquad \text{Eq. 26}$$

The viscosity is expressed by η, α is the heat conductivity, ΔT is the temperature rise, v is a characteristic velocity, R_R is the radius of the rotor and v_p is the peripheral velocity.

The Hersey number additionally depends on a characteristic time t and the mean distance of the compound material to the mixer wall d_w:

$$Hs = \left(\frac{\eta \cdot t}{\alpha \cdot \Delta T}\right) \frac{R_R^2 \cdot v_p^2}{g \cdot d_w} \qquad \text{Eq. 27}$$

In actual practice temperature control is one of the core problems in scaling up. The following scaling rules for similar energy balances can be deducted from the Hersey- and Brinkmann numbers:

$$g' = g'' \qquad \text{Eq. 28}$$

$$\frac{v'}{v''} = \frac{R_R''}{R_R'} \qquad \text{Eq. 29}$$

The tip clearances at the different scales have to be identical, and the peripheral rotor velocity v_p has to decrease with increasing rotor radius.

2.11. ALTERNATIVE APPROACHES

In general, combinations of the above-mentioned criteria are used for scale-up, because none of the models is sufficient to characterize the system completely. One example is the combination of dynamic, shear stress and energy balance scaling. [11] Dynamic scaling in this context means by definition that the flow pattern remains the same, and this implies that the Weissenberg numbers at the different scales have to be similar. At a constant temperature, the ratio of the Weissenberg numbers at the different scales can be expressed by the radius of the rotor R_R, the peripheral velocity v_p and the tip clearance g:

$$\frac{R'_R \cdot v'_p}{g'} = \frac{R''_R \cdot v''_p}{g''}$$

Eq. 30

In comparison to Equation 20, the relaxation time λ is excluded from the ratio: λ is constant as the temperature is kept the same at the different scales. The geometrical coefficient a is replaced by the ratio of the rotor radius R_R to the tip clearance g, and the rotor speed N is replaced by the peripheral velocity v_p. Shear stress scaling as defined in Equation 2 leads to the same ratio as given in Equation 30, if N is replaced by v_p and D_R is replaced by R_R. The energy balance is given by the Hersey and Brinkmann numbers, as given in Equation 26 and 27.

The combination of these scale-up rules results in the following expressions:

$$\frac{1}{v} \cdot \frac{R_R^2 \cdot v_p^2}{g} = const$$

Eq. 31

$$\frac{R_R^2 \cdot v_p^2}{g \cdot d_w} = const$$

Eq. 32

$$\frac{R_R \cdot v_p}{g} = const$$

Eq. 33

Another approach is to use the same linear scale factor for upscaling of all dimensions and the same rotational frequency at the different scales. In this case shear stress, shear strain rate, power input per unit of volume and number of passes of a particle over the tip region will be identical. The critical aspect of this approach again is the temperature balance: energy consumption will

increase with the third power of the scaling factor, whereas the cooling surface area will increase only with the second power of the scaling factor. This leads to a lower cooling capacity of a larger mixer, finally resulting in higher temperatures, lower stresses and reduced dispersive action. [12,13]

Taking a closer look at the actual mixer designs on different scales shows that the most common practice for mixer scaling is the use of a basically linear dimensional scale factor combined with upscaling the power in relation to the increased chamber volume. The less effective cooling with increasing chamber volume can be improved by increasing the rotor length while maintaining the rotor diameter. Theoretical considerations require a power input in proportion to the increase in mixer volume. However, practical cases have shown that the increase in power is in the range of 60% when doubling the batch volume. One of the reasons for this effect are energetic losses, which depend on the scale of the mixer. [14]

3. EXPERIMENTAL

The experiments described in paragraph 4 of this chapter were carried out using a premixed masterbatch containing all compounding ingredients except for the curing agents. They were done in intermeshing mixers differing in mixing chamber volume: The I5 mixer has a net volume of 5.5 liter, compared to 49.0 liter for the I45 mixer. For the experiments the masterbatch was fed into the mixer, the material was heated up using a constant rotor speed and then silanized at a constant temperature and time. The fill factor for the experiments in an open mixer was optimized in terms of silanization efficiency and intake behavior. Machine and process parameters are given in Table I.

The heating phase is the period after charging the mixer with the masterbatch until the temperature reaches the silanization temperature. During this period, the rotor speed was chosen to be as high as possible with the pertinent mixer in order to have a short heating period and to avoid silanization as far as possible. During the silanization period the rotor speed was adjusted in order to keep the temperature constant.

Table I: Experimental setup

		Figure 2		Figure 3		Figure 4	
		I5	I45	I5	I45	I5	I45
Mixer							
Net volume	[liter]	5.5	49.0	5.5	49.0	5.5	49.0
Fill factor	[%]	40	40	70	67	40	40
Coupling agent [1]	[TESP*T*/TESP*D*]	D	D	D	D	T	T
TCU settings	[°C]	60	40	60	40	60	40
Heating phase	Ram position [up/down]	down	down	down	down	down	down
	Duration [seconds]	var.	var.	var.	var.	var.	var.
	Temperature [2] [°C]	145	145	145	145	145	145
	Rotor speed [rpm]	140	66	80	66	100	66
Silanization phase	Ram position [up/down]	down	down	down	down	up	up
	Duration [seconds]	150	150	150	150	150	150
	Temperature [2] [°C]	145	145	145	145	145	145
	Rotor speed [rpm]	var.	var.	var.	var.	var.	var.

[1] D: TESPD, T: TESPT
[2] Heating up: final temperature
Silanization: constant temperature during the silanization phase

4. RESULTS

4.1. INFLUENCE OF UPSCALING ON SILANIZATION EFFICIENCY AND PROCESSING PARAMETERS FOR SILANIZATION IN A CLOSED MIXER AT DIFFERENT FILL FACTORS

Figure 2 and 3 show the results of silanization in the intermeshing mixer with a volume of 5.5 liter (I5) compared to the same type of mixer with a volume of 49 liter (I45). Silanization was done in a closed mixer. The experiments shown in Figure 2 and Figure 3 differ in fill factor (see Table I).
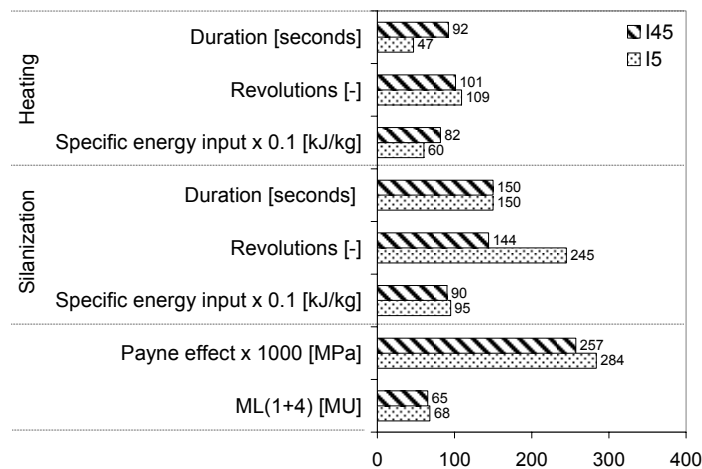
Figure 2: Scaling in a closed mixer at a fill factor of 40%

The Payne effect as well as the viscosity of the compound silanized in the larger mixer are slightly lower than the values for the compound mixed in the smaller mixer: Silanization is more efficient in the larger mixer. The heating period is shorter, the smaller the mixer size, and the specific energy input during heating is lower. The total number of revolutions during this period is comparable on both scales. In the silanization period, during which the process was run isothermally, the specific energy input is comparable, but the number of revolutions during this period is higher for the I5 mixer.
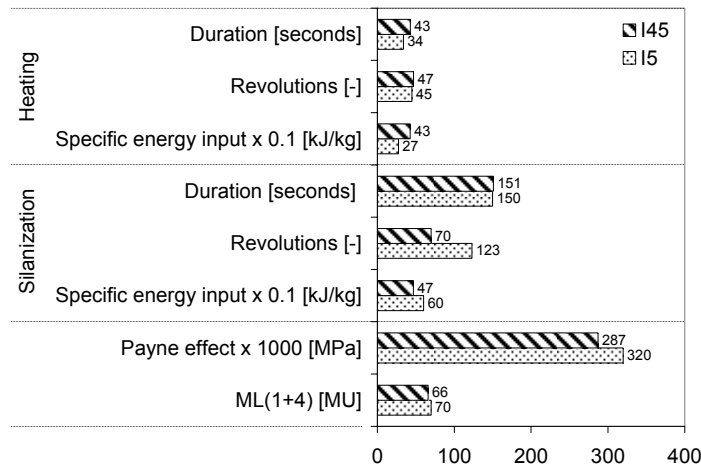
Figure 3: Scaling in a closed mixer at a fill factor of 67/70%

Figure 3 shows the results of a series of experiments carried out under the same conditions as described for Figure 2, but at a higher fill factor: The fill factor is in the range used in actual practice. The final properties of the compound are comparable with the properties of the compound mixed at a lower fill factor: Silanization on a larger scale again results in a lower Payne effect and viscosity, indicating that silanization is more efficient. During the heating period, the total number of revolutions is comparable in both cases, but the duration of this period is shorter and the specific energy input is lower in the smaller size mixer. During the silanization period the total number of revolutions as well as the specific energy input are higher in the smaller mixer.

Comparing Figures 2 and 3, thus looking at the effect of the fill factor, a slight difference in the absolute level of the Payne effect is found: The average level of the values is lower for silanization in the mixer with a lower degree of filling. During the silanization period the specific energy input is significantly higher in the case of the lower fill factor, and the number of revolutions is doubled.

4.2. Influence of Upscaling on the Silanization Efficiency and Processing Parameters for Silanization in an Open Mixer

Figure 4 shows the results of a series of experiments using a fill factor, that was optimized for the silanization process carried out in an open mixer. The conditions during the heating and silanization phase are given in Table I.

When silanization is done in an open mixer, the smaller mixer performs better in terms of silanization. Differences are found in the processing parameters depending on the size of the mixer: The compound in the smaller mixer reaches its final temperature after a slightly longer heating period and consumes more energy per unit mass of the compound. The total number of revolutions during this period is higher for the smaller mixer. During the silanization period, the compound in the I5 mixer consumes less energy. The total number of revolutions is significantly higher for the smaller mixer.
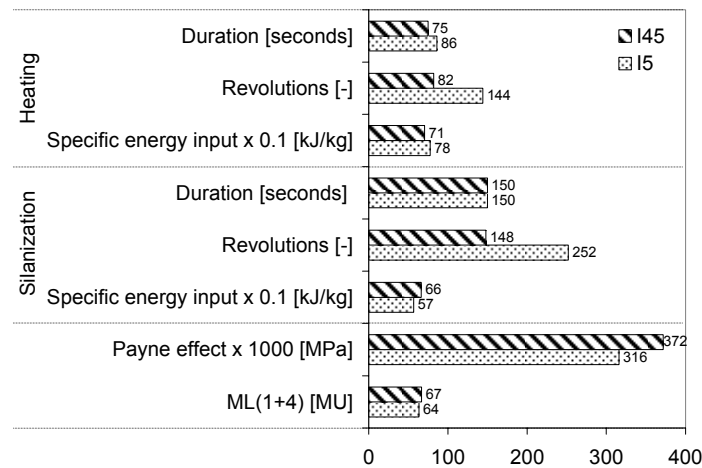
Figure 4: Scaling in an open mixer with a fill factor of 40%

Table II qualitatively summarizes the influence of upscaling on the silanization efficiency and the processing parameters.

Table II: The influence of upscaling from a 5.5 liter to a 49.0 liter
mixer on the silanization efficiency and processing parameters

		Figure 2	Figure 3	Figure 4
	Silanization in a	closed mixer		open mixer
	Fill factor [%]	40	67/70 [1)]	40
	Silanization efficiency	↑	↑	↓
Heating	Time	↑	↑	↓
	Total number of revolutions	=	=	↓
	Specific energy input	↑	↑	↓
Silanization	Time	=	=	=
	Total number of revolutions	↓	↓	↓
	Specific energy input	=	↓	↑

[1)] *I5: 70%, I45: 67%*
↓ Value is decreasing with increasing scale
↑ Value is increasing with increasing scale
= No influence of mixer size

5. DISCUSSION

It is general experience that the efficiency of physical mixing decreases with increasing mixer size. Figure 2 shows, that the situation is different in the present case: The Payne effect of the compound silanized in the I45 mixer is lower compared to the Payne effect of the compound silanized in the I5 mixer. In terms of processing parameters during the silanization period, the main difference between the mixing processes at the different scales is found in the number of revolutions during the silanization step: The small scale mixer requires a larger number of revolutions, in other words a higher rotor speed, to maintain the temperature. This is expected, as the cooling efficiency of the small scale mixer is higher due to the higher surface-to-volume ratio. However, the higher number of revolutions should improve the silanization efficiency as the frequency of the surface renewal is higher and devolatilization therefore should be more efficient (see chapter 4).

An explanation for this contradictory behavior is found in the heating phase: The heating period in the I5 mixer is shorter by a factor of approximately 2; in absolute values shorter by 45 seconds in the 49 liter mixer. Far before the end of the heating period the compound is already on a temperature above the threshold for silanization: The temperature increase of the compound is steep at low temperatures, as long as the viscosity of the compound is still high and the mechanical energy input is very efficient. Once the temperature is on a higher level and viscosity has largely decreased, energy input is less efficient and the heating rate is decreasing significantly. In the I45 mixer, silanization takes place already to a significant extent during the heating period, resulting in a longer effective silanization period compared to the situation in the smaller mixer. During the heating period, the specific energy input is higher for the larger size mixer, and again this is in contradiction with the common experience: An increasing mixer size results in a reduced cooling efficiency, and therefore the energy required to keep a certain temperature level should decrease. But as the period of heating in the large scale mixer is longer, the total energy transfer to the cooling water is higher. Furthermore, the temperature of the cooling media is lower for the I45 mixer, resulting in an increase of heat transfer from the compound to the cooling water. A third factor is the energy loss, electrical and mechanical loss as well as heating of the mixing equipment, depending on the size of the equipment. The total balance of these three factors results in an increased energy dissipation for the larger scale mixer, thus in a higher energy input required for keeping the temperature constant.

During the silanization phase at constant temperature, the specific energy input is comparable for both mixer sizes. The sum of energy losses and energy transfer to the cooling water is similar for the different mixer sizes. The relative energy loss, mechanical and electrical losses together with the energy transferred to the mixing equipment, is increasing with mixer size. This effect is

171

counterbalanced by a reduced energy dissipation into the cooling water with increasing mixer size. The total number of revolutions during the silanization period is about 60% higher in the case of the smaller mixer, which should result in a more efficient silanization due to a better devolatilization. The fact, that the compound in this mixer still has a higher Payne effect, shows, that in this case a different phenomenon is counterbalancing the improved devolatilization. This phenomenon might be an early saturation of the vapor phase in the mixer due to a better sealing of the mixing chamber, limiting the mass transfer from the compound to the gas phase.

Figure 3 shows the results of a comparable series of experiments, but carried out at a higher fill factor. The trends in Payne effect and viscosity are equal to the trends found in the case of the low fill factor: Silanization in the larger mixer is more efficient. During the silanization phase the number of revolutions required to keep the temperature level is lower for the larger mixer, comparable to the situation for a lower fill factor. However, in the case of a higher fill factor, energy input during silanization is higher for the smaller mixer due to the better cooling efficiency. As the fill factor is higher, the contact between the compound and the mixer wall is more intensive, resulting in a more efficient energy transfer from the compound to the cooling water and a higher sensitivity to the changing surface to volume ratio in upscaling.

During the heating phase, a difference in the specific energy input is found with the same trend as in the case of a lower fill factor (Figure 2 and Figure 3). The factors discussed for the silanization in the mixer with a lower fill factor, energy losses and energy dissipation into the cooling water, influence the energy balance in this case as well. The absolute values of the specific energy input are significantly lower compared to the energy input at lower fill factors: Energy input is more effective when the mixer is highly filled, because the high shearing areas are permanently and completely filled.

Figure 4 shows the results of scale up experiments with a fill factor of 40%, but silanization was carried out in an open mixer. In this mode the compound silanized in the small size mixer showed a lower Payne effect compared to the compound silanized in the larger mixer. This result is in a better accordance with the total number of revolutions during this phase: The value for the I5 mixer was significantly higher than the number of revolutions in the I45 mixer. In this case the higher frequency of surface renewal is effective, as the ethanol can now freely evaporate out of the mixing chamber, resulting in a lower concentration of ethanol in the vapor phase and a higher driving force for the mass transfer across the rubber/vapor interphase. Comparing the silanization in an open mixer with the situation in the closed mixer (Figures 4 and 2), the number of revolutions during the silanization phase is equal for the same mixer in both cases. However, the level of the specific energy input is much higher in the closed mixer, indicating that the cooling efficiency is more effective. One possible explanation is stick-slip behavior: When the compound slips, energy is

consumed to move the material in the mixing chamber, but the energy input into the rubber material is very limited as shearing forces are not effective. During silanization in the closed mixer, slip is more likely to occur as ethanol can not escape from the mixing chamber and is condensed on the mixer walls. Another difference between the two series is the coupling agent used, but this is not expected to influence the energy absorption: The coupling agents are similar in structure and reaction mechanism, and the viscosities of the compounds are comparable.

During heating, the specific energy consumption as well as the number of revolutions to reach the required silanization temperature are both significantly lower in the larger mixer: The lower cooling efficiency of the larger mixer is dominating the energy balance. This result is in contradiction with the results shown in Figure 2, where the specific energy input of the larger mixer was higher under basically the same conditions. An explanation for this contradiction is found by relating the specific energy input to the duration of the heating phase: In the I45 mixer the energy input per unit mass and unit time is comparable in the experiments shown in Figure 2 and the experiments shown in Figure 4. For the I5 mixer the energy input calculated from the results shown in Figure 2 is 13 kJ/kg·s, whereas a value of 9 kJ/kg·s is resulting using the data shown in Figure 4. This difference is due to differences in rotor speed: At a higher rotor speed the energy transfer to the cooling water is more efficient, resulting in a higher energy input necessary to keep the temperature constant, as shown in Figure 2.

In this study of a combination of simple mixing, dispersion and chemical reaction, the main processes, which are influenced by upscaling, are energy and mass transfer. The most important factors influencing energy and mass transfer identified in these investigations are:

o Volume of the mixing chamber
o Surface area of the rubber material during the process
o Rotor speed
o Compound temperature
o Cooling water temperature
o Fill factor
o Ventilation of the mixing chamber

The volume of the mixing chamber together with the fill factor determine the volume of the compound. The larger the volume of the compound, the more ethanol is formed, and the higher the required surface area to efficiently devolatilize the compound. The energy consumption is also influenced by this factor: the larger the mixer, the smaller the relative energy losses per unit mass of the compound. Energy transfer is influenced by the surface area of the compound in contact with the mixer wall, whereas mass transfer is determined by the surface area in contact with the vapor phase in the mixing chamber.

Both transfer rates are influenced by the surface renewal rates, determined by the rotor speed. The difference between compound temperature and the cooling water temperature is the driving force for energy dissipation into the cooling water. The temperature of the compound is determining the silanization rate, thus the rate of ethanol formation. It is also influencing the efficiency of energy input due to the temperature-dependence of the compound viscosity. The absolute level of the temperature of the mixer walls determines the ethanol condensation rate, a crucial factor for stick-slip behavior and wall contact. The energy input into the compound is influenced by the fill factor: the higher the fill factor, the more efficient the energy input. The surface area depends only slightly on the fill factor above a certain threshold value, at which the mixer wall is completely covered. However, a lower fill factor results in a reduced ethanol concentration in the rubber compound, as the mass transfer across the compound/vapor interphase is more efficient due to the higher volume of the vapor phase. Finally, in terms of fill factor a proper compromise has to be found to optimize the efficiency of the respective mixers.

Another crucial factor is ventilation of the mixing chamber: if the vapor phase is renewed at a higher frequency, the ethanol concentration in the vapor phase is on a lower level and mass transfer across the interphase with the compound is increased. The tip clearance has an influence on the dispersion of the filler, as this is the area with the highest shearing forces.

To summarize, the most crucial factor for upscaling of this process of dispersion and chemical reaction is the ratio of surface area to volume of the compound, as it influences the energy as well as the mass transfer. Equation 34 shows the parameters that have to be taken into consideration in the upscaling process:

$$\left[\frac{D_R}{g}\right] \cdot \left[N \cdot RR_V \cdot t_{mix}^2\right] \cdot \left[\frac{T_{CW}}{T_{comp}}\right] \cdot \left[\frac{A_{wall} \cdot A_{vapor}}{V_b \cdot h}\right] = const. \qquad \textit{Eq. 34}$$

D_R: Diameter of the rotor

g: Tip clearance

N: Rotor speed

RR_V: Renewal rate of the vapor phase in the mixer

t_{mix}: Mixing time

T_{CW}: Temperature cooling water

T_{comp}: Temperature of the rubber compound

A_{wall}: Surface area of the compound in contact with the mixer wall

A_{vapor}: Surface area of the compound in contact with the vapor phase

V_b: Batch volume

h: Height of the channel between rotor shaft and mixer wall

The factor $(N \cdot D_R/g)$ is the criterion for upscaling with similar maximum shear stress and can be deduced from Equation 2. It is also the scaling rule for a constant flow pattern by using the Weissenberg number (Equation 30). The product of v_p or N and R_R, as given in Equation 29, is one of the two conditions for energy balance scaling. The second condition is a constant tip clearance on the different scales. The tip clearance g and the channel height h do influence the heat and mass transfer, but only to a limited extent. Mass transfer is mainly influenced by the renewal rate of the vapor phase in the mixing chamber RR_V, by the temperature of the compound T_{comp} and the ratio of surface area of the compound/vapor interphase to the batch volume (A_{vapor}/V_b). Energy transfer is determined by the ratio of cooling water temperature to compound temperature (T_{CW}/T_{comp}) and the ratio of the surface area of the compound in contact with the mixer wall to the batch volume (A_{wall}/V_b). The mixing time t_{mix} has a strong influence as indicated by the square power, because it determines the degree of dispersion and distribution of the filler as well as the degree of silanization.

6. CONCLUSIONS

The investigation of the scaling behavior of a dispersion and silanization process of a silica filled rubber compound shows, that this process is dominated by mass transfer and energy transfer. When scaling this process, the main factors to be taken into consideration are the ratio of surface area to volume of the compound, the tip clearance, the absolute level of and the difference between compound temperature and cooling water temperature, rotor speed, the renewal rate of the vapor phase in the mixing chamber and the fill factor.

Linear scaling should be avoided, as this would negatively influence the energy dissipation into the cooling water as well as the transfer of ethanol across the interphase between the compound and the vapor phase in the mixer, both factors reducing the silanization efficiency. The tip clearance as the high-shear area determines the dispersion of the filler. The temperature during the silanization step as well as the cooling water temperature are crucial: Besides the influence on the cooling efficiency, it is determining the silanization rate and the extent, to which condensation on the mixing chamber walls occur. The renewal rates of the surface area and the vapor phase are important, as they also determine the condensation in the mixer and influence the devolatilization of the compound. In terms of the fill factor a compromise between energy input efficiency and absolute ethanol formation has to be sought.

7. REFERENCES

1.   Funt, J.M., *Mixing of rubbers*. 1977, Rubber and Plastics Research Association of Great Britain: Shawbury (Great Britain).
2.   Sunder, J., in *Mixing and compounding of polymers*, I. Manas-Zloczower, Tadmor, Z., Editor. 1994, Hanser: Cincinnati, Munich. p. 189.
3.   Bernhardt, E.C., *Processing of thermoplastic materials*. 1959, van Nostrand Reinhold: New York.
4.   Bebris, K.D., Sov. Rubber Technol., 1971. **30**(8): p. 8.
5.   Bebris, K.D., Shikhirev, N.I., Sov. Rubber Technol., 1972. **30**(6): p. 10.
6.   van Buskirk, P.R., Tugretzky, S.B., Gunberg, P.F., Rubber Chem.Technol., 1975. **48**: p. 577.
7.   Guber, F.B., Sov. Rubber Technol., 1966. **25**(9): p. 30.
8.   Tanaka, V., Int. Polym. Sci. Technol., 1982. **9**(1): p. 86.
9.   White, J.L., in *Science and technology of rubber*, J.E. Mark, Erman, B., Eirich, F.R., Editor. 1994, New York: Academic Press: New York. p. 257.
10. Kuipers, N.J.M., University Twente, Dept. Chem. Technol., Separation Technology, *Scale modification in chemical engineering*. 2003.
11. White, J.L., Polym. Eng. Sci., 1979. **19**(11): p. 818.
12. McKelvey, J.M., in *Polymer processing*. 1962, Textile Book: New York, ch. 12.
13. Bourne, J.R., New Scientist, 1967. **33**: p. 334.
14. Palmgren, H., Rubber Chem. Technol., 1975. **48**: p. 462.

CHAPTER 8

COMPARATIVE INVESTIGATION OF

VARIOUS NEW SILANES

IN SILICA COMPOUNDS

After the discussion of the influence of the mixing process and equipment parameters on the silanization reaction in the previous chapters, this chapter focuses on the influence of the type of coupling agent on the silanization efficiency. The results of a comparative investigation of different types of coupling agents will be discussed. Silanes are chosen from the groups of sulfur-rich silanes (bis(triethoxysilylpropyl)disulfane, TESPD, and the corresponding tetrasulfane, TESPT), silanes with blocked sulfur moieties (S-[3-(triethoxysilyl)propyl]ester of octanethionic acid) and sulfur-free silanes (bis(triethoxysilyl)polybutadiene, bis(triethoxysilyl)decane, DTES). These silanes connect to the filler surface by siloxane bonds between the silyl groups of the silane and silanol groups of the silica filler. They differ in hydrophobation effect, determined by the number of alkyl groups, and the orientation of the molecule on the filler surface.

Compared to the compound with TESPD, the compound with the blocked silane shows a stronger decrease in viscosity as well as Payne effect indicating fast and effective silanization, together with low concentrations of ethanol in the compound. Mixing and dispersion of this compound is easy and not sensitive to the fill factor.

The oligomeric silane results in a higher compound viscosity and higher values of the Payne effect. This is due to the structure of this silane: The long alkyl chains reduce the peptizing effect compared to the smaller silane molecules, and the high molecular mass of the molecule makes it immobile resulting in a low reaction rate with the silica particles. Additionally, the highly entangled shell of silane and polymer molecules around the filler particle increases the viscosity.

The comparison of the three silanes with similar structure and different sulfur ranks did not show significant differences in terms of thermal stability or scorch safety, contrary to earlier observations. This is due to a better temperature control of the intermeshing mixer used in the present investigation, versus a tangential mixer used in prior test series.

177

1. INTRODUCTION

A wide variety of different coupling agents is proposed for silica compounds in order to get a better dispersion of the filler and to reinforce the rubber. These coupling agents belong in general to the group of silanes, with some exceptions such as thiophosphoryl compounds [1], and they differ concerning the following features:

○ *Type and number of functional groups coupling to the filler surface:* The most common group chosen for this purpose is the ethoxysilyl group, showing a good balance between reaction rate and handling, but higher alkoxy groups can be used as well. Most common are three alkoxy groups connected to the silyl group, but silanes with only one ethoxygroups have been successfully tested as well. [2]

○ *Symmetry of the silanes:* Symmetrical silanes contain two silyl end groups, while unsymmetrical silanes contain only one silyl group. Unsymmetrical silanes have a single connection to the filler surface.

○ *Number of alkyl groups between the silyl groups:* The higher the number of alkyl groups in the molecule connected to the filler surface, the higher the hydrophobation effect of this coupling agent.

○ *Sulfur-containing groups:* These groups can directly connect to the polymer. Sulfur chains with different lengths are used, showing increasing stability with decreasing number of sulfur atoms. The length of this sulfur chain is also an important factor with respect to scorch safety of these silanes. [3, 4] Bis(triethoxysilylpropyl)tetrasulfane (TESPT) [5-7] was initially most commonly used, but is reactive towards the rubber polymer during mixing causing premature scorch and negatively influencing processability. At the present time bis(triethoxysilylpropyl)disulfane (TESPD) is more commonly used, because it is less prone to premature scorch. [8, 9] The newest approach is that the sulfur-moiety is blocked by a thermally stable group like a thioester group, which splits under curing conditions. [10-12] Sulfur-free silanes can not react with the polymer as such, they need an activator. [13]

○ *Polar groups in the molecule:* Polar groups can stabilize a parallel orientation of the molecule on the filler surface, the most effective orientation for a good hydrophobation. [14]

The functional parts of the silane being subject to most of the variations are the mid alkyl chain and the sulfur moiety, as well as the end group in an unsymmetrical silane. An immense number of alternative silanes is proposed in literature [1, 15-39], but for most of them no experimental or practical data are available. The most commonly used silanes are still the bis(triethoxysilyl-

propyl)sulfanes. Other silanes being successfully tested are silanes with a blocked sulfur moiety and sulfur-free oligomeric silanes.

In the first part of the investigation a blocked silane (S-[3-(triethoxysilyl)propyl] ester of octanethionic acid) and an oligomeric silane (bis(triethoxysilyl)poly-butadiene) were chosen, and TESPD was used as reference. Comparative studies using these silanes instead of TESPD and TESPT were published earlier with focus on compounding, mixing and mechanical properties, but without special attention to silanization. In terms of mechanical properties of the vulcanized material, only slight differences were found depending on the type of silane, mainly in modulus and tensile strength. [10, 13]

For the second part of this investigation, 3 silanes with different sulfur ranks were chosen: TESPT with an average number of sulfur atoms of 3.8 and TESPD with approximately 2 sulfur atoms per molecule. The third silane was sulfur-free: bis(triethoxysilyl)1,10-decane, DTES, a silane in which the sulfur moiety is replaced by 4 alkyl groups. These silanes were compared concerning their scorch-sensitivity and hydrophobation strength, measured by the Payne effect.

2. COMPARATIVE INVESTIGATION OF A BLOCKED SILANE AND AN OLIGOMERIC SILANE WITH TESPD

2.1. BLOCKED SILANE

2.1.1. Chemistry
The investigated blocked silane has one silyl group and one sulfur atom connected to the propyl group. In contrast to the bifunctional silanes such as TESPT (bis(triethoxysilylpropyl)tetrasulfane) and TESPD (bis(triethoxysilyl-propyl)disulfane), the sulfur moiety of this silane is blocked by esterification with octanethionic acid (see Figure 1).

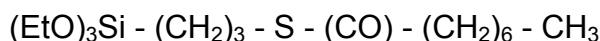$(EtO)_3Si$ - $(CH_2)_3$ - S - (CO) - $(CH_2)_6$ - CH_3
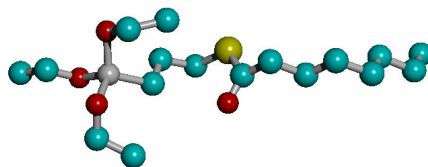
Figure 1: Chemical structure of the blocked silane
S-[3-(triethoxysilyl)propyl]ester of octanethionic acid
(NXT Silane, GE Silicones, Wilton, CT, USA)

This silane contains a monosulfane group bound to a carbonyl group, resulting in a more stable sulfur-moiety compared to the di- and polysulfide groups in

TESPD and TESPT, respectively. The blocked sulfur group prevents sulfur-donation during processing and is supposed to split during the productive mixing step, thermally or with the aid of a deblocking agent such as an amine. The coupling agent contains a higher number of alkyl groups compared to the commonly used silanes, resulting in a better hydrophobation effect. The ratio of ethoxy groups to alkyl groups is lower, resulting in less ethanol generation for a similar hydrophobation effect. [40]

2.1.2. Processing

The blocked silane can be processed according to the mixing procedure of addition of the silica in two portions, and adding the silane together with the first part of the filler. Due to the high temperature stability of the silane, the compound may be heated up to temperatures of 170ºC. The advantage of this temperature-stable silane is the possibility to mix and silanize a compound using less mixing and remilling steps compared to the compounds containing the sulfur-rich silanes.

During the deblocking reaction, the ester-part of the molecule splits off and the extremely reactive monosulfane or thiol group immediately binds to the polymer molecule. Deblocking is supposed to occur mainly during curing of the rubber compound, and is thermally initiated. However, the deblocking reaction can be boosted by special additives such as amines. These additives might be present in the compound as accelerator or activator or can be added together with the curing system.

2.2. OLIGOMERIC SILANE

2.2.1. Chemistry

The oligomeric silane used in this investigation is consisting of 27 butadiene-units in average, with triethoxysilyl groups as terminal groups as shown in Figure 2.

The average molecular weight of the oligomer is 1800 g/mol. The filler-polymer network has to be established during the vulcanization reaction, and a special filler-activator has to be added for this purpose during the final mixing step. The high molecular weight of this silane results in a lower volatility compared to the commonly used silanes. The ratio of alkoxy groups to alkyl groups is low, resulting in a reduction of ethanol generation. The compound is sulfur-free, therefore no scorch reaction can occur and the material can be processed at higher temperatures, up to 175ºC.

$(EtO)_3Si-(CH_2-CH=CH-CH_2)_n-Si(EtO)_3$
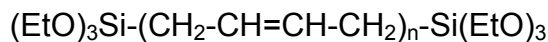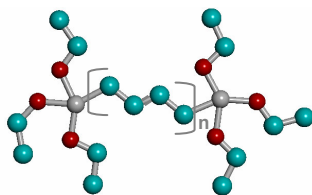
Figure 2: Chemical structure of the oligomeric silane
bis(triethoxysilyl)polybutadiene, $n \approx 27$
(Rhenofit 1715, Rheinchemie, Mannheim, Germany

As this coupling agent does not contain a sulfur-moiety for the reaction with the polymer, a sulfur donor has to be added during the productive mixing step. This molecule donates sulfur during the curing step and enhances the reaction of the double bond of the coupling agent with the polymer. The following compound is used as sulfur donor:
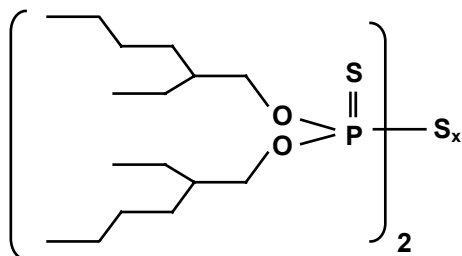
Figure 3: Chemical structure of the sulfur-donor
used to establish the filler-polymer bonds
Bis(O,O-2-ethylhexyl-thiophosphoryl)polysulfide

2.2.2. Processing

Compounds containing this oligomeric silane can be mixed and silanized in one step. The compound can be heated up to 175°C without the risk of scorch. The ratio of the amount of silane to the amount of filler is higher for the oligomeric material: If TESPT or TESPD are replaced by the oligomeric silane, 1.50 respectively 1.34 times the weight of the sulfur-containing coupling agent has to be added. In contrast to the commonly used mixing protocol for silica compounds, the full amount of filler should be added first, followed by the addition of the silane. The filler activator is added during the final mixing step, in a concentration of 1.5 times the concentration of sulfur.

2.3. EXPERIMENTAL

2.3.1. Compound recipe

All investigations were done using a passenger car tire tread masterbatch based on a blend of S-SBR and BR with 83.5 phr silica (Zeosil 1165MP, Rhodia Silices, Boulogne-Billancourt, France). TESPD was used as reference, in a concentration of 5 phr. The blocked silane was added with the same

molecular concentration of silicone, amounting to 7.7 phr, and the amount of oligomeric silane was 1.34 times the amount of TESPD, resulting in 6.7 phr, following the recommendations of the suppliers. All other compounding ingredients and quantities were similar to the reference compound.

2.3.2. Processing

All compounds are mixed according to the same protocol as far as possible, but with implementation of the special mixing advices for the blocked silane and the oligomeric silane. A mixer fill factor of 67% was chosen, based on the results of a fill factor study. All compounds were mixed in a 5.5 liter intermeshing mixer with PES5 rotor. In Table I to III the details are given.

Table I to III: Mixing and silanization protocol for the compound containing the blocked silane, the oligomeric silane and TESPD

Blocked silane	Duration [seconds]	Rotor speed [rpm]	Temperature [ºC]
Addition of the polymer		65	
Mixing	30	60	
½ Silica, silane		60	
Mixing	30	60	
½ Silica, oil, carbon black, chemicals		60	
Mixing	30	65	
Ram up, cleaning		65	
Mixing		70	to silanization temperature
Silanization	variable	variable	temperature controlled
Dump			

Oligomeric silane	Duration [seconds]	Rotor speed [rpm]	Temperature [ºC]
Addition of the polymer		60	
Mixing	30	65	
½ Silica		65	
Mixing	30	65	
½ Silica, silane, oil, carbon black, chemicals		60	
Mixing	30	60	
Ram up, cleaning		65	
Mixing		65	to silanization temperature
Silanization	variable	variable	temperature controlled
Dump			

TESPD	Duration [seconds]	Rotor speed [rpm]	Temperature [ºC]
Addition of the polymer		65	
Mixing	30	65	
½ Silica, silane		60	
Mixing	30	60	
½ Silica, oil, carbon black, chemicals		65	
Mixing	30	60	
Ram up, cleaning		60	
Mixing		75	to silanization temperature
Silanization	variable	variable	temperature controlled
Dump			

Mixer parameters: Fill factor: 67%, mixer TCU settings: 60ºC

Milling parameters: 1 pass, gap: 3,5 mm, 10 rpm, no friction, TCU settings: 40ºC

2.4. RESULTS

2.4.1. *Compound viscosity as a function of silanization time and temperature*

Compounds containing TESPD show a decrease in Mooney viscosity with increasing silanization time and temperature (Figure 4A). The temperature range used for the experiments with this coupling agent was limited from 135ºC to 145ºC; at 155ºC the compound already suffered from scorch.

The blocked silane shows a similar effect for short silanization times in the temperature range from 135ºC to 145ºC (Figure 4B): A higher temperature and longer silanization times result in a lower viscosity due to a higher degree of silanization. With higher degrees of silanization the difference between the viscosities of the samples diminishes. At 145ºC after 2.5 minutes of silanization no significant difference was measured any more. The average level of viscosity is lower for equal silanization times and temperatures compared to compounds containing TESPD and the oligomeric silane.

For increasing temperatures the oligomeric silane shows the same trend of decreasing viscosity values. However, the influence of time is different (Figure 4C): With increasing silanization time the viscosity of the compound increases. The final viscosity for high degrees of silanization is higher compared to the other coupling agents, in spite of the expected higher hydrophobation efficiency due to the higher number of alkyl groups.

The absolute value of viscosity is highest for the compound with TESPD at low silanization rates; the compound with the oligomeric silane has an intermediate position. After 5 minutes of silanization, the compound with the oligomeric silane has the highest viscosity. The compound with the blocked silane shows the lowest values over the whole period at all temperatures.

Figure 4: Viscosity of the compounds containing different coupling agents as a function of silanization time at various temperatures
A: TESPD; B: blocked silane; C: oligomeric silane

Similar to the data on viscosity, TESPD shows the expected behaviour (Figure 5A): decreasing Payne effect values with increasing silanization time and temperature. The blocked silane also shows the same trend for short silanization times and low temperatures (Figure 5B), in accordance with the trend in viscosity. No significant change is observed any more for higher degrees of silanization: The Payne effect reaches a minimum value for maximum silanization after approximately 2.5 minutes at 145°C. The absolute value of the Payne effect in this case is comparable to the Payne effect after 20

minutes of silanization, the lowest achievable value. The starting value for the compound containing the blocked silane is already low, and the Payne effect decreases slowly. In contradiction to this, the starting value of the Payne effect for the compound containing TESPD is high, and the Payne effect decreases strongly over the whole silanization period.

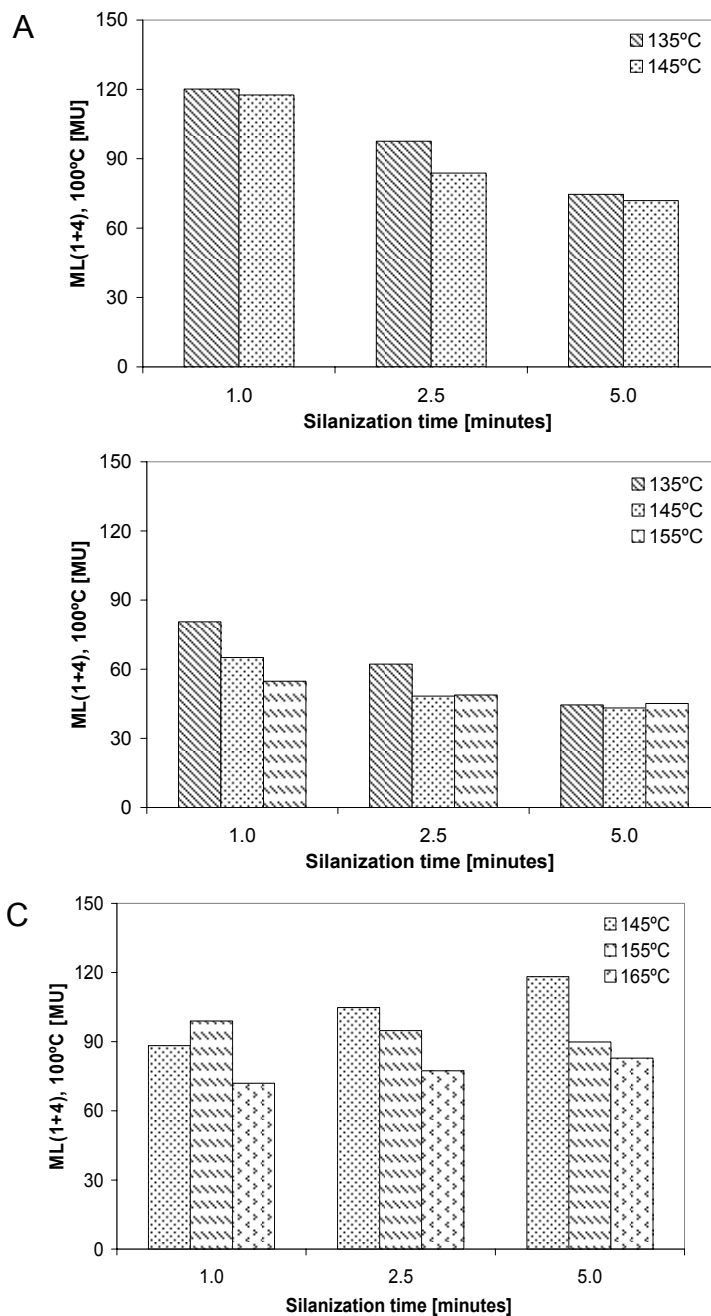### 2.4.2. Payne effect of the compounds as a function of silanization time and temperature
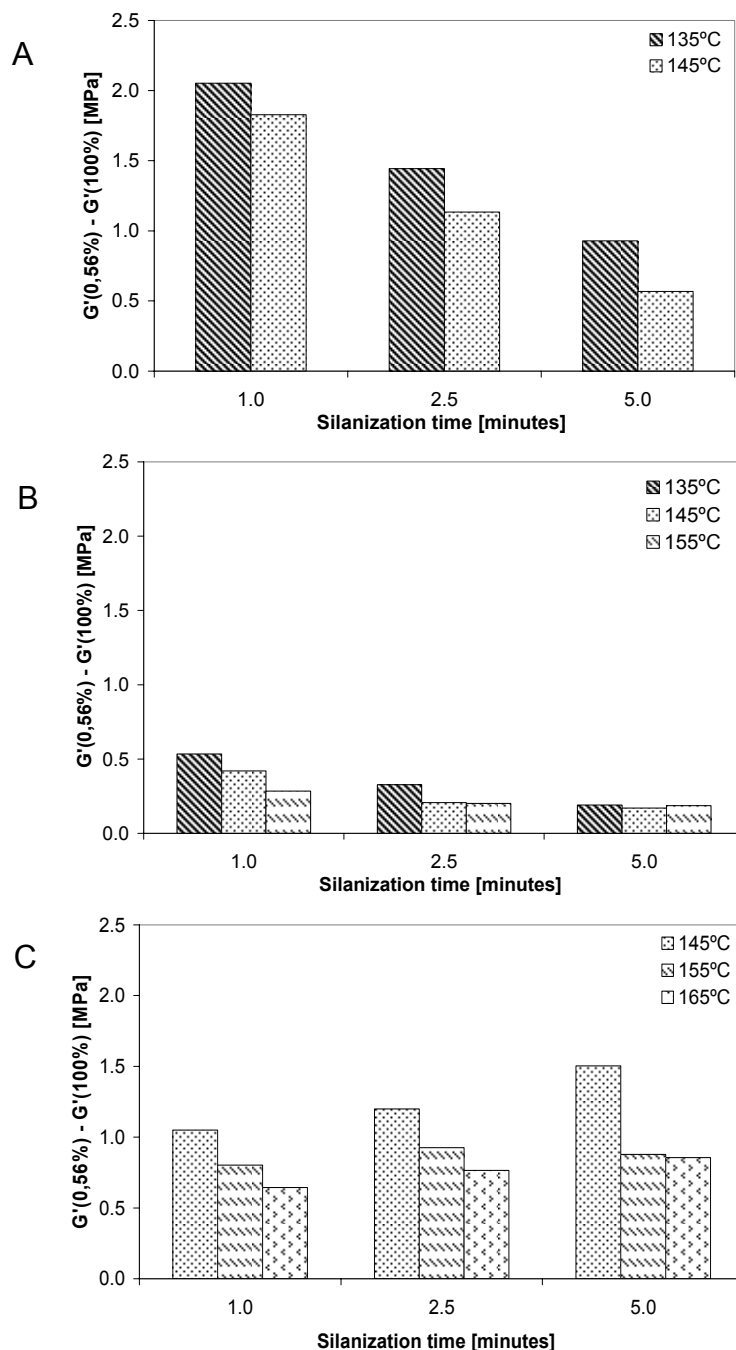
Figure 5: Payne effect of the compounds containing different coupling agents as a function of silanization time at various temperatures
A: TESPD, B: blocked silane, C: oligomeric silane

For the oligomeric silane the Payne effect decreases with increasing temperature, as expected (Figure 5C). The effect of time on the Payne effect is similar to the trend found for viscosity: a longer silanization time results in a higher Payne effect. The influence of time is very strong at a silanization temperature of 145ºC; at 155ºC and 165ºC the increase in Payne effect is less pronounced. The lowest value for the Payne effect is found at 165ºC after a silanization time of 1 minute. Compared to the compounds with TESPD, the Payne effect for short periods of silanization is lower, but after 5 minutes of silanization this ratio reverses.

A comparison of the Payne effect values of the compounds after silanization at 145ºC shows, that the blocked silane is the most efficient one, followed by TESPD. The silanization efficiency of the oligomeric silane is slightly higher than the silanization efficiency of TESPD for shorter silanization times, but does not reach the Payne effect levels of the TESPD containing compounds for longer silanization periods.
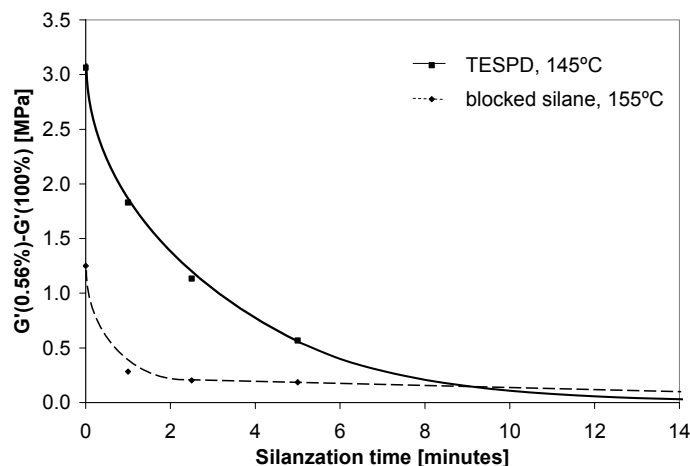
Figure 6: Decrease of the Payne effect for compounds containing TESPD and the blocked silane at their maximum silanization temperatures

Figure 6 shows the decrease of the Payne effect for compounds containing TESPD and the blocked silane. This evaluation could not be done for the compound containing the oligomeric silane, as the Payne effect increases with silanization time. The silanization temperature was chosen just below the temperature at which scorch occurs: 145ºC in the case of TESPD and 155ºC in the case of the blocked silane. The silanization time for the lowest degree of Payne effect, corresponding to the highest achievable degree of silanization, was approximately 2 minutes for the compound containing the blocked silane and 9 minutes for the compound containing TESPD.

2.4.3.   Ethanol concentration in the compound

Figure 7 shows the ethanol content of the various compounds for different silanization periods at 145ºC. The highest values are measured for TESPD; both the blocked silane and the oligomeric silane show lower values of alcohol

concentration in the compound. The compounds containing TESPD show only a slight decrease of ethanol concentration in time, and the absolute values are approximately twice as high compared to the concentrations measured in the compound containing the blocked silane at silanization times of 2.5 minutes and 5 minutes.
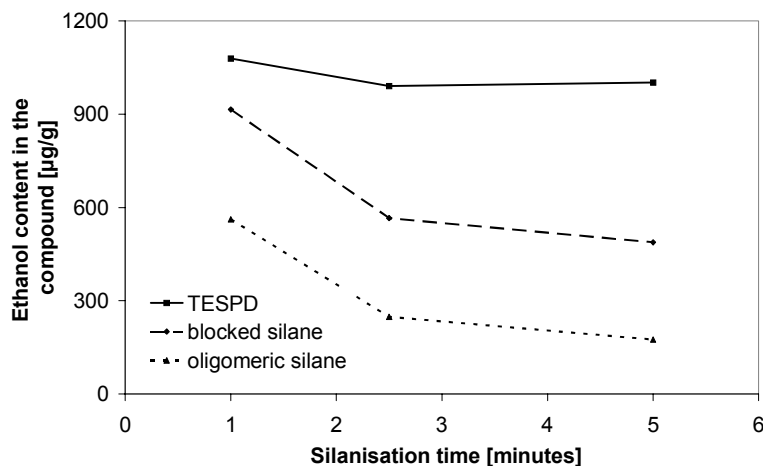
Figure 7: Ethanol concentration in the compound at 145°C

The blocked silane takes an intermediate position between TESPD and the oligomeric silane, even though the Payne effect, as a measure of the degree of silanization, is lowest. The ethanol concentration of the compounds containing the blocked silane decreases within the first minute of silanization and remains more or less constant during further silanization. When the oligomeric silane is used, the concentration of ethanol in the compound is generally low. Compared to TESPD as coupling agent, the concentration of ethanol is reduced by a factor of approximately 2 after one minute of silanization and by a factor of approximately 6 after 5 minutes of silanization. Again the strongest decrease in ethanol concentration is found between 1 minute and 2.5 minutes of silanization time.

2.4.4. Energy consumption

The energy consumption during the silanization step at the preselected constant temperature (Figure 8A) as well as the total energy consumption during heating up and silanization together (Figure 8B) show slight differences, depending on the type of coupling agent used. The compound with the oligomeric silane shows the lowest energy consumption; for a longer silanization period the difference between the energy consumption of this compound compared to the compounds containing TESPD and the blocked silane increases. For a mixing time of 5 minutes the compound containing the blocked silane consumes more energy than both other compounds.

The increase in energy consumption in time is roughly linear for the compound with TESPD and the oligomeric silane, but shows an exponential increase for the compound with the blocked silane.
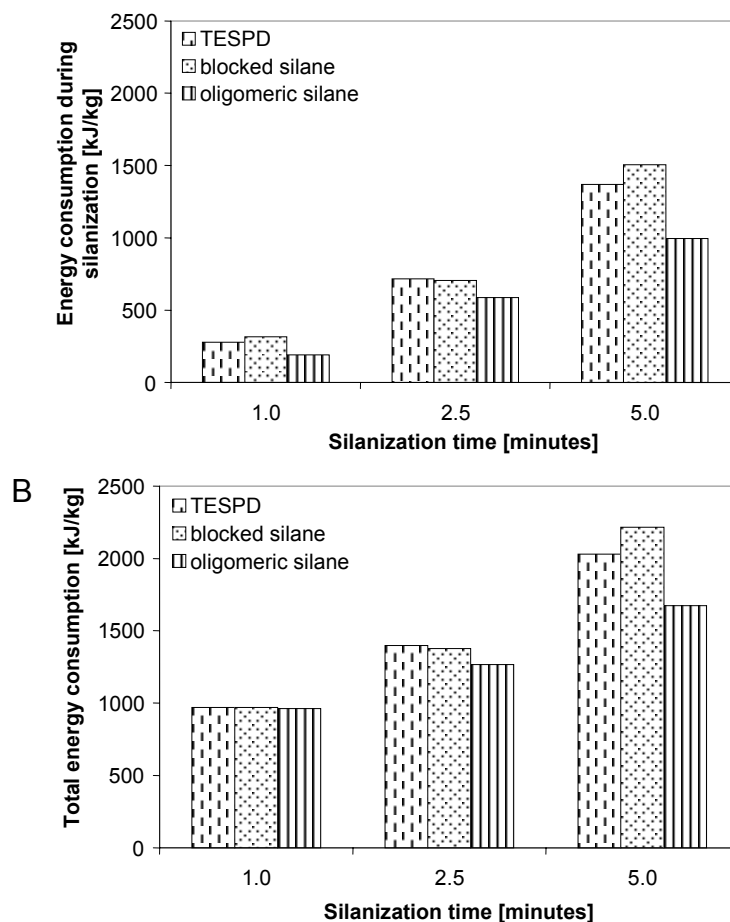
*Figure 8: Energy consumption of the compounds
containing different coupling agents at 145°C
A: during the silanization step, B:total energy consumption*

The number of revolutions required to maintain the silanization temperature shows the same trend as the energy consumption, but the differences between the compounds are amplified (Figures 9A and 9B). Evaluating this process parameter, the compounds containing the blocked silane show significantly higher values than the compounds with both other coupling agents during the whole period of silanization, but with a very strong effect for 5 minutes of silanization time. The number of revolutions needed for this silanization period is double compared to the number of revolutions applied to the compound containing the oligomeric silane.
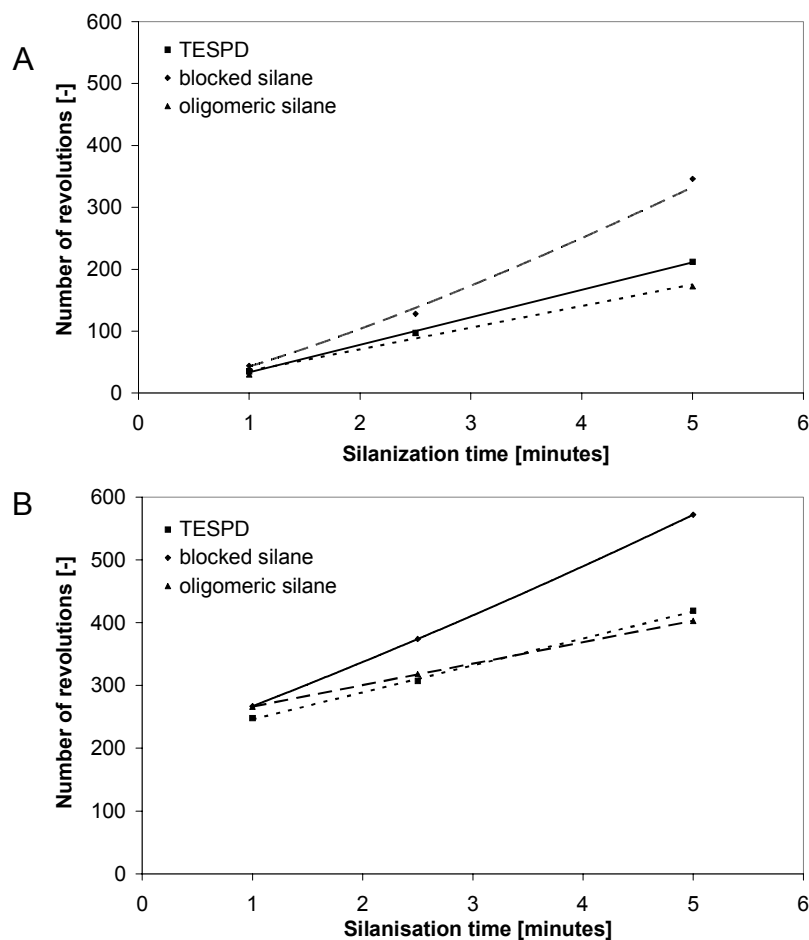
*Figure 9: Number of revolutions for the compounds
containing different coupling agents at 145°C
A: during the silanization step, B: total revolutions*

2.4.5. Kinetic study

Table IV: Kinetic data of the silanization with TESPD and the blocked silane

Rate of silanization		
	TESPD	blocked silane
Temperature [°C]	k_r [minute^{-1}]	k_r [minute^{-1}]
135	0.2119	0.4511
145	0.3475	0.4932
155	-	0.2514
Activation energy (135-145°C)		
	[kJ/mol]	[kJ/mol]
	70	13

TCU settings: 60°C
Ram position: down
Ventilation: on
Air injection: off
Fill factor: 0.67

Table IV shows the results of a kinetic study, based on the Payne effect values. For compounds containing TESPD, a strong increase of the reaction rate k_r is found with temperature rise, as expected. For the blocked silane the reaction rate increases only slightly when the temperature is increased from 135°C to 145°C and it seems to decrease with further temperature rise. For the compounds containing the oligomeric silane the Payne effect values did not follow the expected pattern of decrease in time as stated before; therefore a kinetic evaluation was not possible.

A considerable difference in activation energy between the two coupling agents was found: The silanization reaction of the compound containing TESPD has an activation energy of 70 kJ/mol, and the value for the compound containing the blocked silane for the same temperature range is only 13 kJ/mol.

2.4.6. Fill factor study of the alternative silanes
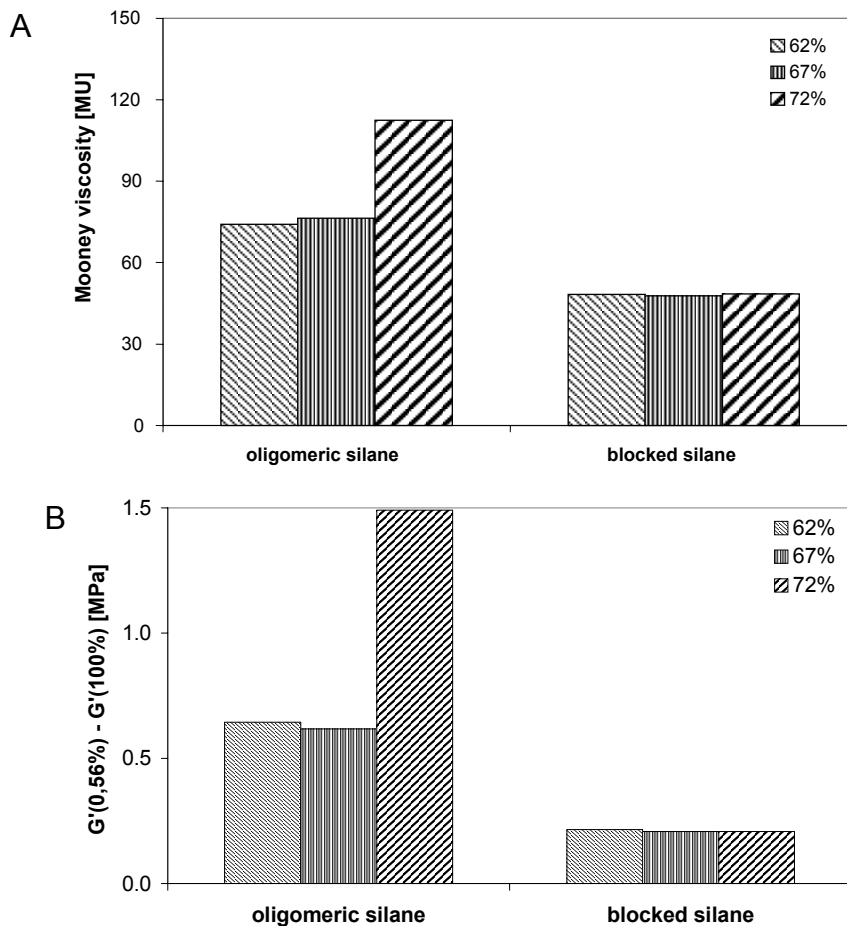
Figure 10: Fill factor study for the blocked silane and the oligomeric silane at 145°C
A: viscosity, B: Payne effect

190

A fill factor study was done for the alternative silanes in the range between 62% and 72% (Figure 10). Higher fill factors were used as well, but resulted in very poor mixing for both silanes, and were therefore not further investigated.

Compounds with the blocked silane as coupling agent are not affected in terms of viscosity and Payne effect by the variation of the fill factor: neither Payne effect nor viscosity show a significant change.

The application of the oligomeric silane as coupling agent results in an increased sensitivity to fill factors higher than approximately 70%: Up to 67% no significant influence of the fill factor is found. At a fill factor of 72%, the Payne effect and viscosity increase significantly, indicating that dispersion and silanization are poor.

2.5. DISCUSSION

All compounds are expected to show a decrease in viscosity as well as Payne effect with increasing temperature, time of mixing and silanization: The longer the mixing time, the higher the degree of mastication of the polymer and the degree of dispersion of the filler. Both processes are faster for lower compound temperatures. The degree of silanization increases with time, and the silanization rate is increasing with temperature. This trend is indeed found for the compounds containing TESPD and the blocked silane (Figures 4A and 4B, 5A and 5B).

For short silanization times, around 1 minute, the difference in viscosity between 135ºC and 145ºC for the compounds containing TESPD are rather small (Figure 4A): At these temperatures the silanization rate is low, and the main effect is based on mastication and dispersion. For longer processing times the silanization rate is determining the viscosity and Payne effect level, and a stronger temperature-dependence is found, especially for the Payne effect (Figure 5A).

Contrary to TESPD, compounds with the blocked silane show the strongest influence of silanization temperature for short processing times. With higher degrees of silanization the differences between the viscosities and Payne effect values at different temperatures diminish, and after 5 minutes of silanization no significant difference is measured any more (Figures 4B, 5B). The silanization rate is very high, and after 2.5 minutes of silanization time at 145ºC the minimum viscosity is reached. After this period the viscosity of the compound is constant, as polymer breakdown is taking place only to a very limited degree due to the low viscosity and the high temperature of the compound; the degree of dispersion is stable because the shearing forces are low at these viscosity levels. The hydrophobation of the filler surface by the alkyl groups of the silane has already reached its maximum. Compared to TESPD, the blocked silane performs better due to the higher number of alkyl groups in the molecule.

The oligomeric silane was tested in a temperature range from 145ºC to 165ºC. At lower temperatures the viscosity of the compound turned out to be too high, with the consequence that processing of this compound was difficult. Temperatures higher than 165ºC should be possible thanks to the high temperature stability of the coupling agent and the absence of sulfur, but again processing was the limiting factor: Keeping all the other processing parameters constant, higher compound temperatures could be reached only by rotor speeds out of the range for the mixer used for this investigation. In terms of viscosity, the oligomeric silane shows a different behavior compared to TESPD and the blocked silane (Figure 4C): with increasing silanization time the viscosity of the compound increases. This effect might be caused by a highly entangled polymer shell: The long alkyl chains in the polymeric coupling agent are entangled with the chains of the polymer. When the silane is fixed to the filler by the silanization reaction it becomes immobilized, and as a consequence it immobilizes on its turn a significant fraction of the polymer, resulting in a bound rubber shell around the filler: The polymer is physically bound to the filler by this highly entangled shell. By virtue of the higher volume fraction of the filler particles and their bound shell, the reinforcing effect of these filler particles is significantly increased leading to the higher viscosity by the hydrodynamic effect. The temperature effect for the oligomeric silane is comparable to the effect for TESPD and the blocked silane: higher temperatures result in lower viscosities. The above-mentioned effect of immobilization depends also on temperature, as the rate of coupling of the silane to the filler is increasing with increasing temperature. However, this effect might be superimposed by the reduction of the viscosity due to an increasing (thermal) mobility and flexibility with increasing temperature, finally resulting in a viscosity reduction.

The average level of viscosity is highest for the compounds with the oligomeric silane compared to the other two silanes. The viscosity is directly influenced by the addition of the silane, a highly viscous liquid that has a smaller peptizing effect compared to the other coupling agents. The high molecular mass of this silane results in a lower rate of silanization, because the molecule is less mobile in the rubber compound.

The trends found for the Payne effect values are comparable to the trends in viscosity for compounds containing TESPD and the blocked silane (Figure 5): higher silanization temperatures and longer silanization times result in lower values of the Payne effect, due to a higher degree of dispersion and silanization. For the compound containing the blocked silane the minimum level is reached after silanization for 2.5 minutes at 145ºC, and a longer silanization period does not result in a further reduction of the Payne effect. A significant part of the silanization is taking place during the mixing and heating period, as the starting value of the Payne effect after warming of the compound is less than half the value found for the compounds with TESPD or the oligomeric silane. This indicates, that for this blocked silane the silanization reaction starts at lower temperatures, and that the silanization rate is not neglectible at

temperatures below 135ºC. The average level of the Payne effect is significantly lower for the blocked silane (Figure 5B); and the time to reach the lowest achievable Payne effect at the highest possible silanization temperature is reduced by a factor of 4 to 5 compared to the compound containing TESPD: This silane has a stronger hydrophobation effect due to the higher number of alkyl groups. However, it should also be taken into consideration that the molar concentration of the blocked silane is higher, as it was added in equimolar quantities of silyl groups compared to TESPD.

The Payne effect values of the compounds with the oligomeric silane follow the trends of the viscosities: Increasing values of the Payne effect for longer silanization times, but decreasing Payne effect values for higher silanization temperatures (Figure 5C). The explanation given for the viscosity holds here as well: The polymer is physically bound to the filler and immobilized. With a higher degree of silanization, this physical network might even become enough extended to trap neighbouring filler particles resulting in a filler-filler network and, consequently, in a higher Payne effect. Temperature has an opposite effect: It increases the mobility of the molecules and loosens the network.

The absolute level of the Payne effect values for the compound containing the oligomeric silane is approximately twice as high as the level found for the compounds containing the blocked silane. The lowest value is found for silanization at 165°C after 1 minute: This indicates that these silanes are preferably processed at high temperatures, resulting in short silanization times. The reduced mobility of the long chains of this coupling agent influences the silanization efficiency: The frequency of contact between filler particles and ethoxy-moieties of the coupling agent is lower for the oligomeric silane compared to the blocked silane and TESPD, resulting in a lower probability of the condensation reaction.

A further explanation of the phenomena observed is that the orientation of the silane on the filler surface influences the hydrophobation effect: Figure 11 shows the possible orientations modeled for the different silanes: A parallel orientation is more effective in shielding the filler surface than a perpendicular orientation. TESPD initially connects with one silyl group to the filler surface. It will then be oriented in a perpendicular manner, and homocondensation can occur (Figure 11c). Connecting with both silyl groups to the silica surface is only possible in a parallel orientation (Figure 11a). For the blocked silane the parallel orientation will be very stable, as the molecule is bound to the filler surface with additional hydrogen bridges from the carbonyl group to a silanol group on the silica. Once the molecule splits, the silyl-part will orient in a perpendicular manner. The octyl part of the molecule might stay connected to the silica surface in a perpendicular position or it might be removed and dissolved in the compound. For the oligomeric molecule the more perpendicular orientation is the most likely one. Contrary to the blocked silane as well as TESPD, a parallel orientation of these molecules is not very

probable: It is very unlikely that the long alkyl chains of this coupling agent are straightened and arranged to the filler surface in a parallel position. The molecules can connect to the filler surface by both silyl groups, but the alkyl chain will orient in a perpendicular manner to the surface, as it has a low affinity with the silanol groups and does not contain any polar groups to stabilize a parallel orientation. An improvement for this coupling agent would be the introduction of polar groups into the molecule, either for chemisorption or for physisorption on the filler surface.

Looking at the ethanol concentration in the compound containing TESPD (Figure 7), the concentration remains nearly constant throughout the silanization cycle. Equilibrium between ethanol removal due to mass transfer and ethanol formation due a to chemical reaction is reached very fast. For both other silanes the ethanol concentration is reduced for longer mixing times: The increase in the concentration of ethanol, the sum of ethanol formation due to silanization and ethanol consumption due to the reaction of the alcohol with the silanol groups on the filler surface, is slower than the ethanol removal.

The changes in Payne effect for the compounds containing TESPD and the blocked silane are reflected in the decrease of ethanol concentration with time. For TESPD high values of ethanol concentration are measured, together with a significant reduction of the Payne effect by the silanization reaction. The compounds with the blocked silane show a high concentration of ethanol for short reaction times, when the silanization reaction is still very fast. The concentration decreases after one minute of silanization due to the lower silanization rate as the reaction is almost complete. The compound with the oligomeric silane shows a similar trend in terms of ethanol concentration, but the trend in Payne effect is different, as seen in Figure 5C. The ethanol concentration values show that the silanization reaction has taken place; the increase in Payne effect with time must thus be due to a different phenomenon (entangled silane and polymer molecules).

The difference in the average levels of ethanol concentration, depending on the type of silane, can be explained using the model described in chapter 4. The only factor being varied during these experiments was the rotor speed, resulting in different numbers of revolutions during the silanization phase (Figures 8 and 9): For the compounds with the oligomeric silane, the lowest rotor speed was required in order to keep the temperature at 145°; the highest rotor speeds had to be applied for the compound with the blocked silane. The higher the rotor speed, the higher the number of revolutions per unit time and the higher the rate of surface renewal, improving the mass transfer of ethanol through the interphase between the compound and the gas phase. The effect is most conspicuous in the compounds with the blocked silane for longer silanization times, significantly reducing the ethanol concentration.

TESPD:

$R_2Si(CH_2)_3S_x(CH_2)_3SiR_3$
|
O
|
SiR_2
|
$(CH_2)_3$
|
S_x
|
$(CH_2)_3$
|
SiR_2
|
O

$\cdot S_n$
|
$(CH_2)_3$
|
SiR_2
|
O

$(CH_2)_3S_x(CH_2)_3$
SiR_2 SiR_2
| |
O   O
Si   Si
a: parallel

Si
b: perpendicular

Si
c: perpendicular with homocondensation

Blocked silane:

$(CH_2)_3S$ — C — $(CH_2)_6$ — (CH_3)
SiR_2 ‖
| O ⋯⋯ H
O   O
Si   Si
d: parallel

$\cdot S$
|
$(CH_2)_3$
|
SiR_2
|
O
Si
e: perpendicular

$(CH_2)_6CH_3$
|
$\cdot C$
‖
O
H
O
Si
f: perpendicular

Oligomeric silane:

CH_2 CH_2
| |
SiR_2 SiR_2
| |
O   O
Si   Si

g: perpendicular
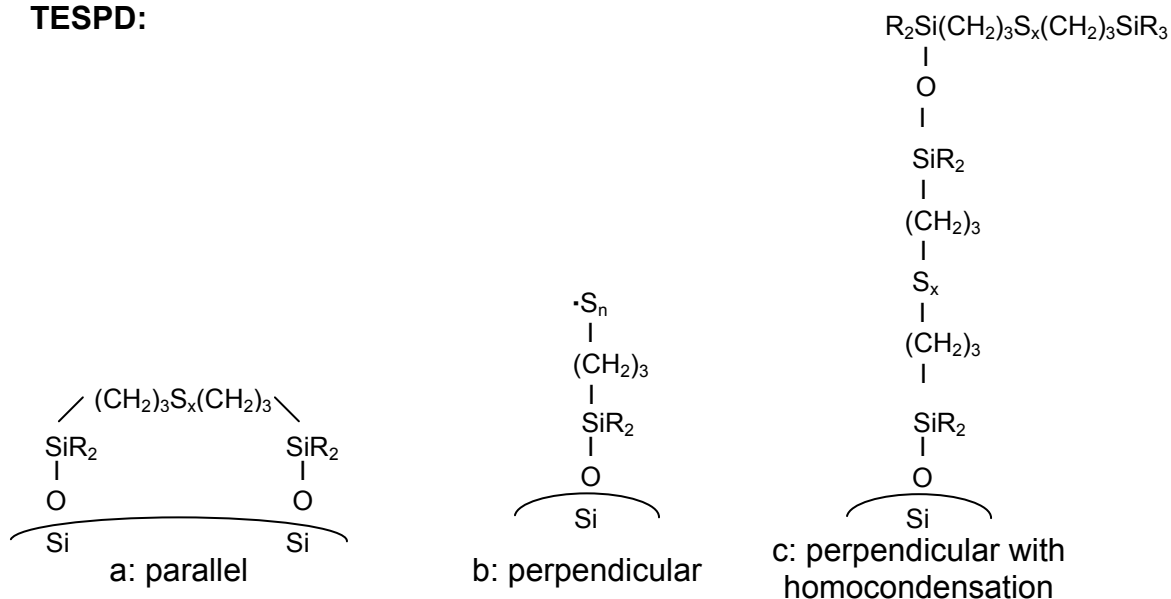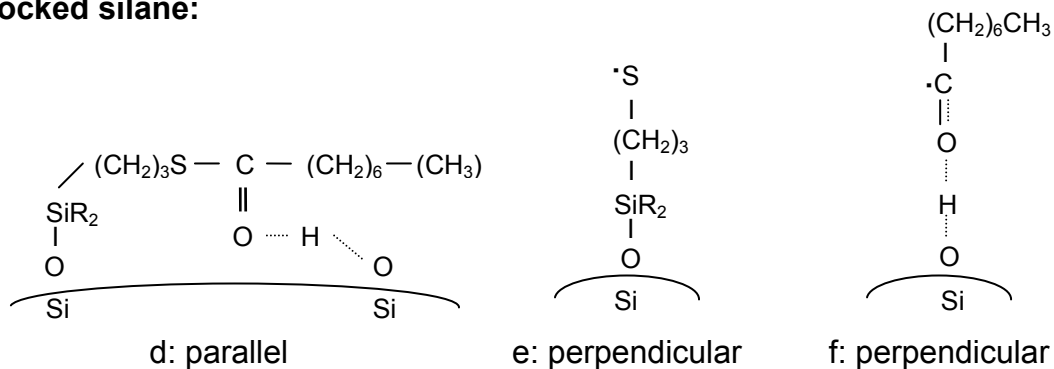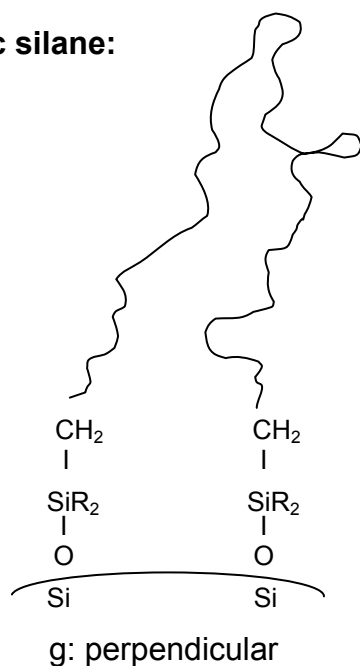
Figure 11: Possible configurations of the different silanes on the silica surface

195

The concentration of ethanol in the compound is proportional to the ratio of ethoxy groups and alkyl groups, decreasing from TESPD over the blocked silane to the oligomeric silane. However, if the ethanol concentration is evaluated in terms of silanization efficiency, the blocked silane is the most efficient one, followed by TESPD and the oligomeric silane.

The energy consumption during the complete mixing and silanization process as well as the energy consumption during the silanization step is comparable for all three coupling agents for shorter mixing times (Figures 8A and 8B.) Only for the longest mixing time, 5 minutes, the energy consumption for the compound containing the oligomeric silane is significantly lower. At this silanization time the difference in the viscosities for the compounds containing different silanes is highest due to the high viscosity of the compound containing the oligomeric silane, resulting in a more efficient energy input for the latter. In general, energy input necessary to hold a given temperature level increases with longer silanization times and higher silanization temperatures, because the viscosity is reduced. The high energy input for the compound containing the blocked silane is caused by the very low viscosity of this compound.

The processing time to achieve the same degree of silanization will vary depending on the different coupling agents. The application of the oligomeric silane results in higher viscosity and Payne effect values compared to both other coupling agents, so the silanization time will be significantly longer at equal temperatures. The viscosity even stays on a high level caused by the high molecular weight of the coupling agent. The energy consumption of a compound containing this silane is slightly lower compared to the other coupling agents, but this advantage will be more than counterbalanced by the longer silanization time.

The application of the blocked silane has certain advantages over TESPD such as a lower viscosity and Payne effect, indicating a higher efficiency of this silane. The energy consumption for equal silanization periods is comparable to the energy consumption of the compounds containing TESPD within the first 2.5 minutes of the silanization. This period is long enough to reach the minimum viscosity and Payne effect of the compound containing the blocked silane.

The blocked silane performs best in terms of ethanol content related to the Payne effect. This indicates that the rate of the Payne effect reduction, the sum of silanization and hydrophobation, is higher for this molecule; and this explains the low values for the Payne effect in comparison to both other silanes. As compounds containing this coupling agent can be processed at higher temperatures compared to TESPD, this results in an additional reduction of the concentration of ethanol in the compound and in an additional increase of the silanization rate.

The kinetic evaluation of the silanization reaction for the compound containing TESPD shows the expected trend of higher reaction rates at higher temperatures. However, for the compounds with the blocked silane this effect is limited to the temperature range between 135ºC to 145ºC; with further temperature rise the reaction rate decreases again. This effect might be due to side reactions such as scorch reactions or the start of a deblocking reaction. The latter reaction will change the hydrophobation efficiency of the coupling agent as the number of alkyl groups is reduced, and the orientation of the molecules will change from parallel to perpendicular. The ratio of attached to dissolved octyl groups influences the hydrophobation.

A considerable difference in the activation energy between the two coupling agents, TESPD and the blocked silane, is found (Table IV). From the point of view of the coupling group - an ethoxy group in both cases - no difference was anticipated. The difference measured in this investigation must be due to the experimental setup: The Payne effect is not a direct measurement of the silanization reaction as such, but it also measures the related effect of hydrophobation. Therefore, differences in kinetics are measured as a consequence of differences in the hydrophobation efficiency. The low value of the activation energy for the compound with the blocked silane reflects the limited influence of temperature on the silanization rate: Within the experimental temperature window, the silanization is fast, even at low temperatures; therefore the impact of increasing temperature is limited. High values of the activation energy, as found for TESPD, were found in other experiments as well, and these activation energies indicate a high temperature dependence of the reaction within the temperature window and under the specific conditions of the experiment.

The compound with the blocked silane is very insensitive to variations of the fill factor in the range between 62% and 72% (Figure 10).This is an indication that the filler is easily dispersed as a result of the high efficiency of the coupling agent. It is an advantage, as the optimal fill factor depends on the viscosity, and major changes in viscosity therefore can result in mixing difficulties. An application of the oligomeric silane as a coupling agent makes the compound more sensitive to high fill factors: up to 67% no significant influence of the fill factor was found, but at 72% the Payne effect and viscosity increase significantly, indicating poor dispersion and silanization. This is mainly due to the insufficient mixing of this highly viscous compound, together with the effect of reduced diffusion of the coupling agent due to its high molecular weight.

3.   COMPARATIVE INVESTIGATION OF SILANES DIFFERING IN SULFUR RANK

3.1. THE DIFFERENT SILANES INVESTIGATED

The following silanes are investigated:

TESPT

(EtO)$_3$Si - (CH$_2$)$_3$ - *S-S-S-S* - (CH$_2$)$_3$ - Si(EtO)$_3$

TESPD

(EtO)$_3$Si - (CH$_2$)$_3$ - *S-S* - (CH$_2$)$_3$ - Si(EtO)$_3$

DTES

(EtO)$_3$Si - (CH$_2$)$_3$ - *(CH$_2$)$_4$* - (CH$_2$)$_3$ - Si(EtO)$_3$
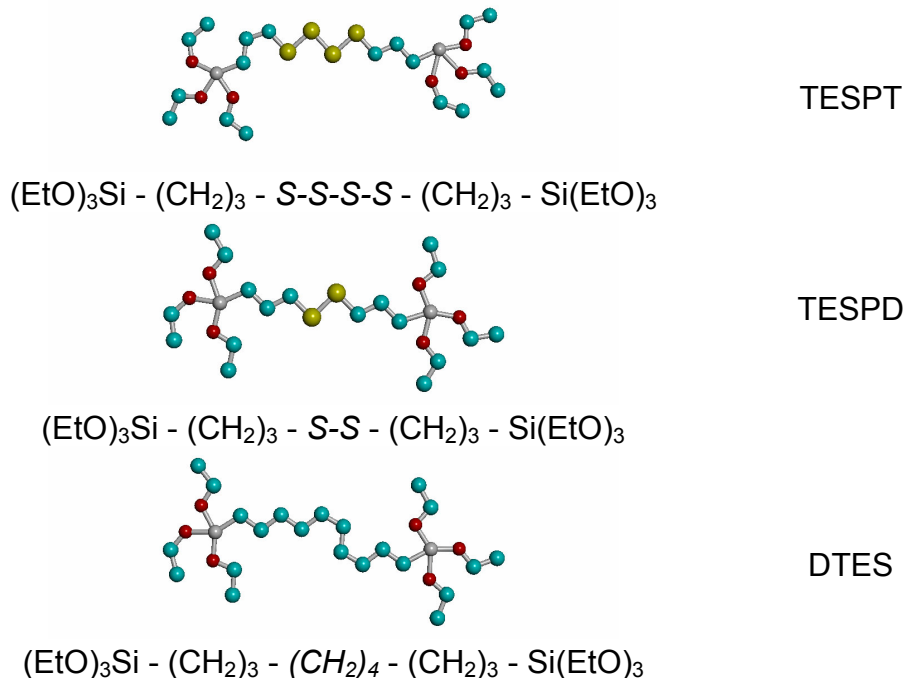
Figure 12: Silanes with different sulfur ranks

The main difference between these silanes is the sulfur rank: The lower the sulfur rank, the less scorch sensitive is the silane. TESPT and TESPD are widely used in the rubber industry as coupling agent for silica, and compounds containing TESPD are reported to be less scorch sensitive compared to compounds containing TESPT. [41-46] DTES, the sulfur-free silane, is used in this investigation to compare the hydrophobation strength: In this molecule, the sulfur moiety is replaced by a butyl group, allowing a direct comparison of the hydrophobation effect of the sulfur moieties with alkyl groups. This silane can not be used as coupling agent for reinforced compounds, as it can not react with the polymer. [1] For the mixing and silanization process the protocol given in Table I is used.

3.2. RESULTS

3.2.1. Viscosity of the compounds as a function of silanization time and temperature
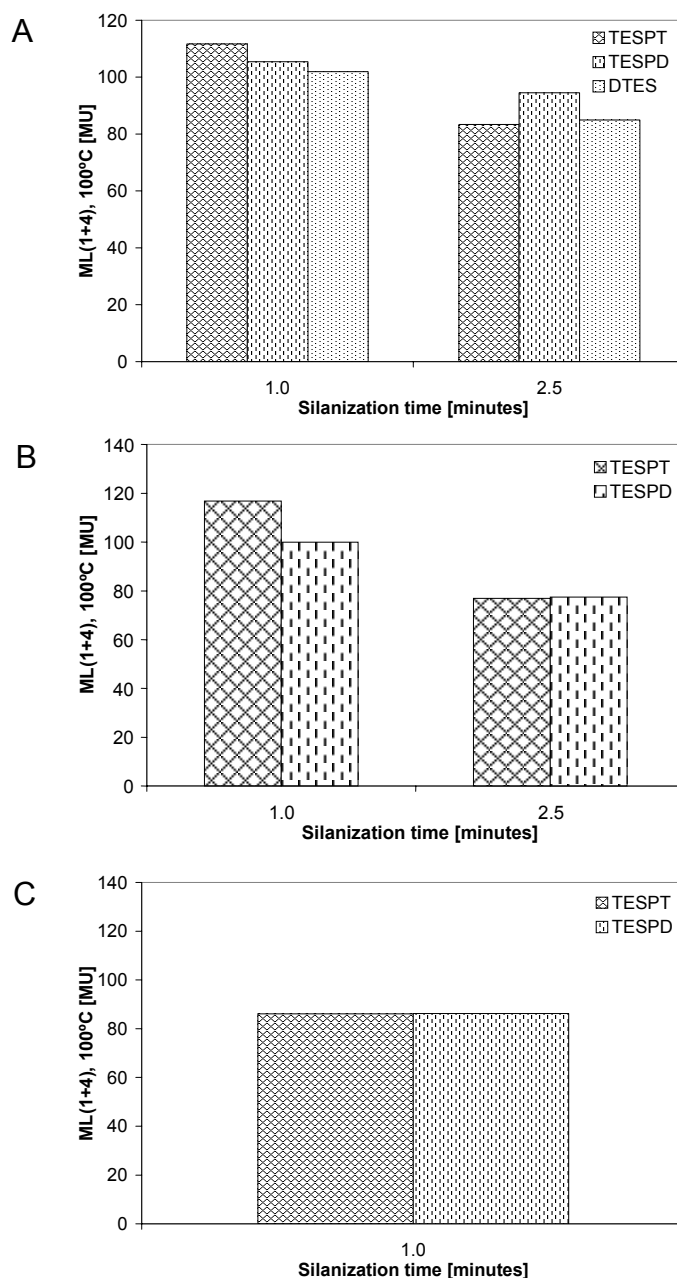
Figure 13: Comparison of the viscosity of compounds
containing silanes with different sulfur ranks
Silanization temperature: A: 135°C, B: 150°C, C: 165°C

In terms of viscosity, slight differences are seen for low silanization degrees: At 135°C and 150°C after one minute of silanization, the viscosity is slightly higher for the compound containing TESPT, followed by the compound containing TESPD. The compound with the sulfur-free silane, DTES, has the lowest viscosity. The absolute values have to be taken with care, as the viscosities are

high and the measurements are less accurate, but the trends are clear. For higher silanization degrees no significant difference is found any more between TESPT and TESPD. The viscosity is decreasing within the whole temperature window of these experiments up to 165ºC, implying that both silanes are temperature-stable under the experimental conditions and scorch is not occurring.

3.2.2. *Payne effect of the compounds as a function of silanization time and temperature*
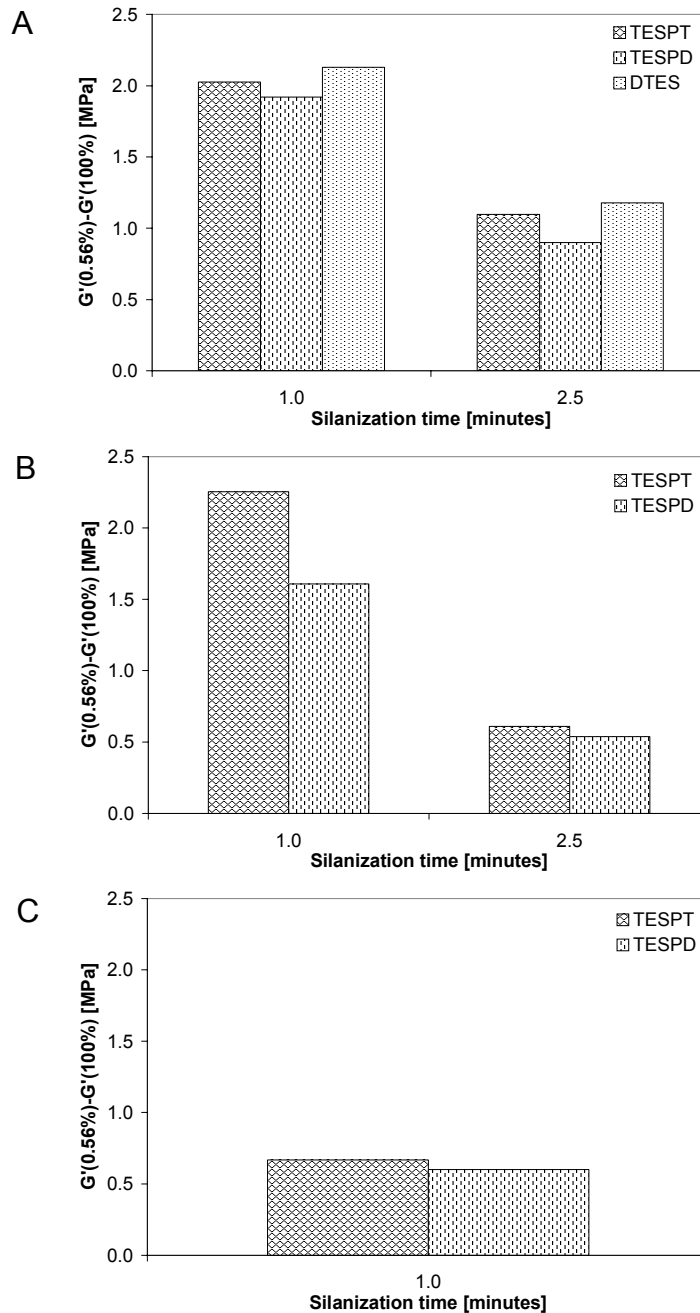
Figure 14: Comparison of the Payne effect of compounds containing silanes with different sulfur ranks
Silanization temperature: A: 135ºC, B: 150ºC, C: 165ºC

The Payne effect values of the compounds at different silanization temperatures are shown in Figure 14. Comparing the compounds containing TESPT and TESPD, respectively, lower values of the Payne effect are found for the TESPD-containing compound. TESPD as coupling agent results in a lower Payne effect especially for medium silanization degrees. At low degrees of silanization, at 135ºC after 1 minute of silanization, as well as at higher degrees of silanization, after 1 minute of silanization at 165ºC, the Payne effect values differ only slightly.

When the sulfur-free silane is used, the Payne effect values of the compound stay on a high level, compared to the compounds containing TESPT and TESPD.

3.3. DISCUSSION

The comparison of the sulfur-containing silanes shows the same trends for viscosity and Payne effect: Lower values for both properties for the disulfidic silane, and the difference between the two compounds becomes less pronounced with increasing degrees of silanization. This is a surprising result as the only difference between the two silanes is the number of sulfur atoms separating the two ethoxysilylpropyl groups. There should be no influence on the kinetics of the silanization reaction, as these groups are separated from the silyl groups by the propyl group. A possible explanation for the lower hydrophobation strength of the tetrasulfane is the degree of separation of the sulfur-moiety and, as a consequence, a difference in the orientation on the surface of the silica. The tetrasulfanegroup is thermally less stable compared to the disulfanegroup; therefore this group might break open to a higher extent during the silanization reaction at moderate temperatures, resulting in a perpendicular orientation of the attached part of the molecule. TESPD stays in a parallel orientation. At 155ºC after a longer period of silanization and at 165ºC no significant differences in viscosity and Payne effect were measured: TESPT and TESPD show the same reactivity in terms of silanization and splitting of the sulfur-moiety. The fact that even at 165ºC no indication of scorch was observed is surprising in view of earlier experiences, but this may be due to the experimental conditions: The experiments were carried out in an small size intermeshing mixer, characterized by a good temperature control and effective cooling, which helps to avoid scorch and allows operation at higher temperatures.

Comparing the sulfur-free silane with the sulfur-containing silanes, it was expected that the hydrophobation strength of the sulfur-free silane would be higher than that of the other two silanes. It is not clear whether or not the sulfur-moiety contributes to the hydrophobation effect; if yes, its effect should be lower compared to the alkyl groups. The experimental result is just the opposite: The compound with DTES has a higher Payne effect than the compounds with the sulfur-containing silanes. The difference in the chemical

201

structure between the two types of silanes will influence the reaction mechanism of the silanization and the orientation of the silane, once connected to the filler surface. As DTES contains only highly stable carbon-carbon-bonds between the silyl groups, it is less prone to thermal scission of these bonds, and the molecule will not split into two parts, which could react separately. Furthermore no polar groups are present in the molecule to stabilize a parallel orientation of the molecule on the filler surface, thus the preferred orientation will be perpendicular, resulting in a less effective shielding of the surface.

4. CONCLUSIONS

The blocked silane shows shorter silanization times for equal Payne effect levels compared to TESPD: Using this silane the maximum hydrophobation is achieved after app. 2.5 minutes of silanization at 145ºC. The hydrophobation rate is significantly faster due to a higher number of alkyl groups in the blocked silane, compared to TESPD. The ethanol-generation for comparable Payne effects is lower. The oligomeric silane shows a different behavior: viscosity and Payne effect increase with longer silanization times. This effect might be caused by a highly entangled bound layer: The coupling agent is chemically bound to the filler, and the polymer is immobilized by the long chains of the coupling agent. Ethanol-generation for a given silanization period is lowest for the oligomeric silane. If the ethanol concentration in the compound is related to the silanization efficiency, the blocked silane performs best.

Energy consumption for higher degrees of silanization is higher for the compounds containing TESPD or the blocked silane, compared to the compound containing the oligomeric silane. It follows the trend of the viscosity of these compounds.

A considerable difference is found for the activation energy of the silanization reaction with TESPD compared to the blocked silane. The blocked silane shows a very low activation energy value, because the silanization is very fast at low temperatures, limiting the impact of temperature increase on the silanization rate.

Only slight differences are found when comparing silanes with different sulfur ranks. Under the experimental conditions TESPT and TESPD perform in a similar manner in terms of temperature stability.

5. REFERENCES

1. ten Brinke, J.W., in *Thesis: Silica reinforced tyre rubbers*. 2002, Dept. Rubber Technol., Univ. Twente: Enschede (the Netherlands).
2. Reuvekamp, L.A.E.M., in *Thesis: Reactive mixing of silica and rubber for tyres and engine mounts*. 2003, Dept. Rubber Technol., Univ. Twente: Enschede (the Netherlands).
3. ten Brinke, J.W., van Swaaij, P.J., Reuvekamp, L.A.E.M., Noordermeer, J.W.M., Rubber Chem. Technol., 2003. **76**(1): p. 12.
4. ten Brinke, J.W., van Swaaij, P.J., Reuvekamp, L.A.E.M., Noordermeer, J.W.M., Kautsch. Gummi Kunstst., 2002. **55**(5): p. 244.
5. Hashim, A.S., Azahari, B., Rubber Chem. Technol., 1998. **71**: p. 289.
6. Wolff, S., Kautsch. Gummi Kunstst., 1981. **34**(4): p. 280.
7. Datta, R.N., Das, P.K., Mandal, S.K., Basu, D.K., Kautsch. Gummi Kunstst., 1988. **41**: p. 157.
8. Luginsland, H.-D., Kautsch. Gummi Kunstst., 2000. **53**(1-2): p. 10.
9. Kim, K.-J., Van der Kooi, J., Rubber world, 2002. **226**(5): p. 39.
10. Technical information from the OSI/Crompton website ([www.cromptoncorp.com)](www.cromptoncorp.com), 2001.
11. Non-confidential personal information from OSI Crompton, currently GE Silicones, 2002.
12. Luginsland, H.-D., Krafczyk, R., Forster, F., *Geblockte mercaptosilane, Verfahren zu deren Herstelleung und die enthaltenden Kautschukmischungen*. 29.08.2002, Degussa AG: EP 1 298 163 A1.
13. Früh, T., Steger, L., Heiliger, L. in *Kautschuk-Herbst-Kolloquium*. 2002. Hannover (Germany).
14. Sindorf, D.W., Maciel, G.E., J. Am. Chem. Soc., 1983. **105**: p. 3767.
15. Agostini, G., *Rubber composition and tire having tread thereof*. 17.02.1999, The Goodyear Tire & Rubber Company: EP 0 896 978 A2.
16. Ahmad, S., Schaefer, R.J., *Energy-saving tire with silica-rich tread*. 28.05.1985, The B. F. Goodrich Company: UP 4,519,430.
17. Kayser, F., Lauer, W., Materne, T.F.E., *Ether containing siloxy compounds*. 14.02.2001, The Goodyear Tire & Rubber Company: EP 1 076 061 A1.
18. Kayser, F., Lauer, W., Materne, T.F.E., *Unsaturated siloxy compounds*. 14.02.2001, The Goodyear Tire & Rubber Company: EP 1 076 060 A1.
19. Materne, T.F.E., Agostini, G., Visel, F., Cohen, M.P., *Unsymmetrical siloxy compounds*. 01.09.1999, The Goodyear Tire & Rubber Company: EP 0 939 081 A1.
20. Materne, T.F.E., *Siloxy compounds*. 01.09.1999, The Goodyear Tire & Rubber Company: EP 0 939 080 A1.
21. Materne, T.F.E., Agostini, G., Junio. M., *Rubber composition containing silanol modified carbon black*. 12.04.2000, The Goodyear Tire & Rubber Company: EP 0 992 535 A1.
22. Sandstrom, P.H., Smith, R.R., Pyle, K.J., *Tire with silica reinforced tread and/or sidewall components*. 29.03.2000, The Goodyear Tire & Rubber Company: EP 0 989 161 A1.
23. Wideman, L.G., Sandstrom, P.H., *Rubber composition containing a pyrazine compound*. 21.11.2001, Goodyear Technical Center Luxembourg: EP 0 860 469 B1.
24. Zimmer, R.J., Visel, F., Frank, U.E., Agostini, G., *Asymmetrical siloxy compounds*. 29.09.1999, The Goodyear Tire & Rubber Company: EP 0 945 456 A2.
25. Ishida, H., Polym. Comp., 1984. **5**(2): p. 101.
26. Wolff, S., Tire Sci. Technol., 1987. **15**(4): p. 276.
27. Tesoro, G., Wu, Y., J. Adhesion Sci. Technol., 1991. **5**(10): p. 771.
28. Yamaguchi, M., Nakamura, Y., Iida, T., Polym. & Polym. Comp., 1998. **6**(2): p. 85.
29. Mariciniec, B., Gulinski, J., Mireki, J., Foltynowicz, Z., Int. Polym. Sci. Technol., 1990. **18**(8): p. T/62.
30. Mariciniec, B., Urbaniak, W., Maciejewski, H., Int. Polym. Sci. Technol., 1993. **20**(2): p. T/53.
31. Mariciniec, B., Gulinski, J., Int. Polym. Sci. Technol., 1993. **22**(1): p. T/83.
32. Ghatge, N.D., Khisti, R.S., Elastomerics, January 1985: p. 23.
33. Thammathadanukul, V., O'Haver, J.H., Harwell, J.H., Osuwan, S., Na-Ranong, N., Wadell, W., J. Appl. Polym. Sci., 1996. **59**: p. 1741.

34.   Vondracek, P., Hradec, M., Rubber Chem. Technol., 1984. **57**: p. 675.
35.   Kornetka, Z.W., Int. Polym. Sci. Technol., 1988. **15**(1): p. T/76.
36.   Thurn, F., Wolff, S., Kautsch. Gummi Kunstst., 1975. **28**(12): p. 733.
37.   Maisel, J.W., Seeley, W.E., Rubber Plast. News. **August 11, 1986**: p. 26.
38.   Krysztafkiewicz, A., Domka, L., Plast. Rubber Proc. Appl., 1986. **6**: p. 197.
39.   Materne, T.F.E., Kayser, F., *Silica reinforced rubber composition used in tires*. 20.12.2000, The Goodyear Tire & Rubber Company: EP 1 061 097 A1.
40.   Joshi, P.G., Cruse, R.W., Pickwell, R.J., Weller, K.J., Sloan, W.E., Hofstetter, M., Pohl, E.R., Stout, M.F., Tire Technol. Int. **2004**: p. 166.
41.   Fröhlich, J., Luginsland, H.-D., Rubber World. **April 2001**: p. 28.
42.   Luginsland, H.-D. *Reactivity of the sulfur functions of the disulfane silane TESPD and the Terasulfane silane TESPT*. in *Am. Chem. Soc. Rubber Div. conference*. April 13-16, 1999. Chicago, Illinois.
43.   Stone, C.R., Menting, K.-H., Hensel, M. *Optimising the use of disulfide silane in a silica green tyre compound*. in *Am. Chem. Soc. Rubber Div. conference*. October 17-19, 2000. Cincinnati, Ohio.
44.   Luginsland, H.-D., Kautsch. Rubber Kunstst., 2000. **53**(1-2): p. 10.
45.   Cruse, R.W., Hofstetter, M.H., Panzer, L.M., Pickwell, R.J., Rubber Plast. News, 1997: p. 14.
46.   Cruse, R.W., Hofstetter, M.H., Panzer, L.M., Pickwell, R.J. in *Am. Chem. Soc. Rubber Div. conference*. October 8-11, 1996. Louisville, Kentucky.

SUMMARY AND OUTLOOK

1. MOTIVATION

The work of this thesis is related to a practical problem of processing of rubber compounds containing silica as a filler and a silane coupling agent. These compounds, which are mainly used in tire treads due the improved performance in terms of rolling resistance and wet grip compared to carbon black filled compounds, suffer from a poor processability: The dispersion of the filler is difficult, and the compounds are very temperature-sensitive. The current way to process these compounds is to mix them in several steps in order to get a good dispersion and a sufficient degree of silanization and to reduce the temperature load. But this solution is a compromise between processability and mixing capacity, as the total mixing time for silica compounds is longer than the mixing time for carbon black compounds, especially when handling time for discharge, cooling and recharge between the mixing steps is taken into consideration.

Within this thesis, a fundamental investigation of the mixing process of silica compounds is done, and the factors influencing the mixing and silanization efficiency are analyzed. However, the final aim of the work is a very practical one: The proposition of adjustments of the production process and mixing equipment, which enhance the mixing and silanization process of silica compounds on production scale and which are easy to implement into the existing mixing equipment.

2. GENERAL SUMMARY

The core problem of silica mixing coming to the fore in all the experiments of *chapter 3,* the phenomenological approach to the dispersion and silanization process in an internal mixer, is the devolatilization of the compound. During the silanization reaction ethanol is generated, which interferes with the mixing process and the silanization reaction, as ethanol is partly evaporated into the free volume of the mixing chamber and partly dissolved in the rubber compound.

High concentrations of ethanol in the vapor phase in the free volume of the mixing chamber are reducing the transfer of ethanol from the compound into the vapor phase. Additionally, the alcohol tends to condensate in the mixing chamber causing slippage of the compound. This reduces mixing as well as cooling efficiency.

Dissolved ethanol influences the processing behavior as well by a reduction of the compound viscosity, which results in an influence on the flow pattern in the mixer and on the energy input into the compound. But the main influence is on the silanization reaction: The alcohol is competing with the silane for adsorption and reaction sites on the filler surface. During the primary reaction, which is assumed to be a direct reaction of one ethoxy group of the silyl moiety with a silanol group of the filler, ethanol is formed in the proximity of the filler surface. The ethanol in statu nascendi is very reactive and the probability is high, that this molecule is chemically or physically adsorbed onto the filler surface. This has several implications for the adsorption of the silane, next to the reduction of the surface concentration of available silanol groups on the filler surface. Adsorbed ethanol will disturb the formation of a silane-shell around the silica particle, because it prevents silane molecules to be bound to vicinal silanol groups and to undergo homocondensation during the secondary reaction. Furthermore, it will influence the sterical arrangement of the silane molecules on the silica surface, because it prevents a parallel orientation of the silane to the filler surface: the preferred position for an optimal hydrophobation effect. The adsorbed ethanol molecules provide a hydrophobation effect as well, but the effect is less due to the lower number of alkyl groups compared to the coupling agent. Even more important is the fact that the alcohol molecules can not react with the polymer during the vulcanization reaction, resulting in a reduced reinforcing effect of the filler. The secondary reaction is assumed to be a condensation reaction of two silanol groups, either from two silane molecules or from one silane molecule and a silanol group from the filler surface. Prior to the condensation reaction, the ethoxy groups of the silane need to be hydrolyzed, again resulting in the formation of ethanol throughout the rubber matrix. Ethanol generated at a distance to a filler particle will have a higher probability to be transported to the compound interphase and be transferred into the vapor phase rather than being adsorbed onto the filler surface.

The overall conclusion from *chapter 3* is, that all measures improving the devolatilization of the compound are finally enhancing the silanization efficiency. In this context, different mixing equipment and processing parameters are investigated: working in an open mixer with varying fill factors, application of air injection under various conditions, variation of the rotor type as well as the temperature settings of the mixing chamber and the rotor. The factors with the strongest positive effect on the silanization efficiency are working in an open mixer and air injection.

Both measures considerably reduce the ethanol concentration in the free volume of the mixing chamber, resulting in a positive effect on mixing and silanization: Condensation of ethanol in the mixing chamber is reduced and the devolatilization rate of the compound is increased. A reduced condensation results in less slip, thus a better contact of the compound to the mixer wall and to the rotor. This increases the cooling efficiency and the energy input into the compound by the rotor movement. The cooling efficiency is indirectly influencing the devolatilization of the compound: A higher cooling efficiency effectuates a higher energy input necessary to keep the temperature level constant. This can be achieved by an increase of the rotor speed, the determining factor for the surface renewal rate of the compound in the mixer: The higher the surface renewal rate, the higher the average ethanol concentration in the surface layer. The difference between the ethanol concentration in the surface layer of the compound and the vapor phase in the free volume of the mixer is the driving force for the mass transfer across this interphase. Not only mass transfer depends on rotor speed, but also energy transfer across the interphase between the compound and the mixing chamber wall, resulting in a superimposed positive effect on cooling and devolatilization efficiency.

The reduced ethanol concentration in the vapor phase results in a reduction of the ethanol concentration in the rubber matrix, as a consequence of the improved devolatilization of the compound. This results in an increased silanization rate and efficiency, as explained above.

When air injection is applied, the effect of dragging ethanol out of the compound is combined with an additional positive effect of cooling. A limiting factor in this mode can be the outlet of the air, and a further improvement can be achieved by providing an outlet. One possibility to realize this is to work in an open mixer; another possibility is to replace the massive ram by a device allowing the air to escape, but still exerting pressure on the compound. However, the latter adjustment of the mixer is rather complicated and the additional positive effect on the silanization efficiency is low. Air injection is the preferred measure, as it is the most effective one and easy to implement.

Working in an open mixer is also effective in improving the silanization efficiency. Ethanol vapor can escape from the mixing chamber, thus reducing ethanol condensation on the mixer walls and increasing the devolatilization rate. However, the fill factor of the mixing chamber has to be adjusted in order to improve the intake behavior and to avoid, that the compound is forming a bank in the upper part of the mixing chamber. The optimal fill factors determined for this mixing mode were 40 to 45%, compared to fill factors of 65% and higher when working in a closed mixer. The preferred solution will be a combination of working in an open mixer with further adjustments of the equipment and the mixing process: The best combination would be an internal mixer applying high shear forces for mastication, dispersive and distributive

mixing, and a separate reactor for the silanization reaction. During the silanization reaction, shearing forces are no longer required, but the creation of fresh surfaces and a constant temperature level are crucial.

Other factors identified to have a positive effect on the silanization efficiency are fill factor, compound temperature, temperature control unit settings and rotor geometry. The variation of the fill factor has a direct influence on the distribution of the rubber compound in the mixing chamber: The lower the fill factor, the lower the ratio of the volume of material in the rolling pool to the volume of material sheeted out thinly on the mixer walls in the case of tangential rotors. Thus, a reduction of the fill factor will improve the devolatilization of the compound, as it increases the relative surface area of the compound and the surface to volume ratio. This correlation between fill factor and silanization efficiency is valid for a limited range of fill factors; below a certain threshold of the fill factor, the flow in the mixing chamber will change significantly and energy input will decrease with a negative influence on the silanization efficiency. However, the increase of the silanization efficiency with decreasing fill factors is accompanied by a decrease of the mixing capacity.

When working in an open mixer, the silanization efficiency is even more sensitive to a variation of the fill factor due to the strong influence on intake behavior. At high fill factors, the rubber is pulled into the area between the rotors with a delay, and effective mixing time is reduced.

Compound temperature is an ambivalent parameter: On one hand, the temperature should be high enough to guarantee a high rate of silanization. On the other hand, low compound temperatures result in a higher viscosity of the compound, and this improves the dispersion of the filler as shearing forces are higher. The temperature is also limited due to the presence of sulfur in most of the coupling agents: If the temperature is too high, the sulfur reacts with the polymer resulting in scorching of the compound. Temperature is not a very flexible parameter; it should be chosen as close as possible to the scorch limit, given that dispersion of the compound is sufficiently accomplished in the early stages of mixing.

The temperature control settings directly influence the cooling efficiency, as the temperature difference between the compound and the mixer wall is the driving force for energy transfer. A higher cooling efficiency has a positive effect on the silanization rate, as explained above. Therefore, lower temperature control unit settings are preferred. The influence of the cooling temperature on the condensation of ethanol in the mixing chamber is of minor importance.

Rotor geometry has an influence on the silanization efficiency. When working in an open mixer, the intake behavior is the most prominent characteristic of the rotor: A good intake behavior of the rotor means that the compound is pulled into the mixing chamber regularly and frequently, resulting in a good mixing and

sheeting of the rubber compound. When silanization is done in a closed mixing chamber, the homogenization and cooling capacities of the rotor are other important characteristics, together with the creation of fresh surface.

In *chapter 4* a model is developed for the devolatilization of a rubber compound including a chemical reaction, the basic situation during the silanization step of silica compounds. This model is based on the penetration theory, which assumes a constant exposure time of the interphase between the compound and the vapor phase. In an internal mixer, the interphase to the vapor phase is formed by rolling pools of material in front of the rotor flights and by a wall layer, which is wiped onto the mixing chamber walls with each rotor revolution. Both interphases are periodically renewed, resulting in a constant exposure time. Devolatilization occurs according to two different mechanisms: diffusion of ethanol and mass transfer by the movement of volume elements of the rubber matrix to the interphase. The main contribution to devolatilization in the present case is mass transfer caused by the intensive movement of the compound, as diffusion of ethanol in a polymer matrix is relatively low. The model qualitatively predicts the influence of the processing conditions and mixer parameters. A comparison of experimental data with model calculations shows, that the process does not reach a steady state: The devolatilization of the rubber compound by mass transfer is faster than the replenishment of the ethanol by the silanization reaction, resulting in a decreasing rate of ethanol evaporation from the compound during the time scale of the experiments.

In *chapter 5*, the kinetics of the reaction between silane and silica in a rubber matrix are compared to the kinetics of the same reaction in model compounds from literature. The influence of a variation of the mixing equipment and processing parameters, as described above, on the kinetics of the silanization reaction is investigated. Once again the general conclusion is, that all measures reducing ethanol concentration either in the rubber compound or in the vapor phase are increasing the silanization rate. Again, air injection is the most effective measure: For a silanization temperature of 145°C, the reaction rate more than doubled when silanization was done with air injection.

The automatically registered fingerprints of the mixing and silanization process allow an estimation of the energy streams. In *chapter 6,* these data are used to make the balance of the different energy streams during the heating and silanization period. The adsorption energy as well as the enthalpy of the silanization reaction contribute only marginally to the total energy balance. These evaluations confirm the earlier drawn conclusion, that ethanol formed during the silanization reaction is one of the main influencing factors of the cooling efficiency. Alcohol condenses on the mixing chamber walls and thus limits the contact between the rubber compound and the walls, resulting in a lower cooling efficiency and a lower silanization rate. Fill factor and rotor speed also influence the cooling efficiency, with generally a linear correlation. Other

influencing factors are rotor design, processing mode (open/closed mixer) and air injection.

The analysis of the mixing and silanization step of silica-filled compounds has so far shown, that the process is dominated by mass transfer and energy transfer. As mass transfer occurs through the interphase between the compound and the vapor phase in the mixing chamber, and energy transfer occurs through the interphase between the compound and the mixing chamber wall, the ratio of the surface area to the volume of the compound is one of the most important parameters in upscaling. Therefore, linear upscaling should be avoided. Rotor speed is another important parameter in this context, as it determines the surface renewal rate. The fill factor influences the energy input and the ethanol generation per unit volume of the mixer, and the gap size is determining the dispersion efficiency. A dimensionless number correlating all parameters which are influenced by a scale up of the mixer, in order to keep the silanization efficiency constant, is proposed in *chapter 7.*

In *chapter 8* different types of coupling agents are compared in terms of processability and silanization efficiency. One series of coupling agents are silanes with basically the same structure of two triethoxysilylpropyl groups, but differing in the sulfur rank: a tetrasulfane, a disulfane and a sulfur-free silane, in which the sulfur moiety is replaced by a butyl group, are chosen. The latter silane can react with the filler, but has no moiety for a reaction with the polymer. It will form a hydrophobic shell around the filler particles and thus improve the processing behavior of the compound, but will not be reinforcing. The two sulfur containing silanes are commonly used as coupling agents in silica compounds, with a growing importance of the disulfane due to the higher temperature stability reducing the scorch risk. In this investigation, no significant differences in scorch were found between these two silanes. The apparently similar temperature sensitivity of the two compounds is due to the mixing equipment used: The experiments are done in an intermeshing mixer on laboratory scale, which is known to have very good temperature homogeneity, thus avoiding hot spots in the mixing chamber at which scorch reactions can occur.

The hydrophobation effect of the disulfane is higher compared to the effect of the tetrasulfane. This might be an effect of the lower thermal stability of the tetrasulfane: The terasulfane molecule splits to a higher degree at the processing temperature, resulting in a re-orientation of the two parts on the filler surface: The orientation possibly changes from a parallel to a perpendicular one after splitting, while the disulfane molecule is predominantly oriented in a parallel manner, stabilized by polarization of the disulfane group. The sulfur-free silane shows a smaller hydrophobation effect, what might be explained by a perpendicular orientation of the molecule on the filler.

The second series of coupling agents was a blocked silane, an oligomeric silane and a disulfane. In the blocked silane the sulfur moiety is blocked by esterification with octanethionic acid, resulting in a more stable sulfur-moiety compared to the disulfide group in TESPD. The blocked sulfur group is supposed to split during the vulcanization mixing step, thermally or with the aid of a deblocking agent such as an amine. It contains a higher number of alkyl groups compared to the commonly used silanes, resulting in a better hydrophobation effect. The ratio of ethoxy groups to alkyl groups is lower, resulting in a positive effect on ethanol generation for a similar hydrophobation effect.

The oligomeric silane has a molecular weight of approximately 1800 g/mol, resulting in a low ratio of alkoxy groups to alkyl groups; therefore ethanol generation is reduced. The compound is sulfur-free: Scorch reaction can not occur and the material can be processed at higher temperatures up to 175ºC. The filler-polymer network has to be established during the vulcanization reaction, and a special filler-activator has to be added for this purpose during the final mixing step as this molecule does not contain a moiety for a direct reaction with the polymer.

The compound with the blocked silane performed best in comparison to both other silanes under the experimental conditions: The Payne effect of this compound decreased very rapidly, accompanied by low concentrations of ethanol in the compound, indicating a fast and effective silanization. Mixing and dispersion of this compound was very efficient, and the sensitivity to variations of the fill factor was low. The compound with the oligomeric silane in general has a higher viscosity and Payne effect under comparable conditions: The degree of hydrophobation and silanization was low compared to the other silanes. Furthermore, a highly entangled shell of the silane and the polymer molecules around the filler particle increases the viscosity of the compound. The advantage of this coupling agent is the scorch safety, making it possible to process the compounds at very high temperatures.

3. OUTLOOK

The results of this investigation give an answer to a lot of questions, but at the same time they raise new questions. This area of investigation is still very wide, and finding an answer to all open questions and solutions to the practical problems will require a considerable further effort.

From a theoretical point of view, one of the most interesting open questions is the mechanism of the silica-silane reaction under processing conditions. The interference with other compounding ingredients and the influence of the processing conditions should be elaborated. The influence of the adsorption kinetics of the silane prior to the silica-silane reaction is not investigated yet,

and especially the competing adsorption of ethanol and other compounding ingredients should be elucidated. The hydrophobation effect is an important characteristic of the coupling agent, and the influence of the structure of the coupling agent, in particular the number of alkyl groups, is discussed in the literature. However, the sterical orientation of the molecules on the filler surface might even be more important for the hydrophobation strength, but this aspect is only marginally mentioned in literature. In terms of processing behavior, the influence of mastication, temperature increase and silanization on the compound viscosity was a subject of long discussions within the project, without obtaining a satisfying answer.

The most urgent practical problems are related to the ethanol generation and the scorch risk of the silica-silane compounds. New coupling agents should be developed, which do not form ethanol or other problematic chemical compounds during the silanization reaction. This problem can also be approached from the silica side by introducing silica types with an activated surface which can directly react with the polymer. Another option is the application of new fillers combining the good processing behavior and the physical interaction with the polymer of carbon black with the chemical interaction of the silica filler with the polymer. First attempts to introduce this kind of fillers are made by developing the 'dual phase fillers', in which a silica phase is finely distributed in a carbon black phase. The scorch risk of silica-silane compounds can drastically be reduced by using sulfur-free silanes, but these silanes are difficult to connect to the rubber. Silanes, which do not react under mixing and silanization conditions, but which can be activated during curing by temperature, pressure or an activator, are one solution to this problem. The blocked silane described in chapter 8 of this thesis is one example of this type of coupling agents, but there is still a need for further developments and improvements.

SAMENVATTING

1. DOEL VAN HET ONDERZOEK

Het uitgangspunt van dit onderzoek is de moeilijke verwerkbaarheid van rubbermengsels, die een silica/silaan-systeem als versterkende vulstof bevatten. Deze mengsels worden met name in loopvlakken van autobanden gebruikt, omdat zij de rolweerstand van banden verlagen en de grip op natte wegen verhogen, in vergelijking met banden waarin roet als vulstof wordt toegepast. Deze mengsels leveren grote problemen: de dispersie van de silica vulstof is moeilijk en de mengsels zijn temperatuurgevoelig. Tegenwoordig worden deze mengsels in meerdere stappen gemengd, om een goede dispersie en silanisering te bereiken en de temperatuur niet te ver te laten oplopen. Deze werkwijze is een compromis tussen verwerkbaarheid en mengcapaciteit, want de totale mengtijd voor silica-mengsels is beduidend langer dan de mengtijd voor vergelijkbare roetmengsels. Hier telt niet alleen de effectieve tijd in de menger, maar ook de tijd om te lossen, af te koelen en het mengsel opnieuw in de menger te brengen.

In het huidige project is fundamenteel onderzoek verricht naar het mengproces van silica-rubber mengsels; de parameters, die van invloed zijn op verwerkingsgedrag en mengefficiëntie zijn geanalyseerd. Het doel van dit onderzoek was gericht op de praktijk: de aanpassing van het mengproces en de mengapparatuur, om mengen en silaniseren van silica-rubber mengsels op productieschaal te verbeteren.

2. SAMENVATTING

Het kernprobleem dat bij alle experimenten van *hoofdstuk 3*, een fenomenologisch onderzoek naar dispersie en silanisering van silica-rubber mengsels in een interne menger, naar voren komt is 'ontluchting': het verwijderen van ethanol uit het mengsel en uit de menger. Tijdens de silaniseringsreactie wordt ethanol gevormd, dat gedeeltelijk in de rubber oplost en gedeeltelijk in de vrije ruimte van de mengkamer terechtkomt en daar het verdere silanisings- en mengproces negatief beïnvloedt.

Een hoge ethanol concentratie in de dampfase in het vrije volume van de mengkamer belemmert de overdracht van ethanol vanuit het mengsel naar de dampfase. Bovendien condenseert ethanol op de mengkamerwanden en veroorzaakt slip, met als gevolg een verlaging van de mengefficiëntie. Verder beïnvloedt ethanol in het mengsel het verwerkingsgedrag door verlaging van de viscositeit, met als gevolg een verandering van het vloeigedrag en de

energie-opname van het mengsel. Bovendien wordt de silaniseringsreactie beïnvloed: ethanol en silaan concurreren om adsorptieplaatsen op het silica-oppervlak. Tijdens de eerste stap van de silaniseringsreactie, de rechtstreekse reactie van één ethoxygroep per silylgroep van de silaan coupling agent met een silanolgroep op de silica, wordt ethanol dicht bij het silica-oppervlak gevormd. Deze ethanol in statu nascendi is bijzonder reactief en wordt daarom gemakkelijk zelf op het silica-oppervlak geadsorbeerd. Dit betekent, dat er effectief minder silanolgroepen overblijven voor de silaanadsorptie. Bovendien wordt de afscherming van het silica-oppervlak door een dicht silaanlaagje belemmerd, omdat de kans kleiner wordt, dat silaanmoleculen dicht genoeg naast elkaar kunnen aanhechten om te kunnen condenseren tijdens de tweede stap van de silaniseringsreactie. De tweede stap van de silaniseringsreactie is een condensatie van twee silanolgroepen van naburige silanen of van silica. Daarvoor moeten de ethoxygroepen van het silaan ook eerst gehydrolyseerd worden: ook weer een bron voor ethanol. Verder wordt de parallelle plaatsing van de silaan-moleculen op het silica-oppervlak verstoord, waardoor het afschermingseffect verkleind wordt. Geadsorbeerde ethanol moleculen hebben ook een hydrofoberend effect, maar dit effect is klein vergeleken met de hydrofobering door silaan moleculen, omdat zij minder alkylgroepen bevatten. Een belangrijk verschil tussen ethanol en silaan is het feit dat ethanol tijdens vulkanisatie niet kan koppelen aan het polymeer, waardoor het versterkend effect van het silica/silaan-systeem negatief beïnvloed wordt.

De conclusie van *hoofdstuk 3* is, dat alle maatregelen die de ethanolconcentratie in het rubbermengsel verlagen, ook een positief effect hebben op de silanisering. Verschillende mengconfiguraties en verwerkingscondities zijn onderzocht: silaniseren in een open menger met variatie van de vulgraad, luchtinjectie, variatie van rotortype en temperatuur van de mengkamer en rotor. De grootste verbetering kan worden bereikt door silaniseren in een open menger of door luchtinjectie. Beide maatregelen verlagen de ethanolconcentratie in de vrije ruimte in de menger, met positieve gevolgen voor het mengen en silaniseren, door minder condensatie en betere devolatilisatie. Door het eerste effect wordt slip voorkomen en het contact tussen mengsel en mengkamerwand verbeterdverbetert, resulterend in verbeterde koeling van het mengsel en efficiëntere energieoverdracht. Een verbeterde koeling zal indirect ook een positief gevolg hebben voor de devolatilisatie van het mengsel: om de mengseltemperatuur desondanks constant te houden, moet meer energie ingebracht worden door middel van een hoger toerental van de rotor. Het toerental bepaalt de vernieuwingsfrekwentie van het mengseloppervlak, en de efficiëntie van de devolatilisatie wordt hoger met een hogere vernieuwingsfrekwentie: voor vers oppervlak is het concentratieverschil tussen ethanol in het mengsel en de omgeving maximaal, de drijvende kracht voor stoftransport. Naast stoftransport wordt ook energietransport tussen mengsel en mengkamerwand

beïnvloed door het toerental van de rotor, resulterend in een verdere verbetering van devolatilisatie.

Een lagere ethanol concentratie in de dampfase in de menger brengt ook een lagere ethanol concentratie in het rubbermengsel met zich mee door een efficiëntere devolatilisatie, resulterend in een hogere silaniseringsnelheid en -efficiëntie.

Bij luchtinjectie wordt ethanol uit het mengsel verwijderd én tegelijkertijd het mengsel gekoeld. Een limiterende factor voor deze maatregel is de afvoer van lucht; een goede afvoer van de lucht kan de effectiviteit van deze maatregel nog verder verbeteren. De combinatie van luchtinjectie en een open menger is één voorbeeld; een andere mogelijkheid is het werken met een stempel, die van uitlaatgaatjes is voorzien. Het verschil tussen de twee werkwijzen is, dat in het laatste geval nog steeds onder druk wordt gewerkt, hetgeen een extra positief effect op de silanisering geeft. Nadeel van deze werkwijze is wel, dat de implementatie in de praktijk moeilijker is. De meestbelovende maatregel ter verbetering van de silanisering is luchtinjectie, vanwege een hoge efficiëntie en een gemakkelijke implementeerbaarheid.

Het silaniseren in een open menger brengt ook een verbetering met zich mee door betere ontluchting, met als gevolg minder condensatie en efficiëntere devolatilisatie. Deze maatregel vraagt wel om een aanpassing van de vulgraad, om het intrekgedrag van het mengsel in de menger te verbeteren en om te voorkomen dat een bank boven de rotoren ontstaat. De optimale vulgraad voor deze werkwijze is 40 tot 45%, terwijl een vulgraad van 65% en meer wordt toegepast bij het werken in een gesloten menger. Wordt in een open menger gewerkt, dan kunnen verdere aanpassingen van mengapparatuur en -proces van voordeel zijn: de beste oplossing is de combinatie van een standaard interne menger met hoge afschuifkrachten voor masticeren, dispersief en distributief mengen en een speciale reactor voor de silaniseringstap. Tijdens de silanisering zijn geen hoge afschuifkrachten meer nodig; alleen de temperatuur moet op niveau worden gehouden en ethanol moet worden afgevoerd.

Andere factoren, die de silanisering positief kunnen beïnvloeden, zijn vulgraad, mengseltemperatuur, koelwatertemperatuur en rotorgeometrie. De vulgraad is binnen grenzen bepalend voor de verdeling van het mengsel in de mengkamer: hoe lager de vulgraad, hoe lager de verhouding van het volume rubbermengsel in de rol vóór de rotorvleugel en de rubberlaag aan de mengkamerwand. Daardoor werkt een verlaging van de vulgraad positief op de devolatilisatie, maar wel met een gelijktijdige reductie van de mengcapaciteit. Bij een te lage vulgraad wordt de krachtinbreng moeilijk en neemt de silaniseringefficiëntie af.

Wordt met een open menger gewerkt, dan is de invloed van de vulgraad nog groter door beïnvloeding van het intrekgedrag: hoe hoger de vulgraad, hoe

onregelmatiger en langzamer het mengsel door de rotoren wordt ingetrokken, waardoor de mengeffectiviteit verlaagd wordt.

De mengseltemperatuur is een ambivalente parameter: aan de ene kant moet de temperatuur hoog genoeg zijn om een hoge silaniseringsnelheid te waarborgen, maar aan de andere kant verhoogt een lage temperatuur de viscositeit van het mengsel, waardoor hogere afschuifkrachten optreden en de menging beter wordt. De bovengrens voor de mengseltemperatuur wordt bepaald door het risico van scorch door de aanwezigheid van zwavel in het silaan. De grenzen voor de mengseltemperatuur zijn redelijk nauw, en de beste werkwijze is het aanhouden van een temperatuur tegen de scorchgrens aan, mits de dispersie van het mengsel reeds voldoende is.

De koeleffectiviteit wordt rechtstreeks bepaald door de koelwatertemperatuur, omdat het temperatuurverschil tussen mengsel en mengkamerwand de drijvende kracht is. Een lage koelwatertemperatuur verbetert de silanisering, met name door een verhoging van de vernieuwingsfrekwentie van het oppervlak; de invloed op ethanolcondensatie in de menger is van ondergeschikt belang.

De silaniseringeffectiviteit wordt beïnvloed door de rotorgeometrie. Wordt in een open menger gesilaniseerd, dan is het intrekgedrag van de rotoren de meest belangrijke eigenschap: een regelmatige en frekwente intrek van het mengsel resulteert in een goede menging en uitsmering van het mengsel langs de mengkamerwand. In een gesloten menger is met name het meng- en koelgedrag belangrijk, naast de vorming van vers oppervlak.

In *hoofdstuk 4* wordt een model voor de devolatilisatie van een rubbermengsel in samenspel met een chemische reactie in een interne menger ontwikkeld. De basis voor dit model is de penetratietheorie, gebaseerd op een constante contacttijd tussen het oppervlak van het mengsel en de dampfase in de menger. In een interne menger wordt het contactvlak tussen mengsel en dampfase gevormd door het oppervlak van het mengsel vóór de rotorvleugels en de rubberlaag aan de mengkamerwand. Beide oppervlaktes worden periodiek vernieuwd, resulterend in een constante contacttijd. Devolatilisatie gebeurt op twee verschillende manieren: diffusie van ethanol en transport van kleine volume-eenheden naar het oppervlak. Het belangrijkste proces voor dit systeem is massatransport door de intensieve menging van het materiaal; de bijdrage van diffusie is in dit geval klein. Het ontwikkelde model is in staat om de invloed van de mengparameters kwalitatief te beschrijven. Een vergelijking van experimentele gegevens met modelberekeningen maakt duidelijk, dat het proces onder de experimentele omstandigheden geen stabiele toestand bereikt: de devolatilisatie van het mengsel door stoftransport verloopt sneller dan de vorming van ethanol door de chemische reactie, waardoor de ethanolconcentratie constant afneemt.

De kinetiek van de silica-silaan reactie is het onderwerp van *hoofdstuk 5*. In dit hoofdstuk wordt de invloed van bovengenoemde variaties van mengapparatuur en silaniseringproces op de kinetiek van de silaniseringsreactie onderzocht, en worden de resultaten vergeleken met gegevens uit de literatuur. De conclusie op basis van de kinetiekgegevens bevestigt de conclusie, dat de silaniseringsreactie sneller afloopt, naarmate de ethanolconcentratie in het mengsel lager is. Luchtinjectie komt als de meest efficiënte maatregel naar voren: bij een silaniseringtemperatuur van 145ºC wordt de silaniseringsnelheid door luchtinjectie verdubbeld.

Met behulp van automatisch geregistreerde 'fingerprints' van de meng- en silaniserings-cycli kan een energiebalans opgemaakt worden. In *hoofdstuk 6* wordt de balans opgesteld van verschillende energiestromen voor de opwarm- en silaniserings-fase. De enthalpie van de silaniseringsreactie en de adsorptiewarmte zijn te verwaarlozen ten opzichte van de totale energiestromen. Ook hier blijkt, dat ethanol een belangrijke rol speelt voor de koeleffectiviteit: condensatie van ethanol in de menger belemmert het contact tussen mengsel en mengkamerwand, resulterend in een lagere koeleffectiviteit en derhalve lagere silaniseringssnelheid. Er wordt een lineaire correlatie gevonden tussen zowel vulgraad als ook rotorsnelheid en koeleffectiviteit. Andere invloedfactoren zijn rotorgeometrie, werkwijze (open/gesloten menger) en luchtspoeling.

De analyse van het meng- en silaniseringsproces geeft duidelijk aan, dat de meest belangrijke processen stof- en energietransport zijn. Omdat beide processen afhangen van het contactoppervlak, is de verhouding van oppervlak en volume van het mengsel van groot belang voor schaalvergroting van een menger. Rotorsnelheid is een andere belangrijke invloedfactor, omdat deze bepalend is voor de vernieuwingsfrekwentie van het oppervlak. De vulgraad beïnvloedt energieopname en ethanolvorming. De afstand tussen rotor en mengkamerwand, de zone met hoge afschuifkrachten, is bepalend voor de efficiëntie van de dispersie. Een dimensieloos kengetal wordt in *hoofdstuk 7* voorgesteld, dat alle invloedparameters voor de schaalvergroting van een 'silaniseringmenger' bundelt..

In *hoofdstuk 8* worden de verwerkbaarheid en silaniseringseffectiviteit van verschillende silanen vergeleken. Eén groep van silanen is vergelijkbaar qua structuur (twee triethoxysilylpropylgroepen), maar de silanen verschillen in het aantal zwavelatomen: één tetrasulfide, één disulfide en een silaan, waarvan de zwavel door een butylgroep is vervangen, zijn onderzocht. Het zwavelvrije silaan reageert met de vulstof, maar de mogelijkheid om een binding met het polymeer aan te gaan ontbreekt. Dit silaan zal de verwerkbaarheid van de mengsels verbeteren door hydrofobering van silica, maar zal geen versterkend effect hebben. Het disulfide en tetrasulfide worden in praktijk toegepast en het tetrasulfide wordt in toenemende mate vervangen door het disulfide vanwege de hogere thermische stabiliteit en daardoor een lager risico op scorchreacties.

217

Het huidige onderzoek heeft echter geen significant verschil aangetoond tussen de twee zwavelhoudende silanen. Dit is te verklaren door de gebruikte mengwijze: de mengsels zijn op laboratorium-schaal met in-elkaar-grijpende rotoren geproduceerd, de meest efficiënte werkwijze voor een goede koelwerking. Daardoor is het risico van hotspots en scorchreacties klein.

Door gebruik van het disulfide in plaats van het tetrasulfide is de hydrofobering van de silica vulstof efficiënter. Het disulfide is thermisch stabieler en wordt daarom in mindere mate gesplitst, waardoor de moleculen met grotere waarschijnlijkheid liggend op het oppervlak van de vulstof worden gebonden, gestabiliseerd door polarisatie van de disulfidegroep. Wordt het tetrasulfide gesplitst, dan gaat het bij voorkeur loodrecht op het oppervlak staan en zal het afgesplitste gedeelte van het molecuul niet meer in contact staan met het oppervlak. Het zwavelvrije silaan heeft het laagste hydrofoberingeffect, wat ook door een sterisch effect verklaard zou kunnen worden.

De tweede serie van silanen die onderzocht is, bevat een geblokkeerde silaan, een silaan-oligomeer en als referentie bis-(triethoxysilylpropyl)disulfide, TESPD. In de eerste silaan is de zwavelgroep geblokkeerd als ester, resulterend in een stabiel monosulfide. Deze groep reageert alleen bij hogere temperatuur tijdens vulkanisatie, al dan niet met behulp van bijvoorbeeld een amine. Het molecuul bevat meer alkylgroepen dan in een gebruikelijk silaan, waardoor het hydrofoberende effect groter is. De verhouding van ethoxygroepen en alkylgroepen is kleiner, met als voordeel dat minder ethanol gevormd wordt bij een vergelijkbare hydrofoberings-graad.

Het silaan-oligomeer met een moleculaire massa van ca. 1800 g/mol heeft een nog lagere verhouding van ethoxygroepen ten opzichte van alkylgroepen en daardoor komt nog minder ethanol vrij. Het molecuul bevat geen zwavel; het is niet temperatuurgevoelig en een verwerkingstemperatuur van 175°C is mogelijk. Ook hier wordt de binding met het polymeer tijdens vulkanisatie gevormd met behulp van een activator.

Het geblokkeerde silaan levert de beste resultaten op: het Payne-effect als maat voor de silaniseringsgraad daalt snel en de ethanolconcentraties in het mengsel zijn laag, indicaties voor een snelle en efficiënte silaniseringsreactie. Het meng- en dispersieproces bleek efficiënt en de invloed van de vulgraad was laag. Mengsels met het silaan-oligomeer hebben een hogere viscositeit onder vergelijkbare condities: een lagere hydrofoberings-graad vergeleken met de andere silanen. De hoge viscositeit zou mede veroorzaakt kunnen zijn door 'entanglements', die gevormd worden tussen het silaan en het polymeer rond de silicadeeltjes.

3. VOORUITBLIK

De resultaten van dit onderzoek geven antwoord op veel vragen, maar zij roepen ook nieuwe vragen op. Dit onderzoeksgebied is groot en het vinden van een antwoord op alle vragen en oplossingen voor alle problemen is een moeilijke opgave.

De meest interessante vraag vanuit academisch perspectief is het mechanisme van de reactie tussen silica en silaan in rubber tijdens het mengen. De interactie met andere mengseladditieven en de invloed van het mengproces zouden moeten worden onderzocht. De competitieve adsorptie van ethanol en silaan op het silica-oppervlak is een belangrijk, maar weinig onderzocht proces. Het hydrofoberingseffect is mede bepalend voor de effectiviteit van silanen. De invloed van het aantal alkylgroepen in het silaanmolecuul is reeds eerder onderzocht. Echter, het sterische effect van verschillende silanen zal waarschijnlijk ook een belangrijke rol spelen; maar dit effect is nauwelijks onderzocht. Een conclusie van het huidige project is, dat de verwerkingscondities een belangrijke rol spelen voor de silaniseringsreactie, en de invloed van masticering, temperatuurverhoging en silanisering op de viscositeit van het mengsel was een onderwerp van lange discussies zonder dat een bevredigend antwoord is gevonden.

Het meest urgente praktijkprobleem met betrekking tot het mengen van silica-silaan-rubber mengsels is de vorming van ethanol en de scorchgevoeligheid van de mengsels. Nieuwe verbindingen zouden ontwikkeld moeten worden, die geen ethanol of anderszins problematische stoffen vormen. Dit probleem zou ook vanuit de vulstof benaderd kunnen worden: de ontwikkeling van nieuwe silica-types met een geactiveerd oppervlak, dat rechtstreeks met het polymeer zou kunnen reageren. Een andere optie is het ontwikkelen van nieuwe vulstoffen, die een combinatie bieden van het goede verwerkingsgedrag en de fysische interactie van een roet/polymeer-systeem en de chemische netwerkvorming van een silica/rubber-systeem. Dit is het concept van 'dual phase fillers', waar silica fijn verdeeld is in een roetfase.

De scorchgevoeligheid kan verbeterd worden door stabielere silanen te ontwikkelen, bij voorkeur zwavelvrije silanen. In het laatste geval zal de binding van silaan aan het polymeer een knelpunt zijn. Het concept van het geblokkeerde silaan, zoals beschreven in hoofdstuk 8, is een mogelijkheid om dit te realiseren, maar er zijn nog verdere verbeteringen mogelijk en vereist.

TIRE TESTING

1. TEST PROCEDURE

Tires:	Standard tire types produced by Vredestein
	Tires with treads made with air injection produced by Vredestein
	Standard tires and development products produced by Continental as reference
Tire type:	205/55 R 16 H, all weather
Start mileage:	1000 km
Start of the tests:	December 2003
Test cars:	VW Passat, VW Golf, Audi A4, MB C class

TESTS ON SNOW:

Region:	East Tirol (Austria), Engadin (Switzerland), Sweden
Temperature:	-3 to -13°C
Humidity:	86% to 43%
Snow type:	Very soft, soft, well prepared, very well prepared
Tests:	Traction, breaking, performance on alpine passes

TESTS ON ICE:

Ice type:	Natural, artificial (indoor)
Region:	Sweden, Grefrath (Germany)
Tests:	Traction, breaking

2. TEST RESULTS

As reference standard winter tires from Continental and a new tire still under development are tested simultaneously. Their performance is put to 100%. Marks higher than 100% are better than the reference.

Reference: Standard winter tire		Standard tire		'Air injection' tire	
		Maximum	Average	Maximum	Average
Traction on snow	[%]	77	75	79	77
Breaking on snow	[%]	96	90	94	89
Performance on alpine pass	[%]		120		115
Traction on natural ice	[%]		90		91
Breaking on natural ice	[%]		105		113

Reference: Newly developed tire		Standard tire		'Air injection' tire	
		Maximum	Average	Maximum	Average
Traction on snow	[%]	104	102	98	96
Breaking on snow	[%]	100	98	102	100
Performance on alpine pass	[%]		98		97
Traction on natural ice	[%]		85		87
Breaking on natural ice	[%]		100		109

Results are average values from 100 drives

3. SUMMARY

The tire having a tread made from a compound produced with air injection is significantly better in terms of breaking on ice and slightly better in terms of traction on snow. The breaking distance on snow and ice is shorter. The performance of breaking on snow is slightly inferior. The overall performance of the 'air injection' tire is better than the tire with a tread from conventional material, and comparable to the performance of the high quality winter tires.

SYMBOLS AND ABBREVIATIONS

Symbol	Description
$\overline{\dot{\gamma}}_{max}$	Maximum shear rate
$\dot{\gamma}$	Shear rate
$\dot{m}$	Mass flux
ID	Diffusion coefficient
τ	Shear stress
κ	Heat transfer coefficient
A	Surface area
Å	Angstrom (10^{-10} m)
A_{ct}	Area under the current-time curve of the mixing process
A_{HT}	Heat transfer area
A_l	Area of the layer on the mixer wall
a_m	Coefficient related to filler morphology
A_p	Area of the pool material surface
a_S	Coefficient related to filler surface
B	Proportion of the mixing chamber wall, where the rotor does not make contact
$b_{ad/de}$	Ratio of adsorption rate to desorption rate
BBP	Dibutylpthalate
BIT	Black incorporation time
Br	Brinkmann number
BR	Bound rubber
C	General coefficient
c	Concentration
c_0	Starting concentration
c_{CA}	Concentration of the coupling agent
c_{eq}	Equilibrium concentration
c_{Et}	Concentration of ethanol
c_i	Initial concentration at time t=0
c_j	Concentration at the end of step j
c_{j-1}	Concentration at the end of step j-1
c_L	Concentration of absorbed molecules
cm	Centimeters
c_{nR}	Concentration after n_R steps

C_o	Einstein-Smallwood parameter
c_p	Heat capacity
CR	Chemical reaction term in the microscopic mass balance
c_{rp}	Concentration of the reaction product
$C_{rp,eq}$	Concentration of the reaction product in equilibrium
c_{sm}	Concentration of the starting components
c_{ss}	Concentration of the volatile component in the material bulk
D_C	Channel diameter between rotor shaft and mixing chamber wall
De	Deborah number
D_M	Mixing chamber diameter
d_{mw}	Mean distance of the compound to the mixing chamber wall
D_N	Network desity
$D_{N,C}$	Density of a chemical network formed by stable bonds
$D_{N,S}$	Density of a stable physical network
$D_{N,U}$	Density of an unstable physical network
D_R	Rotor diameter
DR	Dispersion rate
D_s	Diameter at rotor shaft
D_T	Diameter at rotor tip
d_{wall}	Thickness of the mixer wall
e	Width between rotor tip and mixing chamber wall
E	Overall efficiency
E'	Elastic or storage modulus
E"	Viscous or loss modulus
E_A	Activation energy
E_f	Young's modulus of the reinforced material
E_g	Young's modulus of the gum stock
E_j	Efficiency of a single step
EPDM	Ethylene-propylene-diene polymer
EPM	Ethylene-propylene polymer
erf	Error function
E_W	Work or energy input
F	General proportionality factor
F4W	Full four wing rotor geometry
FF	Fill factor
FID	Flame ionization detector
F_o	Occluded volume effectiveness factor
f_s	Shape factor
G	Shear modulus
g	Gram
g	Clearance between rotor tip and mixing chamber wall
G'	Storage modulus
G_0	Shear modulus of the pure elastomer
GC	Gas chromatograpy
g_{ij}	Molar transfer rate of the volatile component
G_o	Modulus of the unfilled matrix
Gr	Griffiths number
G_v	Modulus of a filled rubber matrix

Gz	Graetz number
h	Clearance of the channel between rotor shaft and mixing chamber wall
H	Height
$h_{1/2}$	Gap half width
He	Hersey number
HPLC	High pressure liquid gas chromatography
HTU	Height of transfer unit
Hz	Hertz
I(+number)	Intermeshing mixer (size)
I5	5.6 liter mixer with intermeshing PES5 rotors
J	Joule
K	Dispersibility index
K	Kelvin
k_a	Rate constant of the re-agglomeration process
k_B	Boltzmann constant
K_{CR}	Constant ratio of the concentrations for the equilibrium state of a chemical reaction
k_H	Henry's constant
k_I	1st order reaction constant
KJ	Kilojoule
k_L	Overall liquid phase mass transfer coefficient
K_{MT}	Mass transfer coefficient
K_P	Proportionality factor summarizing geometrical factors of a mixer
k_R	Reaction rate constant
L	Length
τ_I	Shear stress in the wall layer
L_M	Length of the mixing chamber
L_R	Rotor length
LTU	Length of transfer unit
LV	Line voltage
m	Meter
min	Minute
m_I	Flow of a volatile component out of the wall layer
ML(1+4)	Mooney viscosity after 1 minute of preheating and 4 minutes of measuring, measured with a large rotor
mm	Millimeter
m_p	Flow of a volatile component out of the pool of material
MPa	Megapascal
MPS	3-methacryloxypropyltrimethoxysilane
MU	Mooney units
N	Number of elastically active contacts
N	Rotor speed
n	Power law index
N_0	Number of elastically active contacts at zero deformation
n_f	Number of flights
nm	Nanometer (10^{-9} meter)
n_r	Number of rotors
n_R	Number of reactors in a series

NR	Natural rubber
n_s	Number of steps
P	Power consumption
p (subscript)	Pressure
PE	Polyethylene
PE	Payne effect
PES5	Brand name of a standard intermeshing rotor
phr	Parts per hundred rubber
PVC	Polyvinylchloride
Q	Volumetric flow rate
q	Amount of a compound removed per unit time from a unit area of the surface
Q_C	Energy input to the compound
Q_{CR}	Energy of a chemical reaction
Q_{DC}	Drag flow in the channel between rotor shaft and mixer wall
Q_{DT}	Drag flow between rotor tip and mixer wall
Q_E	Energy losses to the environment
Q_{EML}	Electrical and mechanical energy losses
Q_M	Energy losses to the mixing equipment
Q_N	Net energy input
Q_{PC}	Pressure flow in the channel between rotor shaft and mixer wall
Q_{PP}	Energy balance a physical process
Q_{PT}	Pressure flow between rotor tip and mixer wall
Q_T	Total energy input
Q_W	Energy transfer to cooling water
R	Reaction rate
R	Gas constant
R_a	Rate of agglomeration
R_M	Radius of the mixing chamber
RPA	Rubber Process Analayzer
rpm	Revolutions per minute
R_R	Radius of the rotor
RR	Fractional renewal rate of the area exposed to penetration
RR_V	Renewal rate of the vapor phase in the mixer
SBR	Styrene butadiene rubber
sec	second
SI rotor	Rotor developed for silica mixing
S-SBR	Solution styrene butadiene rubber
S_v	Ratio of evaporation area to batch volume
$S_{v,l}$	Ratio of evaporation area of the wall layer to batch volume
$S_{v,p}$	Ratio of evaporation area of the material pool to batch volume
T	Absolute temperature [Kelvin]
T	Torque
t	Time
t (subscript)	Rotor tip
T(number)	Tangential mixer (size)
T4	3.6 liter mixer with tangential ZZ2 rotors
T7	7.6 liter mixer with Intermeshing F4W rotors or SI rotor

226

tan δ	Loss angle
T_{comp}	Temperature of the rubber compound
TCU	Temperature control unit
T_{CW}	Temperature cooling water
t_e	Exposure time
$t_{e,l}$	Exposure time of the wall layer
$t_{e,p}$	Exposure time of the pool surface
TESPD	Bis(triethoxysilylpropyl)disulfane
TESPT	Bis(triethoxysilylpropyl)tetrasulfane
t_m	Mixing time
TS	Tensile strength
U	Scaling factor
V	Volume
v	Velocity
v_a	Angular velocity
var.	variable
V_b	Batch volume
v_f	Volume fraction of the filler
V_i	Volume element in the mixer
V_M	Volume of the mixing chamber
v_p	Peripheral rotor speed
V_s	Volume of the high-shear zone in the mixing chamber
v_x	Velocity in x-direction
v_y	Velocity in y-direction
v_z	Velocity in z-direction
W	Watt
w	Equilibrium mass fraction
W	Width
W	Work
We	Weissenberg number
x	Coordinate x-direction
X', X"	Different scales of mixer size
y	Coordinate y-direction
y_p	Average number of strain-invariant units of the polymer trains between the adsorption sites
$y_{p,v}$	Reduced average size of polymer segments in a filled compound under consideration of the filler-polymer contacts
Z	Flow field
z	Coordinate z-direction
Z_R	Length of the rotor
ZZ2	Brand name of a standard tangential rotor
α	Heat transfer coeffcient
$α_{RS}$	Heat transfer coefficient between rubber and steel
$α_{SW}$	Heat transfer coefficient between steel and water
Γ	Surface concentration of adsorbent
γ	Strain
$Γ_0$	Concentration of a monolayer of adsorbent
$γ_c$	Strain half-width amplitude

γ_s	Surface free energy
γ_s^d	Dispersive component of the surface free energy
γ_s^{sp}	Specific component of the surface free energy
δ	Hildebrand solubility parameter
δ	Layer thickness
Δc	Concentration gradient
ΔT	Temperature difference
η	Viscosity of an elastomer-filler blend
η_0	Viscosity of a pure elastomer
λ	Relaxation time
λ_H	Heat conductivity
λ_m	Maximum uniaxial strain that can be applied to a single chain
$\lambda_{m,v}$	Reduced strain in the polymer-filler system under consideration of polymer-polymer and filler-polymer bridges
μ	Velocity of a suspending fluid
μ	Apparent viscosity
μm	Micrometer (10^{-6} meter)
v	Concentration of elastically active network chains
ξ	Characteristic time
ρ	Density
Φ	Volume fraction of the filler
Φ'	Volume fraction of the filler including the immobilized fraction of the polymer
χ	Geometry of the breakup process
Ψ	Relative efficiency of one step in a series

ANNEX 3

PUBLICATIONS, PAPERS, PATENTS

1. H. Schaarschmidt, W. Dierkes
   Kontinuierliche Herstellung von Gummibahnen aus modifiziertem Altgummipulver
   Kautschuk Gummi Kunststoffe, **48**, 3, 198-200 (1995)

2. W. Dierkes
   Lösung der Reststoff-Problematik: die Wiederverarbeitung von Produktionsabfällen im
   Rahmen des Recyclingkonzeptes
   Proceedings 2. German-Dutch Rubber Symposium, Maastricht, The Netherlands, 175-187
   (1995)

3. W. Dierkes
   A New Development in Rubber Recycling
   147th Spring Technical Meeting of the American Chemical Society, Rubber Division,
   Philadelphia, Pennsylvania (1995)

4. W. Dierkes
   Die Wiederverarbeitung von Gummiabfällen - ein Recycling-Konzept
   Gummi Fasern Kunststoffe, **48**, 6, 398-404 (1995)

5. W. Dierkes
   Surface Activated Crumb Rubber: A New Development in Rubber Recycling
   Proceedings IRMRA 17th Rubber Conference, Madras, India, 131-149 (1995)

6. W. Dierkes
   Solutions to the Rubber Waste Problem Incorporating the Use of Recycled Rubber
   148th Fall Technical Meeting of the American Chemical Society, Rubber Division,
   Cleveland, Ohio (1995)
   Published in: Rubber World, **214**, 25-31 (1996)

7. R. Burlet, W. Dierkes
   The place of recycled rubber in the modern industry
   Proceedings International Rubber Forum, Phuket, Thailand, 143-157 (1996)

8. W. Dierkes
   The Recycling of Rubber Waste: Our Challenge and Your Opportunity
   Proceedings Nordic Rubber Conference NRC '96, Helsinki, Finland (1996)

9. W. Dierkes
   State-of-the-art reduction of tire waste
   Proceedings ETRA: Third European Conference, Brussels, Belgium, 102-111 (1996)

10. W. Dierkes
    Opportunities and Challenges for Rubber Recycling
    Proceedings International Rubber Conference IRC '99, Manchester, Great Britain (1996)

11. W. Dierkes
    Surface activated rubber crumb : A new development in rubber recycling
    Journal of Elastomers and Plastics, **28**, 3, 257-278 (1996)

12. W. Dierkes
    Tomorrow's Technology Today
    150th Fall Technical Meeting of the American Chemical Society, Rubber Division,
    Louisville, Kentucky (1996)

13. R. Burlet, W. Dierkes
    Market- and Legislation-driven Change in the Rubber Recycling Industry
    Polymer Recycling, **2**, 3, 177-182 (1996)

14. W. Dierkes
    Rubber Re-use is best all around
    European Rubber Journal, 36-38 (November 1996)

15. H.-J. Manuel, W. Dierkes
    Recycling of Rubber
    RAPRA Review Report no. 99, 9, 3, RAPRA Technology Limited (1997) [ISSN 0889-3144]

16. W. Dierkes
    New developments in rubber recycling
    7th Brazilian Congress of Rubber Technology, São Paulo, Brazil (1997)

17. W. Dierkes, H. Leeuw, H.-J. Manuel, R. Smits
    Granulate developments
    ETRA : Fifth European Conference, Brussels, Belgium (1998)

18. W. Dierkes
    Rubber Recycling: is it a burden or opportunity for the rubber industry?
    Materials Congress '98, Cirencester, Great Britain (1998)

19. W. Dierkes
    Recycling – a changing scene
    Tire Technology International UK & International Press, 170-175 (1998)

20. H. Leeuw, W. Dierkes, H.-J. Manuel
    Size does matter
    Tire Technology International, 46-50 (September 1998)

21. W. Dierkes
    Tire recycling is a reality
    Proceedings Technical Meeting of the American Chemical Society, Rubber Division,
    Nashville, Tennessee (1998)

22. W. Dierkes
    Recycled rubber: a valuable raw material!
    Elastomery, **1**, 14, 18-25 (1999)

23. W. Dierkes
    Customer service: from production waste to a raw material
    Proceedings International Rubber Conference IRC`99, Manchester, Great Britain (1999)

24. H.-J. Manuel, W. Dierkes, A. Hendriks
    Butyl reclaim in innerliner applications
    Kautschuk Gummi Kunststoffe, **53**, 12, 730-734 (2000)

25. W. Dierkes
Wiederverwertung und Recycling von Elastomeren
in: Handbuch der Kautschuktechnologie, chapter 16, Dr. Gupta Verlag (2001)
[ISBN 3-9803593-2-8]

26. Dierkes, W., Klamt, G., Hasenkox, U., Mueller, L., Vogt, A.,
Wiper Blade
DE10125045, WO02094624, appl.: Robert Bosch GmbH, 28.11.2002:

27. Baun, R., Dierkes, W., Gruhn, H., Schmid, H., Leutsch, W.
Method for the production of a rubber article and corresponding rubber article
WO03080717, appl.: Robert Bosch GmbH, 02.10.2002

28. W. Dierkes
Recyclingmogelijkheden voor rubber
Materialen & Processen, **1**, 20-23 (2002) [ISSN 0926-8979]

29. L.A.E.M. Reuvekamp, J.W. ten Brinke, W.K. Dierkes, J.W.M. Noordermeer
Mechanistic aspects of the role of coupling agents in silica-rubber composites
Proceedings Kautschuk-Herbst Kolloquium, Hannover, Germany, 75-84 (2002)

30. W. Dierkes, J.W.M. Noordermeer, C. van de Pol, M. Rinker, K.-U. Kelting
Increasing the silanisation efficiency of silica compounds: upscaling
Proceedings Kautschuk-Herbst Kolloquium, Hannover, Germany, 297-307 (2002)
Published in: Kautschuk Gummi Kunststoffe, **56**, 6, 338-344 (2003)

31. W. Dierkes, K.-U. Kelting
Optimization of the mixing process and equipment for silica compounds
Proceedings International Rubber Conference '03, Nürnberg, Germany, 245-249 (2003)

32. L.A.E.M. Reuvekamp, W.K. Dierkes, J.W.M. Noordermeer
Fulfilling potential
Tire Technology International, **3**, 44-47 (2003)

33. W. Dierkes
Review article: Rubber Recyling
Recent Research Developments in Macromolecules **7**, 265-292 (2003)

34. L.A.E.M. Reuvekamp, W. Dierkes, A.J.W. ten Brinke, J.W.M. Noordemeer
Silane coupling agents for silica filled tire compounds: the link between chemistry and performance
Proceedings Fourth International Symposium on Silanes and other Coupling Agents, Orlando, Florida (2003); published in: Silanes and other coupling agents, vol. 3, editor: K.L. Mittal, VSP, Utrecht, the Netherlands (2004)

35. W. Dierkes, J.W.M. Noordermeer, K.-U. Kelting, A. Limper
Improvements in processing of silica compounds: optimization of the mixing equipment
Proceedings Technical Meeting of the American Chemical Society, Rubber Division, Cleveland, Ohio, USA (2003)
published in: Rubber World, **229**, 6, 33-40 (2004)

36. W. Dierkes
Untreated and treated rubber powder
Chapter 'Rubber Recycling Handbook', CRC Press, Boca Raton, Florida, USA; to be published in 2005

37. W. Dierkes, J.W.M. Noordermeer
Improvements in processing of silica compounds: optimization of the mixing equipment
Proceedings of the Polymer Processing Society conference, Akron, Ohio, USA (2004)

38. W. Dierkes, V.V. Rajan, J.W.M. Noordermeer
Model compound studies on the devulcanization of natural rubber using 2,3-dimentyl-2-butene
Proceedings Kautschuk Herbst Kolloqium, Hannover, Germany, (2004); to be published in
      Kautschuk Gummi Kunststoffe

39. P. Sutanto, F. Picchioni, L.P.B.M. Janssen, K. Dijkhuis, W.K. Dierkes, J.W.M.
      Noordermeer
State of the art: Recycling of EPDM rubber vulcanizates
To be published in Polymer Processing International

40. V.V. Rajan, W.K. Dierkes, J.W.M. Noordermeer, R. Joseph
Mechanisms involved in the reclamation of NR based rubber products
Proceedings Technical Meeting of the American Chemical Society, Rubber Division, Columbus,
      Ohio, USA (2004), to be published in: Rubber Chemistry and Technology

CURRICULUM VITAE

Date of birth   December 24, 1964 (Werlte, Germany)

EDUCATION

08/1975 - 06/1984   Gymnasium Sögel (Lower Saxony, Germany)
10/1984 - 09/1990   Technical University Hanover: Chemistry (Diplom)
02/1990 - 09/1990   Institute for Physical Chemistry and
                           Electrochemistry of the Technical University
                           Hannover, masters thesis: `FT-IR investigation on
                           the physisorption of hydrogen on specially prepared
                           NaCl-crystal surfaces´

09/1991 - 12/1993   Fondation Universitaire Luxembourgeoise, Arlon
                           (Belgium), post-academical education: European
                           Environmental Sciences

07/1992 - 06/1993   Vredestein Rubber Recycling, Maastricht,
                           masters thesis: `Surface-activation of rubber
                           powder´

PROFESSIONAL EXPERIENCE

10/1990 - 02/1991   Institute for Physical Chemistry and
                           Electrochemistry of the Technical University
                           Hannover: Assistant in education, research

03/1991 - 08/1991   Degussa Belgium: Chemical analyst
10/1993 - 07/1999   Vredestein Rubber Recycling, Maastricht (the
                           Netherlands): Research & Development, Technical
                           Service, marketing

08/1999 – 07/2001   Robert Bosch Produktie (Belgium): Product
                           development, head of the chemical laboratory

since 08/2001   University Twente, Enschede (the Netherlands):
                           Assistant Professor